![rps MAKING COMPLEX EASY]

ENBRIDGE LINE 5 WISCONSIN SEGMENT RELOCATION PROJECT
22-P-216493

Technical Appendix B – Hydrocarbon Trajectory, Fate, and Effects Assessment

Appendix to Operations Assessment: Oil Spill Report

www.rpsgroup.com

Contents

Figures

www.rpsgroup.com

Tables

1   INTRODUCTION

As described in the Oil Spill Report, Enbridge Energy, Limited Partnership (Enbridge) is proposing to relocate the existing Line 5 pipeline (Line 5) around the Bad River Reservation ("the Reservation") in northern Wisconsin to a more southerly route in Ashland, Bayfield, Douglas, and Iron Counties, Wisconsin. The Proposed Route and each route alternative (RA) of the Line 5 Wisconsin Segment Relocation Project (L5WSRP) would divert a small portion of the Line 5 pipeline from the existing route through the Reservation and instead route the pipeline from a starting point west of the Reservation, south around the Reservation, and then back to the north to reconnect at another point farther east in Iron County. Depending on the route alternative, the relocated route would add between 50.5 km (31.4 mi.) and 163.4 km (101.5 mi.) of new pipeline. The pipeline would carry the same products to the same ultimate Line 5 destination in Sarnia, Ontario, Canada. The Proposed Route, as well as alternate routes RA-01 and RA-02, would bypass the Reservation to the south and pass through the upper portions of the Bad River watershed. Along this path, the Proposed Route would cross both the Bad River and the White River, a large tributary of the Bad River (Figure 1-1). These two crossing locations are the focus of this high-resolution three-dimensional trajectory, fate, and effects modeling assessment. A full suite of hypothetical crude oil release scenarios was used to bound the range of effects that multiple release volumes, geographic and environmental variability, and the inclusion or absence of emergency response mitigation measures may have on hypothetical releases into large waterways.
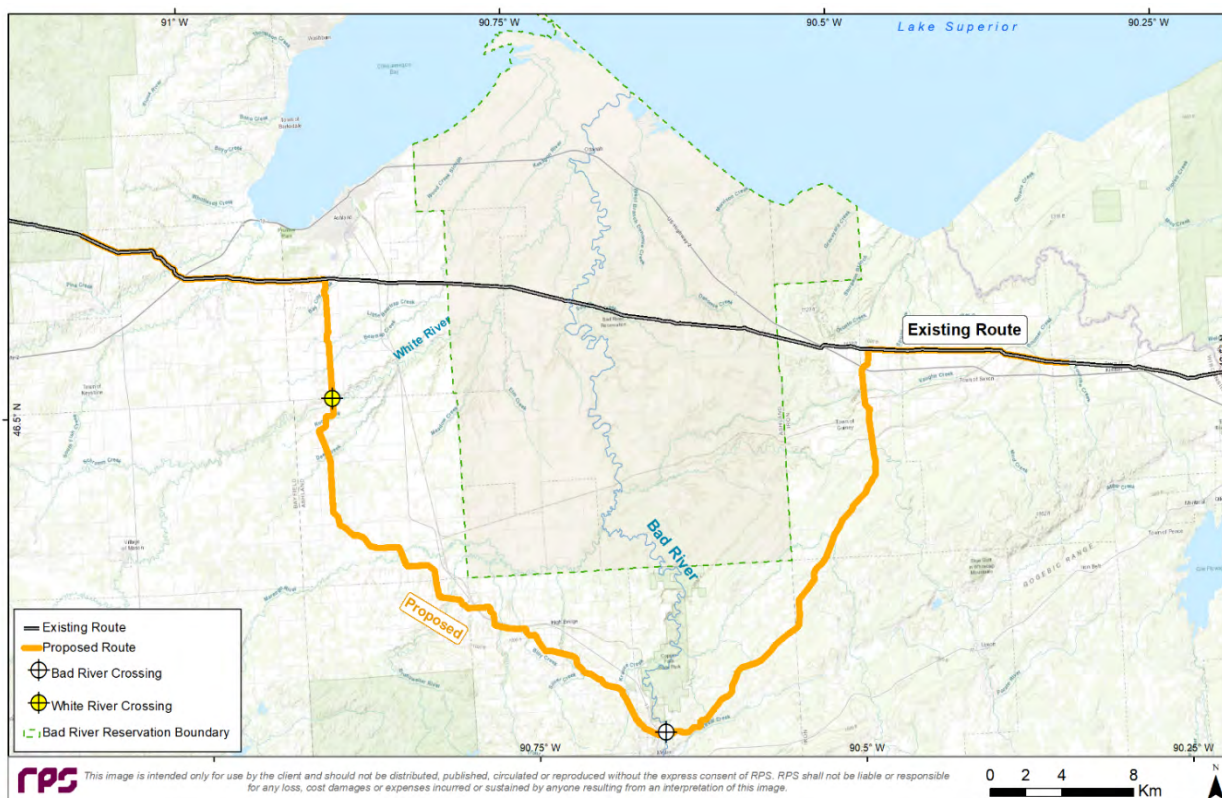
Figure 1-1. Map of Proposed Route in the DEIS and crossings with the Bad River and White River.

The draft Environmental Impact Statement (DEIS) for the proposed relocation project, which was prepared by the Wisconsin Department of Natural Resources (WDNR), provided a high-level analysis of potential environmental impacts from the Proposed Route of the pipeline and three route alternatives (RA-01, RA-02, and RA-03). The Oil Spill Report and this Technical Appendix B seek to supplement the DEIS with quantitative analyses, using computational oil spill modeling. The goal was to provide a high-resolution modeling assessment of trajectory, fate, and effects that considered potential hydrocarbon releases from the Proposed Route of the L5WSRP.

The modeling approach for this assessment is described in Section 2.2 of the Oil Spill Report. To recap, each scenario was simulated as a near-instantaneous release (13 minutes) under a variety of geographic and environmental conditions throughout the year using multiple hypothetical release volumes. The trajectory, fate, and potential effects were simulated for a total of four days following the release, enabling a longer period of time for oil to reach Lake Superior (Table 1-1, Table 1-2). Simulations bounded representative environmental conditions throughout the year. April was identified as being representative of the high river flow season, June was representative of the average river flow during summer and autumn seasons, and January was representative of low river flow wintertime conditions. In winter, the presence of 100% ice cover was assumed, which would effectively prevent the evaporation of subsurface oil and maximize the potential for in-water contamination.

Each representative release scenario was run separately in RPS' three-dimensional Spill Impact Model Application Package (SIMAP) as a deterministic (i.e., single trajectory) model simulation. Three release volumes were modeled at the crossings of each river, including an FBR release (9,874 bbl for the Bad River crossing and 8,517 bbl for the White River crossing), a HARV discharge of 1,911 bbl, and a RARV discharge of 334 bbl (Table 1-1, Table 1-2). Each FBR and HARV discharge was modeled during high, average, and low river flow conditions. The RARV discharges were only simulated under average river flow conditions for comparison to the larger volume releases. In comparison to the largest release volume (FBR), the HARV and RARV capture potentially smaller release scenarios other than the worst-case FBR. The HARV was identified based on an analysis of the average release volume since 1985 from all pipelines that carry crude oil on the entire Enbridge Mainline System (PHMSA, 2017). The smaller-volume RARV was identified based on an analysis of the average release volumes of any reportable size (recorded as >5 gallons or >0.12 bbl) from 2010 to 2019 for all of Enbridge's liquids pipelines. The RARV still represents a conservatively high release volume because, since 2010, Enbridge has transported approximately 25% of the crude oil produced in North America in its pipelines and recorded only 122 total releases, of which 90% were less than 10 bbl, with both the mode and median of these release volumes being less than 1 bbl. In each hypothetical release scenario, a constant release rate was assumed during the period of release.

The same suite of scenarios (i.e., FBR, HARV, and RARV during high, average, and low river flow conditions) was modeled both with and without emergency response mitigation. This mitigation was implemented at a set of pre-identified downstream Control Points (CPs) that included various containment and collection tactics (see details in Section 2.1 of the Oil Spill Report). Response actions modeled in this study included surface and shoreline containment booming, as well as surface oil skimming technologies. At each Modeled Control Point (MCP), a variable number of surface skimming equipment were utilized. Booms were positioned at an angle across the channel in order to funnel oil flowing downstream into the point of collection, where skimmers were placed to maximize surface oil recovery. Response planning information was provided to RPS by Enbridge, which identified the placement of each CP, as well as the timing, response equipment present, and the assumed efficiency for each piece of equipment (Enbridge 2022a). In the event of an actual release, containment and recovery/collection locations would be tailored to the specific release, the environmental

conditions at the time, and the exact location of the oil when responders arrived to target containment and collection activities most effectively.

Table 1-1. Bad River Crossing Scenarios modeled in SIMAP.

Scenario ID	Spill Site	Spill Event & Response	River Flow Condition	Season	Spill Duration	Total Spilled Volume (bbl)	Model Duration
1		FBR Unmitigated	High	Spring		9,874	
2			Average	Summer			
3			Low	Winter (Ice)			
4		HARV Unmitigated	High	Spring	13 min	1,911	4 days
5	Proposed Route Crossing of Bad River		Average	Summer			
6			Low	Winter (Ice)			
7		RARV Unmitigated	Average	Summer		334	
8	46.3360 °N, 90.6494 °W	FBR Mitigated	High	Spring		9,874	
9			Average	Summer			
10			Low	Winter (Ice)			
11		HARV Mitigated	High	Spring	13 min	1,911	4 days
12			Average	Summer			
13			Low	Winter (Ice)			
14		RARV Mitigated	Average	Summer		334	

Table 1-2. White River Crossing Scenarios modeled in SIMAP.

Scenario ID	Spill Site	Spill Event & Response	River Flow Condition	Season	Spill Duration	Total Spilled Volume (bbl)	Model Duration
1	Proposed Route Crossing of White River 46.502 °N, 90.895 °W	FBR Unmitigated	High	Spring	13 min	8,517	4 days
2			Average	Summer			
3			Low	Winter (Ice)			
4		HARV Unmitigated	High	Spring		1,911	
5			Average	Summer			
6			Low	Winter (Ice)			
7		RARV Unmitigated	Average	Summer		334	
8		FBR Mitigated	High	Spring	13 min	8,517	4 days
9			Average	Summer			
10			Low	Winter (Ice)			
11		HARV Mitigated	High	Spring		1,911	
12			Average	Summer			
13			Low	Winter (Ice)			
14		RARV Mitigated	Average	Summer		334	

This Technical Appendix B provides background on the SIMAP modeling package, underlying fate processes, and hydrodynamic characterization used in the computational spill modeling (Section 2). Section 3 describes the input data used in each aspect of the modeling, as well as the characterization of response mitigation tactics (Section 3.10). Section 4 provides the results of the deterministic SIMAP simulations, including time histories of the fate and weathering of oil over the duration of the release (mass balance) and footprints of the instantaneous maximum for individual spill trajectories over the course of the entire modeled duration. The mass balance results are expressed as the percentage of released oil on the water surface, on the shoreline, evaporated to the atmosphere, entrained in the water column, and naturally degraded. The maximum oiling footprints depict the cumulative path of floating surface oil thickness, mass of shoreline oil, and the maximum concentration of dissolved hydrocarbons (i.e., the soluble fraction) in the water column at any point in time. The results of further biological effects modeling of the scenarios are also presented (Section 4.2), at two different sensitivity thresholds, to bound the potential impacts that each release may have on the ecological receptors in the environment. These results have been calculated and presented in the same, consistent way as the oil spill modeling work and assessments that were completed for proceedings related to the Enbridge Line 3 Replacement Program (L3RP) in Minnesota and other documents such as the Rebuttal Report and Technical Appendix of Dr. Matthew Horn prepared for proceedings related to Line 5 litigation associated with the Bad River Reservation.

2   MODEL DESCRIPTIONS

2.1   SIMAP Model Description

The SIMAP modeling system is a comprehensive three-dimensional modeling system that was developed by RPS over the last roughly forty years to provide an understanding of the movement, behavior, and potential effects of crude oil for releases into the water. SIMAP originated from the oil fate and biological effects sub-models in the Natural Resource Damage Assessment Models for Coastal and Marine Environments (NRDAM/CME) and Great Lakes Environments (NRDAM/GLE), which ASA (predecessor to RPS) developed in the early 1990s for the U.S. Department of the Interior for use in "Type A" Natural Resource Damage Assessment (NRDA) regulations under the Comprehensive Environmental Response, Compensation, and Liability Act of 1980 (CERCLA). The most recent version of the Type A models, the NRDAM/CME (Version 2.4, April 1996) was published as part of the CERCLA type A NRDA Final Rule (Federal Register, May 7, 1996, Vol. 61, No. 89, p. 20559-20614). The technical documentation for the NRDAM/CME is in French et al. (1996). This technical development involved several in-depth peer reviews, as described in the Final Rule.

While the NRDAM/CME and NRDAM/GLE were developed for simplified natural resource damage assessments of small spills in the U.S., SIMAP was designed to evaluate fate and effects of both real and hypothetical spills in marine, estuarine, and freshwater environments worldwide. Additions and modifications to prepare SIMAP were made to increase model resolution, allow modification and site-specificity of input data, allow incorporation of spatially- and temporally-varying current data, evaluate subsurface releases and movements of subsurface oil, track multiple chemical components of the oil, enable stochastic modeling, and facilitate analysis of results.

The 3D physical fate model estimates the distribution of whole oil and oil components on the water surface, on shorelines, in the water column, and in sediments as both mass and concentration. Because oil contains many chemicals with varying physical and chemical properties, and the environment is spatially and temporally-variable, the oil rapidly separates into different environmental compartments through multiple fate processes. Oil fate processes included in SIMAP are oil spreading (gravitational and by shearing), evaporation, transport, randomized dispersion, emulsification, entrainment (natural and facilitated by dispersant [although dispersant application was not modeled in this assessment]), dissolution of the soluble fraction of oil into the water column, volatilization of dissolved hydrocarbons from the surface water, adherence of oil droplets to suspended sediments, adsorption of soluble and sparingly-soluble aromatics to suspended sediments, sedimentation, and degradation. Oil trajectory and weathering endpoints include surface oil, emulsified oil (mousse), tar balls, suspended oil droplets, oil adhered to particulate matter, dissolved hydrocarbon compounds in the water column and pore water, and oil on and in bottom sediments and shoreline surfaces.

Consideration of the effects of subsurface oil is important, particularly in the evaluation of effects on aquatic organisms. Surface floating oil primarily affects wildlife (birds, mammals, reptiles, and adult amphibians) and shoreline biota (emergent vegetation), rather than aquatic biota (fish, invertebrates, early life-stages of amphibians, aquatic plants) in submerged habitats. In turbulent waters (e.g., riverine environments) and at higher wind speeds than about 12 knots (approximately 14 mph) (or at lower wind speeds if dispersant is applied), oil will entrain into the water column, unless it has become too viscous to do so after weathering and the formation of mousse. Once oil is entrained in the water in the form of small droplets, monoaromatic and polycyclic aromatic hydrocarbons (MAHs and PAHs) dissolve into the water column over time. The MAHs and PAHs are the most toxic portion of the oil by virtue of their relative solubility in water, making them available to

aquatic biota for uptake. The dissolution rate of MAHs and PAHs from entrained oil is very sensitive to the droplet size because it involves mass transfer across the surface area of the droplet, and the amount of hydrocarbon mass dissolved is a function of the mass entrained and droplet size distribution. These are, in turn, a function of soluble hydrocarbon content of the oil, the amount of evaporation of these components before entrainment, oil viscosity (which increases as the oil weathers and emulsifies), oil surface tension (which may be reduced by surfactant dispersants), and the energy in the system (the higher the energy the smaller the droplets). Large droplets (greater than a few hundred microns in diameter) resurface rapidly, and so their dissolution is inconsequential. Dispersant application (which was not modeled in this assessment) facilitates the entrainment of oil into the water in a smaller size distribution than would occur naturally, with the median droplet size of about 20 μm (Lunel, 1993a; 1993b).

Thus, the fate of MAHs and lighter or more volatile PAHs in surface oil is primarily volatilization to the atmosphere, rather than to the water unless entrainment of the surface oil into the water is significant. If oil is entrained before it weathered and lost the lower molecular weight aromatics to the atmosphere, dissolved MAHs and PAHs in the water can reach concentrations where they can affect water column organisms or bottom communities (French-McCay and Payne, 2001).

Detailed descriptions of the algorithms and assumptions in the model are in published papers (French-McCay, 2002; 2003; 2004; 2009). The model has been validated with more than 20 case histories, including the *Exxon Valdez* and other large spills (French and Rines, 1997; French-McCay, 2003; 2004; French-McCay and Rowe, 2004) as well as test spills designed to verify the model (French et al., 1997).

Floating surface oil is calculated within the model as a mass per unit area, averaged over a defined (grid cell) area. If the oil is evenly distributed in that area, it would be equivalent to a mean thickness, where 1 micron (μm) of thickness corresponds to a layer of oil with a mass concentration of approximately 1 g/m^2. Surface oil thickness is typically determined by the visual appearance of the oil observed by responders conducting aerial overflights of the impacted area (NRC, 1985; Bonn Agreement, 2009, 2011; NOAA, 2016a; Table 2-1). As an example, barely visible sheens may be observed above 0.01 μm and silver sheens correspond with surface oil thickness of approximately 0.3 μm. Crude oils and heavy fuel oils greater than 1 mm thick typically appear as black oil while light fuels and diesels that are greater than 1 mm thick may appear brown or reddish. Because of the differences between oils and their degree of weathering, floating oil will not always have the same appearance. As oil weathers, it may be observed in the form of scattered floating tar balls and tar mats where currents converge. Typically, oil slicks in the environment would be observed as a range of visual appearances including silver sheen, rainbow sheen, and metallic areas simultaneously, as a combination of thicknesses may be present (Figure 2-1). Thus, a model result presented as average oil mass per unit area or "thickness" is actually a region with patches of oil of varying thickness, which when distributed evenly in the area of interest, would be on average a certain thickness.

Table 2-1. Oil appearances based on NOAA (2016a) and BAOAC (2011) and how these values are conservatively generalized for use in oil spill modeling.

Code	Description	Layer-Thickness			Concentration			Generalized Thickness Used in Modeling Results[*]	Nomenclature Used for Modeling Results**
		range	microns (μm)	inches (in)	range	m³/km²	bbl/acre	microns (μm)	oil description
S	Silver Sheen	min	0.04	1.6×10^{-6}	min	0.04	1×10^{-3}	<0.01	Colorless Silver Sheen
		max	0.30	1.2×10^{-5}	max	0.30	7.8×10^{-3}		
R	Rainbow Sheen	min	0.30	1.2×10^{-5}	min	0.3	7.8×10^{-3}	0.1-1	Rainbow Sheen
		max	5.0	2.0×10^{-4}	max	5.0	1.28×10^{-1}		
M	Metallic Sheen	min	5.0	2.0×10^{-4}	min	5.0	1.28×10^{-1}	1-10	Dull Brown Sheen
		max	50	2.0×10^{-3}	max	50	1.28		
T	Transitional Dark (or true) Color	min	50	2.0×10^{-3}	min	50	1.28	10-100	Dark Brown Sheen
		max	200	8×10^{-3}	max	200	5.1		
D	Dark (or true) Color		>200	$>8 \times 10^{-3}$		>200	>5.1	100-1,000	Black Oil
								>1,000	Heavy Black Oil
E	Emulsified	Thickness range is very similar to that of dark oil.						>1,000	Heavy Black Oil

Chart from Bonn Agreement Oil Appearance Code (BAOAC) 2011, modified by A. Allen

[*]Visual appearances and corresponding thicknesses of surface oil vary by oil type and environmental condition. Therefore, generalized thicknesses are used the portrayal of modeling results.

**Although results are displayed in this report as cumulative maxima over the entire modeled time frame, individual slicks and sheens at any specific point in time are predicted to be patchy, discontinuous, and short lived at any point, as the river transports oil downstream (see Figure 4-1). Modeled concentrations portrayed on the results figures in Section 4 are generalized into the above-listed thicknesses and nomenclature, but actually vary dynamically in time and space, as well as within individual slicks and sheens (see Figure 2-1).
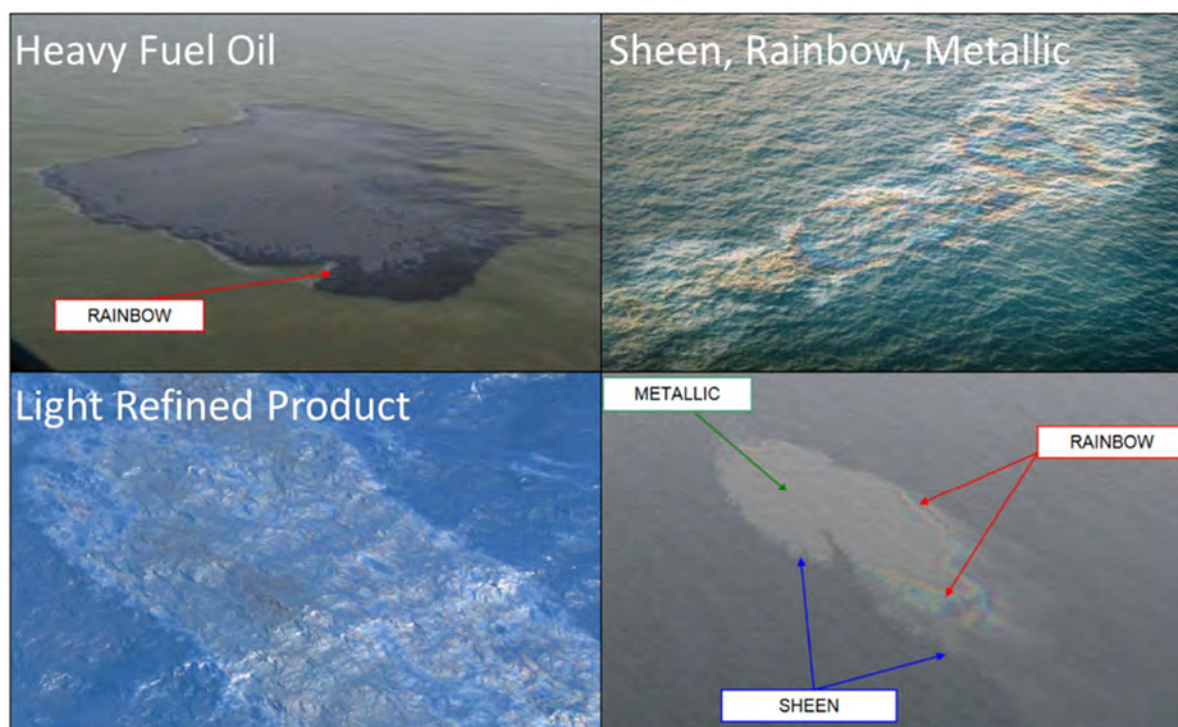
Figure 2-1. Aerial surveillance images of discharged oil in the environment as examples of different visual appearances based on surface oil thickness and product type (Bonn Agreement, 2011).

It is important to note that because of the high degree of variability in environmental conditions within the study region, a spill occurring at a different date or time than those modeled may result in slightly different trajectory, fate, and potential effects results than reported here. Therefore, the area of surface oiling, mass of oil along the shoreline, and mass of oil within the water column, may be different for each simulation. Overall, this modeling methodology provides a range of representative results for trajectory, fate, and biological effects for each modeled hypothetical release.

2.1.1   SIMAP Physical Fate Model Description

The three-dimensional physical fate model estimates distribution (as mass and concentrations) of whole oil and oil components on the water surface, on shorelines, in the water column, and in sediments. Oil fate processes included in SIMAP are oil spreading (gravitational and by shearing), evaporation, transport, randomized dispersion, emulsification, entrainment (natural and facilitated by dispersant), dissolution, volatilization of dissolved hydrocarbons from the surface water, adherence of oil droplets to suspended sediments, adsorption of soluble and sparingly-soluble aromatics to suspended sediments, sedimentation, and degradation.

Oil is a mixture of hydrocarbons of varying physical, chemical, and toxicological characteristics, which have the potential for varying fate and effects on organisms. In the model, oil is represented by component categories, and the fate of each component is tracked separately. The "pseudo-component" approach (Payne et al., 1984;

1987; French et al., 1996; Jones, 1997; Lehr et al., 2000) is used, where chemicals in the oil mixture are grouped by physical-chemical properties, and the resulting component category behaves as if it were a single chemical with characteristics typical of the chemical group.

The most toxic components of oil to aquatic organisms are low molecular weight aromatic compounds (MAHs and PAHs), which are both volatile and soluble in water. Their acute toxic effects are caused by non-polar narcosis, where toxicity is related to the octanol-water partition coefficient (K_{ow}), a measure of hydrophobicity. The more hydrophobic the compound, the more toxic it is likely to be. However, as K_{ow} increases, the compound also becomes less soluble in water, so there is less exposure to aquatic organisms. The toxicity of compounds with $\log(K_{ow})$ values greater than about 5.6 is limited by their very low solubility in water and consequent low bioavailability (French-McCay, 2002, Di Toro et al., 2000). Thus, the potential for acute effects is the result of a balance between bioavailability, toxicity once exposed, and duration of exposure. French-McCay (2002) contains a full description of the oil toxicity model in SIMAP and French-McCay (2003, 2009) describes the implementation of the toxicity model in SIMAP.

Because of these considerations, the SIMAP fate model focuses on tracking the lower molecular weight aromatic (AR) and aliphatic (AL) components divided into chemical groups based on volatility, solubility, and hydrophobicity. In the 19-pseudo-component model, the oil is treated as comprising eighteen components (defined in Table 2-2), with a nineteenth spot available to handle additional compounds (e.g., dispersant). Sixteen of the components (i.e., all but the non-volatile residual components representing non-volatile aromatics and aliphatics) evaporate at rates specific to the pseudo-component. Solubility is strongly correlated with volatility, and the solubility of aromatics is higher than aliphatics of the same volatility. The MAHs are the most soluble. The 2-ring PAHs are less soluble, and the 3-ring PAHs are slightly soluble (Mackay et al., 1992). Both the solubility and toxicity of the non-aromatic hydrocarbons are much lower than for the aromatics, and dissolution (and resulting in-water concentrations) of non-aromatics is safely ignored. Thus, dissolved concentrations are calculated only for each of the eight soluble aromatic pseudo-components. In this modeling approach, "aromatic" compounds (groups AR1-AR9) refer to chemicals that are both soluble and volatile, while "aliphatic" compounds (groups AR1-AR8) refer to chemicals that are insoluble and volatile. It is understood that this naming framework is slightly different than a true chemical definition, however, the actual physical and chemical parameters of each compound were used to define which compound was assigned to each group (i.e., low molecular weight aliphatic compounds, which are soluble, are included in AR groups within the model). Note that the nineteenth pseudo-component (reserved for compounds like dispersants) was not used in this application of the model.

Table 2-2. Definition of nine distillation cuts and the eighteen pseudo-components used in the SIMAP model.

AR or AL	All HCs	Soluble and semi-soluble HCs		Non-soluble aliphatic HCs	
Component #	Volatility	Compounds	Range of log(K_{OW})	Compounds	Boiling Point Range (°C)
1	Volatiles	MAHs (BTEX)	1.9-2.8	Volatile aliphatics	< 150
2		C3-benzenes	2.8-3.6	Volatile aliphatics	150-180
3	Intermediate Volatility	C4-benzenes	3.1-3.8	Semi-volatile aliphatics	180-200
4		Decalins	4.1-6.0	Semi-volatile aliphatics	200-230
5		C0-C2 Naphthalenes	2.3-4.3	Semi-volatile aliphatics	230-280
6	Semi-Volatile	C3-C4 Naphthalenes	4.2-5.20	Low volatility aliphatics	280 - 300
7		Fluorenes & C0-C2 3-ring PAHs	4.0-5.6	Low volatility aliphatics	300-350
8		4-ring PAHs & C2-C3 3-ring PAHs	4.9-6.0	Low volatility aliphatics	350-380
9	Highly Volatile and Soluble Aliphatics	Alkanes, Isoalkanes, Cycloalkanes	2.3-5.6	N.A. (Used for Dispersant Indicators)	<180
Residual	Residual (non-volatile) Component 19	High MW PAHs	>6.0	High molecular weight aliphatics	>380

Monoaromatic hydrocarbons, MAHs; benzene + toluene + ethybenzene + xylene, BTEX; polycyclic aromatic hydrocarbons, PAHs.

The lower molecular weight aromatics dissolve from the whole oil and are partitioned in the water column and sediments according to equilibrium partitioning theory (French et al., 1996; French-McCay, 2004). The residual fractions in the model are composed of non-volatile and insoluble compounds that remain in the "whole oil" that spreads, is transported on the water surface, strands on shorelines, and disperses into the water column as oil droplets or remains on the surface as tar balls. This is the fraction that composes black oil, mousse, and sheen.

2.1.2 Modeled SIMAP Oil Fates Processes

The schematic in Figure 2-2 depicts the oil fate processes simulated in the SIMAP model near shore and in riverine environments. Because oil contains many chemicals with varying physical-chemical properties and the environment is spatially and temporally variable, the oil rapidly separates into different compartments within the environment including:

- Surface oil,
- Emulsified oil (mousse) and tar balls,
- Oil droplets suspended in the water column,
- Oil adhering to suspended particulate matter in the water,
- Dissolved lower molecular weight components (MAHs, PAHs, and other soluble components) in the water column,
- Oil on and in the sediments,
- Dissolved lower molecular weight components (MAHs, PAHs, and other soluble components) in the sediment pore water, and
- Oil on and in the shoreline sediments and surfaces.
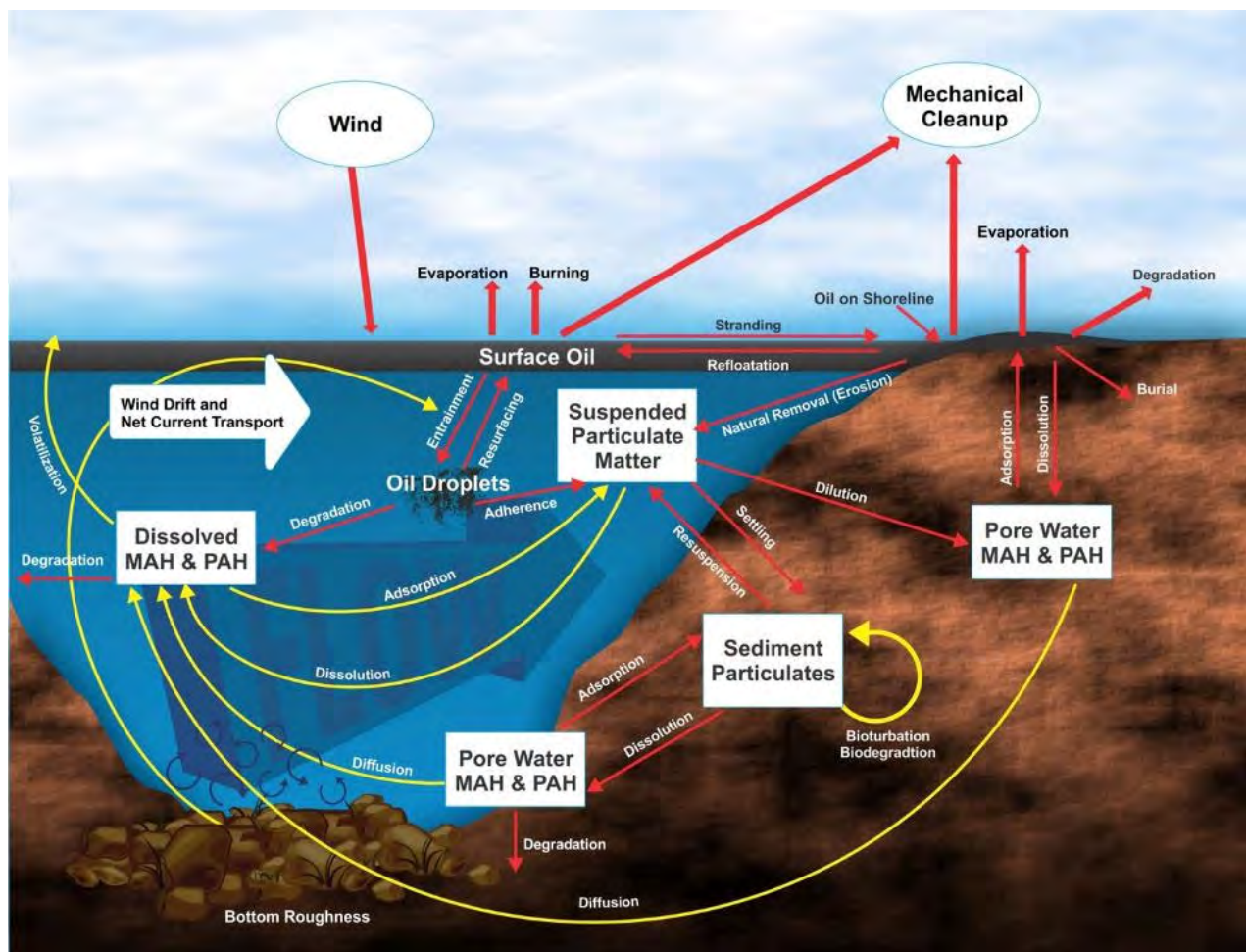
Figure 2-2. Simulated SIMAP oil fate processes in lakes and rivers.

The schematic in Figure 2-2 represents oil fate processes that are simulated in the SIMAP model:

- **Spreading** is the thinning and broadening of surface slicks caused by gravitational forces and surface tension. Spreading occurs rapidly after oil is spilled on the water surface. The rate of spreading is faster if oil viscosity is lower. Viscosity decreases as temperature increases. Viscosity increases as oil emulsifies,

- **Transport** is the process where oil is carried by currents,

- **Turbulent dispersion:** Typically, there are also "sub-scale" currents (not included in the current data), better known as turbulence, that move oil and mix it in three dimensions. The process by which turbulence mixes and spreads oil components on the water surface and in the water column is called turbulent dispersion,

- **Evaporation** is the process where volatile components of the oil diffuse from the oil and enter the gaseous phase (atmosphere). Evaporation from surface and shoreline oil increases as the oil surface area, temperature, and wind speed increase. As lighter components evaporate off, the remaining "weathered" oil becomes more viscous,

- **Emulsification** is the process where water is mixed into the oil, such that the oil makes a matrix with embedded water droplets. The resulting mixture is commonly called mousse. It is technically referred to as a water-in-oil emulsion. The rate of emulsification increases with increasing wind speed and turbulence on the surface of the water. Viscosity increases as oil emulsifies,

- **Entrainment** is the process where waves break over surface oil and carry it as droplets into the water column. At higher wind speeds, or where currents and bottom roughness induce turbulence, wave heights may reach a threshold where they break. In open waters, waves break beginning at wind speeds of about 12 knots (14 mph) and wave breaking increases as wind speed becomes higher. Thus, entrainment becomes increasingly important (higher rate of mass transfer to the water) the higher the wind speed. As turbulence from whatever source increases, the oil droplet sizes become smaller. Application of chemical dispersant (which was not modeled in this assessment) increases the entrainment rate of oil and decreases droplet size at a given level of turbulence. Entrainment rate is slower, and droplet size is larger, as oil viscosity increases (by emulsification and evaporation loss of lighter volatile components). The droplet size determines how fast and whether the oil resurfaces,

- **Resurfacing** of entrained oil rapidly occurs for larger oil droplets. Smaller droplets resurface when the wave turbulence decreases. The smallest droplets do not resurface, as typical turbulence levels in the water keep them in suspension indefinitely. Local winds at the water surface can also prevent oil from surfacing. Resurfaced oil typically forms sheens. In open water where currents are relatively slow, surface slicks are usually blown down wind faster than the underlying water, and resurfacing droplets come up behind the leading edge of the oil, effectively spreading the slicks in the down-wind direction,

- **Dissolution** is the process where water-soluble components diffuse out of the oil into the water. Dissolution rate increases the higher the surface area of the oil relative to its volume. As the surface area to volume ratio is higher for smaller spherical droplets, the smaller the droplets the higher the dissolution rate. The higher the wave turbulence, the smaller the droplets of entrained oil. Dissolution from entrained small droplets is much faster than from surface slicks in the shape of

flat plates. The soluble components are also volatile, and evaporation from surface slicks is faster than dissolution into the underlying water. Thus, the processes of evaporation and dissolution are competitive, with evaporation being the dominant process for surface oil,

- **Volatilization** of dissolved components from the water to the atmosphere occurs as the components are mixed, diffused to the water surface boundary, and then enter the gas phase. Volatilization rate increases with increasing air and water temperature,

- **Adsorption** of dissolved components to particulate matter in the water occurs because the soluble components (MAHs and PAHs) preferentially adsorb to particulates when the latter are present. The higher the concentration of suspended particulates, the more adsorption occurs. Also, the higher the molecular weight of the compound, the less soluble it is, and the more it tends to adsorb to particulate matter,

- **Adherence** is the process where oil droplets combine with particles in the water. If the particles are suspended sediments, the combined oil/suspended sediment agglomerate is heavier than the oil itself. If turbulence subsides sufficiently, the oil-sediment agglomerates will settle,

- **Sedimentation** (or settling) is the process where oil-sediment agglomerates, and particles with adsorbed sparingly-soluble components (MAHs and PAHs) settle to the bottom sediments. Adherence and sedimentation can be an important pathway of oil in near shore areas when waves are strong and subsequently subside. Generally, oil-sediment agglomerates transfer more PAH to the bottom than sediments with PAHs that were adsorbed from the dissolved phase in the water column,

- **Resuspension** of settled oil-sediment particles and particles with adsorbed sparingly-soluble components (MAHs and PAHs) may occur if current speeds and turbulence exceed threshold values where cohesive forces can be overcome,

- **Diffusion** is the process where dissolved compounds move from higher to lower concentration areas by random motion of molecules and micro-scale turbulence. Dissolved components in bottom and shoreline sediments can diffuse out to the water where concentrations are relatively low. Bioturbation, groundwater discharge, and hyporheic flow of water through stream-bed sediments can greatly increase the rate of diffusion from sediments (see below),

- **Dilution** occurs when water of lower concentration is mixed into water with higher concentration by turbulence, currents, or shoreline groundwater,

- **Bioturbation** is the process where animals in the sediments mix the surface sediment layer while burrowing, feeding, or passing water over their gills. In open-water, soft-bottom environments, bioturbation effectively mixes the surface sediment layer about 10 cm (3.9 in) thick (in non-polluted areas),

- **Degradation** is the process where oil components are changed either chemically or biologically (biodegradation) to another compound. It includes breakdown to simpler organic carbon compounds by bacteria and other organisms, photo-oxidation by solar energy, and other chemical reactions. Higher temperature and higher light intensity (particularly ultraviolet wavelengths) increase the rate of degradation, and

- **Stranding and Refloatation** may occur when floating oil meets the shorelines and then refloats as water levels rise, allowing the oil to move further down current (downstream).

2.1.3   Summary of Spill Dynamics

For a spill on the water surface, gravitational spreading occurs very rapidly (within hours) to a minimum thickness. Thus, the area exposed to evaporation is high, relative to the oil volume. Evaporation proceeds faster than dissolution resulting in most of the volatiles and semi-volatiles evaporating with a smaller fraction dissolving into the water column. Degradation (photo-oxidation and biodegradation) also occurs at a relatively slow rate compared to these processes.

Evaporation is more rapid as wind speed increases. However, above approximately 12 knots (approximately 14 mph) of wind in open water, white caps begin to form, and the breaking waves entrain oil as droplets into the water column. Higher wind speeds (and turbulence) increase entrainment resulting in smaller droplet sizes. From Stokes' Law, larger droplets resurface faster and form surface slicks. Thus, a dynamic balance evolves between entrainment and resurfacing. As high-wind events occur, the entrainment rate increases. When the winds subside to less than 12 knots, the larger oil droplets resurface and remain floating, while smaller droplets may remain entrained in the water column. Similar dynamics occur in turbulent streams.

The smallest oil droplets remain entrained in the water column longer than larger oil droplets. Larger oil droplets rise to the surface at varying rates. While the droplets are under water, dissolution of the light and soluble components occurs. Because the dissolution rate is a function of the surface area available, most dissolution occurs from droplets, as opposed to from surface slicks, since droplets have a higher surface area to volume ratio, and they are not in contact with the atmosphere. In addition, the soluble components do not preferentially evaporate as they do from surface oil).

If oil is discharged or driven underwater, it forms droplets of varying sizes. The more turbulent the conditions, the smaller the droplet sizes. From Stokes' Law, larger droplets rise faster and surface if the water is shallow. Resurfaced oil behaves as surface oil after gravitational spreading has occurred. The surface oil may be re-entrained. The smallest droplets in most cases remain in the water permanently. As a result of the higher surface area per volume of small droplets, the dissolution rate is much higher from subsurface oil than from floating oil on the water surface.

Because of these interactions, the majority of dissolved constituents (which are of concern because of potential effects on aquatic organisms) are from droplets entrained in the water. For a given spill volume and oil type/composition, with increasing turbulence either at the water surface and/or at the stream bed, the following impacts occur on the oil fate. There is an increasing amount of oil entrained, and the oil is increasingly broken up into smaller droplets. In addition, there is more likelihood of the oil remaining entrained rather than resurfacing, and the dissolved concentrations will be higher. Entrainment and dissolved concentrations increase with: (1) higher wind speed, (2) increased turbulence from other sources of turbulence (rapids, waterfalls in rivers, etc.), (3) subsurface releases (especially under higher pressure and turbulence), and (4) application of chemical dispersants. Chemical dispersants both increase the amount of oil entrained and decrease the oil droplet size. Thus, chemical dispersants increase the dissolution rate of soluble components. Note that chemical dispersants are unlikely to be used in a stream when effects on aquatic biota are a primary concern.

These processes that increase the rate of supply of dissolved constituents are balanced by loss terms in the model: (1) transport (dilution), (2) volatilization from the dissolved phase to the atmosphere, (3) adsorption to

solid particles within the water column, referred to as suspended particulate material (SPM) or total suspended solids (TSS), and sedimentation through the formation of Oil Mineral Aggregates (OMA) or Oil Particle Aggregates (OPA) that are more dense than the surrounding water and sink, and (4) degradation (photo-oxidation or biologically mediated). There are other processes that slow the entrainment rate: (1) emulsification increases viscosity and slows or eliminates entrainment, (2) adsorption of oil droplets to SPM and settling removes oil from the water, (3) stranding on shorelines removes oil from the water, and (4) mechanical cleanup and burning removes mass from the water surface and shorelines. Thus, the model-predicted concentrations are the resulting balance of all these processes and the best estimates based on our quantitative understanding of the individual processes.

2.1.4 SIMAP Model Oil Fates Algorithms

The algorithms used to model oil fate processes are described in French-McCay (2004). Lagrangian elements (spillets) are used to simulate the movements of oil components in three dimensions over time. Surface floating oil, subsurface droplets, and dissolved components are tracked in separate spillets. Transport is the sum of advective velocities by currents input to the model, surface wind drift, vertical movement according to buoyancy, and randomized turbulent diffusive velocities in three dimensions. The vertical diffusion coefficient is computed as a function of wind speed in the surface wave-mixed layer. The horizontal and deeper water vertical diffusion coefficients are model inputs.

The oil (whole and as pseudo-components) separates into different phases or parts of the environment, i.e., surface slicks; emulsified oil (mousse) and tar balls; oil droplets suspended in the water column; dissolved lower molecular weight components (MAHs and PAHs) in the water column; oil droplets adhered and hydrocarbons adsorbed to suspended particulate matter in the water; hydrocarbons on and in the sediments; dissolved MAHs and PAHs in the sediment pore water; and hydrocarbons on and in the shoreline sediments and surfaces.

The algorithms used to calculate these fate processes are briefly described in the subsections below.

2.1.4.1 Transport

Lagrangian particles (spillets) are moved in three dimensions over time. For each model time step, the new vector position of the spillet center is calculated from the old location plus the vector sum of east-west, north-south, and vertical components of advective and diffusive velocities:

$$X_t = X_{t-1} + \Delta t \, (U_t + D_t + R_t + W_t) \qquad\qquad (1)$$

where X_t is the vector position at time t, X_{t-1} is the vector position the previous time step, Δt is the time step, U_t is the sum of all the advective (current) velocity components in three dimensions at time t, D_t is the sum of the randomized diffusive velocities in three dimensions at time t, R_t is the rising or sinking velocity of whole oil droplets in the water column, and W_t is the surface wind transport ("wind drift"). The magnitudes of the components of D_t are scaled by horizontal and vertical diffusion coefficients (Okubo and Ozmidov, 1970; Okubo, 1971). The vertical diffusion coefficient is computed as a function of wind speed in the surface wave-mixed layer (which ranges from centimeter scales in rivers and near lee shorelines to potentially meters in large water bodies away from shore when wind speeds are high) based on Thorpe (1984). The velocity R_t is computed by Stokes' Law, where velocity is related to the difference in density between the particle and the

water, and to the particle diameter. The algorithm developed by Youssef and Spaulding (1993) is used for wind transport in the surface wave-mixed layer (Wt, described above).

2.1.4.2 Shoreline Stranding

The fate of spilled oil that reaches the shoreline depends on characteristics of the oil, the type of shoreline, and the energy environment. The stranding algorithm is based on work by CSE/ASA/BAT (1986), Gundlach (1987) and Reed and Gundlach (1989) in developing the COZOIL model for the U.S. Minerals Management Service. In SIMAP, deposition occurs when an oil spillet intersects the shore surface. Deposition ceases when the volume holding capacity for the shore surface is reached. Subsequent oil coming ashore is not allowed to remain on the shore surface. It is refloated by rising water and carried away by currents and wind drift. The remaining shoreline oil is then removed exponentially with time. Data for holding capacity and removal rate are taken from CSE/ABA/BAT (1986) and Gundlach (1987) and are a function of oil viscosity and shore type. The algorithm and data are in French et al. (1996).

2.1.4.3 Spreading

Spreading determines the areal extent of the surface oil, which in turn influences its rates of evaporation, dissolution, dispersion (entrainment), and photo-oxidation, all of which are functions of surface area. Spreading results from the balance among the forces of gravity, inertia, viscosity, and surface tension (which increases the diameter of each spillet); turbulent diffusion (which spreads the spillets apart); and entrainment followed by resurfacing (which can spatially separate the leading edge of the oil from resurfaced oil transported in a different direction by subsurface currents).

For many years, Fay's (1971) three-regime spreading theory was widely used in oil spill models (ASCE, 1996). Mackay et al. (1980; 1982) modified Fay's approach and described the oil as thin and thick slicks. Their approach used an empirical formulation based on Fay's (1971) terminal spreading behavior. They assumed the thick slick feeds the thin slick and that 80-90% of the total slick area is represented by the thin slick. In SIMAP, oil spillets on the water surface increase in diameter according to the spreading algorithm empirically derived by Mackay et al. (1980; 1982). Sensitivity analyses of this algorithm led to the discovery that the solution was affected by the number of spillets used. Thus, a formulation was derived to normalize the solution under differing numbers of surface spillets (Kolluru et al., 1994). Spreading is stopped when an oil-specific terminal thickness is reached.

2.1.4.4 Evaporation

The rate of evaporation depends on surface area, thickness, vapor pressure, and mass transport coefficient, which in turn are functions of the composition of the oil, wind speed, and temperature (Fingas, 1996; 1997; 1998; 1999; Jones, 1997). As oil evaporates, its composition changes, affecting its density and viscosity as well as subsequent evaporation. The most volatile hydrocarbons evaporate most rapidly, typically in less than a day and sometimes in under an hour (McAuliffe, 1989). As the oil continues to weather, and particularly if it forms a water-in-oil emulsion, evaporation will be significantly decreased.

The evaporation algorithm in SIMAP is based on accepted evaporation theory, which follows Raoult's Law that each component will evaporate with a rate proportional to the saturation vapor pressure and mole fraction present for that component. The pseudo-component approach (Payne et al., 1984; French et al., 1996; Jones, 1997; Lehr et al., 2000) is used, such that each component evaporates according to its mean vapor pressure,

solubility, and molecular weight. The mass transfer coefficient is calculated using the methodology of Mackay and Matsugu (1973), as described in French et al. (1996).

2.1.4.5 Entrainment

As oil on the water surface is exposed to wind and waves, or if oil moves into a turbulent area of a stream or river, it is entrained (or dispersed) into the water column. Entrainment is a physical process where globules of oil are transported from the water surface into the water column due to breaking waves or other turbulence. Observations show that entrained oil is broken into droplets of varying sizes. Smaller droplets spread and diffuse in the water column, while larger ones rise back to the surface.

Entrainment by Breaking Surface Wave Action

In open waters, breaking waves created by the action of wind and waves on the water surface are the primary sources of energy for entrainment. Entrainment is strongly dependent on turbulence and is greater in areas of high wave energy (Delvigne and Sweeney, 1988).

Delvigne and Sweeney (1988), using laboratory and flume experimental observations, developed a relationship for entrainment rate and oil droplet size distribution as a function of turbulent energy level and oil viscosity. Entrained droplets in the water column rise according to Stokes' Law, where velocity is related to the difference in density between the particle and the water, and to the particle diameter. The data and relationships in Delvigne and Sweeney (1988) are used in SIMAP to calculate mass and particle size distribution of droplets entrained. Particle size decreases with higher turbulent energy level and lower oil viscosity. The natural dispersion particle sizes observed by Delvigne and Sweeney (1988) are confirmed by field observations by Lunel (1993a; 1993b).

Use of chemical dispersants (not modeled in the scenarios examined here, nor likely to occur in freshwater) decreases the median particle size, increasing the number of droplets in the <70 μm range (Daling et al., 1990; Lunel, 1993a; 1993b). Particle size distributions for dispersed oil are available for several oils from these studies. When dispersant is applied, the model entrains surface oil, creating subsurface droplets in the appropriate size distribution for dispersant use. The median particle size for permanently dispersed droplets is set at 20 microns, the median size observed by Lunel (1993a; 1993b). The fraction of oil permanently dispersed is set by the assumed dispersant efficiency. The IKU/SINTEF studies provide data on the viscosity range where oils may be dispersed chemically. Typically, dispersants are effective up to about 10,000 cP (centipoise) (Aamo et al., 1993; Daling and Brandvik, 1988; 1991; Daling et al., 1997). In the model, oil is dispersed up to 10,000 cP.

Entrained oil is mixed uniformly throughout the wave-mixed zone. Vertical mixing is simulated by random placement of particles within the wave-mixed layer at each time step. Settling of particles does not occur in water depths where waves reach the bottom (taken as 1.5 times wave height). Wave height is calculated from wind speed, duration, and fetch (distance upwind to land), using the algorithms in CERC (1984). Wave height is on the scale of centimeters in small rivers and streams and near lee shorelines. In open water under windy conditions, it may increase to meters.

Entrainment by Bottom Roughness in Streams

When modeling oil releases in rivers, entrainment of oil into the water column by turbulent flow over bottom structures and around obstacles must be taken into consideration. It is clear that in rapid flow where turbulence

is large, rocks or other obstacles may break the surface and a plunging wake may occur where the possibility of entrainment increases. Delvigne (1993) demonstrated that breaking wave dispersion to fast flow past an obstacle, such as a pile, generates a plunging wake. This is sufficiently similar to breaking waves from alternative sources of turbulence such as the fast flow past an obstacle, flow over a dam, cataract with a hydraulic jump, or a ship crossing an oil slick. In the breaking wave model, the dispersion of energy leads to the plunging of oil into water and the formation of oil droplets. To relate this more generally to a river formulation, an energy dissipation relationship was developed. In this formulation, energy dissipation is proportional to the stream flow rate and bottom roughness and is inversely proportional to the local depth. The generation and propagation of turbulent energy through the water column due to bottom roughness is applied with a typical quadratic stress equation to the plunging flow (Anderson et al., 1995). The dispersed mass of oil is determined by scaling the surface area covered by oil at the dispersion source and the range of oil droplet sizes, which is a function of the dispersion energy.

2.1.4.6 Emulsification (Mousse Formation)

The formation of water-in-oil emulsions, or mousse, depends on oil composition and turbulence level. Emulsified oil can contain as much as 80% water in the form of micron-sized droplets dispersed within a continuous phase of oil (Daling and Brandvik, 1988; Fingas et al., 1997). Viscosities are typically much higher than that of the parent oil. The incorporation of water also dramatically increases the oil/water mixture volume.

The Mackay and Zagorski (1982) emulsification scheme is implemented in SIMAP for floating oil. Water content increases exponentially, with the rate related to the square of wind speed and previous water incorporation. Viscosity is a function of water content. The change in viscosity feeds back in the model to the entrainment rate.

2.1.4.7 Dissolution

Dissolution is the process by which soluble hydrocarbons enter the water from a surface slick or from entrained oil droplets. The lower molecular weight hydrocarbons tend to be both more volatile and more soluble than those of higher molecular weight. For surface slicks, since the partial pressures tend to exceed the solubilities of these lower molecular weight compounds, evaporation accounts for a larger portion of the mass than dissolution (McAuliffe, 1989), except perhaps under ice. Dissolution and evaporation are competitive processes. The dissolved component concentration of hydrocarbons in water under a surface slick shows an initial increase followed by a rapid decrease after some hours due to the evaporative loss of components. Most soluble components are also volatile, and direct evaporation (volatilization) from the water column depletes their concentrations in the water. Dissolution is particularly important where evaporation is low (dispersed oil droplets and ice-covered surfaces). Dissolution can be significant from entrained droplets because of the lack of atmospheric exposure and because of the higher surface area per unit of volume.

The model developed by Mackay and Leinonen (1977) is used in SIMAP for dissolution from a surface slick. The slick (spillet) is treated as a flat plate, with a mass flux (Hines and Maddox, 1985) related to solubility and temperature. It assumes a well-mixed layer with most of the resistance to mass transfer lying in a hypothetical stagnant region close to the oil. For subsurface oil, dissolution is treated as a mass flux across the surface area of a droplet (treated as a sphere) in a calculation analogous to the Mackay and Leinonen (1977) algorithm. The dissolution algorithm was developed in French et al. (1996).

2.1.4.8 Volatilization from the Water Column

The procedure outlined by Lyman et al. (1982), based on Henry's Law and mass flux (Hines and Maddox, 1985), is followed in the SIMAP fate model. The volatilization depth for dissolved substances is limited to the maximum of one half the wave height. Wave height is computed from the wind speed and fetch (CERC, 1984). The volatilization algorithm was developed in French et al. (1996).

2.1.4.9 Adsorption and Sedimentation

Hydrocarbons dissolved in the water column are carried to the sediments primarily by adsorption to suspended particulates and subsequent settling. The ratio of adsorbed (C_a) to dissolved (C_{dis}) concentrations (whereby concentrations are reported as mg per mg of sediment and mg per mg of water) is computed from standard equilibrium partitioning theory as

$$C_a / C_{dis} = K_{oc} \, C_{ss} \qquad\qquad (2)$$

K_{oc} is a partitioning coefficient (L/mg), and C_{ss} is the concentration of SPM in the water column expressed as mass of particulate per volume of water (mg/L). As a default, the model uses a mean value of TSS of 10 mg/L (Kullenberg, 1982). Alternatively, suspended sediment concentration is specified as model input.

Sedimentation of oil droplets occurs when the specific gravity of oil increases over that of the surrounding water. Several processes may act on entrained oil and surface slicks to increase density: weathering (evaporation, dissolution, and emulsification), adhesion or sorption onto suspended particles or detrital material, and incorporation of sediment into oil during interaction with suspended particulates, bottom sediments, and shorelines. Rates of sedimentation depend on the concentration of suspended particulates and the rates of particulate flux into and out of an area. In areas with high suspended particulate concentrations, rapid dispersal and removal of oil is found due to sorption and adhesion (Payne and McNabb, 1984).

Kirstein et al. (1985) and Payne et al. (1987) used a reaction term to characterize the water column interactions of oil and suspended particulates. The reaction term represents the collision of oil droplets and suspended matter, accounting for both oiled and unoiled particulates. The model formulation developed by Kirstein et al. (1985) is used to calculate the volume of oil adhered to particles. In the case where the oil mass is larger than the adhered sediment (i.e., the sediment has been incorporated into the oil), the buoyancy of the oil droplet will control its settling or rise rate. The Stokes' Law formulation is used to adjust vertical position of these particles. If the mass of adhered droplets is small relative to the mass of the sediment it has adhered to, the sediment settling velocity will control the fate of the combined particulate.

2.1.4.10 Degradation

Degradation may occur as the result of photolysis or photo-oxidation, which is a chemical process energized by ultraviolet light from the sun, and by microbial breakdown, termed biodegradation. In the model, degradation occurs on the surface slick, deposited oil on the shore, the entrained oil and dissolved hydrocarbons in the water column, and oil in the sediments. A first order decay algorithm is used, with a specified (total) degradation rate for each oil type: surface oil, water column oil, and sedimented oil (French et al., 1999).

2.1.5 SIMAP Model Physical Fates Output Description

The physical fate model creates output files recording the distribution of a spilled substance in three-dimensional space and time. The quantities recorded are:

- Cumulative area covered by oil and thickness on the water surface ("swept area"),

- Volumes in the water column at various concentrations of dissolved hydrocarbons,

- Volumes in the water column at various concentrations of total hydrocarbons in suspended droplets,

- Total and dissolved hydrocarbon mass in surface sediment, and

- Lengths and location of shoreline affected by oil, and volume of oil ashore in each shoreline segment.

The dissolved hydrocarbon concentration in the water column is calculated from the mass in the Lagrangian elements, as follows. Concentration is contoured on a three-dimensional Lagrangian grid system. This grid is scaled each time step to cover the volume occupied by aromatic particles, including the dispersion around each particle center. This maximizes the resolution of the contour map at each time step and reduces error caused by averaging mass over large cell volumes. Distribution of mass around the particle center is described as Gaussian in three dimensions, with one standard deviation equal to twice the diffusive distance ($2D_x t$ in the horizontal, $2D_z t$ in the vertical; where D_x and D_z are the horizontal and vertical diffusion coefficients, respectively, and t is the particle age). The plume grid edges are set at one standard deviation away from the outer-most particle. These data are used by the biological effects model to evaluate exposure, toxicity and acute effects.

2.1.6   SIMAP Biological Effects Model

The SIMAP biological exposure model estimates the volume and area of water (and stream length, as appropriate) affected by surface oil, concentrations of oil components in the water, and sediment contamination. Then, the SIMAP biological effects model estimates losses resulting from acute exposure after a spill (i.e., losses at the time of the spill and while acutely toxic concentrations remain in the environment) in terms of direct mortality.

The area potentially affected by the spill is represented by a rectangular grid with each grid cell coded by habitat type. Habitat types are defined by depth, proximity to shoreline(s), bottom/shore type, and dominant vegetation type. The habitat grid is also used by the physical fate model to define the shoreline location and type, as well as habitat and sediment type. A habitat is an area of essentially uniform physical and biological characteristics that is occupied by a group of organisms that are distributed throughout that area. A contiguous grouping of habitat grid cells represents an ecosystem in the biological model. The density of fish, invertebrates, wildlife, and rates of lower trophic level productivity are assumed constant for the duration of the spill simulation and evenly distributed across an ecosystem. While biological distributions are known to be highly variable in time and space, data are generally not sufficient to characterize this patchiness. Since oil is also patchy in distribution, the patchiness is assumed to be on the same scale, so the intersection of the oil and biota is equivalent to overlays of spatial mean distributions.

2.1.6.1 Aquatic Biota

In the SIMAP model, aquatic biota (e.g., fish, invertebrates) are affected by dissolved hydrocarbon concentrations in the water or sediment. This rationale is supported by the fact that soluble aromatics are the most toxic constituents of oil (Neff et al., 1976; Rice et al., 1977; Tatem et al., 1978; Neff and Anderson, 1981; Malins and Hodgins, 1981; National Research Council (NRC), 1985; 2003; Anderson, 1985; French-McCay,

2002). Exposures in the water column are short, and effects are the result of acute toxicity. In the sediments, exposure can be both acute and chronic, as the concentrations may remain elevated for longer periods of time.

The model evaluates mortality and sublethal effects of dissolved hydrocarbon concentrations in the water or sediment. Mortality is a function of duration of exposure – the longer the duration of exposure, the lower the effects concentration (see review in French-McCay, 2002). At a given concentration after a certain period of time, all individuals that will die, will have done so. The LC_{50} is the lethal concentration at which 50% of exposed organisms will die, for a specified duration of exposure. The cumulative percent mortality is a log-normal function of concentration, with the LC_{50} located at the mid-point of the distribution (Figure 2-3). The incipient LC_{50} ($LC_{50\infty}$) is the asymptotic LC_{50} reached after infinite exposure time (or long enough that that level is approached). While toxicity studies may deal with $LC_{50\infty}$ (with known dosing and long-term exposure), the duration of exposure is rarely infinite. Therefore, the concentration and duration of exposure are calculated within the SIMAP model to calculate the fractional mortality that would be predicted with shorter durations of exposure.

French-McCay (2002) provides estimates of $LC_{50\infty}$ for MAH and PAH mixtures in fuel and crude oils for spills under different environmental conditions. Figure 2-3 plots LC_{50} values for total dissolved PAHs for species of average sensitivity under turbulent conditions ($LC_{50\infty}$ = 50 µg/L) for a range of exposure durations and temperatures. The $LC_{50\infty}$ for 95% of species fall in the range 5 – 400 µg/L. This oil toxicity model has been validated using laboratory oil bioassay data (French-McCay, 2002).

In SIMAP, $LC_{50\infty}$ for the dissolved hydrocarbon mixture of the spilled oil is input to the model. For each aquatic biota behavior group, the model evaluates exposure duration and corrects the LC_{50} for time of exposure and temperature to calculate mortality (Figure 2-3). The oil toxicity model is described in the next section, and in detail in French-McCay (2002). However, it is important to note that an $LC_{50\infty}$ = 50 µg/L does *not* correlate to 50% mortality at a concentration of 50 µg/L if the exposure is for less than several days. The SIMAP model accounts for the duration of exposure and scales the predicted mortality to lower values for shorter durations of exposure.
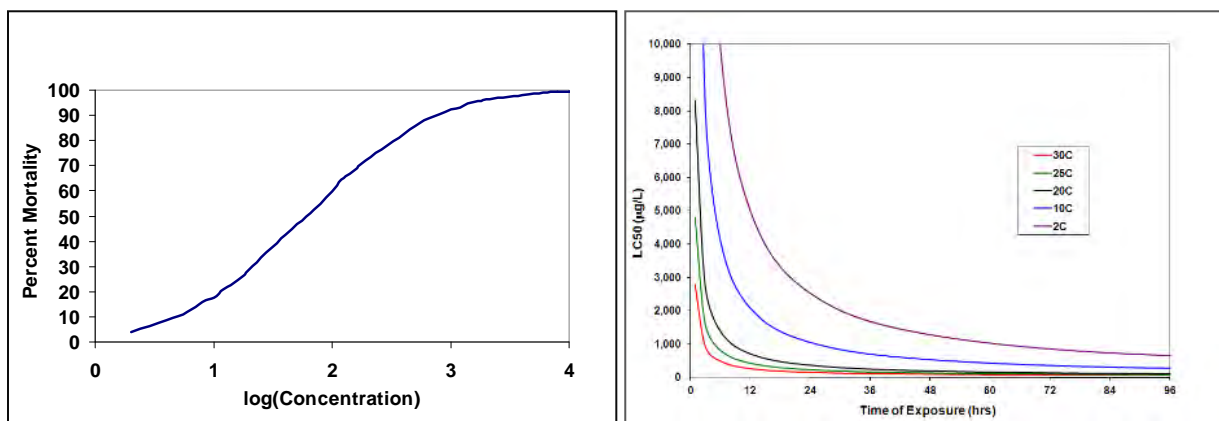
Figure 2-3. Illustration of percent mortality as a function of concentration (left). The LC_{50} is at the center of the log-normal function, aligning with 50% mortality. The LC_{50} of dissolved oil PAH mixtures as a function of exposure duration and temperature (right).

Mortality is calculated as percent loss in specified areas. This is translated into the Equivalent Area of 100% loss (i.e.,EA-100; Figure 2-4). This EA-100 loss is useful when results are compared to one another. As an example, if one scenario resulted in predictions of 20% mortality over 10 km^2, and another resulted in 50% mortality over 4 km^2, then the two would have the same EA-100, which would be 2 km^2. The model performs this fractional loss calculation within each grid cell over the entire model domain. Mortality results from each grid cell are then summed to determine a total area of effects and then the equivalent area (much smaller) that would experience complete mortality. To go one step further, the EA-100 loss can be divided by the total area of habitat available in the region of interest to estimate a percentage of the population in the area affected. The percent mortality of the exposure group is multiplied by abundance at the time exposed and in the habitat type to calculate the species' mortality as numbers of individuals or biomass (kg). Note that the EA-100 is used for comparative purposes between scenarios that may have different concentrations, timing, and contamination over different areas. The EA-100 is not the only area that would have any amount of mortality.
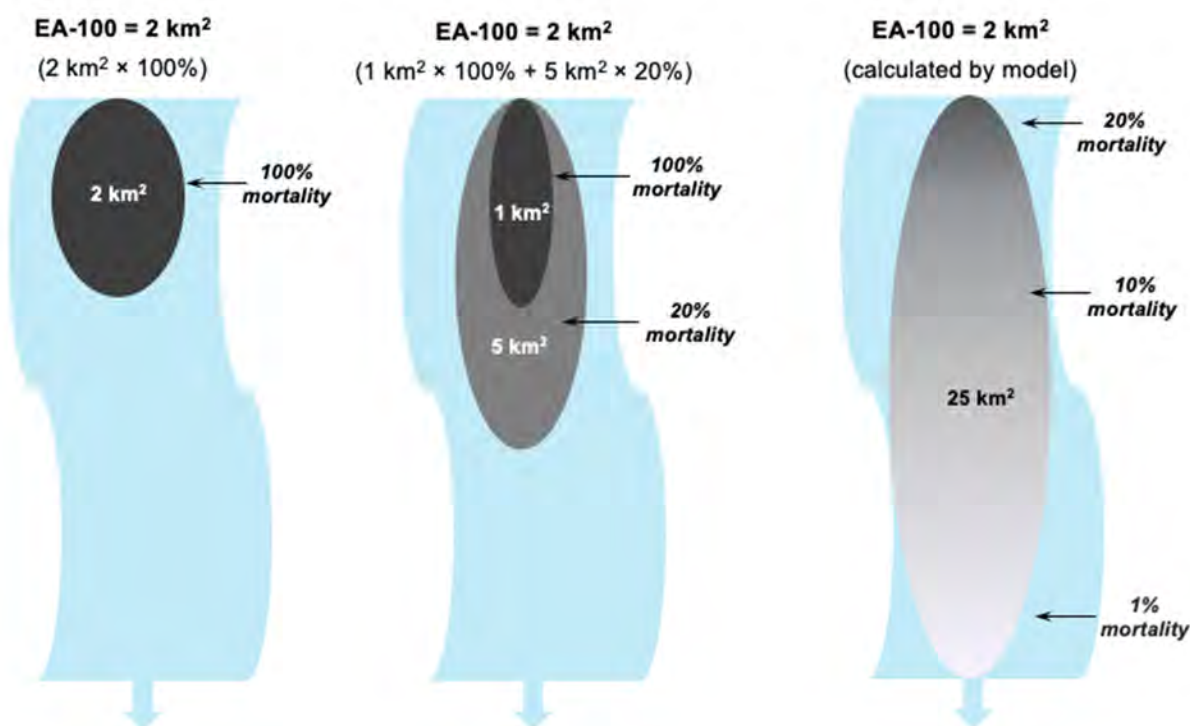
Figure 2-4. Examples of EA-100 calculations (simplified, unrealistic schematics provided for example purposes). The left highlights the unrealistic and extremely unlikely scenario where the presence of any amount of oil would result in 100% mortality of all organisms within the area of contamination. The center highlights greater areas of exposure to oil and the simplification of two fixed fractions killed (either 20% or 100). The right highlights a more realistic (though still highly simplified) scenario with fractional mortality over a much greater area. This later example is closest to what is carried out within the SIMAP model over each grid cell within the entire model domain. In each of these examples, the EA-100 would be the same value of 2 km^2.

2.1.6.2 Oil Toxicity

The following describes the oil toxicity model, OilToxEx, used in the SIMAP exposure model. The full development of OilToxEx and data upon which it is based are in French-McCay (2001; 2002). This model uses the accepted toxic units approach for organic compounds, including MAHs and PAHs, where the primary acute effect is narcosis (Bradbury et al., 1989). The approach was used by the U.S. Environmental Protection Agency (EPA) for development of PAH water and sediment quality criteria (Di Toro et al., 2000; Di Toro and McGrath, 2000; U.S. EPA, 2003; 2008). The oil toxicity model was validated using laboratory oil bioassay data for both fresh and salt-water organisms (French-McCay, 2002) and for lobster mortality in the case of the *North Cape* spill (French-McCay, 2003). The underlying toxicity data used to develop the model is based on bioassays for freshwater and marine fish, invertebrate, and algal species at a variety of life stages. Below is a summary of the oil toxicity analysis in French-McCay (2001; 2002).

The most toxic components of oil to pelagic (fish, plankton, amphibians) and benthic (invertebrates, algae) organisms are lower-molecular-weight compounds, which are both volatile and soluble in water, especially the aromatic compounds (Anderson et al., 1987; French et al., 1996; French-McCay, 2001; 2002; 2003). It has been shown that toxicity of narcotic organic compounds, such as these lower-molecular weight aromatics in oil (MAHs and PAHs), is related to the octanol-water partition coefficient (K_{ow}), a measure of hydrophobicity (Nirmalakhandan and Speece, 1988; Hodson et al., 1988; Blum and Speece, 1990; McCarty, 1986; McCarty et al., 1992a; 1992b; McCarty and Mackay, 1993; Varhaar et al., 1992; Swartz et al., 1995; French et al., 1996; French-McCay, 2001; 2002; 2003). Chemicals with a narcotic mode of action-affect organisms by accumulating in lipids (such as in the cell membranes) and disrupting cellular and tissue function. At the same time, however, the more hydrophobic a compound is, the more it accumulates in the tissues, and the more severe its effect. However, the more hydrophobic the compound, the less soluble it is in water, and the less available it is to aquatic organisms. Compounds of $\log(K_{ow}) > 5.6$ are virtually insoluble, and therefore are not bioavailable and make no meaningful contribution to the acute toxicity of hydrocarbon mixtures to aquatic biota (French-McCay, 2001; 2002). Biological effects are the result of a balance between bioavailability (dissolved-component exposure) and toxicity once exposed.

The acute toxic effects of narcotic chemicals, including lower molecular weight aromatics, are additive (Swartz et al., 1995; French et al., 1996; Di Toro et al., 2000; Di Toro and McGrath, 2000; French-McCay, 2001; 2002; 2003). The Toxic Unit (TU) model is used to estimate the toxicity of a mixture of narcotic chemicals. A TU is defined as the exposure concentration divided by the LC_{50} (lethal concentration to 50% of exposed organisms). For a mixture, the toxic units are additive. When $\Sigma TU = 1$, the mixture is lethal to 50% of exposed organisms.

It has been shown (French et al., 1996; French-McCay, 2001; 2002) that the LC_{50} of the mixture (LC_{50mix}) is related to the LC_{50} of each chemical i in the mixture and the dissolved concentration of chemical i in the total mixture:

$$F_i = C_{w,i} / (\Sigma\ C_{w,i}) \qquad\qquad\qquad (\ 3\ )$$

$$LC50_{mix} = 1 / \Sigma\ (\ F_i / LC50_i\ ) \qquad\qquad (\ 4\ )$$

where $C_{w,i}$ is the dissolved concentration of chemical i in the water. The values of F_i may be measured in the field or F_i may be estimated from data on oil composition. It has been shown that for turbulent surface waters where entrainment of oil has occurred, the values of F_i are nearly proportional to the source oil aromatic composition. The values of LC_{50i} can be estimated using regression models relating LC_{50} to K_{ow} (French-

McCay, 2001; 2002). The 95% confidence range of this regression provides LC_{50} values for average (50th percentile), sensitive (2.5th percentile), and insensitive (97.5th percentile) species. This oil toxicity model is used to estimate the LC_{50} for the dissolved hydrocarbon mixture originating from the spilled oil. Only the soluble compounds of $\log(K_{ow}) \leq 5.6$ are included in the additive toxicity model.

Toxicity varies with duration of exposure, with the LC_{50} decreasing as exposure time increases (Sprague, 1969; Kooijman, 1981; McAuliffe, 1987; Anderson et al., 1987; French and French, 1989; French, 1991; McCarty, 1986; McCarty et al., 1992a; 1992b; McCarty and Mackay 1993; French et al., 1996). This result is due to the accumulation of toxicant over time up to a critical body residue (tissue concentration) that causes mortality. The accumulation is faster at higher temperatures, such that LC_{50} at a given (short) exposure time decreases with increasing temperature.

The following algorithm was developed in French-McCay (2001; 2002). The LC_{50} of an aromatic in the oil mixture varies with exposure time and temperature according to:

$$LC_{50\infty} = LC_{50t} \ (1 - e^{-\varepsilon t}) \qquad\qquad\qquad (5)$$

$$\log_{10}(\varepsilon) = \varepsilon_1 - \varepsilon_2 \log_{10}(K_{ow}) \qquad\qquad\qquad (6)$$

$$d\varepsilon / dT = \tau T \qquad\qquad\qquad (7)$$

where t is time of exposure, LC_{50t} is LC_{50} at time t, $LC_{50\infty}$ is LC_{50} at infinite time of exposure, K_{ow} is the octanol-water partition coefficient, $\varepsilon_1 = 1.47$ and $\varepsilon_2 = 0.414$, T = temperature (°C), and $\tau = 0.11$ (French-McCay, 2002).

LC_{50}s for MAHs and PAHs from the literature were corrected for time and temperature of exposure to calculate $LC_{50\infty}$. The QSAR (Quantitative Structure Activity Relationship) regression for narcotic aromatics in oil was developed:

$$\log_{10}(LC_{50\infty}) = \log_{10}(\phi) + \gamma \log_{10}(K_{ow}) \qquad\qquad\qquad (8)$$

For 278 bioassays on individual aromatics, the slope and intercept of the regression are: $\log_{10}(\phi) = 4.8926$ and $\gamma = -1.0878$. This QSAR describes the mean response for all species (i.e., the response of the average species), and the slope of this relationship is constant for all species (see Di Toro et al., 2000 for theory). The intercept varies by species, with 95% of species falling within the range $\log_{10}(\phi) = 3.9704$ (sensitive species) and $\log_{10}(\phi) = 5.8147$ (insensitive species). The above equation may be used to estimate $LC_{50\infty}$ for any aromatic, assuming an appropriate intercept for the species of concern.

The SIMAP exposure model takes into account the time and temperature of exposure, using the rearrangement of the above: $LC_{50t} = LC_{50\infty} / (1 - e^{-\varepsilon t})$ to correct the LC_{50}. Time of exposure is evaluated by tracking movements of organisms' relative concentrations greater than the concentration lethal to 1% of exposed organisms (LC1, approximated as 1% of $LC_{50\infty}$). Stationary or moving Lagrangian tracers that represent organisms record the concentrations of exposure over time and the dose (summed concentration times duration) to an organism represented by that behavior. Exposure time is the total time concentration exceeds LC1. The concentration is the average over that time, or total dose divided by exposure time. The percent mortality is then calculated using the log-normal function centered on LC_{50t}.

BTEX is very soluble in water, so exposure concentrations can be high. However, BTEX is only moderately hydrophobic (so relatively low in toxicity) and it is also very volatile. Thus, BTEX rapidly volatilizes (in hours) reducing exposure concentrations. For these reasons, the effects due to BTEX after a spill are typically low and of short duration, except potentially for very light fuels such as gasoline or jet fuel, which may contain high percentages of BTEX.

PAHs and many of the alkyl-substituted benzenes are less soluble than BTEX, but they do dissolve in significant bioavailable quantities. Because they are more hydrophobic than BTEX, they more strongly partition into the lipids in membranes and tissues. Thus, they are more toxic and can have significant effects on aquatic organisms.

Lower-molecular-weight aliphatic hydrocarbons (e.g., alkanes and cycloalkanes with boiling points less than about 380°C) may also contribute to toxicity after an oil spill. However, the aliphatics are more volatile (have higher vapor pressure) and less soluble than aromatics of the same molecular weight (Mackay et al., 1992) and would be more readily lost to the atmosphere from surface waters. They are also less toxic than the aromatics of similar molecular weight (French-McCay, 2001; 2002). Anderson et al. (1981) and Anderson (1985) found that 98% of the dissolved hydrocarbons in oil and water dispersions were aromatics (MAHs and PAHs).

The residual fraction in the model is composed of non-volatile and relatively insoluble compounds that remain in the "whole oil" that spreads, is transported on the water surface, strands on shorelines, and disperses into the water column as oil droplets or remains on the surface as tar balls. This is the fraction that comprises black oil, mousse, and sheen. In the model, it is assumed not to be bioavailable or acutely toxic to aquatic biota, although it may have acute effects on wildlife species and contribute to chronic effects on aquatic biota.

The LC_{50mix} of aromatic mixtures from oil were calculated using the additive model, including those aromatics that are measured in the oil and dissolved in the water [with $\log(K_{ow}) \leq 5.6$] for long enough for exposure to aquatic organisms to be significant. Typically, only the PAHs are dissolved in sufficient quantity and remain in the water long enough for their toxic unit values to be significant. The biological effects model uses the calculated ΣPAH (or $\Sigma BTEX + \Sigma PAH$ if BTEX is significant) and the estimated $LC50_{mix}$ corrected for time and temperature of exposure to estimate mortality to aquatic biota. Typically, the appropriate LC_{50mix} for most species is the average sensitivity, as specific data are not available for all species and the most likely LC_{50} for an untested species would be the mean of the observations for other species. However, for certain species known to be sensitive to organics with a narcotic mode of action, the sensitive 2.5[th] or some other percentile LC_{50mix} may be more appropriate. Categorization of species as sensitive, average, or insensitive may be based on bioassay data reviewed in French-McCay (2001) or similar data indicating the percentile of the species' sensitivity to the narcotic lower molecular weight aromatics in oil.

The dissolved concentrations are estimated by the fate model for both the water column and sediments. Dissolved concentrations in the water column result mainly from dissolution of entrained oil droplets, as the soluble compounds evaporate faster from surface slicks. In the sediments, dissolved concentrations in pore waters are calculated using the equilibrium partitioning model. Exposure and mortality of benthic organisms are a function of the dissolved concentrations in pore water. This methodology was validated by Swartz et al. (1995) and used in sediment quality criteria for PAHs (Di Toro et al., 2000; U.S. EPA, 2003; 2008).

2.1.6.3 Wildlife

The likelihood of encounter with oil will be different for each wildlife type depending on its behavior. Terrestrial mammals and birds that do not feed in aqueous habitats would likely avoid the oil, except for those attracted to carrion (e.g., foxes, coyotes, wolverines, bald eagles). Scavengers and wildlife that obtain part of their diet from aquatic habitats (e.g., racoons, moose) would have a moderate probability of becoming oiled. Aquatic mammals (e.g., muskrat, beaver, otter, and mink), waterfowl, wading birds, and turtles would have a high likelihood of being oiled.

In this report, "wildlife" includes the air-breathing vertebrates that occupy primarily terrestrial habitats but also interact with the aquatic environment. Accordingly, wildlife includes birds, mammals, reptiles, and adult stages of amphibians. The potential effects on wildlife that are in the spill-affected area are evaluated based on the probability of encounter with floating and/or shoreline oil and the amount of oil that is likely to accumulate on an individual animal. The threshold of oil thickness that would impart a lethal dose to intersecting wildlife is 10 microns (~10 g/m^2), based on literature reviews by Engelhardt (1983), Clark (1984), Geraci and St. Aubin (1988), Jenssen (1994) and other oil effects literature on aquatic birds and marine mammals. Varoujean et al. (1983) state that 1 g/m^2 of oil on the water surface is 100% lethal to birds when confined to the oil slick in an enclosure, while 0.1 g/m^2 is not enough to cause acute mortality. Peakall et al. (1985) state that blue sheen oil <1 µm thick (equivalent to <1 g/m^2) (NRC, 1985) is not harmful to seabirds. Jenssen and Ekker (1991a; 1991b) studied the effects of exposure of eiders to oil at various doses. The required dose for an effect on metabolism was >20 mL of crude oil on the skin or feathers with hydrocarbons being adsorbed directly and ingested via preening. However, their literature review revealed that an order of magnitude more oil is the required dose for significant and potentially lethal effects.

Birds incubating eggs can transfer oil to the egg from their plumage (Albers and Szaro, 1978; King and Lefever, 1979; Albers, 1980). Clutches of common eider eggs treated with 20 µL of fuel oil had significantly greater embryonic mortality than control clutches (Albers and Szaro, 1978). Hatching success was significantly reduced for mallards with plumage exposed to 100 mL/m^2 (0.1 mm) of Prudhoe Bay crude oil for 48 hours while incubating eggs, whereas the reduction in hatching success was not significant at 5 mL/m^2 of oil exposure. However, survival rates of newly-hatched ducklings and adults exposed to up to 100 mL/m^2 oil were not significantly lowered (Albers, 1980). Mortality rates of mallard eggs treated with 1 and 5 µL South Louisiana crude oil were 35% and 91%, respectively. For chicken eggs, mortality rates were 38%, 80%, and 98% with applications of 1, 5, and 10 µL of oil, respectively (Hoffman, 1978). As these amounts of oil covered only small fractions of the eggshell surface effects were likely due to chemical toxicity and not to physical causes such as reduced gas exchange rates.

To determine the effects on mammalian receptors, Wolfe and Esher (1981) exposed rice rats to 200 mL/m^2 (~200 g/m^2) and 20 mL/m^2 (~20 g/m^2) of crude oil on the water surface. These studies were conducted in laboratory test chambers, with 1 m^2 water and two islands. In both exposures, willingness to enter the water and swim was reduced. Survival 24 hours later was significantly lowered in the higher exposure treatment. Survival rate was not measured beyond 24 hours after exposure. These results suggest that mortality would occur for other semi-aquatic mammals, such as muskrat, mink, and otter that swim through oil. River otters were observed to be killed by *Exxon Valdez* oil (Spies et al., 1996).

Little research is available to quantify oil exposure effects on aquatic reptiles. Much of what is available regarding reptiles includes work on sea turtles, synthesized by Vargo et al. (1986). In addition to direct mechanical and chemical toxicity, effects include reduced hatching rates and developmental deformities (Milton et al., 2003). For turtles of all ages, ingestion of tar balls is a major issue because turtles eat anything that

appears to be the same size as their preferred prey. Ingestion can result in starvation from gut blockage, decreased absorption efficiency, absorption of toxins, buoyancy problems from buildup of fermentation gasses, and other effects (Milton et al., 2003). Inhalation of vapor is also of concern for turtles. Sea turtles have not been shown to exhibit avoidance behavior when surrounded by petroleum fumes (Milton et al., 2003) and presumably freshwater turtles would behave similarly.

The SIMAP model uses an estimate of the minimum external dose of oil that is lethal. During testing that was conducted, there was one observation of a 70 mL dose causing a significant change in metabolic rate. However, 200 – 500 mL was observed as the lethal dose when applied to the plumage of ducks (Jenssen, 1994). In the SIMAP model, 350 mL is assumed to be the lethal dose for all wildlife. Assuming that a swimming bird has a width of 15 cm, it would need to swim through 23 m of oil of 100 µm thickness, 230 m of oil of 10 µm thickness, or 2300 m of oil of 1 µm thickness, to obtain a dose of 350 mL. This distance spent in oil need not be in a straight line. If an animal swims at a rate of 10 m/min, then 23 m would be covered in about 2 minutes. Carrying this calculation forward, 230 m would be covered in 23 min, and 2,300 m would be covered in 230 min (3.8 hours). A slick thickness of 10 µm is assumed as a threshold thickness for oiling mortality, given the sizes of the water bodies involved and likely exposure times of animals within them (French-McCay, 2009). Those animals oiled above a threshold lethal dose may die, given the environmental temperatures involved and the possibility that timely capture and treatment may not be possible.

2.1.6.4 SIMAP Model Biological Output Description

The biological effects model (French et al., 1996; French-McCay, 2003; 2004; 2009) estimates short term (acute) exposure of biota to floating oil and subsurface oil contamination (in-water and sediments) and predicts the resulting percent mortality. Toxicity to aquatic biota in the water column and sediments is estimated from dissolved hydrocarbon concentrations (DHC) and exposure duration, using laboratory-based bioassay data for oil hydrocarbon mixtures (French-McCay, 2002). In each habitat grid cell, acute toxicity to aquatic biota in water column and demersal (bottom one meter of the water immediately above the sediments) habitats are evaluated by tracking exposure for these different behavior groups. In rivers, where water depths are near or less than 1 m, the affected areas for water column and demersal biota are the same. Areas where effects on wildlife might occur are estimated based on the area swept by surface oil over a threshold thickness for acute toxic effects.

The DHC modeling results for all scenarios were post-processed to analyze the extent of dissolved hydrocarbon concentrations and the potential for effects on aquatic organisms (e.g., fish). The threshold value for species toxicity in the water column is based on global data from French-McCay (2002), which showed that species sensitivity to dissolved hydrocarbons exposure > four days (96-hour LC_{50}) varied from 5 to 400 µg/L with an average of 50 µg/L. This range covered 95% of aquatic organisms (fish, invertebrates and eggs) tested. Biological effects were evaluated for species with high sensitivity to dissolved hydrocarbons (e.g., 5 µg/L level) to indicate a protection of 97.5% of species, and for species with an average sensitivity to dissolved hydrocarbons (e.g., 50 µg/L level) to indicate average losses.

The results of the biological exposure model provide estimates of the EA-100 (in km^2) by behavior group for wildlife and fish/invertebrates. Potential acute effects following a release can vary greatly by space, time, and percent kill. In some cases, 100% mortality may be experienced in some localized regions, while much broader areas may experience only partial effects (e.g., 10% mortality). To normalize results, the EA-100s were estimated for both the surface/shoreline and the water column. Thus, the EA-100 would be the same for a release that resulted in 100% mortality over 1 km^2 versus 1% mortality over 100 km^2. This example is an

oversimplification; however, as the SIMAP model will predict the likely percent mortality by grid cell for the entire modeled domain.

It should be noted that injury resulting from non-acute mortality due to a spill [e.g., chronic effects, delayed mortality such as reduced cardiac fitness (Incardona et al., 2015)] are not accounted for in the exposure model. Therefore, the results predicted by the biological exposure model may be considered underestimates for fish and wildlife. This metric was evaluated for both pelagic and demersal species, benthic and planktonic organisms, and other avian, wildlife, and mammalian receptors.

The area of potential effects on wildlife is presented as the area of the open water or shoreline that was covered by oil above the thickness threshold for acute effects at any time during the scenario. In this case, the threshold thickness was 10 μm. It is important to note that this area does not imply direct effects on all wildlife in that area since the actual effects will be different for each wildlife type depending on the percent likelihood of encountering oil, which is based on behavior.

2.1.7   Model Uncertainty and Validation

The SIMAP model was developed over several decades to include past and recent information from laboratory-based experiments and real-world releases to simulate the trajectory and fate of discharged oil. However, there are limits to the complexity of processes that can be modeled, as well as gaps in knowledge regarding the affected environment. Assumptions based on available scientific information and professional judgment were made in the development of the model, which represent a best assessment of the processes and potential exposures that could result from oil releases.

The major sources of uncertainty in the oil fate model are:

- Oil contains thousands of chemicals with differing physical and chemical properties that determine their fate in the environment. The model must, out of necessity, treat the oil as a mixture of a limited number of components, grouping chemicals by physical and chemical properties,

- The fate model contains a series of algorithms that are simplifications of complex physical-chemical processes. These processes are understood to varying degrees,

- The model treats each release as an isolated, singular event and does not account for any potential cumulative exposure from other sources of contamination,

- Several physical parameters including but not limited to hydrodynamics, water depth, total suspended solids concentration, and wind speed were not sampled extensively throughout the entire modeled domain. However, the data that did exist was sufficient for this type of modeling. When data were lacking, professional judgment and previous experience were used to refine the model inputs, and

- Response timing and effectiveness is highly dependent on the specific discharge as well as exact conditions at the time of a discharge.

In the unlikely event of an actual release of oil, the trajectory, fate, and potential biological exposure will be strongly determined by the specific environmental conditions, the precise locations, and a myriad of details related to the specific event and exact timeframe of the release. Modeled results are a function of the scenarios simulated and the accuracy of the input data used. The goal of this study was not to forecast every detail that could potentially occur, but to describe a range of possible consequences and exposures of oil releases under

various representative scenarios. Using these results, an informed analysis can be made as to the likely effects of oil releases under various scenarios. The model inputs are designed to provide representative conditions to inform such an analysis for the scenarios considered.

Despite the uncertainty inherent in this type of modeling, the OilToxEx model in SIMAP and the data upon which it is based (French-McCay, 2001; 2002) have been validated through various studies and applications. The toxic units approach was used by U.S. EPA for development of PAH water and sediment quality criteria (Di Toro et al., 2000; Di Toro and McGrath, 2000; U.S. EPA, 2003; 2008). The oil toxicity model was validated using laboratory oil bioassay data for both fresh and salt-water organisms (French-McCay, 2002) and for lobster mortality in the case of the *North Cape* spill (French-McCay, 2003). The underlying toxicity data used to develop the model is based on bioassays for freshwater and marine fish, invertebrate and algal species at a variety of life stages.

The biological effects model was validated using simulations of over 20 spill events where data are available for comparison (French and Rines, 1997; French-McCay, 2003; 2004; French-McCay and Rowe, 2004). In most cases (French and Rines, 1997; French-McCay, 2004; French-McCay and Rowe, 2004), only the wildlife acute effects could not be verified because of limitations of the available observational data.

2.2 BFHYDRO Model Description

Hydrodynamics for the Bad River were calculated using the RPS BFHYDRO hydrodynamic model. The BFHYDRO model is a general curvilinear coordinate, boundary-fitted hydrodynamic model (Muin and Spaulding, 1997; Mendelsohn et al., 1995; Huang and Spaulding, 1995; Swanson et al., 1989) that can be used to generate tidal or river elevations, velocities, and salinity and temperature distributions. The model uses a boundary-fitting technique, which matches the grid coordinates with shoreline and bathymetric feature boundaries for highly accurate representations of areas with complex coastal or riverine geometries, such as the Bad River. This system also allows the modeling team to adjust the model grid resolution as desired and introduce lower mesh resolution (larger cells) at locations several miles from the proposed route for computational efficiency. BFHYDRO may be applied in either two or three dimensions depending on the nature of the problem and the complexity of the study. A detailed description of the model with associated test cases is described in Muin and Spaulding (1997), and Muin (1993). The model has undergone extensive testing against analytical solutions and has been found to perform accurately and quickly. Specific model comparisons are found in Swanson et al. (2012), Mendelsohn et al. (2003), Muin and Spaulding (1997), Mendelsohn et al. (1995) and Huang and Spaulding, (1995).

A brief description of the model theory follows. The application development and hydrodynamic outputs developed for the Bad River using the BFHYDRO model are described in Section 3.3.

2.2.1 BFHYDRO Model Theory

The boundary-fitted method uses a set of coupled, quasi-linear, elliptic transformation equations to map an arbitrary horizontal multi-connected region from physical space to a rectangular mesh structure in the transformed horizontal plane (Spaulding, 1984). The three-dimensional conservation of mass and momentum equations, with approximations suitable for lakes, rivers, estuaries, and coastal oceans (Swanson, 1986; Muin, 1993) that form the basis of the model, are then solved in this transformed space. A sigma stretching system is used in the vertical to map the free surface and bottom onto coordinate surfaces to resolve bathymetric variations. The vertical mesh stretches and shrinks with the changing tidal elevation or river stage, maintaining

a constant number of layers, so that no interpolation is required to simulate the surface slope or the bathymetry (Figure 2-5). The velocities are represented in their contra-variant form, on an Arakawa-C grid.
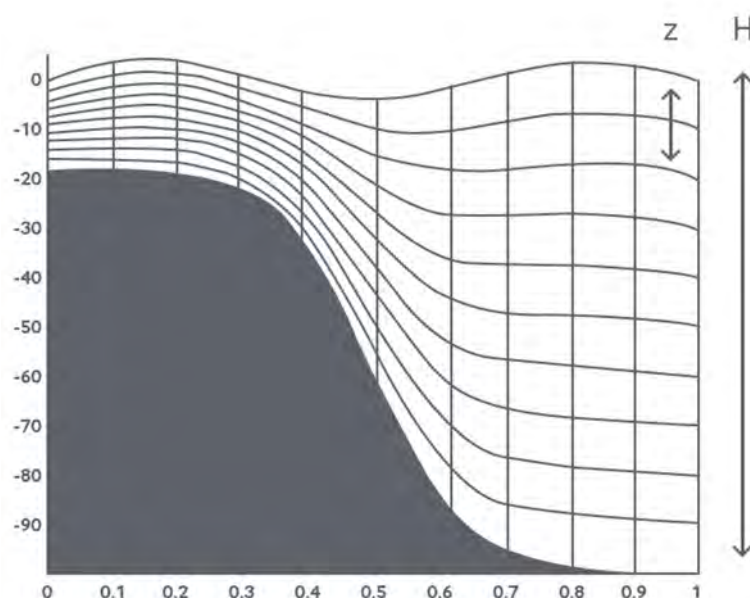
Figure 2-5. Schematic of the BFHYDRO vertical sigma coordinate system.

The basic equations are written in spherical coordinates to allow for accurate representation of large, modeled areas without distortion. The conservation equations for water mass, momentum (in three dimensions) and constituent mass (temperature [heat] and salinity) form the basis of the model and are well established. It is assumed that the discharge is incompressible, that the fluid is in hydrostatic balance, the horizontal friction is not significant and the Boussinesq approximation applies; all customary assumptions.

The boundary conditions are as follows:

- At land, the normal component of velocity is zero,

- At open boundaries, the free surface elevation must be specified, and temperature (and salinity for estuarine and coastal applications) specified on in discharge,

- On outflow, temperature (heat) and salinity are advected out of the model domain,

- At river boundaries, the volume flux must be specified, with positive discharge into the model domain, and temperature (and occasionally salinity) must be specified,

- A bottom stress or a no slip condition can be applied at the bottom. No temperature (heat) is assumed to transfer to or from the bottom, a conservative assumption as some transfer of heat to the bottom is expected to occur, and

- A wind stress, and appropriate heat transfer terms, are applied at the water surface. The surface heat balance includes all the primary heat transfer mechanisms for environmental interaction.

There are various options for specification of vertical eddy viscosity, (for momentum) and vertical eddy diffusivity, (for constituent mass [temperature and salinity]). The simplest formulation is that both are constant throughout the water column. They can also be functions of the local Richardson number, which, in turn, is a function of the vertical density gradient and vertical gradient of horizontal velocity. A 1-equation or 2-equation turbulence closure model may also be used.

The set of governing equations with dependent and independent variables transformed from spherical to curvilinear coordinates, in concert with the boundary conditions, is solved by a semi-implicit, split mode finite difference procedure (Swanson, 1986). The equations of motion are vertically integrated and, through simple algebraic manipulation, are recast in terms of a single Helmholtz equation in surface elevation. This equation is solved using a sparse matrix solution technique to predict the spatial distribution of surface elevation for each grid.

The vertically averaged velocity is then determined explicitly using the momentum equation. This step constitutes the external or vertically averaged mode. Vertical deviations of the velocity field from this vertically averaged value are then calculated, using a tridiagonal matrix technique. The deviations are added to the vertically averaged values to obtain the vertical profile of velocity at each grid cell, thereby generating the complete current patterns. This constitutes the internal mode. The methodology allows time steps based on the advective, rather than the gravity, wave speed as in conventional explicit finite difference methods, and therefore results in a computationally efficient solution procedure (Swanson, 1986; Muin, 1993).

2.3   D-Flow FM Model Description

Hydrodynamic modeling for the White River was performed using Delft3D FM, which is a modeling suite developed and maintained by Deltares. The Delft3D FM modeling suite includes the D-Flow FM finite volume model code that was used for this application, and an interface (Delta Shell) for handling model inputs and outputs (Deltares, 2022). Hydrodynamic outputs from the D-Flow FM model were then converted to a file format that is compatible with RPS's SIMAP model input format, and were used to determine the transport of oil in the water column.

D-Flow FM is a multi-dimensional, boundary-fitted hydrodynamic model that can operate with cartesian or spherical coordinates (Deltares, 2022). The unstructured mesh grid utilizes a boundary-fitting technique, which matches the grid coordinates with shoreline and bathymetric feature boundaries for highly accurate representations of areas with complex coastal or riverine geometries. This allows for easy development of model grids that conform well to complex shorelines and sinuous channels and can include high degrees of mesh resolution in areas only where it is desired. D-Flow FM may be applied in either two or three dimensions depending on the nature of the problem and the complexity of the study. User-specified forcing conditions (e.g., tidal, meteorological) can be applied to the model to generate water elevations, velocities, density, and/or salinity in various coastal, river, lakes, and estuarine environments. The model has undergone extensive validation for a variety of hydrodynamic conditions and water body types and has been found to perform accurately and agree well with measurements of steady and unsteady flow behavior (Gerritsen et al., 2008). A

brief description of the model follows. The application development and hydrodynamic outputs developed for the White River using the D-Flow FM model are described in Section 3.3.2.

2.3.1 D-Flow FM Model Theory

The boundary-fitted model solves a series of non-linear shallow water equations derived from the three dimensional Navier-Stokes equations with Boussinesq approximation for incompressible free surface flow (Deltares, 2022). In cases where non-hydrostatic modeling is required, additional components can be added to make the equations practically equivalent to the incompressible Navier-Stokes equations.

The equations solved in the modeling are conservative toward:

- Water volume (the continuity equation), and
- Linear momentum (the Reynolds-averaged Navier-Stokes equations).

Two vertical grid co-ordinate systems are available, the sigma-grid system (a more common application initially designed for atmospheric models) and the Z-grid system (for simulations of weakly forced stratified water systems). The sigma-grid has several layers bounded by two sigma-planes, which follow the bottom topography and the free surface (Figure 2-6) to obtain a smooth representation of the topography. The Z-grid has horizontal coordinate lines that are (nearly) parallel with density interfaces (isopycnals) in regions with steep bottom slopes, for modeling stratified systems with horizontal density gradient (Deltares, 2022).

The sigma-grid system was used to resolve the vertical direction in this application of the model because there are no steep bed slopes, and no strong stratifications needed to be captured in this study.
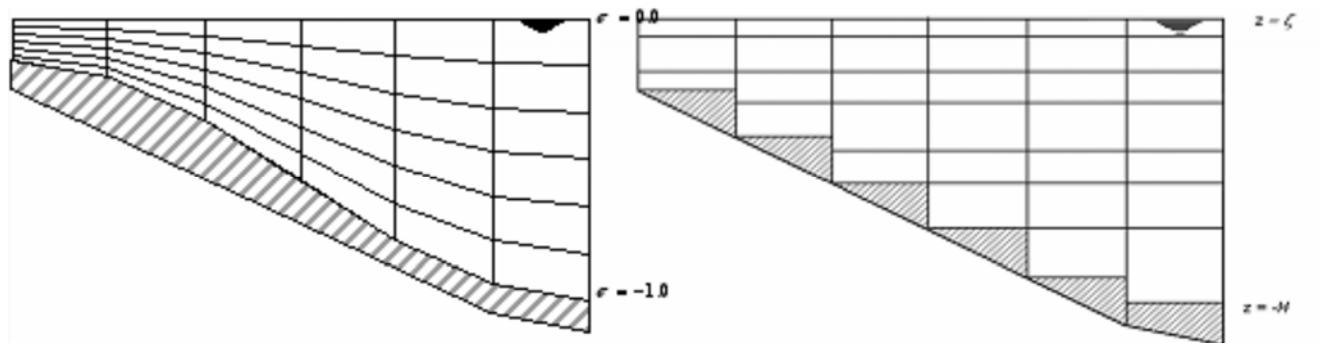
Figure 2-6: Schematic of the D-Flow FM vertical sigma (left) and vertical Z-coordinate (right) systems (Deltares, 2022).

Boundary conditions of the model can be defined as follows:

- The flux of matter through land boundaries and on the bottom is zero, thus creating a zero normal component of velocity,
- Flow and transport boundary conditions (e.g., water levels, currents, gradients, discharges) are input at open boundaries to represent influences from areas outside the model,

- Slip conditions are assumed at the bottom of the waterway, while partial-, free-, or no-slip conditions can be applied at the sides,

- Wind stress can be applied at the free surface, which generates wind-driven flow. Flow can also be driven by pressure gradients or density gradients in the watercourse, and

- Spatial and temporal outputs of velocity and water surface elevation can be obtained at the specified model output locations.

In D-Flow FM, there are various levels of complexity that can be applied to model the turbulent exchange of momentum and mass in the vertical direction. The simplest assumption is that both are constant throughout the water column, although other options are available. Iterative solvers are used for the core equations in the model, allowing for efficient solutions and adaptability to different assumptions and complexities in the system (Gerritsen, et al., 2008).

3   SIMAP MODEL INPUT DATA

Numerous geographic and environmental data sources are required by the SIMAP model to define site-specific characteristics that will be used to determine the likely trajectory, fate, and potential biological effects of discharged oil. Federal, state, and local resources were identified for use in the Bad River and White River SIMAP modeling that capture the site-specific parameters and variability for the region over the modeled time period (Table 3-1). The data types, sources, and preparation of the data for use in the SIMAP modeling are discussed in the following sections.

Table 3-1. Environmental data sources used in the SIMAP modeling at the Bad River and White River.

Input Type	Input Parameter	Source	Time Frame
Geographic and Habitat Data	Bathymetry	Enbridge Field Surveys, Enbridge, 2022b; Enbridge, 2020; WDNR, 1966; USGS, 2022	2019-2022[‡]
	Shoreline Habitat	Enbridge Aerial Photography and National Wetland Inventory version 2 (USFWS-NWI, 2020)	2019[‡]
	Shoreline	USGS NHD (High Resolution) (USGS, 2020b); Esri aerial imagery	2020-2021
Wind		Ashland Kennedy Memorial Airport (NOAA, 2015)	1999 – 2018
Hydrodynamics		NHDPlus RPS – BFHYDRO modeling output D-FLOW FM modeling output	Model steady state solution*
Water Temperature		Monthly averages for USGS Gage #4027000 Bad River near Odanah, WI (USGS, 2020a)	1977, 2012 – 2018
Total Suspended Solids (TSS)		USGS, 2020b	N/A
Wild Rice Habitat		Bad River Tribe (2020) Wisconsin Department of Natural Resources, Water Quality Bureau Great Lakes Indian Fish and Wildlife Commission (WI DNR, 2020; 2023) National Wetlands Inventory Version 2 (USFWS, 2020)	N/A

*Steady state currents refer to fixed current velocities (speed and direction) within each grid cell over the duration of each model run. However, currents for each point within the model domain were spatially variable. Similarly, currents at each fixed point were different between seasons, based upon variable river flow rate (i.e., low, average, and high river flow conditions).

[‡]Field data were collected by Enbridge in 2019 and used as inputs to the oil spill modeling. Values in the Bad River downstream of the existing Line 5 crossing were also verified on two separate field visits by Dr. Horn in 2018 and 2021. Values in the White River were supplemented from other sources cited here.

3.1   Geographic, Bathymetry, and Habitat Data

For geographical reference, SIMAP uses a rectilinear grid to designate the location of the shoreline, the water depth (bathymetry), and the shore or habitat type. The grid is generated from a digital shoreline or other geographical information using the Esri ArcGIS program. The cells are coded for depth and habitat type, and the model identifies the shoreline using this grid. In model outputs, the land-water map is only used for visual reference. It is the habitat grid that defines the actual location of the shoreline in the model. The resolution of the Bad River habitat grid was approximately 5 m (16.40 ft) (north-south) by 3 m (9.84 ft) (east-west), corresponding with dimensions of 0.00004° on each side. The resolution of the White River habitat grid was approximately 3 m (16.40 ft) (north-south) by 3 m (9.84 ft) (east-west), corresponding with dimensions of 0.00004° on each side.

Geographical data including a digital shoreline basemap and habitat mapping were obtained from monthly reservoir statistics, aerial photography, and the USGS National Hydrography Database (Table 3-1). The USGS High Resolution National Hydrography Database (NHD) was used to define the land/water boundary, and data from aerial imagery and Enbridge (2019) were used to define the types of habitats present within the study area (USGS, 2020b). Habitat grids define the bottom type, the wetlands, and the shore type. Habitat data varies throughout the year and three separate grids were constructed for each river to account for the changing conditions over the simulated river flow conditions (Table 3-2, Figure 3-1 and Figure 3-3 [Bad River], Figure 3-2 and Figure 3-4 [White River]). Note that low and average river flow conditions use the same land-water boundaries, and because the assumed habitat for low river flow was entirely ice edge, those habitat grids were not presented here. The high river flow conditions in the Bad River resulted in connection to an oxbow in Extent 7 (Figure 3-3).

Table 3-2. Classification of habitat types used in SIMAP.

Habitat Code (Sw, Lw)	Ecological Habitat	F or W
Shore / Intertidal		
1, 31	Rocky Shore	F
2, 32	Gravel Shore	F
3, 33	Sand Beach or Shore	F
4, 34	Fringing Mud Flat	F
5, 35	Fringing Wetland (Emergent or Forested)	F
6, 36	Macroalgal Bed	F
7, 37	Mollusk Reef	F
8, 38	Coral Reef (marine only)	F
Submerged / Subtidal		
9, 39	Rock Bottom	W
10, 40	Gravel Bottom	W
11, 41	Sand Bottom	W
12, 42	Silt-mud Bottom	W
13, 43	Wetland (submerged areas)	W
14, 44	Macroalgal Bed	W
15, 45	Mollusk Reef	
16, 46	Coral Reef (marine only)	W
17, 47	Submerged Aquatic Vegetation Bed	W
Shore / Intertidal		
18, 48	Man-made, Artificial	F
19, 49	Ice Edge	F
20, 50	Extensive Mud Flat	W
21, 51	Extensive Wetland (Emergent or Forested)	W

Seaward (Sw) and landward (Lw) system codes are listed. Fringing types (indicated by 'F') are only as wide as the intertidal zone or shoreline width where oiling might occur. Other types (indicated by 'W' for 'water') are a full grid cell wide and have a fringing type on the landward side. Note that not all habitat codes (e.g., marine oriented) were used in this modeling study.
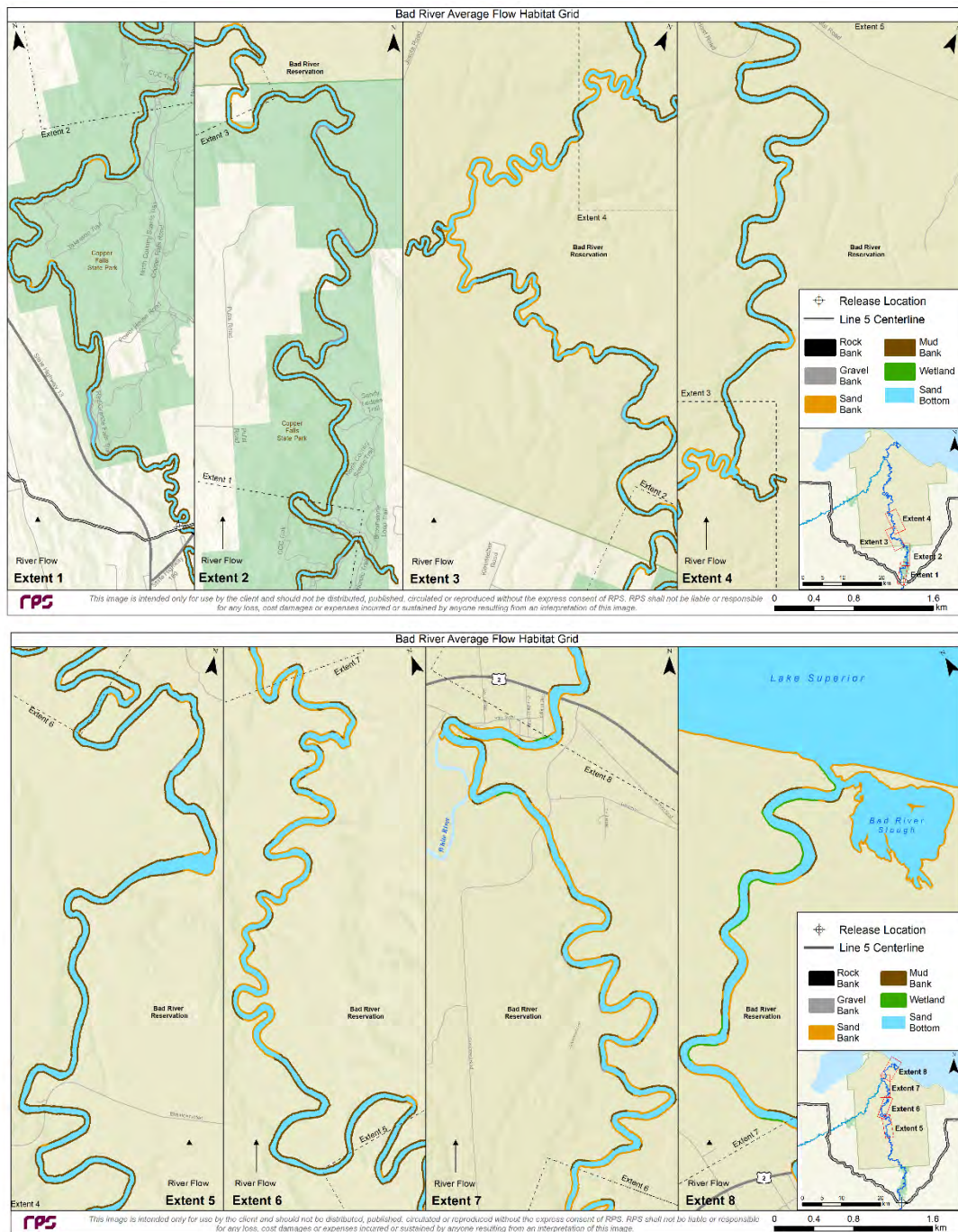
Figure 3-1. Habitat grid shore types for the Bad River Proposed Route crossing under average river flow conditions.
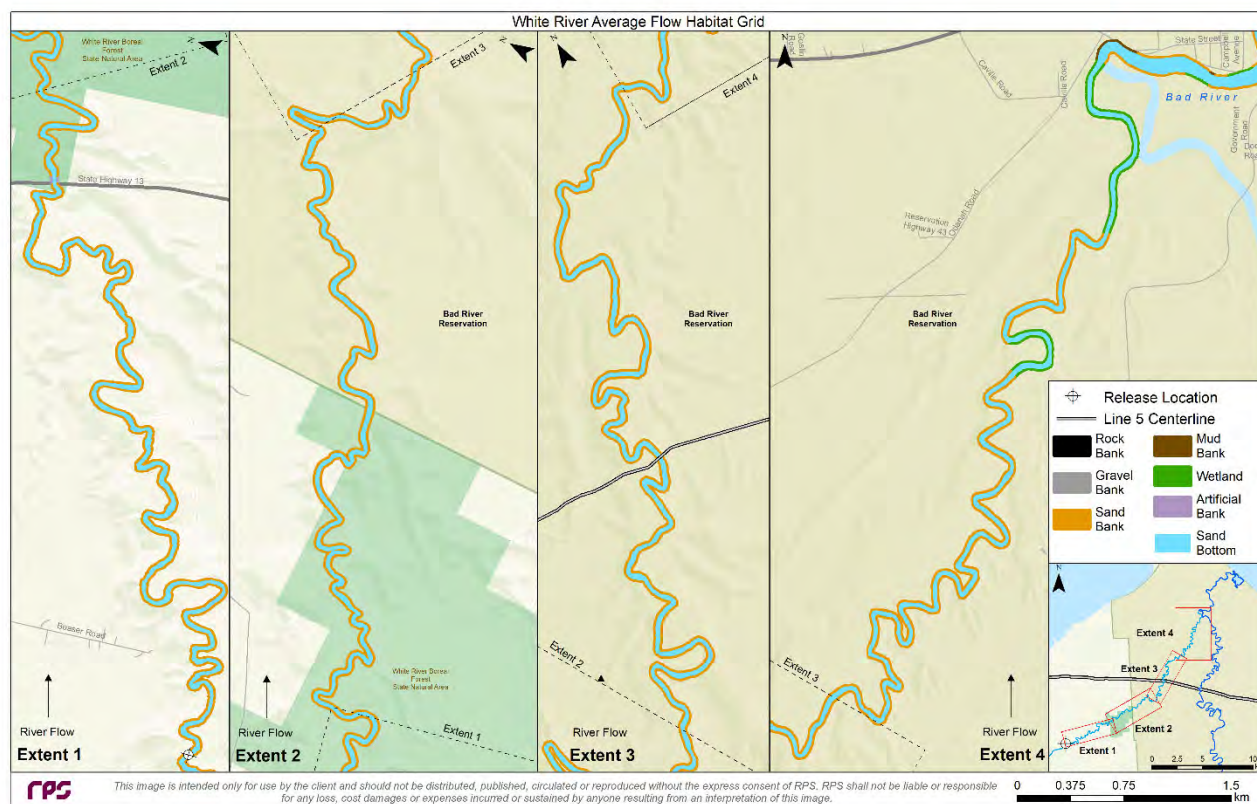
Figure 3-2. Habitat grid shore types for the White River Proposed Route crossing under average river flow conditions.
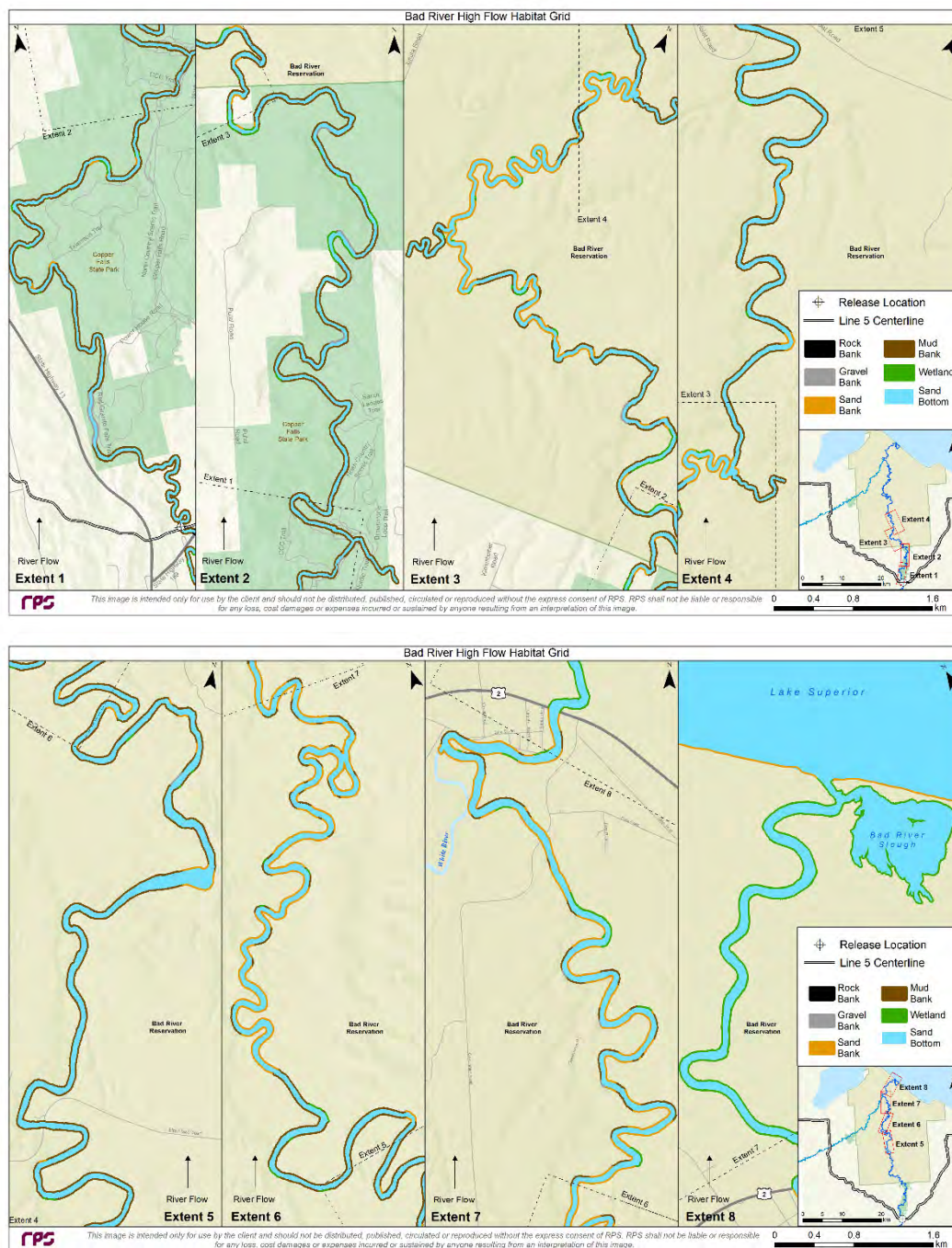
Figure 3-3. Habitat grid shore types for the Bad River Proposed Route crossing under high river flow conditions. Note the inclusion of the oxbow in Extent 7.
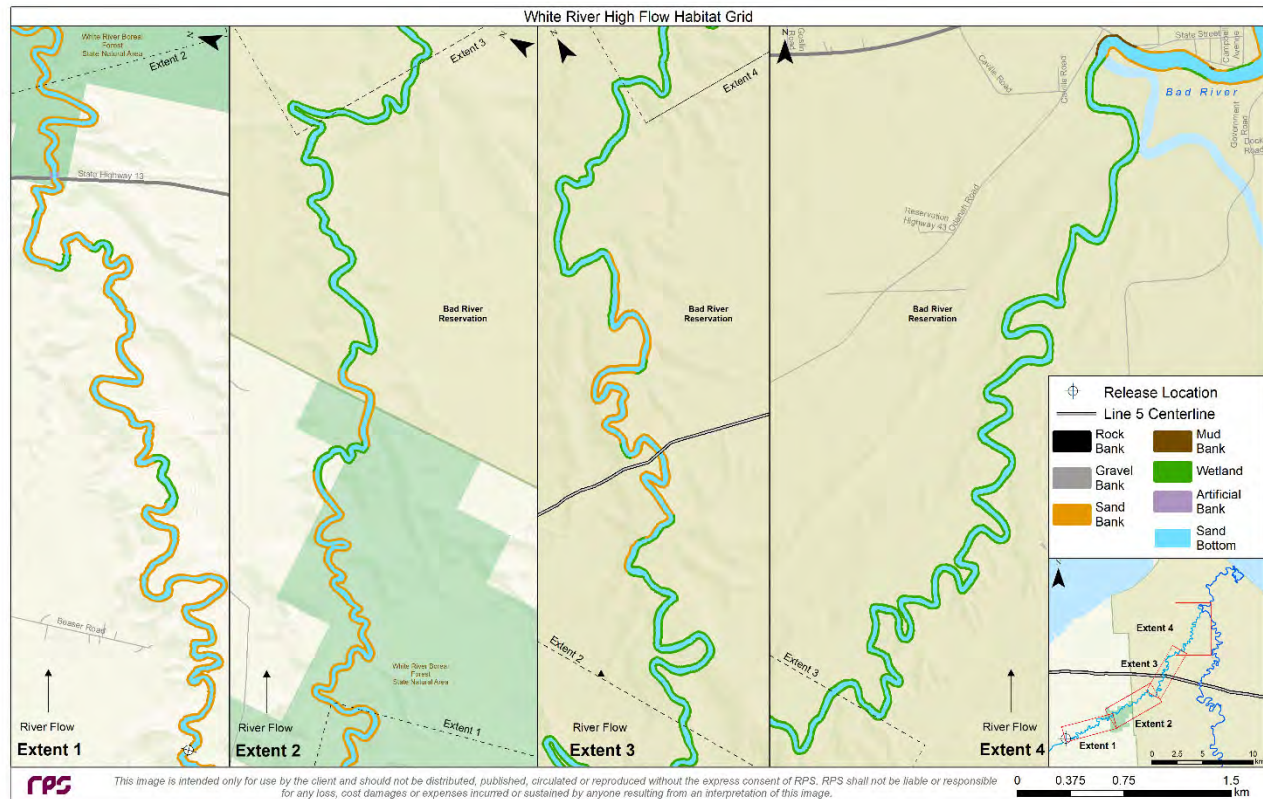
Figure 3-4. Habitat grid shore types for the White River Proposed Route crossing under high river flow conditions.

Regions identified as wild rice habitat were included in the modeling for an overlay assessment to define regions that may be susceptible to effects following a release of oil. The only wild rice habitats within the Reservation are those in the vicinity of the Kakagon-Bad River Slough complex, located more than 72 km (45 mi.) downstream of the Proposed Route crossing of the Bad River and more than 35 km (22 mi.) downstream of the Proposed Route crossing of the White River. Several datasets were combined to map the specific habitat locations within the Reservation. The wild rice habitat data linked to the Tribe's website (Bad River Tribe, 2020) was accessed as an interactive online portal with no download capabilities. The wild rice Esri map service for river and stream as well as lakes (but not wetlands) generated by the Wisconsin Department of Natural Resources (WI DNR) and the Great Lakes Indian Fish and Wildlife Commission (GLIFWC) contains bodies of water within the model domain which have been classified to contain wild rice (WI DNR, 2020; 2023). Wetlands identified in the U.S. Fish and Wildlife Service National Wetland Inventory version 2 (USFWS-NWI, 2020) that were adjacent to the wild rice habitat included in the WI DNR and the Tribe's data were then also classified as wild rice habitat. This conservative approach compiled all wild rice habitat from each of the three datasets for inclusion in the assessment (Figure 3-5). Using the most up-to-date wetlands inventory resulted in some small differences in wetland delineations with wild rice habitat when comparing the Tribe's website and Figure 3-5.
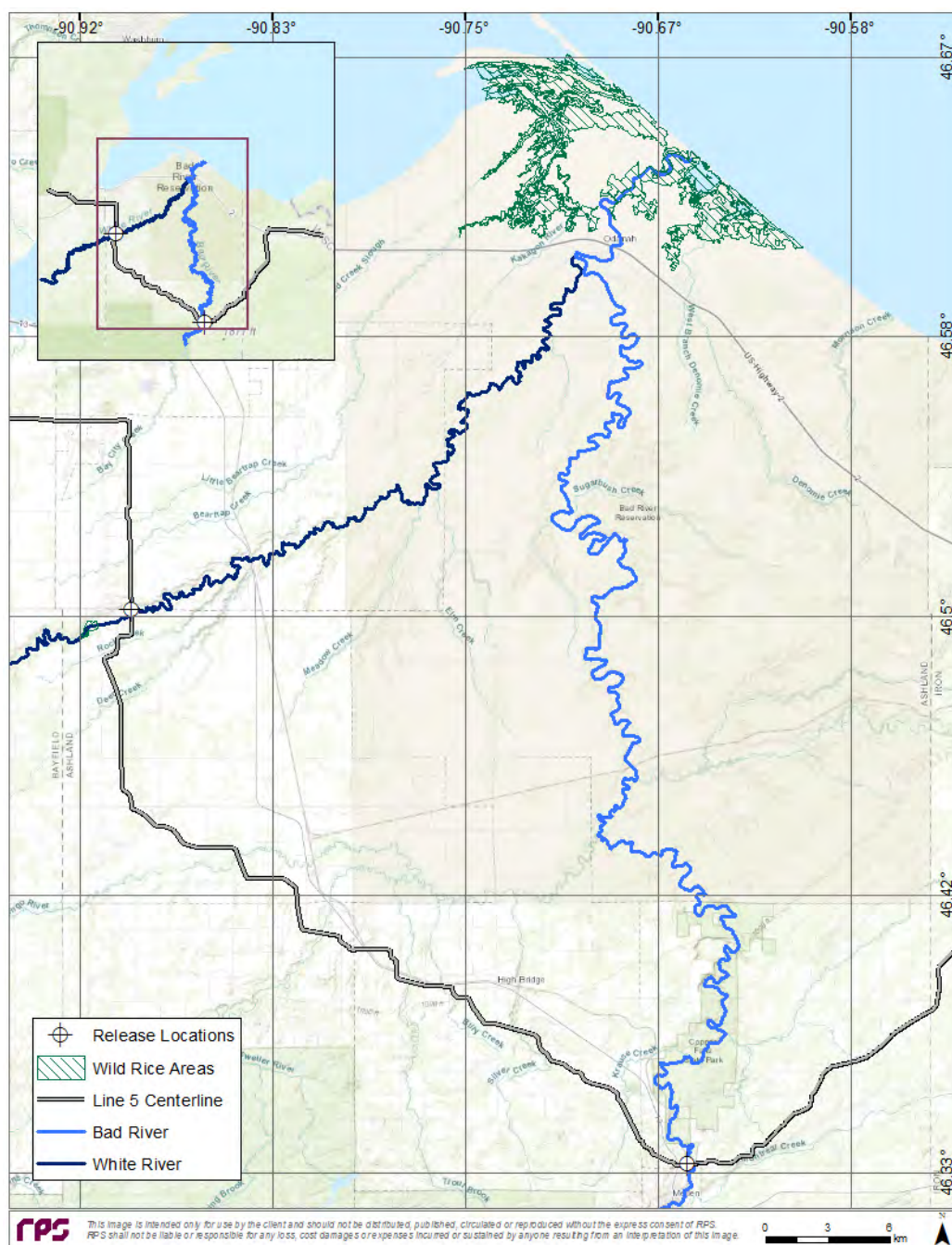
Figure 3-5. Wild rice habitat used in the spill modeling assessment to identify regions that may be impacted by a release of oil using Bad River Tribe data (2020), WI DNR (2020; 2023), and USFWS-NWI (2020).

Each shoreline type corresponds to a characteristic width. In combination with a thickness of oil that may adhere to the shoreline, these parameters can be used to define the total quantity of oil that may adhere to the shoreline. Shore types were defined based upon interpretation of aerial photography and the National Wetland Inventory (USFWS-NWI, 2020). A bottom type of fine-grained material (represented by sand/clay within the model) was assigned for the entire region.

Bathymetry data define the water depths within the study area. Gridded bathymetry for the Bad River was not available; therefore, bathymetry data were derived from point data from field surveys conducted by Enbridge (2019) for the purpose of control point investigation. River depth was determined for each river flow condition (low – January; average – June; and high – April), throughout the model domain. Depths generally ranged from 2-6 ft in upstream sections and 4-10 ft in downstream sections of the Bad River, depending on the location and flow conditions (maps of model bathymetry were provided in Horn et al., 2022).

In the White River, average water depths of 2.4, 3.5, and 4.4 feet were implemented for the three river flow conditions (low, average, and high), respectively. The bathymetry inputs were determined based on information from a CP site sheet, plans for the HDD crossing, bathymetric contours upstream of the White River flowage, data from USGS gage 04027500 on the White River near Ashland, WI, Google imagery, and comparison with the Bad River (Enbridge, 2022b; Enbridge, 2020; WDNR, 1966; USGS, 2022). The higher and lower depths for the low and high flow conditions represent 25% increases and decreases from that 3.5 ft average, based on ratios between gage height and flow rate documented in historical field observations at the White River USGS gage. The suitability of the bathymetry inputs was also confirmed using data from NHDPlus.

It is understood that the location of the land/water boundary and the depth of the river would shift under different river flow conditions. There is the potential for a wider river with deeper depths under higher river flow conditions, when compared to the narrower widths, shallower depths, and potential for small islands to form under low river flow conditions. However, detailed imagery and mapped field data of the three-dimensional structure of the entire Bad and White Rivers were not available. Therefore, a simplifying assumption was made. A single shoreline location was used in this study for each of the three modeled river flow conditions. Because river flow (volume of water moving through the channel) and cross-sectional area (river width and depth) was used to define the velocity of the river, the assumption of a fixed river width would tend to underestimate the velocity of the water under low river flow conditions (low flow volume moving through a wider channel). Similarly, maintaining the river width would tend to overestimate velocity under high river flow conditions. Therefore, the conservative assumption of a fixed river width under low, average, and high river flow conditions resulted in a wider band of predicted results, which further bounded the potential conditions that may exist within the Bad and White Rivers.

3.1.1   Shoreline Oil Retention

Retention of oil on shorelines depends on the shoreline type, width, and angle of the shoreline and viscosity of the oil. In the NRDAM/CME (French et al., 1996), shore holding capacity was based on observations from the *Amoco Cadiz* spill in France and the *Exxon Valdez* spill in Alaska (based on Gundlach, 1987) and later work summarized in French et al. (1996). The maximum potential oil thickness for various shore types as a function of oil viscosity range from as little as 1 mm up to 40 mm (Table 3-3). The shore width (i.e., width of zone where oiling would occur) was set to 1 m (3.3 ft) under high river flow conditions and 10 cm (0.3 ft) under average river flow conditions, as realistic widths for oiling given the spill volumes and river dimensions involved for the Bad River and White River scenarios. The thickness of oil stranding on shorelines was calculated within the model for each stranding event in space and time, as weathering increased oil viscosity through time.

Table 3-3. Maximum oil thickness for various shore types as a function of oil viscosity, measured in centistokes (cSt; from French et al., 1996, based on Gundlach, 1987).

	Oil Thickness (mm) by Oil Type		
Shore Type	Light (<30 cSt)	Medium (30 – 2,000 cSt)	Heavy (>2,000 cSt)
Rocky shore	1	5	10
Gravel shore	2	9	15
Sand beach	4	17	25
Mud flat	6	30	40
Wetland	6	30	40
Artificial	1	2	2

3.2   Wind and Water Temperature Data

Much like other environmental parameters, water temperature and wind speeds at the Bad River and White River vary throughout the year (Table 3-4). The air immediately above the water was assumed to have the same temperature as the water surface, which is the best estimate of the air temperature in contact with floating oil. Average water temperatures for the study area were extracted from the most recent data from a USGS gage in Odanah, WI (Station 04027000) (USGS, 2020a). The model requires that the water temperature be above 0.0°C to allow fluid motion. Therefore, a value of 0.1°C was assumed during wintertime conditions.

Table 3-4. Average water temperature and wind speed for each seasonal condition modeled in SIMAP.

Season	Average Water Temperature (°C)	Average Water Temperature (°F)	Wind Speed (m/s)
High River Flow – April (Spring)	7.7	45.9	3.7
Average River Flow – June (Summer)	18.5	65.3	2.9
Low River Flow – January (Winter)	0.1	32.2	3.8

Winds may physically transport oil on the water surface, and wind speed and direction at the water surface may make a difference between limited or extensive transport, especially in sinuous sections of river. The wind data available is for open areas (e.g., an airport) at some distance (approximately 6-30 km, or 4-19 mi.) from the discharge locations examined, as opposed to in the forested stream areas modeled. Orographic effects and along channel winds are known to exist, however the fine scale resolution in both speed and direction are unknown for this region. Local winds at each point downstream from the release location may be different than

the reported wind speed and direction. Because of these uncertainties and the expected variability in speed and direction, the SIMAP model conservatively assumed wind drift transport was zero (i.e., winds did not laterally transport oil or push it ashore) within the simulation. However, wind speed was still considered, as this is a very important variable for other fates processes such as evaporation and entrainment. The modeled wind was therefore not a true vector as it had magnitude, but no direction. Because of this assumption, non-dimensional winds could be considered conservative, as they may add to the evaporation of surface oil in the model output and could enhance the vertical mixing of the surface water, in some instances keeping subsurface oil entrained or entraining more oil under higher wind speeds but would not strand oil on shorelines. In addition, with wind drift set to zero, oil could not be pinned to shorelines and predicted results would conservatively overestimate the potential for downstream transport.

3.3 Hydrodynamic Data and Applications

The first modeling task was the development, validation, and application of hydrodynamic model applications for the Bad River and White River. The Bad River application was developed using the BFHYDRO model. The White River application was developed using the D-Flow 3D model because the simplified grid generation functionality helped capture fine-scale hydrodynamic changes in a narrow water body with a complex shoreline.

The BFHYDRO and D-Flow 3D models were applied to the Bad River and White River, respectively, over the model domain, assuming within-bank flow at low, average, and high river flow conditions. Each hydrodynamic scenario was used in a different set of modeled spill scenarios, associated with representative seasonal conditions: low flow (January), average flow (June), and high flow (April). The intent was to develop river currents across and down the river channels to assess the potential for downstream transport of discharged hydrocarbons within the rivers. The hydrodynamic grids each covered an area slightly upstream of the hypothetical release location, reaching downstream to Lake Superior. Hydrodynamics within Lake Superior were not modeled. The model applications were used to simulate the volume discharge, current, and stage of each river and to provide discharge conditions (spatially- and seasonally-varying currents). These currents were used as inputs to the oil dispersion models.

3.3.1 Bad River Model Application

3.3.1.1 River Grid

Two hydrodynamic model grids were created to capture the Bad River flow conditions for use in the SIMAP scenarios (one grid for low and average flow conditions and another for high flow conditions). The high river flow gridding included additional current vectors through an open oxbow downstream of the Existing Route crossing (Horn et al., 2022). That oxbow was closed off in the low and average river flow grid. Each Bad River grid extended from more than 10 km (6.2 mi) upstream (i.e., south) of the Proposed Route crossing to approximately 78 km (48.5 mi) downstream (i.e., north) of the Proposed Route crossing at the entrance of Lake Superior and included the Bad River Slough. Note that the hydrodynamic grids were larger than the model domain. Different size grid cells were used to characterize the hydrodynamics, as higher resolution grid cells are required to capture smaller scale differences in the speed and direction of currents in portions of the river that were more variable (especially at river bends and narrow sections). The higher resolution gridding ensured that there were multiple grid cells spanning the channel, allowing for variable flow (i.e., higher river flow in the center of the channel or near the outer bank). Lower resolution, larger grid cells were used in regions where the river was fairly straight and where the river was wider. Grid cell resolution in the Bad River varied from

approximately 6 m x 6 m (20 ft x 20 ft) to 100 m x 20 m (328 ft x 66 ft) within the study area (detailed maps available in Horn et al., 2022).

3.3.1.2 Boundary Conditions

The edges of the BFHYDRO model grid were designated as either closed boundaries for land or open boundaries to allow the model to be driven by volume flow from upstream and contributing tributaries. The model application was developed assuming that fluid was in hydrostatic balance and the discharge was incompressible.

The boundary conditions specified for the model applications were as follows:

- The flux of water through the channel sides and bottom was zero,

- Bottom friction was negligible,

- The upstream White River discharge rate was used for the inflow boundary at the start of the model domain. For the high flow scenario, additional inflow from the White River was integrated at that junction, and

- The outflow exited through the end of the modeling domain (at Lake Superior), which was defined as an open boundary.

3.3.1.3 Flow Inputs

Flow information for the Bad River was obtained from the USGS NHDPlus dataset (USGS, 2020b). The NHDPlus dataset includes information for each segment of the watercourse. The data were then compared with USGS stream gage data at two points along the Bad River near Odanah, WI and Mellen, WI (USGS, 2020a). It was determined that the NHDPlus dataset provided a more complete set of data (i.e., along the entire river, by segment/reach) to use as inputs to the BFHYDRO model, when compared to the USGS gage data at two points. The hydrodynamic model was therefore tuned to the NHDPlus river flow (low, average, and high) throughout the river, with the USGS gage data used to validate the current velocity. The current speeds predicted for the high, average, and low river flow conditions are depicted for the first half of the modeled extent to highlight the variability in river current by season and location (Figure 3-6 through Figure 3-8). Additional figures depicting current velocities for the lower half of the model extent, including the existing Line 5 crossing of the Bad River (at "the meander") downstream to Lake Superior, are provided in Horn et al. (2022).
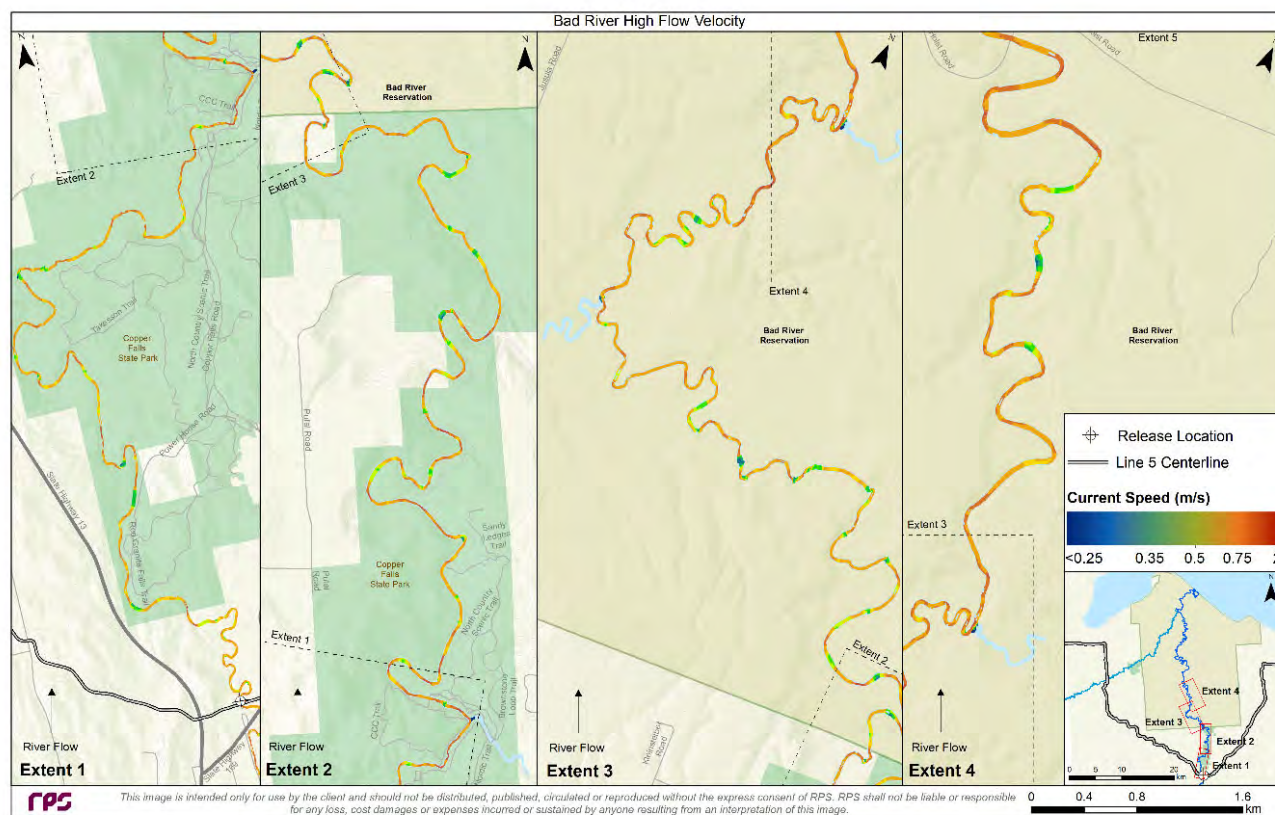
Figure 3-6. Model-predicted current speeds in the first half of the Bad River study area under the high river flow conditions. The inset depicts the full model extent, while the red boxes highlight the segmentation into Extents 1-4 that are provided in the larger panels.
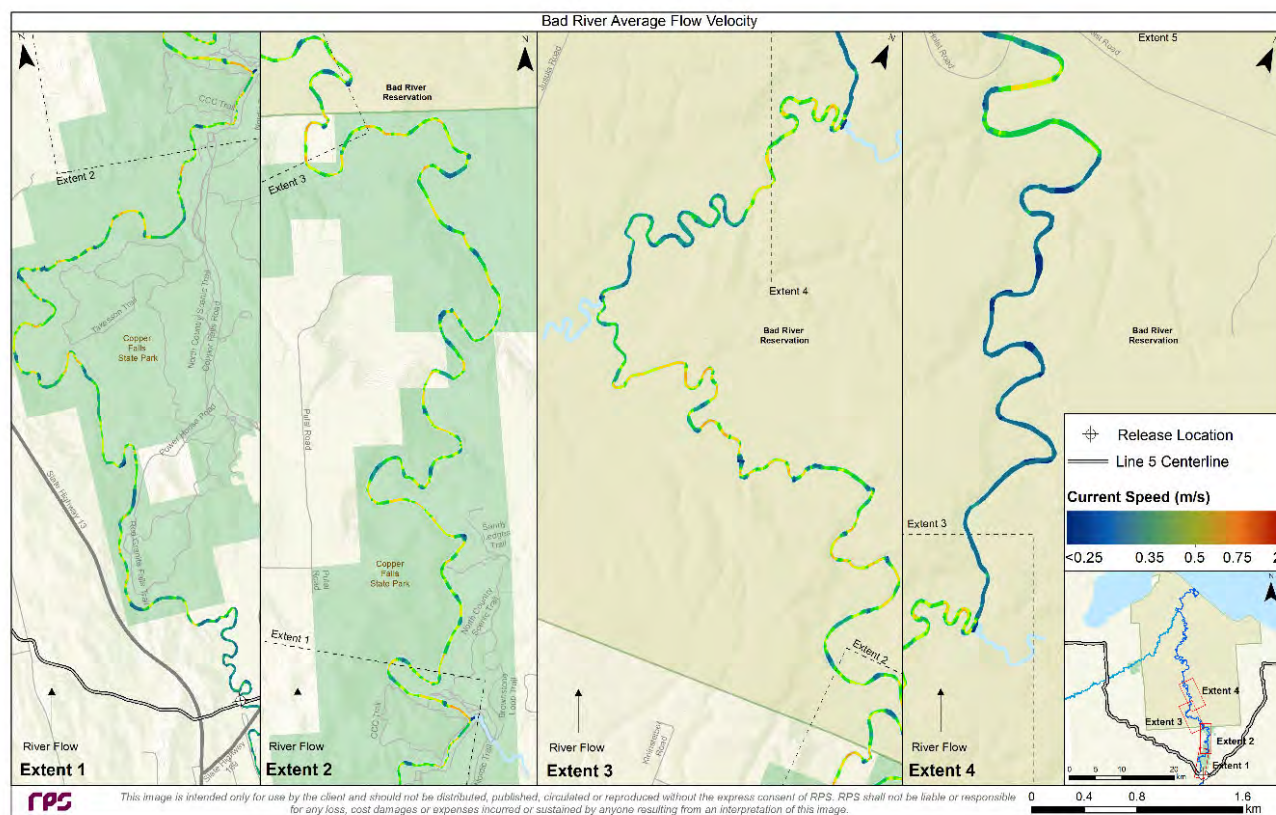
Figure 3-7. Model-predicted current speeds in the first half of the Bad River study area under the average river flow conditions. The inset depicts the full model extent, while the red boxes highlight the segmentation into Extents 1-4 that are provided in the larger panels.
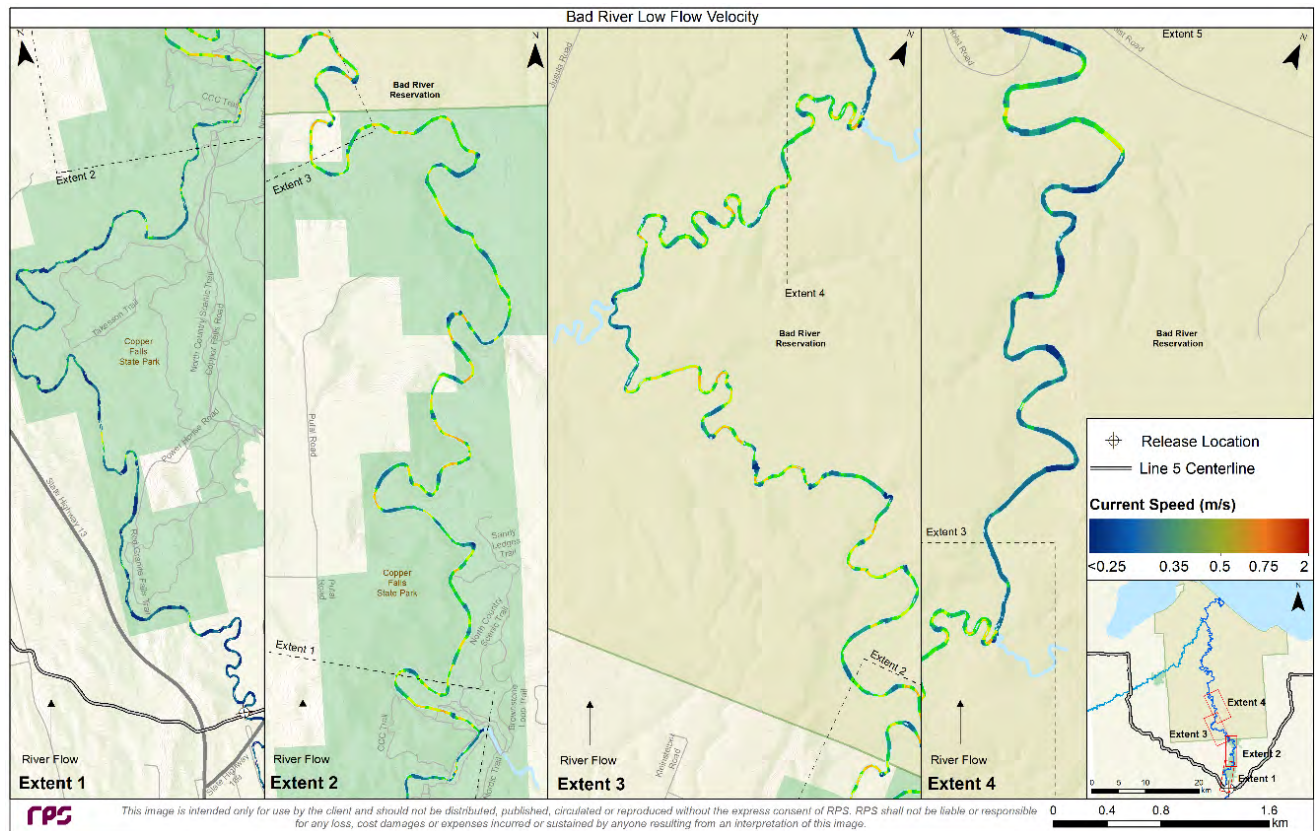
Figure 3-8. Model-predicted current speeds in the first half of the Bad River study area under the low river flow conditions. The inset depicts the full model extent, while the red boxes highlight the segmentation into Extents 1-4 that are provided in the larger panels.

3.3.2   White River Model Application

3.3.2.1 River Grid

One hydrodynamic model grid was created to capture the White River flow conditions for use in the SIMAP scenarios. An unstructured mesh grid (comprised of irregular triangles) was developed to cover the study area and capture varying current flows. The domain starts approximately 2.1 km (1.3 mi) upstream (i.e., southwest) of the Proposed Route crossing of the White River and extends downstream (i.e., northeast) approximately 35.7 km (22.2 mi) to its confluence with the larger Bad River, which continues to flow to the north into Lake Superior. Variable cell edge lengths were used in the unstructured mesh throughout the length of the river. In the upstream portion of the river, cell edge lengths varied from 3 to 10 m, while cell edge lengths varied from 10 to 29 m in the downstream portion. The goal of the grid development process was to ensure that there was sufficient grid resolution throughout the model domain to accurately capture *in situ* conditions while optimizing

computational modeling time. The computational grid for the entire White River domain consists of 46,193 cells and 28,819 nodes. The D-Flow FM model GUI was then used to grid the bathymetry data (Section 3.1), assigning a unique depth value to each cell, either through averaging, for multiple values in a designated cell, or interpolation for the occasional cell where no depth data were available.

3.3.2.2 Boundary Conditions

The edges of the D-Flow FM model grid were designated as either closed boundaries for land or open boundaries to allow the model to be driven by volume flow from upstream and contributing tributaries, including the larger flows from the larger Bad River at the downstream junction. These boundaries facilitated the transfer of external conditions by integrating river flow into the domain, and then allowing the flow to exit through the open boundary at the end of the river.

For the purposes of this model application, it was assumed that the flow was incompressible, the depth was small compared to horizontal length scales (the shallow water assumption), and the fluid was in hydrostatic balance (Deltares, 2022).

The boundary conditions considered for the model applications were as follows:

- The flux of water through the channel sides and bottom was zero,

- Flow boundary conditions were provided as inputs at the start of the model domain (representing inflow from the upstream White River) and at various locations along the channel path to incorporate influxes from different tributaries,

- The outflow exited through the end of the modeling domain (at Lake Superior), which was defined as an open boundary, and

- Free-slip conditions were assumed at the sides.

The models simulations were run until they reached a steady-state condition. The resulting current velocity datasets were used as inputs to the oil spill modeling scenarios.

3.3.2.3 Flow Inputs

River flow information for the White River was obtained from both the USGS stream gage data along the White River (USGS, 2022) and the USGS NHDPlus dataset (USGS, 2020b). The USGS gage is located in the same watercourse segment as the Proposed Route crossing and was therefore directly used to provide boundary flow conditions for the modeling. These data were also used to confirm that the representative low, average, and high river flow conditions in the White River matched those used for the Bad River modeling (January, June, and April, respectively). NHDPlus data, which were available for each segment of the watercourse, were validated against the USGS gage data and used to determine the contributing flow from tributaries over the length of the White River. At the confluence with the Bad River, additional flows from the larger Bad River were used to reflect the combined river flow downstream to Lake Superior. In summary, these various river flow inputs (i.e., gage-based data at the Proposed Route crossing, inflows along the White River from NHDPlus, and Bad River inflows at the confluence) were used to develop the D-Flow 3D hydrodynamic model application for the White River. The current speeds predicted for the high, average, and low river flow conditions demonstrated the variability in river current speeds by season and location (Figure 3-9 through Figure 3-11).
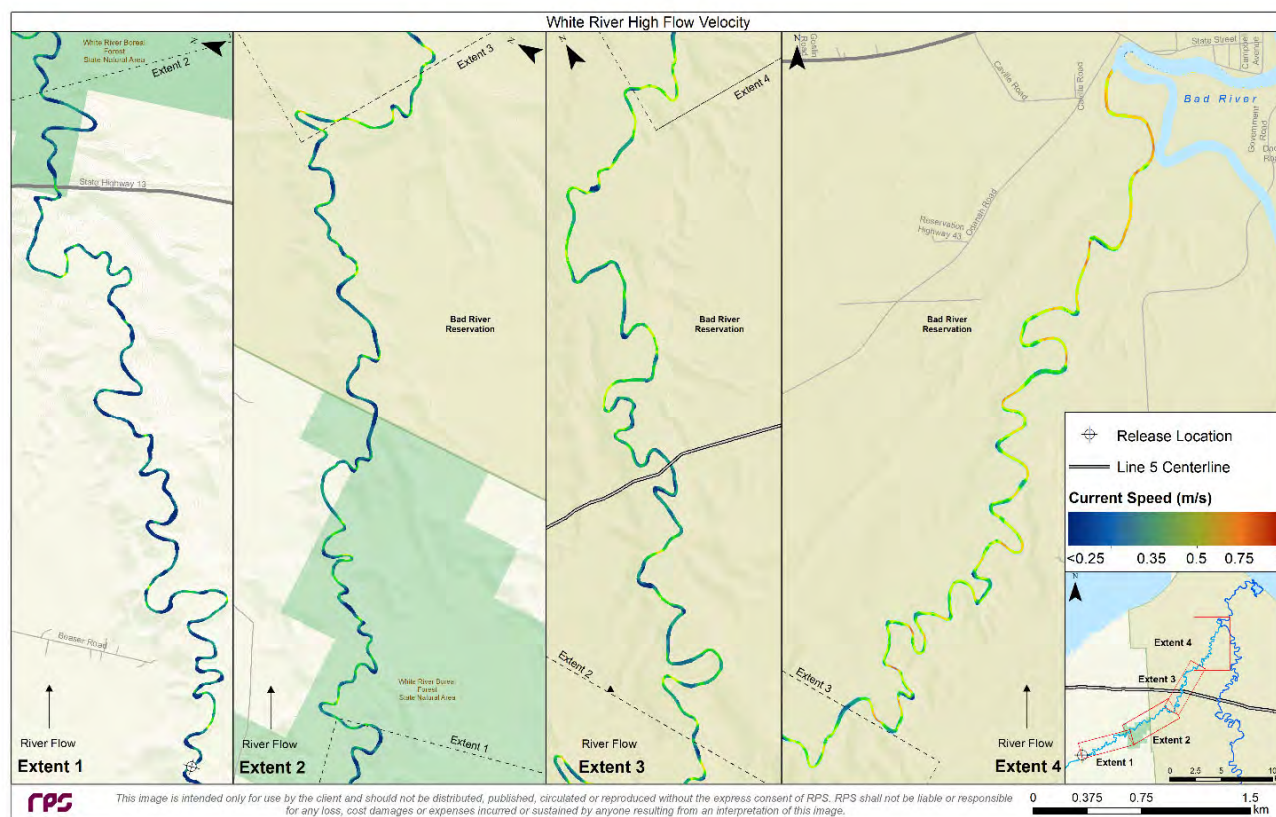
Figure 3-9. Model-predicted current speeds in the White River study area under the high river flow conditions. The inset depicts the full model extent, while the red boxes highlight the segmentation into Extents 1-4, provided in the larger panels.
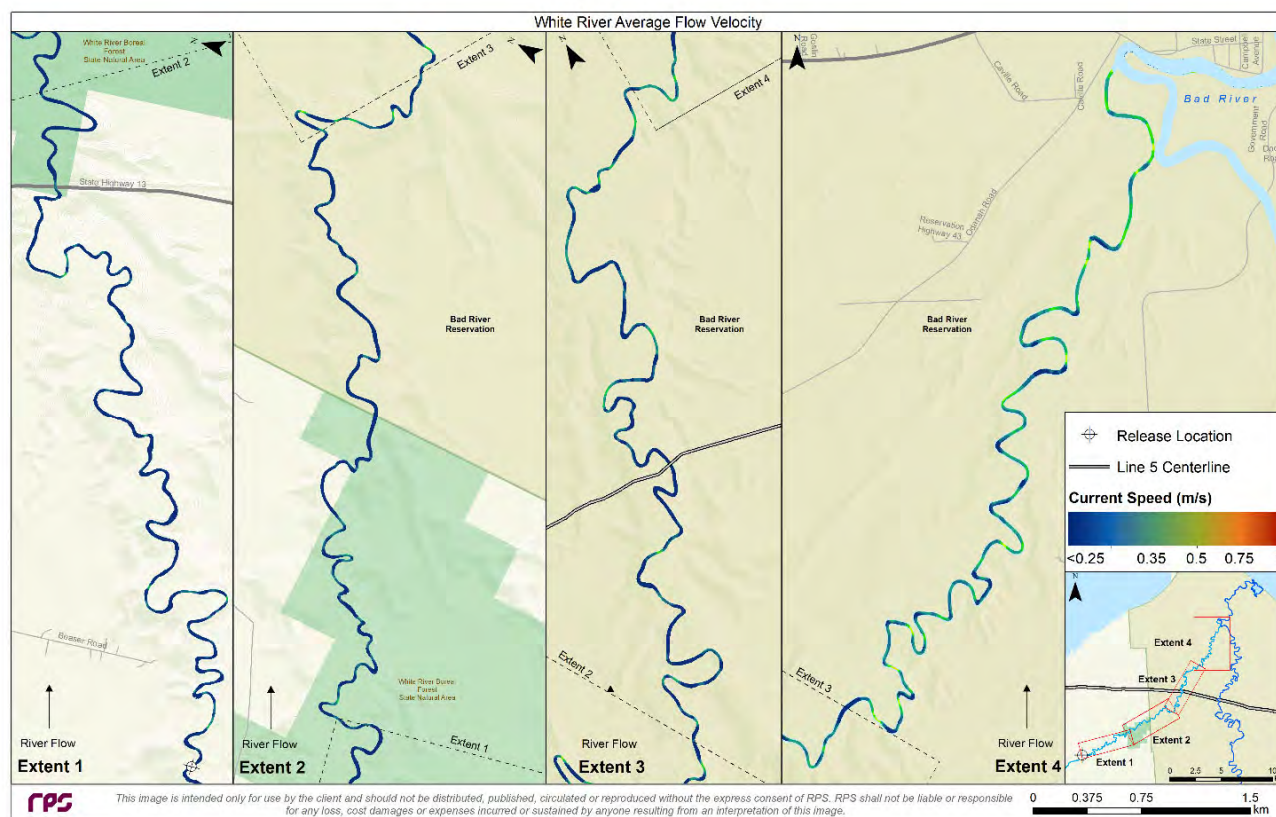
Figure 3-10. Model-predicted current speeds in the White River study area under the average river flow conditions. The inset depicts the full model extent, while the red boxes highlight the segmentation into Extents 1-4, provided in the larger panels.
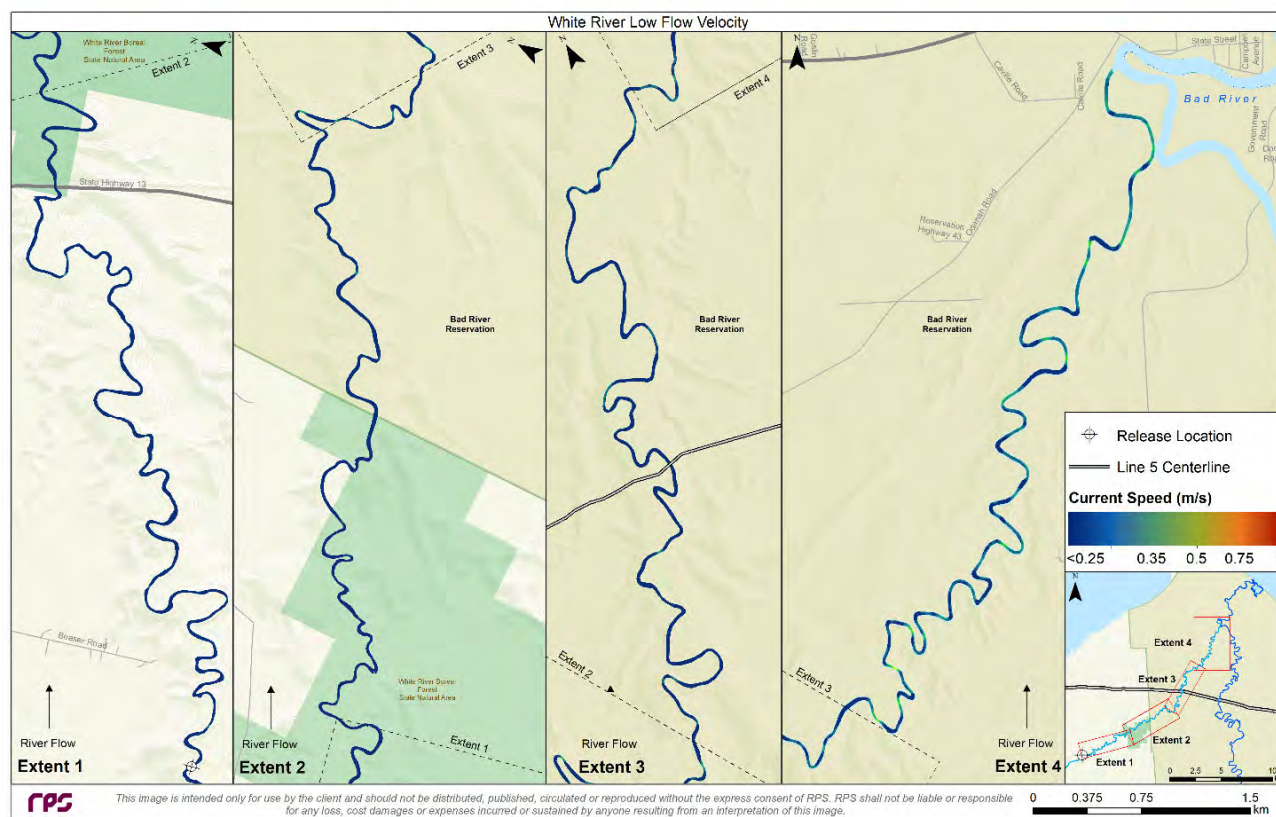
Figure 3-11. Model-predicted current speeds in the White River study area under the low river flow conditions. The inset depicts the full model extent, while the red boxes highlight the segmentation into Extents 1-4, provided in the larger panels.

3.4   Rapids and Waterfalls

There are several waterfalls and areas of rapids within the modeled domain in the Bad River that were considered. These features have the potential to entrain surface oil into the water column. Red Granite Falls and Copper Falls are located 2.6 km (1.6 mi.) and 8.8 km (5.5 mi.) downstream of the Proposed Route crossing of the Bad River, respectively. Both waterfalls are located in the Copper Falls State Park. Red Granite Falls is more similar to a set of large rapids with drops, rather than an actual waterfall, with a cumulative elevation drop of approximately 20 feet (Great Lakes Drive, 2022; Go Waterfalling, 2013). The Copper Falls waterfall is segmented in a multi-tiered series of larger drops, with a cumulative elevation drop of approximately 30 feet (Go Waterfalling, 2009; Territory Supply, 2022; Cheng, 2022). For the purposes of modeling, these waterfalls were included to characterize locations of significant turbulence that could lead to entrainment of surface oil into the water column. While the vast majority of entrained oil would re-surface in quiescent downstream waters, this entrainment can result in sediment interactions within the water column and additional sediment oiling that can be predicted through SIMAP's adsorption and sedimentation algorithms.
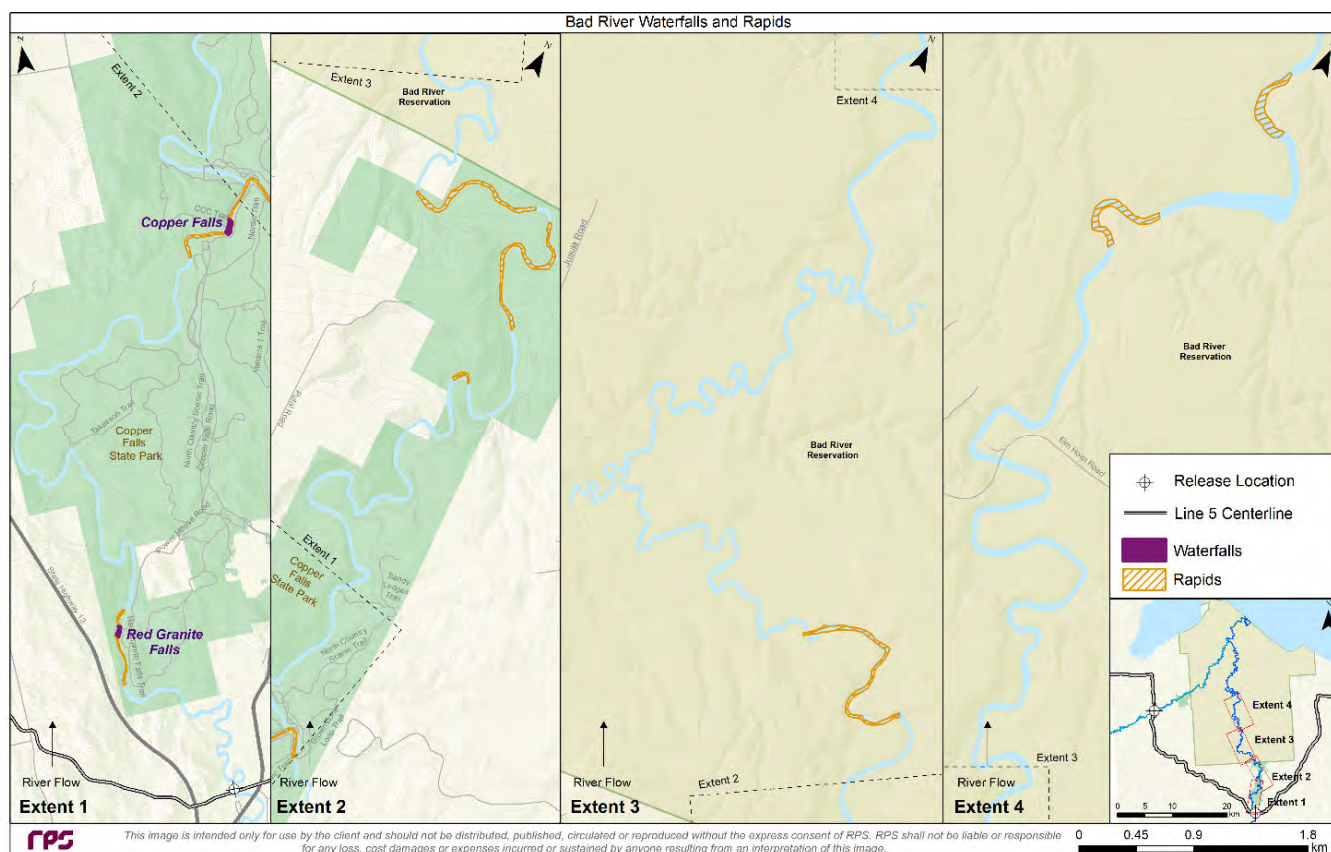
Figure 3-12. Location of waterfalls and rapids modeled in the Bad River.

No waterfalls were present in the White River model domain and therefore did not need to be included in the White River simulations. The crossing of the Proposed Route is located downstream of the White River Flowage at Route 112 in Ashland County. Therefore, a spill from the Proposed Route would not be expected to enter the Flowage or experience turbulence associated with its outflow.

3.5 Suspended Particulate Matter

The amount of total suspended particulate matter (SPM) or sediments in the water column can vary by several orders of magnitude based on location and river flow conditions. Extensive sediment transport and correspondingly high concentrations of SPM are possible during high river flow conditions, especially storm events, and flood conditions. Lower SPM loads, which result in clearer water, typically occur during low river flow conditions such as those found in the winter. Oil droplets may adhere (i.e., stick) to suspended sediments in the water column, which can cause oil or fractions of oil to settle to the bottom as Oil Mineral Aggregates (OMA) or Oil Particle Aggregates (OPA). Data from the USGS gage in Odanah, WI and Mellen, WI, as well as

professional experience, were used to determine the total SPM concentrations during high, average, and low river flow conditions for the Bad River (USGS, 2020b). SPM varied by season ranging from 191 mg/L during high river flow conditions down to 4 mg/L for low river flow conditions (Table 3-5). The settling rate was assumed to be 1 m/day (3.3 ft/day) for all scenarios. However, enhanced vertical turbulence within the water column had the potential to keep sediment in suspension for long periods of time (see Section 3.7).

Table 3-5. Suspended particulate matter concentrations modeled for each seasonal condition.

Season	SPM (mg/L)
High River Flow – April (Spring)	191
Average River Flow – June (Summer)	20
Low River Flow – January (Winter)	4

3.6   Ice Cover

Ice coverage is important to consider, as it may affect the ultimate trajectory and fate of oil within the winter environment. Ice may reduce the quantity or prevent oil from entering a water body altogether. Furthermore, it may affect the potential downstream transport and potential for pooling of oil under ice.

Oil interactions with mobile and immobile ice involve several processes that affect the transport and fate of the oil. Oil discharged under water may become trapped under the ice in ridges and keels or build up along and become trapped (Drozdowski et al., 2011). Many of these interactions and processes are at a finer scale than can be captured in oil spill models using inputs from the available large scale meteorological, hydrodynamic, and coupled hydrodynamic-ice models. SIMAP simulates the influence of ice on net transport and fate processes by considering potential reduction in the surface area of the oil and the water in contact with the atmosphere, which changes the effects of the wave environment, spreading, movements, dissolution, volatilization, and mixing on the discharged oil.

In SIMAP, when oil encounters ice at the surface of the river, it is assumed to trap along the ice edge and remain immobile until ice retreats. In areas deep enough for ice to have subsurface open channels (i.e., where the ice sheet may not extend completely to the riverbed in all areas), SIMAP allows entrained oil to circulate underneath the surface ice using subsurface current data for transport. The 100% ice coverage on the rivers during the winter was assumed to have an ice thickness of 0.1 m. Therefore, subsurface oil spillets continued to move downstream with currents, until the spillets reached the water-ice interface, at which point they "stick." Ice is assumed to prevent all evaporation. However, the soluble fraction of the oil will continue to dissolve into the water column, where it will be transported downstream. Because evaporation has been capped, higher concentrations of soluble constituents are frequently predicted under 100% ice cover conditions.

The presence of ice can shelter oil from the wind and waves (Drozdowski et al., 2011). Thus, weathering processes such as evaporation and emulsification, and behaviors such as spreading and entrainment are slowed (Spaulding 1988). Field data show evaporation, dispersion, and emulsification slowed substantially in ice leads, contrary to some laboratory experiments. Wave-damping, the limitations on spreading dictated by

the presence of sea ice, and temperature appear to be the primary factors governing observed spreading and weathering rates (Sørstrøm et al., 2010).

During the low flow river conditions, corresponding with the month of January, ice cover was assumed to be 100%. With 100% ice coverage, SIMAP stops the processes of evaporation, emulsification, entrainment, volatilization, and surface spreading.

Ice cover was considered in the SIMAP modeling. During winter conditions, complete coverage (100% ice cover) of the water surface is assumed. If a release were to occur into the watercourse from the underground/underwater crossing, then all oil would enter into the water column itself. For the purpose of modeling, oil is assumed to rise through the water column and be trapped by the ice cover at the surface. The model assumes that evaporation is prevented completely (0% evaporation) due to the layer of ice on the water surface. The downstream transport of oil is modeled within river sections at the local water velocity; however, oil pools under the ice in lakes. As modeled in the ice-free conditions, complete shoreline oiling occurs in the complete ice cover season as well. However, rather than referring to true shoreline oiling, this term in the winter would more appropriately be named edge-oiling. Shorelines are set to ice-edge and shoreline retention values are lower than those found during the ice-free seasons. The retention of oil along the banks during winter seasons refers to the oil that would be trapped below the ice surface along the edge of the river in the narrow region between the ice and the bottom. These conservative approximations maximize the extent of potential oiling.

The equilibrium thickness of oil under ice has been measured in many environments. However, the main focus has been in the marine environment, where thicknesses may range from 1-30 centimeters (cm) (Dickins et al. 2008). Freshwater environments, particularly rivers, are quite different than the open ocean, notably with the level of energy within the environment (e.g., waves and other turbulent processes). Assuming that new ice formed in calm conditions and the underside was flat and smooth, the oil will spread beneath ice to an equilibrium thickness based upon the balance between surface tension and buoyancy (Barnes et al. 2013). The equilibrium slick thickness may be determined using the equation of Cox et al. (1980):

$$\delta = -8.5(\rho_w - \rho_o) + 1.67 \quad\quad\quad (9)$$

where δ is the thickness of oil under ice in cm and ($\rho_w - \rho_o$) is the density difference between oil and water. Under the smoothest ice conditions, thicknesses of 5.2 – 11.5 mm (0.20 – 0.45 in) are typical for oils with densities in the range of crude oils (Cox et al. 1980). The minimum stable drop thickness for crude oil under ice is approximately 8 mm (0.31 in) (Lewis 1976). The equilibrium thickness of Bakken was calculated to be 0.07 in. (1.9 mm).

3.7   Horizontal and Vertical Dispersion

Horizontal and vertical dispersion are used to model the randomized mixing at length scales that are smaller than those used in the hydrodynamic dataset. In essence, dispersion is the fine scale mixing that is not captured in coarser hydrodynamic grids under the time scales modeled (1-minute time step). The horizontal dispersion coefficient was assumed to be 5, 2, or 1 m²/s for high, average, and low river flow condition scenarios, respectively, in both the Bad and White Rivers. The vertical dispersion coefficient was assumed to be 1 cm²/s throughout the model domain and is in line with estimated dispersion from bottom roughness. Horizontal dispersion spreads oil laterally, while vertical dispersion may enhance the mixing within the water column, slowing the resurfacing of entrained oils and settling of OMA. Dispersion values are reasonable for coastal and

riverine waters based on empirical data (Fischer, 1973; Okubo and Ozmidov, 1970; Okubo, 1971; Seo and Baek, 2004; Socolofsky and Jirka, 2005) and modeling experience.

3.8 Degradation Rates

Degradation may occur as the result of photodegradation (e.g., photolysis, which is a chemical process energized by ultraviolet (UV) light from the sun, photo-oxidation), and by biological (bacterial) breakdown, termed biodegradation. In the model, degradation occurs on surface floating oil, oil deposited on the shore, entrained oil and dissolved hydrocarbons in the water column, and oil in the sediments. Photodegradation is important for hydrocarbons in floating oil and aromatic hydrocarbons dispersed or dissolved in the upper photic zone where UV light levels are high and not attenuated by SPM in the water column. Biodegradation rates are relatively fast for the soluble and semi-soluble hydrocarbons, higher when these are in the dissolved state or in dispersed small droplets, and relatively slow in floating oil and in sediments (on shore or on the sea floor).

A first-order decay algorithm is used, with degradation rates specified for the whole oil as well as for the individual hydrocarbon components in each of the surface, water column and sediment compartments of the model. The degradation rate (g/day) can be defined as,

$$R_{h,i} = dM_{h,i}/dt = -K_{h,i}C_{h,i} \times V_i \qquad (10)$$

where:

h: hydrocarbon compound (or compound group; i.e., "pseudo-component");

i: environmental compartment (water or shoreline surface, upper and lower water column, and sediments);

$R_{h,i}$: loss rate of the mass of compound (or compound group) h in oil through degradation in environmental compartment i (g/day);

$M_{h,i}$: mass of compound (or compound group) h in oil subjected to degradation in environmental compartment i (g);

$K_{h,i}$: 1st order degradation constant for compound (or compound group) h in environmental compartment i (1/day);

$C_{h,i}$: Aqueous phase concentration of compound (or compound group) h in the environmental compartment i (g/m^3); this is either the solubility saturated concentration or the aqueous phase concentration of compound (or compound group) h calculated based on the partitioning from oil phase and the seawater; the smaller of the two determines the compound (or compound group) h that is available (bioavailability) for biodegradation; and

V_i: The total volume of the environmental compartment i (m^3).

The degradation constant, K_{hi}, may include all degradation processes. Distinct values of K_i may be specified for whole oil and specific constituent groups (n-alkanes, aromatics, etc.) in each compartment.

Degradation rates for each pseudo component group and compartment (surface, water column, and sediments) are user inputs. Default rates are provided in the oil database, supplied with the model, as summarized in Table 3-6 for the 7-component model configuration. These rates are based on data obtained from literature reviews that included estimates for compounds and/or components of crude oil generally and are not specific to the Bad River. Degradation rates in this freshwater environment, especially under low temperature wintertime conditions, may be lower than those modeled. Note that for floating oil, the volatile components (especially AR1

and AL1 of the 19-component model would evaporate (volatilize) before degradation would likely occur. For the semi-volatile components (>AR 4 and >AL4), degradation in floating oil would be considerably slower than volatilization. The rates for residual oil are consistent with studies by Zahed et al. (2011) and Atlas and Bragg (2009). At the time this report was prepared, there were no published oil degradation studies for hydrocarbons within the Bad River. A detailed description of the literature review and derivation of the degradation rate values provided in Table 3-6 may be found in the BOEM OCS Study of the Simulation Modeling of Ocean Circulation and Oil Spills in the Gulf of Mexico including Annex A to Appendix II: Oil Transport and Fate Model Technical Manual, with specific focus on Annex C (French-McCay et al., 2017; Li and French-McCay, 2017).

Table 3-6. Degradation rates (instantaneous, daily) for the 19 modeled pseudo-component groups of oil.

Pseudo-component Group	Instantaneous Degradation Rate (day^{-1})		
	Floating Oil	In Water	Sediments
Aromatic 1	0.01	0.230	0.001
Aromatic 2	0.01	0.290	0.01
Aromatic 3	0.01	0.280	0.01
Aromatic 4	0.001	0.060	0.001
Aromatic 5	0.001	0.326	0.001
Aromatic 6	0.001	0.226	0.001
Aromatic 7	0.001	0.433	0.001
Aromatic 8	0.001	0.405	0.001
Aromatic 9	0.001	0.170	0.001
Aliphatic 1	0.001	0.240	0.001
Aliphatic 2	0.001	0.120	0.001
Aliphatic 3	0.001	0.060	0.001
Aliphatic 4	0.001	0.060	0.001
Aliphatic 5	0.001	0.060	0.001
Aliphatic 6	0.001	0.050	0.001
Aliphatic 7	0.001	0.040	0.001
Aliphatic 8	0.001	0.040	0.001
Aliphatic 9	0.001	0.001	0.001
Residual	0.001	0.020	0.001

Pseudo-component groups are defined in Table 2-2. Volatile (aromatic) components in floating oil would evaporate before degradation would occur (in ice-free conditions) and could be considered inconsequential in the model.

3.9   Oil Characterization and Acute Toxicity

Crude oils and refined petroleum products are complex mixtures of many thousands of different hydrocarbon compounds derived from naturally occurring geological formations. Each has physical and chemical properties (e.g., viscosity, density, solubility, volatility) that reflect its composition and affect its transport and fate, once discharged into the environment (NRC, 2003). The model must out of necessity treat the oil as a mixture of a limited number of components, grouping chemicals by physical and chemical properties.

Line 5 predominantly carries lighter hydrocarbons, including light crude oils through natural gas liquids (NGLs). Based upon its physical and chemical properties, a single Bakken crude oil type was modeled in all scenarios. Bakken Crude Oil is produced in North Dakota, Montana, and the bordering Canadian provinces of Manitoba and Saskatchewan. Bakken is a relatively light crude oil with low density, low viscosity, and a high aromatic content. Bakken Crude Oil is similar to other light crudes and can be considered representative of many light crude oils, including many Canadian crudes, but is a conservative selection for this type of effects assessment as the high aromatic content has the potential to maximize the potential for impacts in the environment. Bakken was therefore conservatively selected to be the "worst-case" compound for in-water effects following a release because it would be more persistent than a NGL (which would evaporate rapidly and nearly completely) and it has a higher percentage (when compared to similar oil types) of BTEX compounds and other monocyclic aromatic hydrocarbons (MAHs), making up 2.5-4% of the total by mass, which would tend to maximize in water effects.

Summaries of the physical and chemical parameters for the Bakken crude oil used in the modeling are provided in Table 3-7 and Table 3-8. Numerous sources were used to gather a sufficient amount of information required to simulate the oil type (Environment Canada Oil Property Database, 2017; API, 2015). As was mentioned previously, the oil (and its many thousands of different components) was broken down into 19 compartments or pseudo-component groups consisting of nine aromatic, nine aliphatic, and the higher molecular weight residual fraction. While these groupings carry titles that are very specific in the field of chemistry, they are meant to imply different behaviors in the model. Aromatic compounds in the SIMAP model are those that are both volatile and soluble, meaning they can evaporate to the atmosphere and dissolve into the water column. Aliphatic compounds in the SIMAP model are those that are volatile and insoluble, meaning they can evaporate to the atmosphere, but cannot dissolve into the water column. The residual fraction is allowed to decay with time but is otherwise considered relatively inert within the model. Bakken is a light crude oil with low viscosity that is similar to those of other light crudes, but with a slightly higher percentage of BTEX compounds and other MAHs (2.5-4%), when compared to similar oil types (Table 3-8).

Table 3-7. Physical parameters of Bakken crude oil simulated in SIMAP.

Oil Property	Value
Oil Name	Bakken
Oil Type	Crude
Surface tension (dyne/cm)	19.62
Pour Point (°C)	0
API Gravity	41.8
Density (g/cm) at 16°C	0.822196
Viscosity (cP) at 15°C	3.80
Viscosity (cP) at 25°C	2.99
Emulsion maximum water content (%)	0.0

Table 3-8. Chemical parameters of Bakken crude oil simulated in SIMAP. Aromatic (AR), aliphatic (AL), and total hydrocarbon concentration (THC) and percentage composition of fresh whole oil for Bakken crude. THC is the sum of AR and AL.

Bakken Crude Oil By Pseudo-Component Group	% AR	% AL	% THC
1	1.6900	6.2822	7.9722
2	0.8770	4.8140	5.691
3	0.0810	4.4646	4.5456
4	0.1863	6.6321	6.8184
5	0.4388	10.9252	11.364
6	0.4882	4.0574	4.5456
7	0.1292	11.2348	11.364
8	0.1295	6.6889	6.8184
9	13.6000	N/A	13.6000
		Residual Percent:	27.2808
		Total Volatile Percent:	72.7192
		Total Aromatic Percent:	17.6200
		Total Aliphatic Percent:	55.0992

AR adjusted from calculated THC values from distillation data from API (2015). AR and THC data used for the adjustment calculations are from Dangerous Goods Transport Consulting (2014).

AL calculated by difference THC- AR.

THC calculated from distillation data from API (2015).

For oil spills at the water surface, 6- to 8-carbon MAHs (i.e., benzene, toluene, ethybenzene and xylenes known as BTEX), may actually have less effect on aquatic organisms than PAHs after the initial release for the following reasons. BTEX compounds are soluble and fractions would dissolve and become bioavailable. However, BTEX are also extremely volatile, and have the potential to evaporate from the water surface and volatilize from the water column very quickly following their release. BTEX compounds evaporate faster than they dissolve, such that toxic concentrations are not reached.

The lowest acute toxicity threshold for aquatic freshwater organisms for benzene is 7.4 ppm (roughly equivalent to 7,400 µg/L) based on standardized toxicity tests (USEPA, 2000). The threshold for toxic effects for BTEX compounds is approximately 500 µg/L for sensitive species (French-McCay, 2002). However, small concentrations of BTEX in the water will be diluted to levels well below toxic thresholds quickly following their release, as a result of dispersion and evaporation. Thus, the assumed values for BTEX concentrations in the oil, as well as their fate, may have less influence on the predicted model results for biological effects. The percentages of PAHs and more highly substituted benzenes (i.e., with 9 or more total carbons in the molecule), which have a higher likelihood of remaining within the environment for a longer period of time, are likely to have a more significant influence on the model results. Thus, data for well-defined oils were used to develop acute toxic endpoints used in the modeling, and the LC_{50} values assumed were for total dissolved PAH concentrations in the water (LC_{50mix}, see Section 2.1.6). The substituted benzenes have similar toxicity to the soluble and sparingly-soluble PAHs.

To estimate LC_{50mix} values for dissolved PAHs in the water, the additive model described in French-McCay (2002) was used (Section 2.1.6). French-McCay (2002) estimated LC_{50mix} = 50 µg/L for typical fuels at infinite exposure time and for the average species and life stage. Ninety-five percent of species and life stages have LC_{50} values between 5 and 400 µg/L.

The LC_{50} values above are for the concentration of dissolved PAHs that would be lethal to 50% of organisms exposed for a long enough time for mortality to occur. For PAHs, this is for at least 10 days of exposure at warm temperature. For chemicals in general, toxicity is higher, and the LC_{50} lower, at longer time of exposure and higher temperature (French et al., 1996; French-McCay, 2002). The model corrects this LC_{50} to temperature and duration of exposure for each group of organisms exposed.

For this exposure assessment, modeling was performed using two acute toxicity endpoints for in-water effects: the LC_{50mix} for species of average sensitivity (50 µg/L) and for sensitive species (5 µg/L). The lower value (5 µg/L) would be protective of 97.5% of species or life stages in the aquatic environments of concern. For surface and shoreline effects, a toxicity endpoint of 10 µm was used.

While it is understood that benzene can result in negative effects, it is only one of hundreds of thousands of compounds in oil and the extremely high volatility and solubility of benzene typically only result in short-lived elevations of this component in the water column. Many other compounds in oil have the potential to cause negative effects and/or acute mortality as they are more persistent than the benzene which volatilizes to the atmosphere. It is very likely that downstream of the initial release, compounds other than benzene may be responsible for the negative effects including the pro-active closure of downstream water intakes. For this reason, total dissolved hydrocarbon concentrations (DHC) are investigated in this study. DHC represents the total amount of hydrocarbons that are in solution.

3.10 Response Inputs

In the unlikely event of a release, there are a range of tactics that Enbridge and its contracted Oil Spill Removal Organizations (OSROs) can deploy based on the specific release, the conditions at the release location, and sites downslope or downstream. As outlined in the Emergency Response Mitigation section of the Oil Spill Report, Enbridge provided RPS with a list of response equipment and tactics that would be available in the event of a release into the Bad River or White River (Enbridge, 2022a). This list included containment booms and various skimmer resources that could be deployed by Enbridge and contracted OSROs, who maintain nearby staging locations with more equipment than that listed in the Oil Spill Report, as well as other types of equipment not modeled here (e.g., X-Tex fabric, pom-pom snares, and sorbent boom for minimizing sheens and capturing submerged).

Enbridge's emergency response for the modeling included seven Control Points (CPs) in the Bad River and five CPs in the White River, downstream of the respective crossings with the Proposed Route (Figure 3-13-Figure 3-16). While the CPs are predetermined locations from where spill containment and recovery operations may be conducted with the expectation of a high degree of success, a response would not be limited by these pre-established CPs. In the event of an actual release, containment and recovery/collection locations would be tailored to the specific release, the environmental conditions at the time, and the exact location of the oil when responders arrived to target containment and collection activities most effectively. Enbridge uses a tracking system that assigns unique IDs to each CP, following the naming mechanism of region (SUR, Superior Region), control point (CP), tracking number (e.g., SURCP0796). Any SURCP that is included in this assessment is a part of Enbridge's operational emergency response tracking system. Because the Proposed Route has not been constructed, some formalized CPs are not in the operational tracking system used by Enbridge. Therefore, additional CPs designed for consideration of the Proposed Route were developed and included. The naming convention for these new CPs include BR for the Bad River and WR for the White River.

Individual information sheets were compiled for each successive downstream CP, providing planned site-specific equipment lists, deployment layouts, and the associated timings for activation of each (Enbridge, 2022a). The timings factored in mobilization and transport from staging locations, through deployment at the timepoint that containment and collection would begin. The activation times at each CP reflect the sum of a 2-hour notification time and the location-specific travel time based on a 35 miles per hour (mph) speed average from the staging location to the CP access. The use of a conservative 35 mph average speed reflects planning standards as identified in the 2021 guidelines for the US Coast Guard OSRO Classification Program (as per 33 CFR § 154), which considers potentially adverse travel conditions (e.g., winter snow, severe storm) that might impact the ability to access a CP location. For the purposes of modeling, an additional 15 minutes was added to account for the period of time under which a release was identified and communication of the spill was relayed to internal responders and external OSROs. It is likely that in a real-world release, these communications could be completed in less time.

Collectively, the response tactics planned at each CP were developed into a series of inputs that were used in the mitigation modeling scenarios. The exact equipment to be used at each CP included varying lengths of containment booms, a number of different skimmer resources, specific equipment layouts, and varying timing for activation. This information was used to develop the Modeled Control Points (MCPs) along the Bad River (Figure 3-13 and Figure 3-14) and White River (Figure 3-15 and Figure 3-16) for modeling, which included each of the MCP-specific tactics and equipment for containment and collection (Figure 3-17 to Figure 3-29). These MCPs were used as inputs to the mitigated modeling scenarios (Tables 2-2 and 2-3 from Oil Spill Report), in conjunction with derated equipment-based recoveries (Table 2-1 from Oil Spill Report), reduced

containment efficiencies (99% for boom), and environmental condition thresholds used to limit the window of potential equipment application (Table 3-9). In low river flow wintertime conditions, if oil was predicted to reach the identified CPs, the most upstream MCPs within the response timeframe were used in the modeling.

Together, the conservatively-based recovery rates and timings used in the modeling depict scenarios where emergency response efforts and success could be reasonably lower than might occur in real-world circumstances. The modeling does not account for full-scale OSRO deployment from additional equipment inventories or emergency response mitigation techniques other than direct containment (through booming) and collection (through skimming). Therefore, submerged oil recovery techniques, sorbent or protective booming, shoreline cleanup, burning, the use of underflow dams, and a number of other strategies and techniques that may improve containment and collection efficiencies were considered but not modeled in the simulations.

Notably, the modeling does not account for the establishment of an additional barrier (as part of overall tactical response planning) that would be used to limit impacts into a watercourse at a point downstream of the expected near-term oil trajectory. In a real-world release, the location of an additional barrier and associated tactics would be determined based on field observations and input from the ICS Operations Sections Chief and Unified Command (Enbridge, 2022c). Resources beyond those modeled in this Technical Appendix would be mobilized, not subtracting from mitigation efforts otherwise available at the upstream CPs. The planned strategy for an additional barrier (Enbridge, 2022c) is as follows:

- Contains sufficient reserve resources for containment and recovery of larger amounts of surface oil in the unlikely event that a loss of containment from an upstream CP occurred;

- Addresses sheens and micro surface oils through the use of sorbents including; sorbent pads, Pillows, Sorbent Sweeps, Pom-poms/snares, sorbent socks;

- Includes tactics that would address entrained and submerged oils that may resurface through the use of filter fences and filter fabrics;

- May include protective and exclusionary booming for environmentally sensitive areas or areas of high consequence (equipment includes vinyl river boom, vinyl creek boom, vinyl shore seal boom, AquaDams™, Tiger Dams™, Water-Gate dams, etc.). The Inland Spill Response Tactics Guide (Enbridge, 2018) is an internal Enbridge document that can be used to select and implement such equipment from a cache of Enbridge-owned oil spill response equipment during the first 72 hours of the response.

Based on the trajectory modeling conducted in this assessment (Table 4-1, Table 4-2), oil would be predicted to reach Highway 2 between 44 hours and 87 hours after release, depending on the release location and river flow conditions. The resources for an additional barrier could therefore be positioned into an area downstream of Highway 2 and upstream of the entry point to the Bad River Slough complex and Lake Superior; the exact location would be determined and adjusted based on real-time observations of the watercourse characteristics at the time of release. These resources were not modeled here due to the dynamic and spill-specific nature of the potential deployment, as well as the variety of equipment that might be used to address very small quantities of oil on the surface (e.g., sheens) or in the water column (i.e., entrained oil). However, such resources would likely be able to stop small amounts of oil (e.g., sheens, which are less than 1/1,000[th] the thickness of heavy black oil; Table 2-1) from transporting beyond this point in the event of a real release from the pipeline.

Figure 3-13. MCP locations modeled on the Bad River (upstream portion).
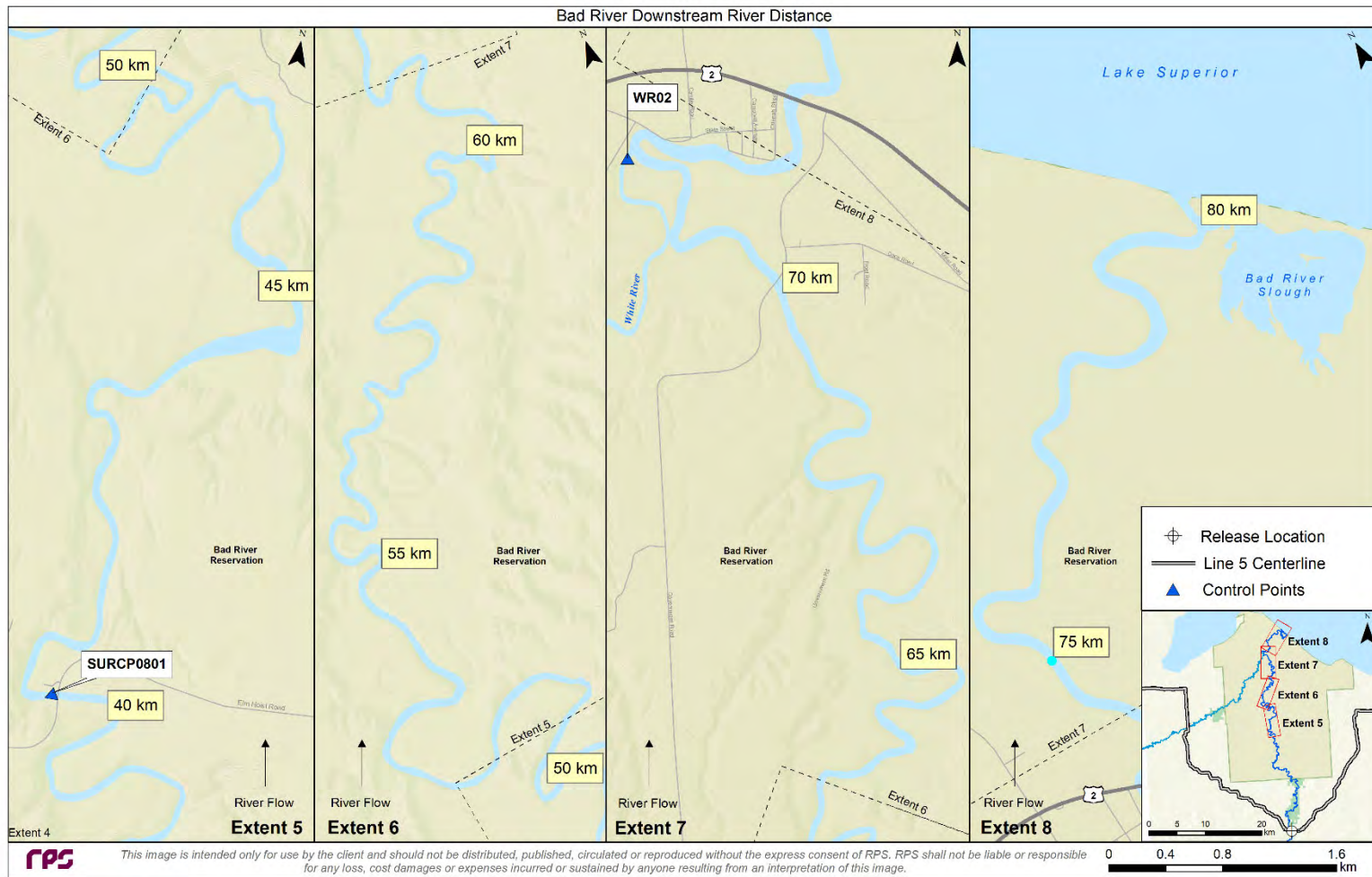
Figure 3-14. MCP locations modeled on the Bad River (downstream portion). An additional barrier would likely be deployed between Highway 2 (Extent 7) and Lake Superior (Extent 8).
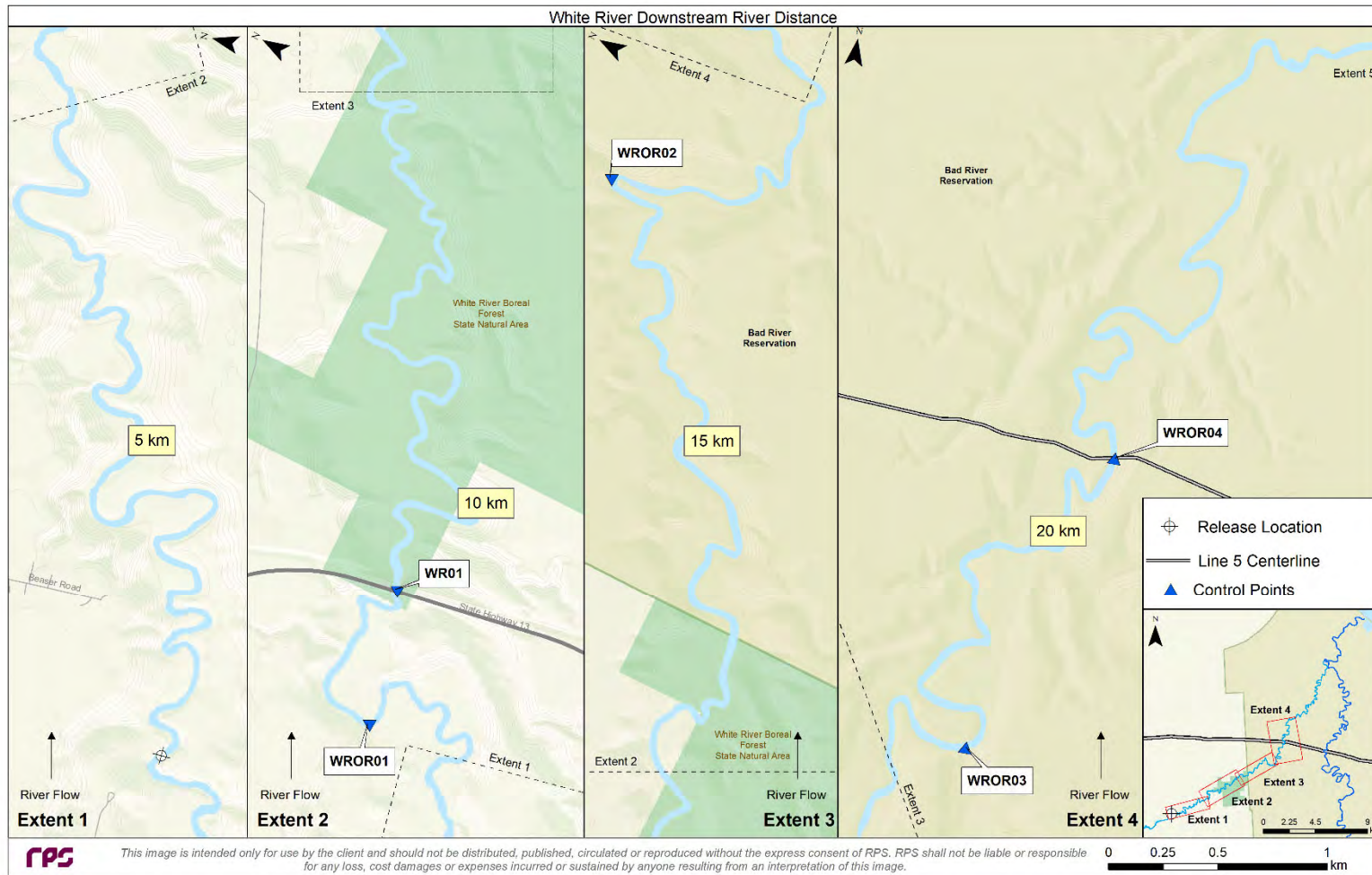
Figure 3-15. MCP locations modeled on the White River (upstream portion).
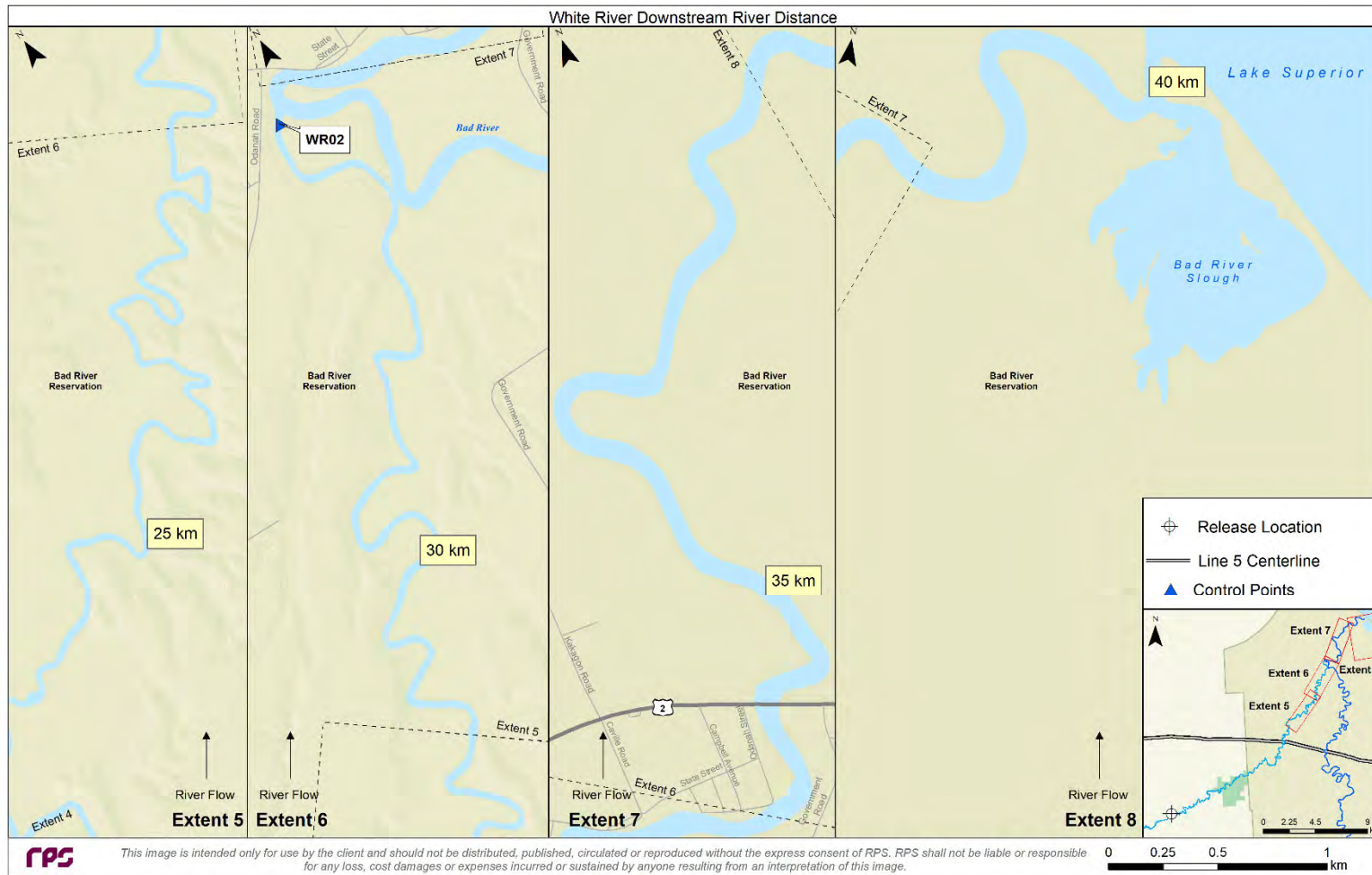
Figure 3-16. MCP locations modeled on the White River (downstream portion).
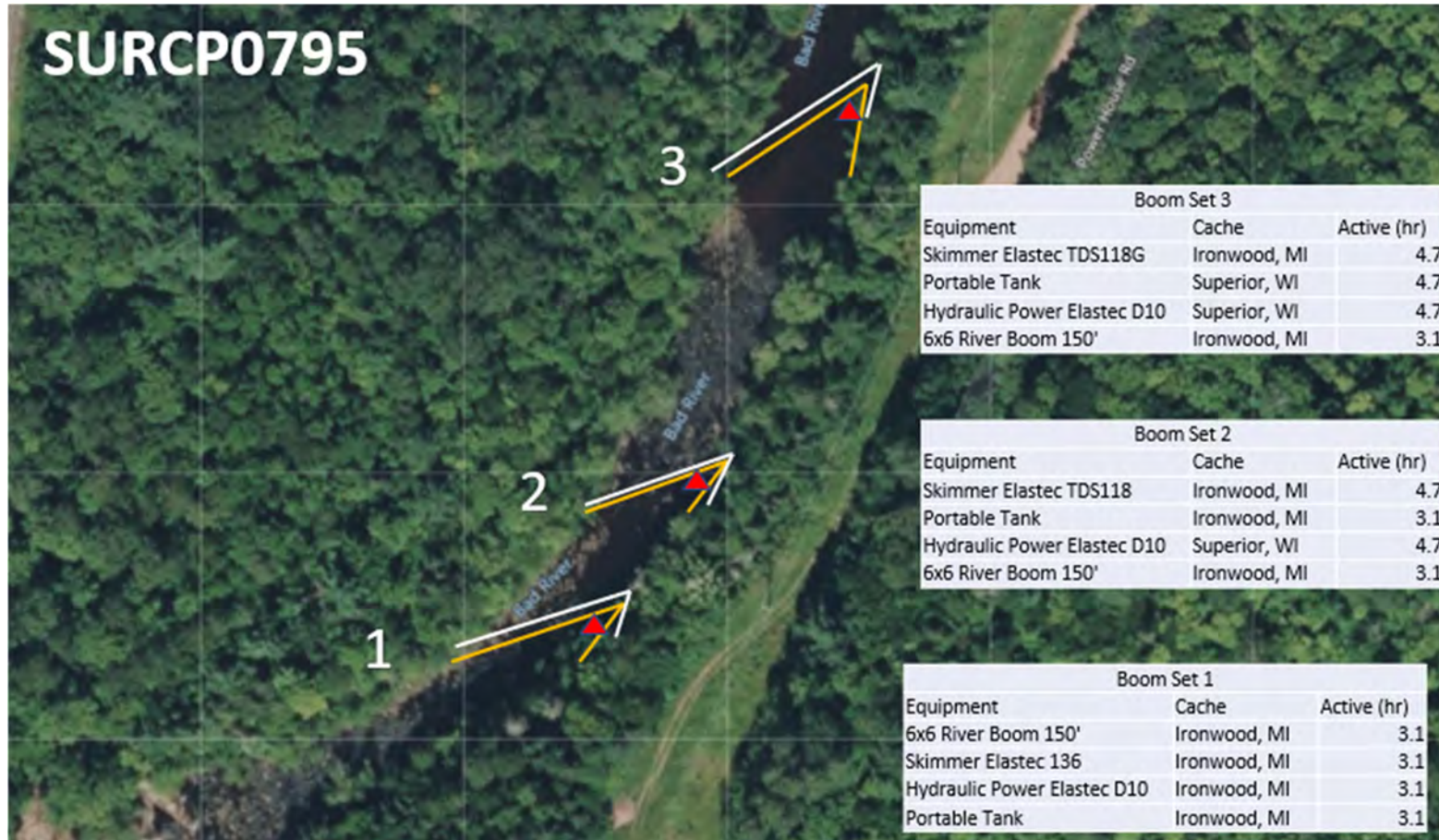
Figure 3-17. Response layout for MCP SURCP0795 on the Bad River. Red triangles are skimmer placement locations, orange lines represent containment boom, and white lines represent sorbent boom. The sorbent boom was not simulated in the model.
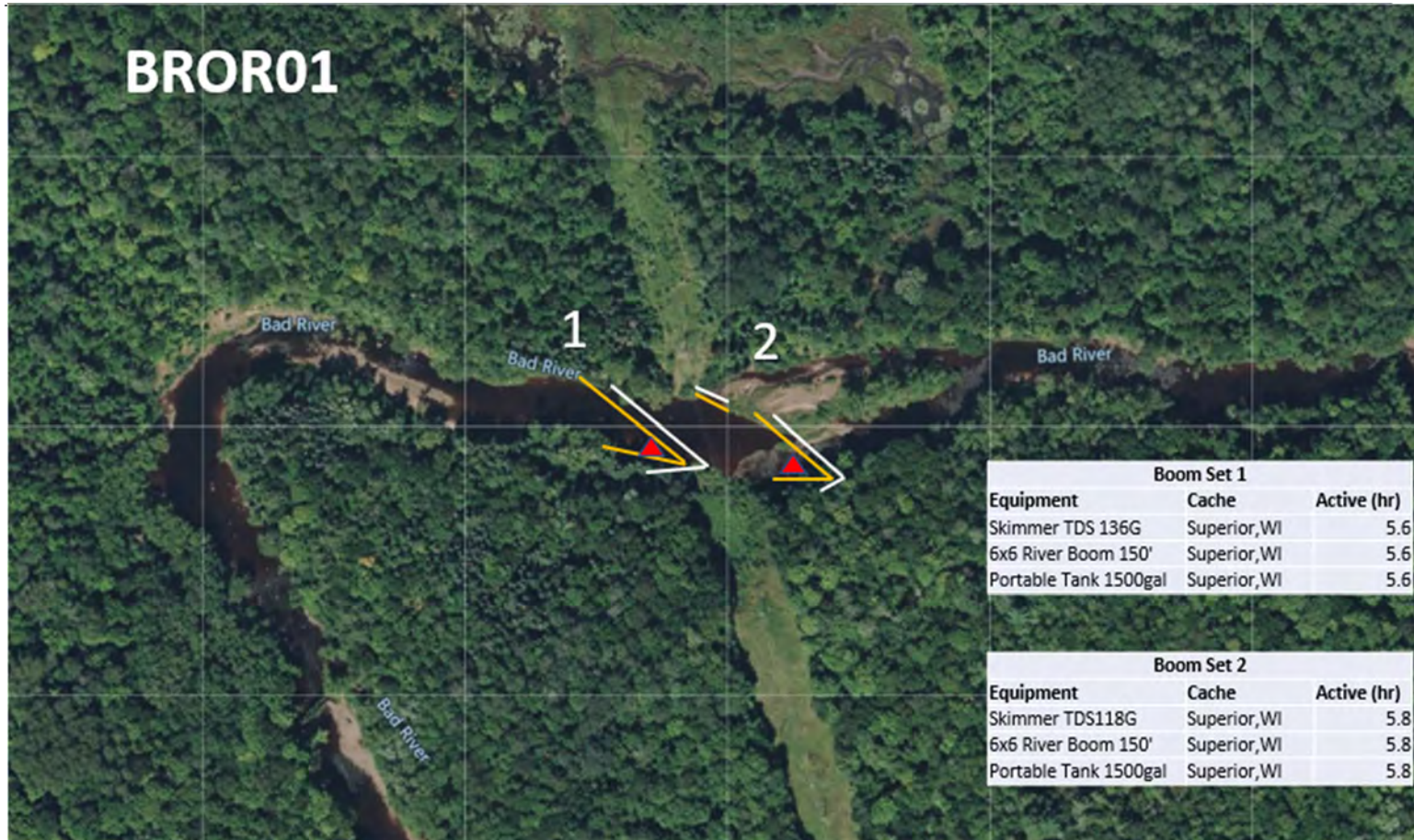
Figure 3-18. Response layout for MCP BROR01 on the Bad River. Red triangles are skimmer placement locations, orange lines represent containment boom, and white lines represent sorbent boom. The sorbent boom was not simulated in the model.
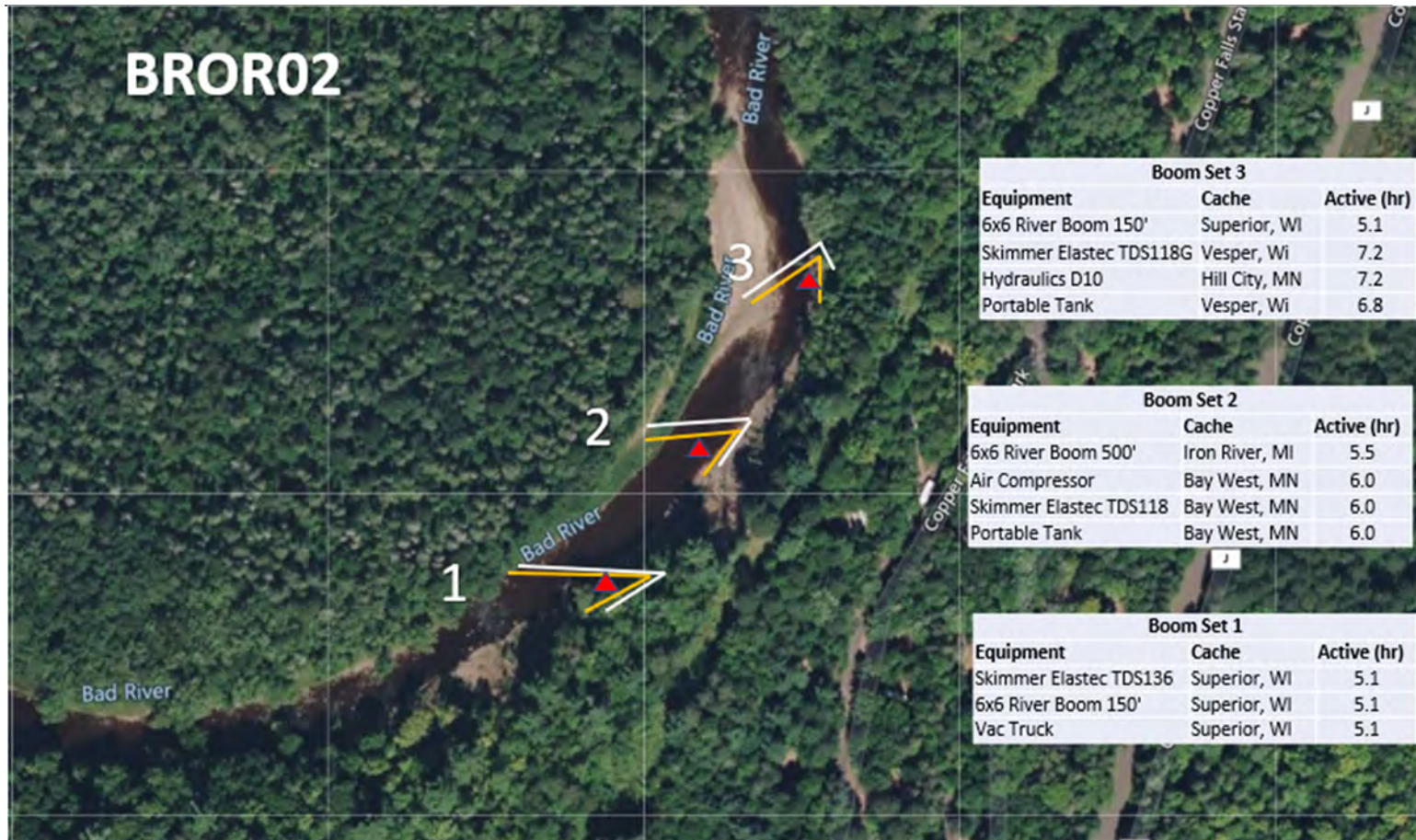
Figure 3-19. Response layout for MCP BROR02 on the Bad River. Red triangles are skimmer placement locations, orange lines represent containment boom, and white lines represent sorbent boom. The sorbent boom was not simulated in the model.
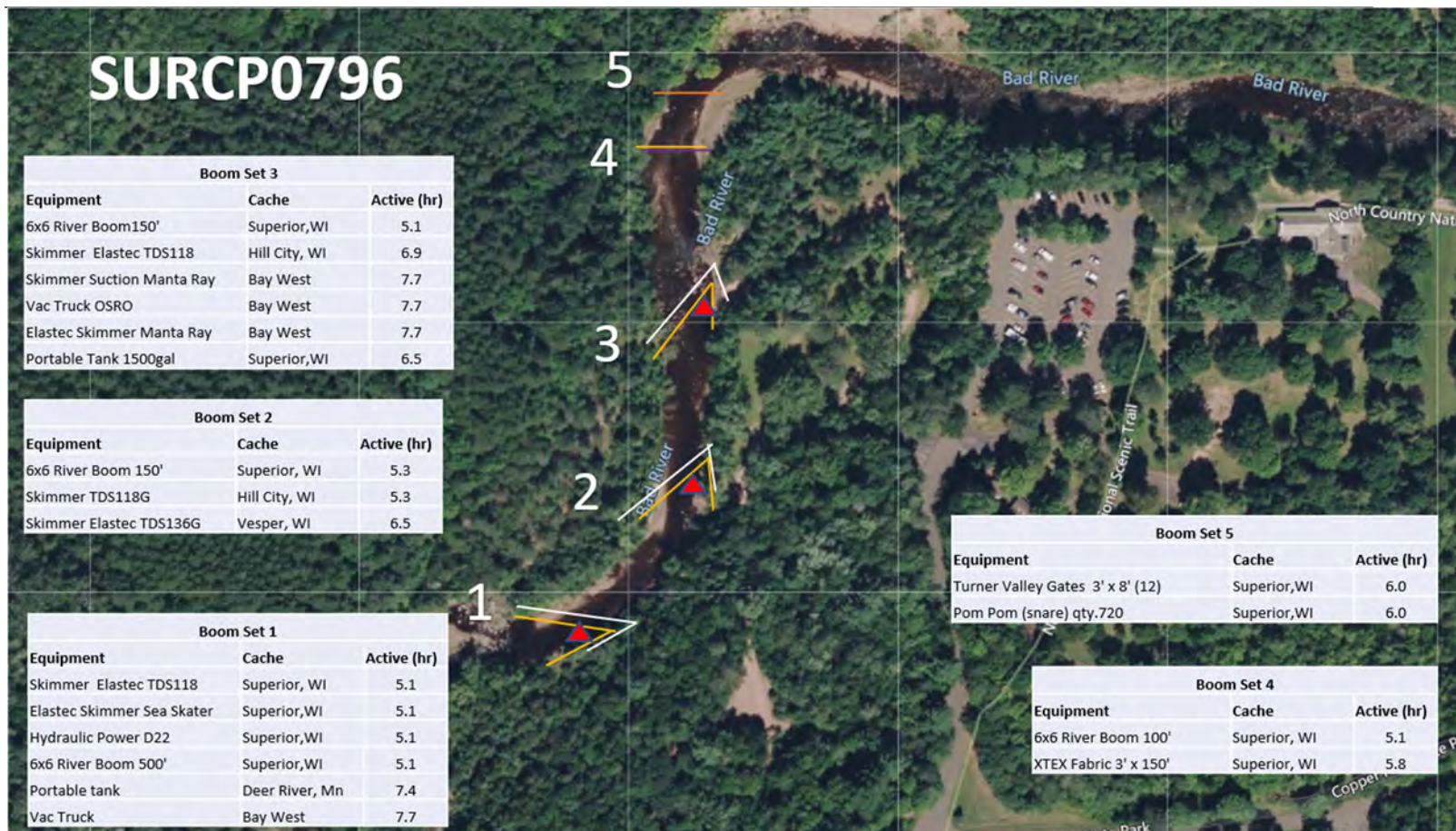
Figure 3-20. Response layout for MCP SURCP0796 on the Bad River. Red triangles are skimmer placement locations, orange lines represent containment boom, white lines represent sorbent boom, the purple line represents X-Tex fabric, and the dark orange line at location 5 represents Pom Pom snares. The sorbent boom, X-Tex fabric, and Pom Pom snares were not simulated in the model.

Figure 3-21. Response layout for MCP SURCP0797 on the Bad River. Red triangles are skimmer placement locations, orange lines represent containment boom, and white lines represent sorbent boom. The sorbent boom was not simulated in the model.
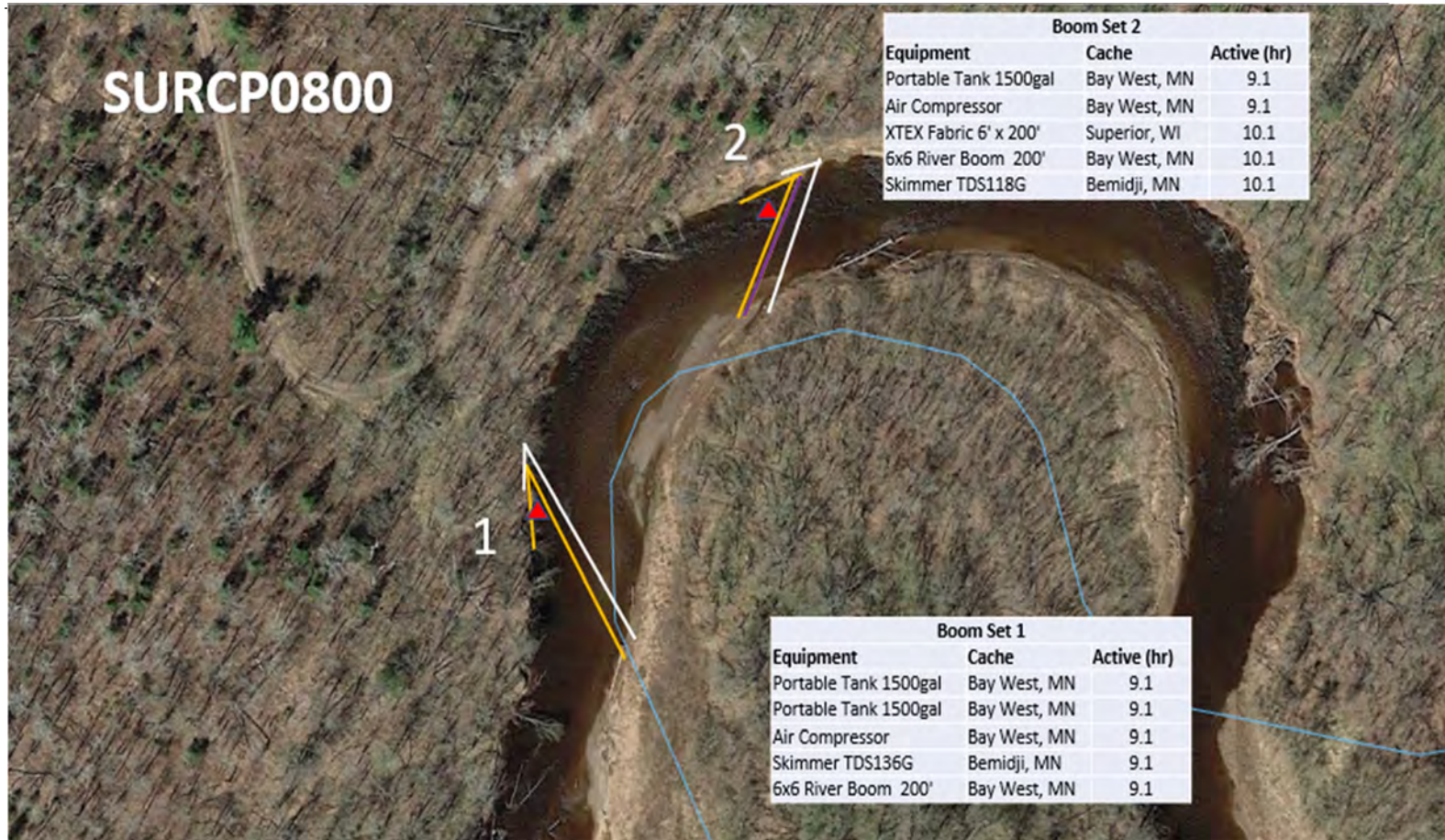
Figure 3-22. Response layout for MCP SURCP0800 on the Bad River. Red triangles are skimmer placement locations, orange lines represent containment boom, white lines represent sorbent boom, and the purple line represents X-Tex fabric. The sorbent boom and X-Tex fabric were not simulated in the model.
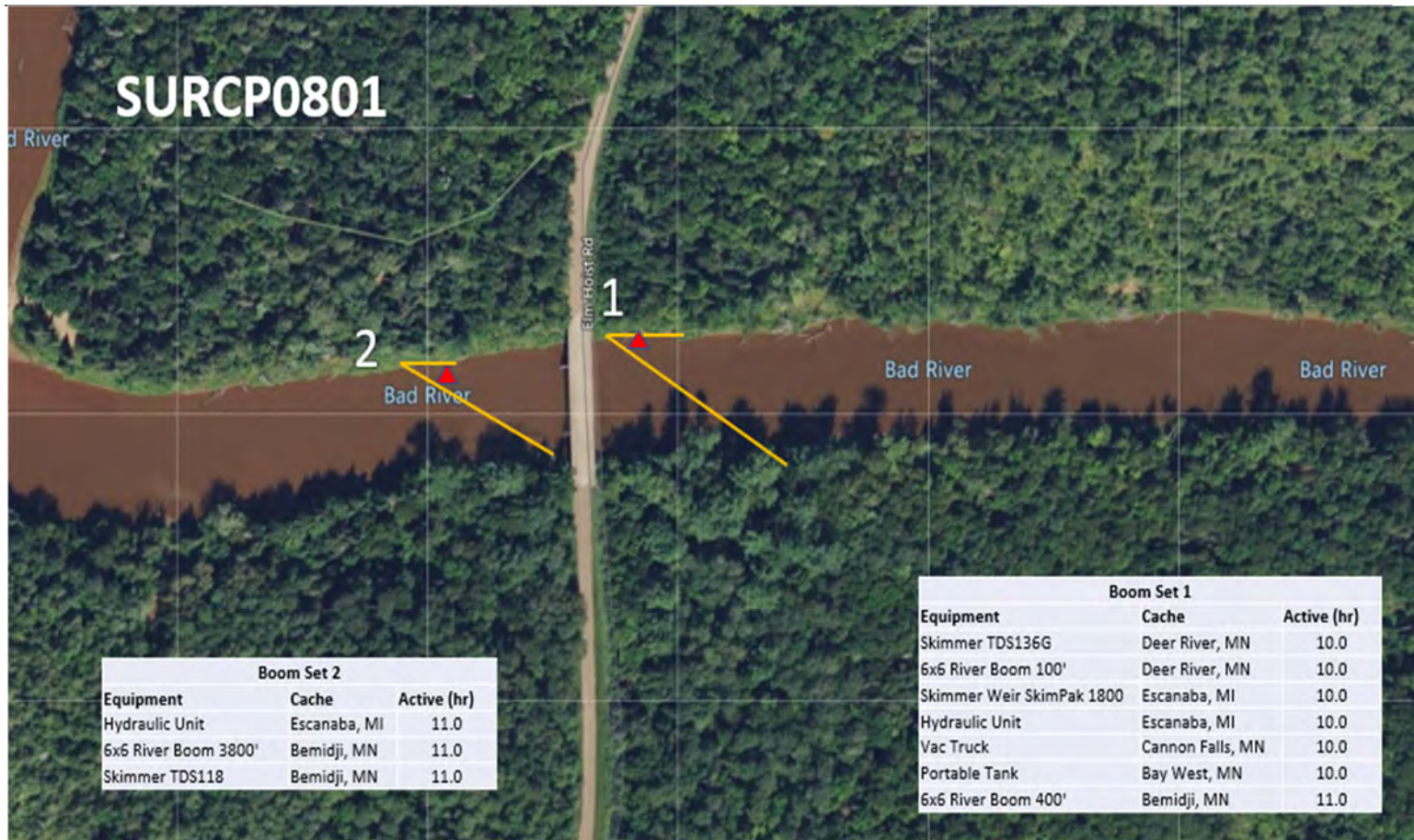
Figure 3-23. Response layout for MCP SURCP0801 on the Bad River. Red triangles are skimmer placement locations and orange lines represent containment boom.
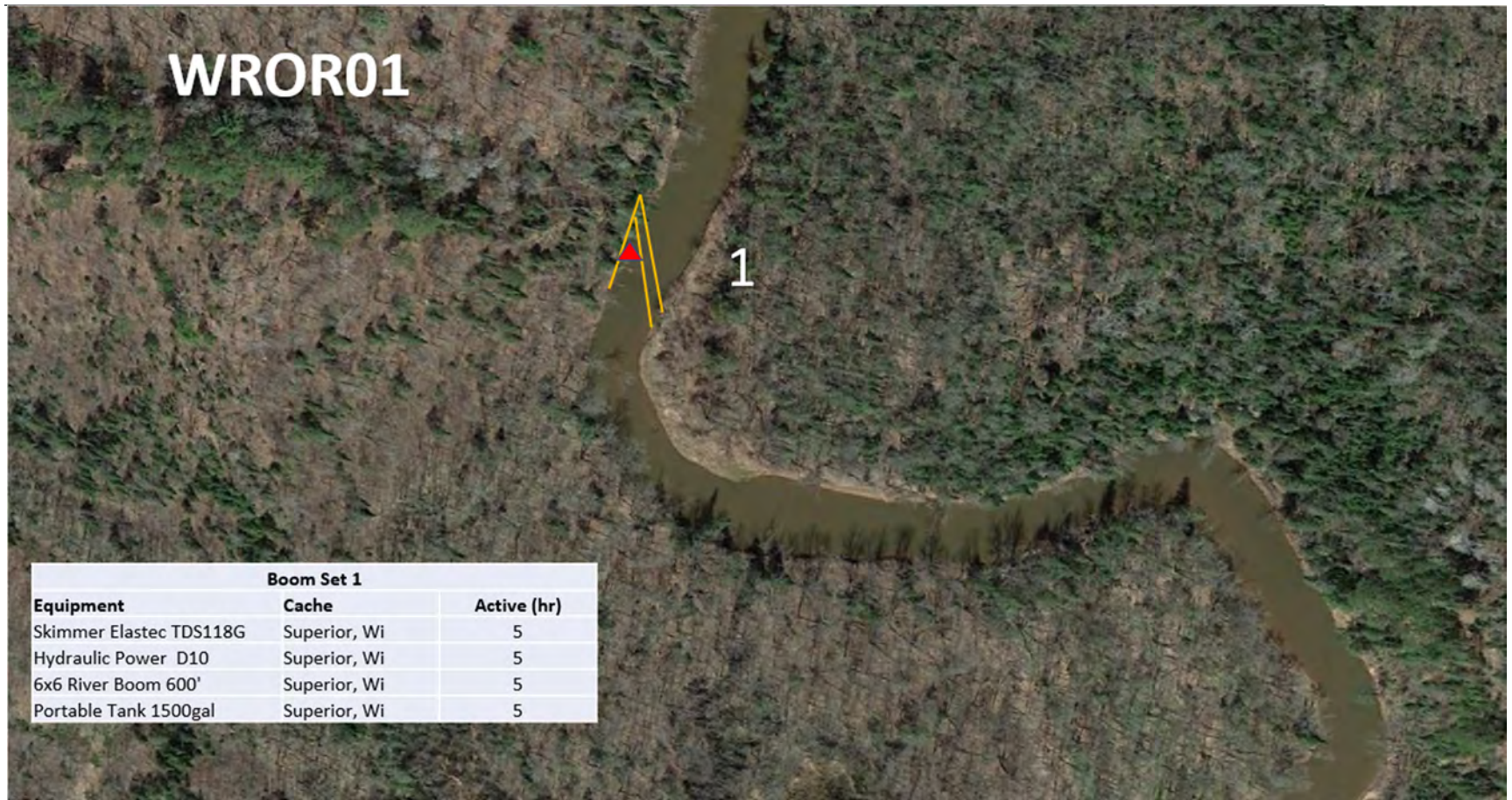
Figure 3-24. Response layout for MCP WROR01 on the White River. Red triangles are skimmer placement locations and orange lines represent containment boom.

Figure 3-25. Response layout for MCP WR01 on the White River. Red triangles are skimmer placement locations, orange lines represent containment boom, white lines represent sorbent boom, and the purple line represents X-Tex fabric. The sorbent boom and X-Tex fabric were not simulated in the model.
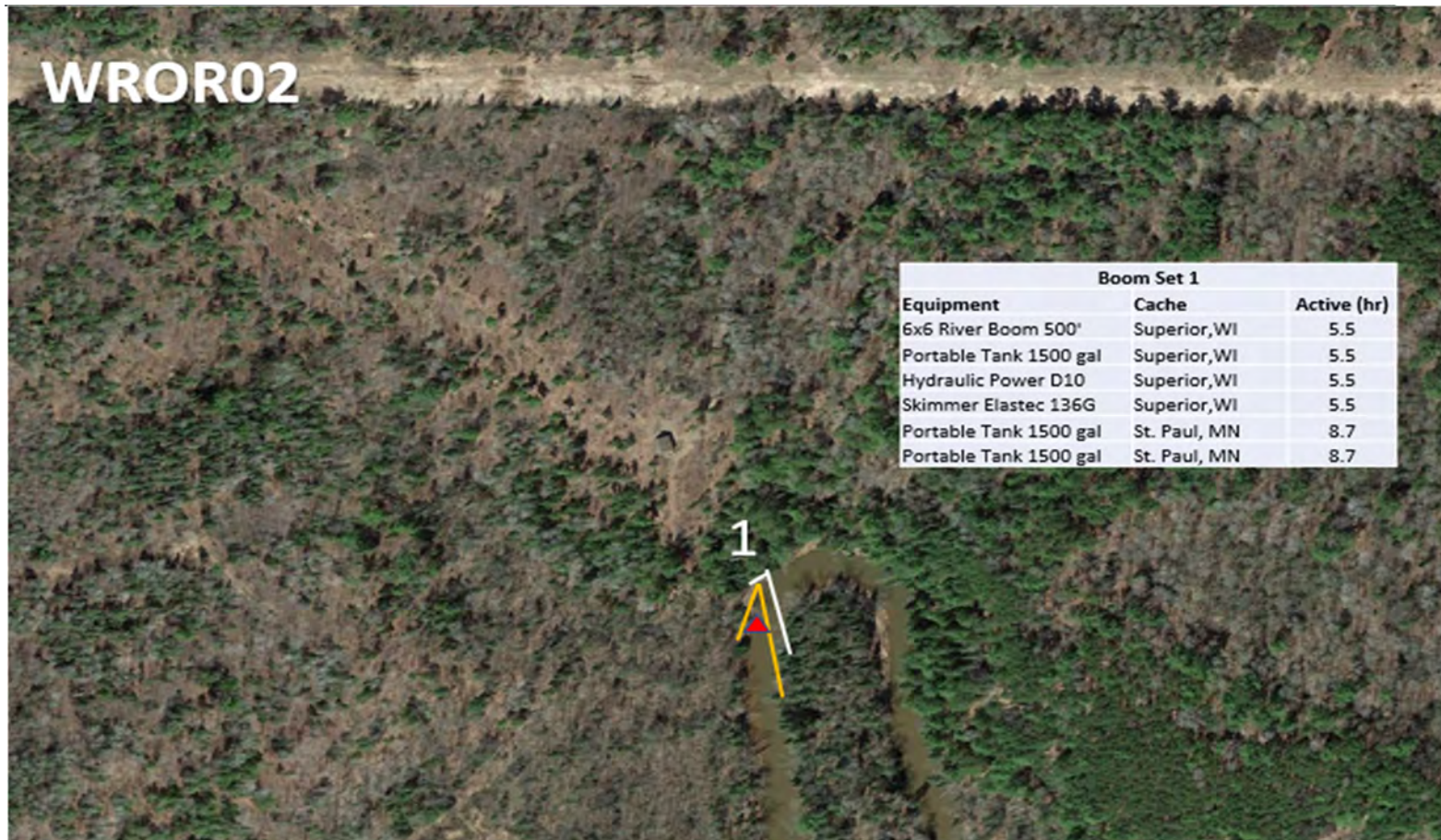
Figure 3-26. Response layout for MCP WROR02 on the White River. Red triangles are skimmer placement locations, orange lines represent containment boom, and white lines represent sorbent boom. The sorbent boom was not simulated in the model.

Boom Set 2		
Equipment	Cache	Active (hr)
XTEX Fabric 6' x 200'	Superior, WI	8.6
6x6 River Boom 500'	Superior, WI	8.6
Skimmer Elastec TDS136G	Deer River, MN	8.6
Portable Tank 1500 gal	Deer River, MN	8.6
Air Compressor	St. Paul, MN	8.6
Portable Tank 1500 gal	St. Paul, MN	8.6
Skimmer Elastec TDS118	Bemidji, MN	8.6
Skimmer Elastec TDS136G	Bemidji, MN	8.6

Boom Set 1		
Equipment	Cache	Active (hr)
Skimmer Elastec TDS136G	Superior, WI	8.6
Hydraulic Power D10	Hill City, MN	8.6
Portable Tank 1500 gal	Vesper, WI	8.6
6x6 River Boom 500'	Superior, WI	8.6
Air Compressor	St. Paul, MN	8.6
Portable Tank 1500 gal	St. Paul, MN	8.6
Skimmer Elastec TDS118G	Bemidji, MN	8.6
Skimmer Elastec TDS118	Bemidji, MN	8.6

Figure 3-27. Response layout for MCP WROR03 on the White River. Red triangles are skimmer placement locations, orange lines represent containment boom, white lines represent sorbent boom, and the purple line represents X-Tex fabric. The sorbent boom and X-Tex fabric were not simulated in the model.

Figure 3-28. Response layout for MCP WROR04 on the White River. Red triangles are skimmer placement locations, orange lines represent containment boom, and white lines represent sorbent boom. The sorbent boom was not simulated in the model.
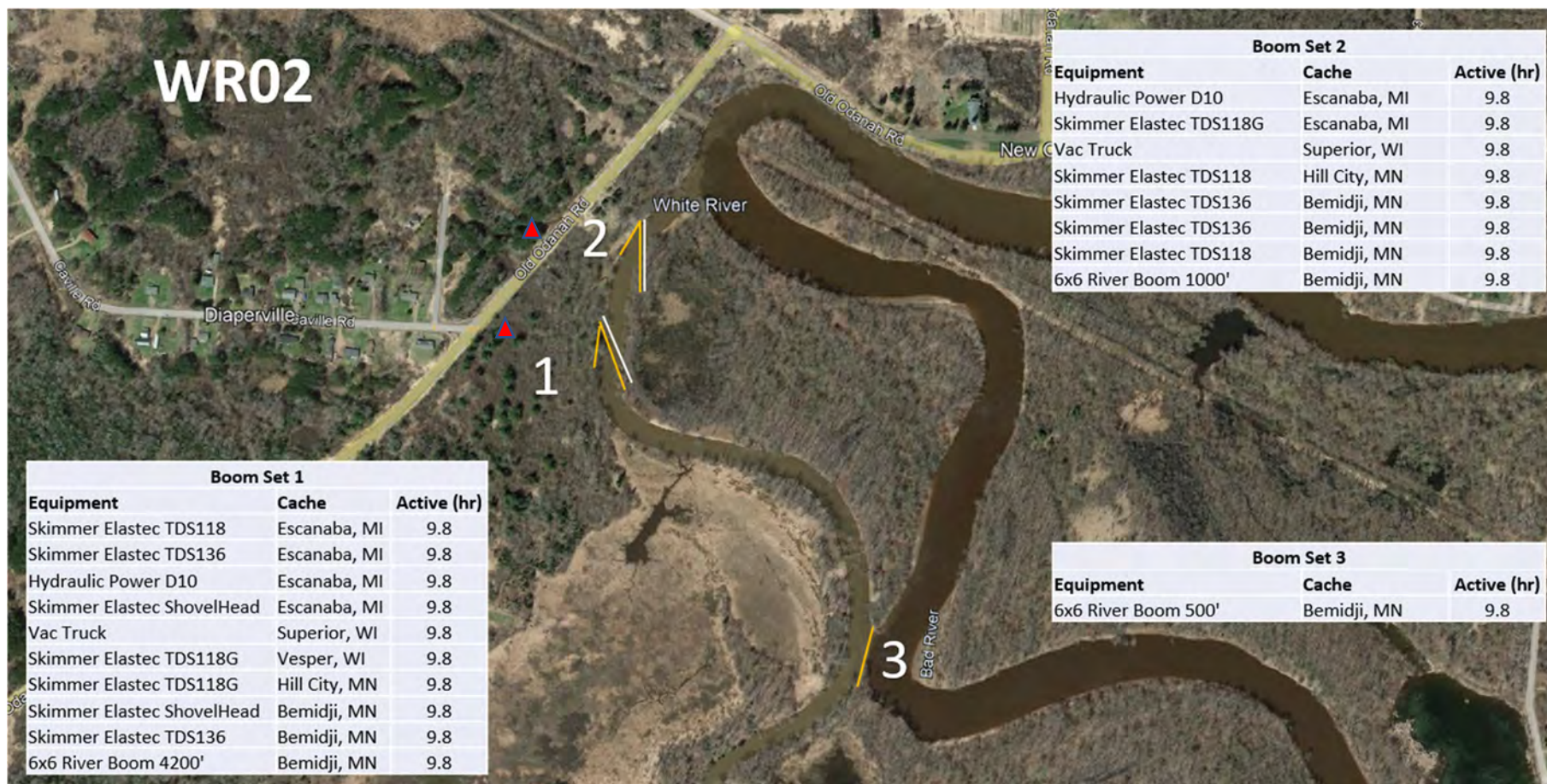
Figure 3-29. Response layout for MCP WR02 on the White River. Red triangles are skimmer placement locations, orange lines represent containment boom, and white lines represent sorbent boom. The sorbent boom was not simulated in the model.

Boom Set 2		
Equipment	**Cache**	**Active (hr)**
Hydraulic Power D10	Escanaba, MI	9.8
Skimmer Elastec TDS118G	Escanaba, MI	9.8
Vac Truck	Superior, WI	9.8
Skimmer Elastec TDS118	Hill City, MN	9.8
Skimmer Elastec TDS136	Bemidji, MN	9.8
Skimmer Elastec TDS136	Bemidji, MN	9.8
Skimmer Elastec TDS118	Bemidji, MN	9.8
6x6 River Boom 1000'	Bemidji, MN	9.8

Boom Set 1		
Equipment	**Cache**	**Active (hr)**
Skimmer Elastec TDS118	Escanaba, MI	9.8
Skimmer Elastec TDS136	Escanaba, MI	9.8
Hydraulic Power D10	Escanaba, MI	9.8
Skimmer Elastec ShovelHead	Escanaba, MI	9.8
Vac Truck	Superior, WI	9.8
Skimmer Elastec TDS118G	Vesper, WI	9.8
Skimmer Elastec TDS118G	Hill City, MN	9.8
Skimmer Elastec ShovelHead	Bemidji, MN	9.8
Skimmer Elastec TDS136	Bemidji, MN	9.8
6x6 River Boom 4200'	Bemidji, MN	9.8

Boom Set 3		
Equipment	**Cache**	**Active (hr)**
6x6 River Boom 500'	Bemidji, MN	9.8

Table 3-9. Modeled response equipment efficiencies by identified weather condition, and cutoff thresholds (i.e., no collection possible while these conditions exist) used in mitigation scenarios.

Equipment	Response Target	Weather Condition	Containment & Collection Efficiency (Derated from Nameplate Capacity)	Wind (m/s)	Currents (knot)	Waves (m)
Containment Boom	Shoreline/ Water Surface	All Mitigated:	99%	7.9	1	1
Skimmer	Water Surface	Non-winter Mitigated:	20% (80% derating)	7.9	n/a	1
		Winter Mitigated:	15% (85% derating)			

4　SIMAP MODEL RESULTS

4.1　Deterministic Trajectory and Fate Results and Discussion

This section provides modeled predictions of the expected trajectory and fate information for hypothetical Bakken crude oil releases under multiple environmental conditions from release locations at the Proposed Route crossings of the Bad River and White River. Trajectory and fate results are provided for both unmitigated and emergency response-mitigated discharge scenarios, with FBR, HARV, and RARV release volumes.

The hydrocarbon trajectories provide a visual depiction of oil transport throughout the modeled domain in both time and space. Components of the oil were tracked as entrained droplets of oil, dissolved hydrocarbons in the water column, floating surface oil, stranded oil on shorelines, and oil on the sediment. This section describes the types of figures produced through the modeling process and the information they portray. Summary figures of trajectory and fate are provided for each scenario with different combinations of release volume, river flow conditions, and response timing.

The mass balance results of the twenty-four deterministic simulations provide a time history of the fate and weathering of oil over the duration of the release, expressed as the percentage of released oil on the water surface, on the shoreline, evaporated, entrained in the water column, degraded, and removed (i.e., successful emergency response activities which clean or remove oil from the environment). Mass balance information at the end of each four-day simulation is provided in tables for each of the release scenarios in terms of percent of oil spilled. Each representative deterministic simulation included its own mass balance, surface oil thickness, in-water concentration of dissolved hydrocarbons, and shoreline length oiled, reported individually. The maximum cumulative footprints of the individual trajectories over the course of the entire modeled duration depict the total area over which floating surface oil was transported, the total length of shoreline being oiled with a mass of oil, and the maximum concentration of dissolved hydrocarbons throughout the water column at every point at all modeled time steps.

The figures described below are provided for the modeled scenarios. Each of the four identified outputs represent composite or cumulative views over the four-day modeled time period. The maps provided below are color-coded indications of the predicted relative magnitude of maximum contamination (i.e., thickness, concentration, or mass) throughout the model domain.

1. **Mass Balance Graphs**: Provide an estimate of the oil's weathering and fate for a specific run for the entire 4-day model duration as a fraction of the oil spilled up to that point. For example, the oil that evaporates (i.e., fate process) ends up in the atmosphere (i.e., environmental compartment). Components of the oil tracked over time include the amount of oil on the water surface, the total entrained hydrocarbons in the water column, the oil on shore, the oil evaporated into the atmosphere, the oil on and in sediments, the oil that decayed (accounts for both photo-oxidation and biodegradation), and the oil removed by response measures.

2. **Surface Oil Thickness Maps:** Maps depicting the predicted cumulative footprint of maximum floating surface oil thickness (μm) at every point in space over all time steps for each of the individual four-day spill simulations. The color-coded value depicted is the maximum associated thicknesses (μm) for each point within the model domain at any time. Note that rather than providing surface oil thickness for the low flow scenarios, a single figure was created that depicts the predicted subsurface thickness of oil that was trapped under the ice (at the ice-water interface). The maximum levels of coverage would not be observed at each location simultaneously.

3. **Water Column DHC Maps:** Maps depicting the predicted cumulative footprint of maximum water column concentration of DHC (µg/L) at every point in space over all time steps for each of the individual four-day spill simulations. The color-coded value depicted is the maximum concentration over all modeled time steps at any depth throughout the water column is reported (i.e., vertical maximum). Dissolved hydrocarbons are the portion of the oil having the greatest potential to affect water column biota, and the footprints were typically smaller than the extent of total oil contamination in the water column. Water column DHC figures depict only concentrations ≥ 1 µg/L. Concentrations below 1 µg/L are considered low and result in little water column impact. The maximum levels of contamination would not be observed at each location simultaneously.

4. **Shoreline and Sediment Impact Maps:** Maps depicting the predicted total mass of oil deposited onto the shoreline and on sediments over the course of each of the four-day spill simulations. Note that 1 µm thickness is equivalent to 1 g/m^2.

It is important to recognize that each cumulative footprint map depicts the highest value that was ever predicted at every location over the entire simulation (i.e., at any point of time). Therefore, these composite figures provide 1) the total swept area of the slick (all areas that were predicted to have any oil at any point in time over the 4-day simulation) and 2) for each point on the map, the maximum value that was ever predicted over the entire simulation. In essence, these composite figures are provided to illustrate the maximum value of contamination, at every point on the map, at any time over the entire simulations. Because of this, if there were a release of the magnitudes portrayed, there would not be enough oil to achieve the depicted level of coverage at all locations at the same time. Rather, these maximum values would be achieved at each location at different points in time as the oil was transported downstream.

To clarify, snapshots of the surface floating oil thickness for the unmitigated FBR discharge of 9,874 bbl at the Bad River channel location during average river flow conditions are provided at 6, 12, 18, and 24 hours into the release (Figure 4-1 and Figure 4-2) for comparison to the cumulative or composite footprint (Figure 4-8). Note that the release moves as a "pulse" of oil that both elongates (roughly 5 km in length at hour 6 and >30 km at hour 24) and thins. The slick of oil was predicted to move downstream with the initial appearance of heavy black oil, but increasingly spread to a heterogeneous, patchy, and discontinuous pulse of dark brown or rainbow sheen. The cumulative footprints do not capture the spatial and temporal variability of the release or any information about the duration of exposure above specific thresholds (e.g., the amount of time an organism at any given location may experience heavy black oil).
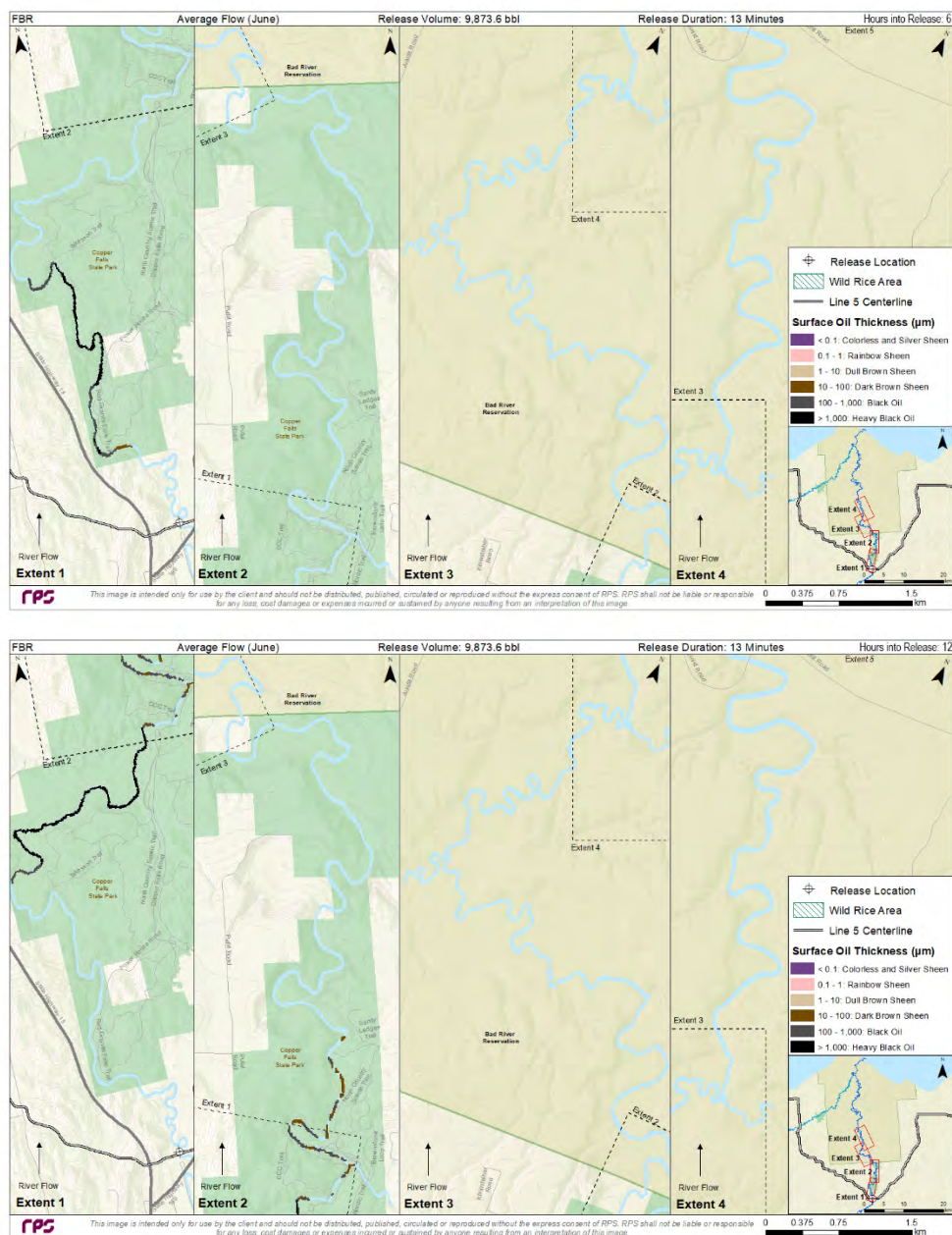
Figure 4-1. Predicted surface oil thickness for the Bad River FBR under average river flow conditions at 6 hours (top) and 12 hours (bottom) into the discharge. Note that the predicted slicks are "snapshots" at specific points in time and are much smaller in area than the provided cumulative figure (Figure 4-8), which depicts the maximum value ever predicted over the course of the four-day simulation for all locations where slicks were predicted to pass through.
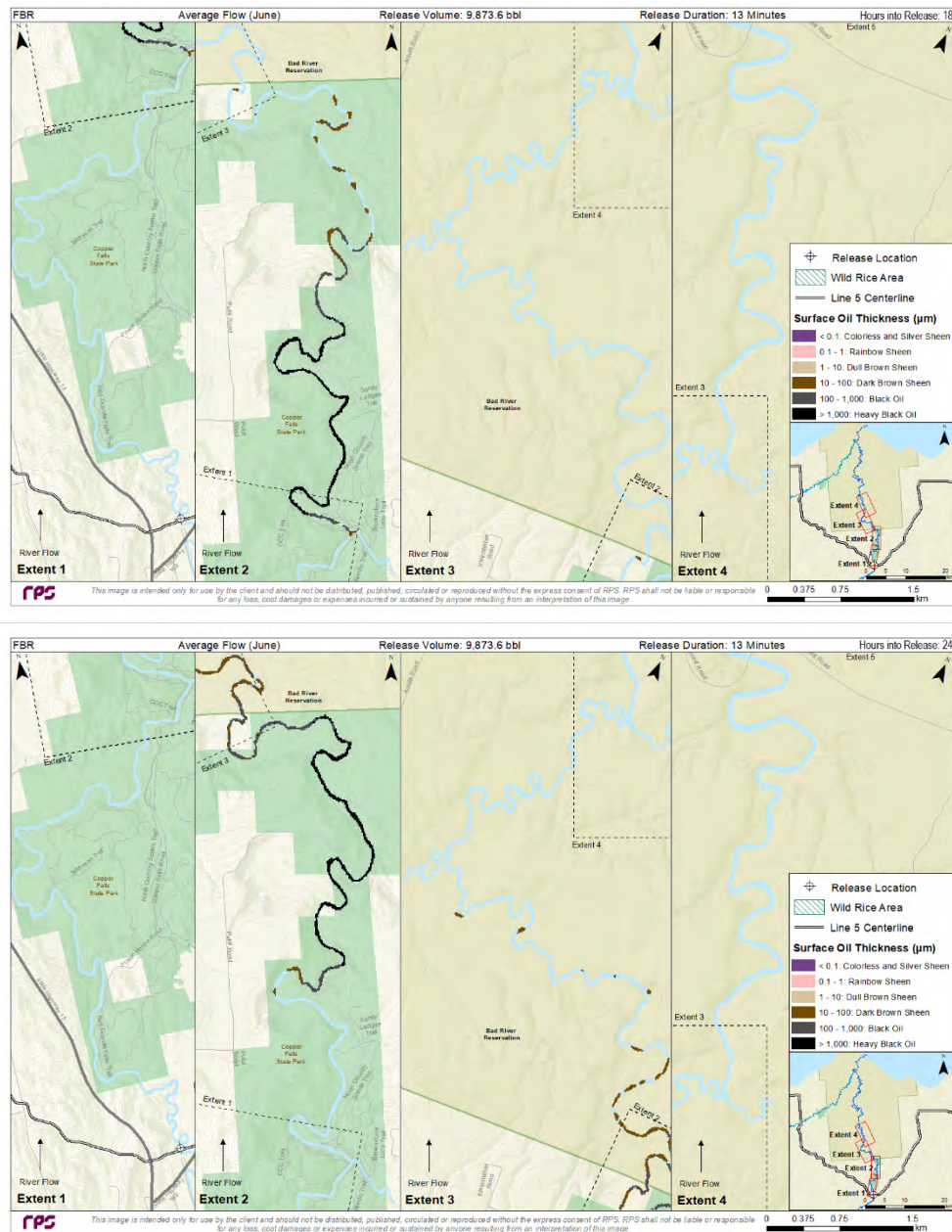
Figure 4-2. Predicted surface oil thickness for the Bad River FBR under average river flow conditions at 18 hours (top) and 24 hours (bottom) into the discharge. Note that the predicted thicknesses are "snapshots" in time and are much smaller than the provided composite or cumulative figure (Figure 4-8), which depicts the maximum value ever predicted over the course of the four-day simulation for all locations where slicks were predicted to pass through.

General Summary

Three main factors influencing the potential for effects following an oil spill were simulated including 1) the river flow conditions at the time of the release (and associated presence or absence of ice), 2) the volume of oil that may be discharged, and 3) whether emergency response efforts were undertaken (unmitigated vs. response mitigated scenarios). The unmitigated scenarios were modeled to illustrate baseline conditions where no response activities were conducted at all, in order to determine the maximum extents of oil that could physically occur and how long it might take oil to reach Lake Superior, if it all. These represent highly conservative "worst-case" scenarios, as it is unrealistic to assume no response would occur for the full 4-day model duration. The trajectory and fate figures and tables provided throughout Section 4.1 highlight the magnitude and extent of downstream movement and behavior of released oil under the modeled conditions, as well as the timing of arrival for contaminants and success of emergency response activities.

In general, river flow conditions had the largest influence on timing and extent of downstream transport in the Bad River (Table 4-1) and White River (Table 4-2). Logically, oil was predicted to reach downstream CPs and Areas of Interest (AOIs) in the least amount of time under high river flow conditions, followed by average river flow, and then low river flow. For the completely unmitigated scenarios, hydrocarbon contamination (e.g., DHC) from hypothetical releases simulated in both rivers would take more than 48 hours to reach Lake Superior. DHC was predicted to have the potential to reach Lake Superior in as little as approximately 2 days under high river flow conditions, approximately 3 days under average conditions, and approximately 4 days under low river flow conditions. In other words, there would be a 2-day to 4-day time period for response activities to be undertaken prior to oil reaching the Lake and downstream-most receptors (e.g., the Kakagon-Bad River Slough Complex). Actual response mitigation activation is anticipated to begin at the first CPs within 3.1 to 3.8 hours (see Section 2.1.3 of the Oil Spill Report).

Under ice-free conditions, limited amounts of hydrocarbons would reach Lake Superior in the form of floating oil and soluble compounds within the water column, especially for FBR unmitigated releases. However, oil slicks (i.e., surface floating oil) were not predicted to reach Lake Superior in any of the unmitigated HARV or RARV scenarios, as all surface floating oil stranded on shorelines prior to reaching these downstream locations. Because of the smaller release volumes simulated in the RARV releases, surface slicks and shoreline oiling were predicted to stop within a few kilometers downstream of the hypothetical release location, well upstream of the larger volume HARV releases which had the possibility of a few patchy and discontinuous surface sheens. When emergency response mitigation was employed, surface floating oil was removed and resulting shoreline oiling ceased within the first few kilometers downstream for both the HARV and RARV releases. In the smaller volume HARV and RARV scenarios, only very limited portions of the oil were predicted to reach the Lake, in the form of the soluble fraction of the hydrocarbons within the water column (i.e., DHC).

Under ice-covered low river flow conditions, whole oil was predicted to remain trapped under the ice. The hydrocarbons were assumed to enter the water column at the river bottom, where they would rise to the surface, becoming trapped beneath the ice with a portion being transported downstream until the equilibrium thickness was achieved. However, the trapped oil would dissolve (to a greater extent than ice free conditions due ice capping evaporation) and soluble hydrocarbons (i.e., the portion that dissolves) were predicted to reach Lake Superior approximately 4 days following the release, regardless of the release volume. In a real-word release, an oil spill on land under wintertime conditions may be prevented from entering the water column by this ice.

The time that discharged oil was first predicted to reach the Reservation ranged from approximately 11.5 hours to over 24 hours on the Bad River and approximately 23 hours to nearly 36 hours on the White River, depending on the river flow condition (Table 4-1, Table 4-2). Downstream times were also provided for additional AOIs,

including Copper Falls on the Bad River, the Highway 13 crossing at the White River, the White River confluence at the Bad River, the Highway 2 crossing at the Bad River, and the entrance to Lake Superior (Table 4-1, Table 4-2). For the mitigated scenarios, oil was predicted to reach the most upstream MCPs starting at approximately 4 to 5 hours after release in the Bad River and 12 to 20 hours after release in the White River. Predicted recovery volumes at each MCP ranged from less than 1 to more than 400 metric tons (MT) over the course of the model duration, depending on the collection capacity of the planned response equipment and timing of thick oil slicks relative to the MCP activation (Table 4-5, Table 4-6). Note that entrained portions of the release (i.e., whole oil in the water column) would not be captured without physical barriers like X-Tex fabric (which were not modeled here), and therefore had the potential to move further downstream, possibly reaching Lake Superior. In a real-world release with an additional barrier, these entrained hydrocarbons are likely to be contained and collected by these enhanced response tactics.

The volume of released oil had the largest influence on the predicted magnitude and downstream/areal extent of oil contamination. While river flow conditions controlled how quickly any amount of oil was predicted to reach a downstream location, the total release volume influenced the total thickness and/or concentration of contaminants that were predicted to arrive. Larger release volumes were predicted to result in more extensive extents with higher concentrations and thicknesses of contamination, thereby increasing the potential for exposure of downstream receptors to levels that may exceed sensitivity thresholds. The smallest release volume modeled (RARV) was predicted to have the smallest extents of potential effects and lighter surface oiling thicknesses, when compared to the other larger volume release scenarios. Other than the average river flow, unmitigated HARV hypothetical release scenarios, no surface oil from any of the other HARV or RARV scenarios (mitigated or unmitigated) in the Bad River or the White River was predicted north of Highway 2, where wild rice areas, the Bad River Slough, and Lake Superior are located. Under average river flow conditions, only the unmitigated HARV scenarios resulted in a patchy and discontinuous sheen slightly north of Highway 2. The potential for exposure of receptors was greatest immediately downstream of each hypothetical release location and lower at points further downstream for all scenarios. This declining exposure was highlighted in the smaller volume release scenarios, where the vast majority of released oil was predicted to be largely evaporated, stranded on shores, or removed through response actions prior to reaching the furthest downstream portions of the Bad River and White River. The wild rice areas and Lake Superior are more than 72 km (45 mi.) downstream of the release location on the Bad River and more than 35 km (22 mi.) downstream of the release location on the White River for the Proposed Route.

Unmitigated releases were simulated to better understand how oil would move through the environment if fully unimpeded by human activities. With nothing done to contain or collect the release, the results would be considered as highly conservative "worst-case" scenarios, as they would maximize the potential downstream movement and potential for effects. Should there be a real-world release, emergency response actions would be undertaken rapidly, identifying and controlling the source and containing and collecting the released oil. The goal of a successful emergency response would be to prevent further release and transport of the product and to remove as much as possible from the environment, thereby reducing the potential for effects. This effects potential is represented by the more realistic, emergency response mitigated release scenarios.

Interactions between released oil and soils, shorelines, and suspended material in the water column can increase the density of the combined Oil-Mineral Aggregates (OMA) to the point that they may sink. In nearly all of the modeled scenarios, oil was predicted to interact in some way (e.g., adsorption) with particulate matter within the water column (SPM or TSS) or sediments (shoreline and bottom) that could result in some sedimentation of oil. However, in all scenarios, oil on sediments (sometimes referred to as "sunken oil") was predicted to be no greater than 325 bbl (or 3.8% of the FBR high river flow scenario in the White River), but

generally averaged approximately 30-36 bbl, making up a few percent or less of the total mass of each release (Table 4-3, Table 4-4).

Unmitigated Trajectory and Fate

The mass balance predictions depict the ultimate fate of the oil over the four-day modeled period for the hypothetical releases that were simulated, under the illustrative baseline assumption of no response mitigation for the full model duration (Table 4-3, Table 4-4). During ice-free periods (scenarios under high and average river flow conditions), the light and volatile Bakken crude oil was predicted to evaporate rapidly to the atmosphere as it was transported downstream. As the oil evaporated, stranded on the shorelines, or re-entrained into the water column due to wind-induced surface breaking waves or waterfalls and rapids, the amount of oil floating on the surface was predicted to decrease. However, entrained oil was predicted to resurface in quiescent waters, re-forming surface slicks. At the end of the unmitigated FBR and HARV simulations that occurred during high river flow conditions, roughly 32-40% of the released oil was predicted to evaporate, while most of the remainder was predicted to have stranded on shorelines (60-64%), where it would continue to evaporate, degrade, and, if mitigation were conducted, be subject to Enbridge's Shoreline Cleanup and Assessment Technique (SCAT) program (Enbridge, 2016). During average river flow conditions without mitigation, the predicted fraction to have evaporated was slightly greater (44-51%), with less accumulated on shorelines (9-55%), leaving a larger portion of the oil on the water surface. Even assuming no response mitigation, surface oil was predicted to take more than 3 days to reach Lake Superior, with at most 39.4% remaining on the water surface at the end of the 4-day simulation, where it may enter the Lake. None of the high or low river flow scenarios for either river were predicted to have surface (whole) oil entering the Lake at any point in the simulations, even unmitigated.

High river flow conditions were predicted to result in greater amounts of oil stranded on the shoreline (up to 5,944 bbl in the Bad River and 5,067 bbl in the White River) because different land cover types were exposed to oil at bank full conditions (Figure 3-1 to Figure 3-4). Vegetated banks at bank full conditions will hold significantly more oil (i.e., higher shoreline oil holding capacity) than the typical mud bank and sand bank shorelines that were exposed under the average river flow conditions, when water levels would be lower. Under low river flow scenarios, with 100% ice-cover on the surface and completely ice-covered riverbanks, even less oil (<0.1% of the total release volume) was able to strand on shorelines.

The second largest amount of oil stranded on the shorelines was predicted to occur under average river flow conditions for the FBR (up to 9.1% or 900 bbl in the Bad River, 15.6% or 1,330 bbl in the White River), because of the large hypothetical release volume. While the HARV and RARV had higher percentages of the total release stranding on shorelines, the smaller volume of the release resulted in lower total volumes of oil predicted to strand on shorelines. HARV and RARV releases, were predicted to have 35-55% or 185-660 bbl of the release volume stranded on shorelines in the Bad River, and 47-52% or 175-890 bbl in the White River. As mentioned previously, the largest percentages and amounts of released oil were predicted to strand on shorelines during high river flow conditions, due to the predominantly grass and forested shore types which were exposed to oil contamination under bank full conditions and predicted to retain more oil than under average river flow conditions (Table 3-3).

For the rest of the oil in the unmitigated, non-winter scenarios, a combined maximum of 4.1% of the oil was predicted to remain entrained in the upper surface of the water column, adhered to the sediment, and/or

degraded at the end of the 4-day simulation. In the Bad River, up to 28% of the oil was predicted to entrain into the water column during the simulation as it passed over Red Granite Falls and then Copper Falls (observed as two purple "humps" in Figure 4-3, Figure 4-7, Figure 4-14, Figure 4-18, Figure 4-25). However, the oil was predicted to resurface downstream of the falls and rapids, where it would generally strand on shorelines, rather than adsorbing to sediments and settling on the river bottom, because the faster current speeds in the Bad River continually exceeded the depositional threshold. Total percentages of sedimented oil were less than 0.1% for all Bad River scenarios. The White River has consistently lower velocities than the Bad River, across all seasons (Figure 3-6-Figure 3-11). Therefore, in the White River, even though entrainment was generally low throughout the simulation, the lower velocity waters and elevated TSS loads allowed for greater amounts of sedimentation to occur, with approximately 3.5% of the oil in sediments at the end of the unmitigated scenarios. For both Bad River and White River simulations under low river flow conditions, with complete ice cover (100%) and capped evaporation, nearly all the oil was predicted to remain in the water column (i.e., trapped under the ice surface), with approximately 1% or less predicted to degrade within the simulated 4-day timeframe.

The floating surface oil in the unmitigated[1] scenarios simulated in the Bad River was predicted to be transported downstream, thinning with distance from heavy black oil (>1,000 μm) near the release locations to predominantly dull brown sheens and rainbow sheens (0.1-10 μm) in the downstream reaches of the Bad River, including at the wild rice areas, Bad River Slough, and outlet to Lake Superior in some scenarios (Figure 4-4, Figure 4-8, Figure 4-15, Figure 4-19). The oil slicks were generally thinner and patchier for high river flow conditions (as compared to average river flow) and the HARV release volumes (as compared to the FBR release volumes). In the White River, the floating surface oil from unmitigated FBR scenarios was predicted to be thicker than the Bad River simulations when it reached these same downstream areas, with oil still present as black oil (100-1,000 μm) or dark brown sheens (10-100 μm) (Figure 4-56, Figure 4-60, Figure 4-68, Figure 4-72). Greater thicknesses were predicted for these White River simulations because the release location was approximately half the distance upstream than in the Bad River release location, and the White River is a narrower, lower flow water body. The release volumes simulated in the RARV scenarios for both rivers, even without mitigation, were small enough that surface oil was not predicted to reach downstream waters north of Highway 2, where the wild rice areas, the Bad River Slough, and Lake Superior are located (Figure 4-26, Figure 4-79).

For all of the unmitigated, Bad River release scenarios, floating surface oil was not predicted to enter or spread into the Bad River Slough, predominantly due to, at most, patchy and discontinuous thin sheens being predicted to reach the downstream reaches of the Bad River itself. Larger volume releases into the White River (again, unrealistically assuming no response mitigation throughout the simulation) were predicted to have surface oil enter the Bad River Slough, reaching thicknesses of primarily rainbow sheen (0.1-1 μm) for the HARV releases and dull or dark brown sheens (1-100 μm) for the FBR releases. However, the sheens predicted in the Bad

---

[1] As described above, the unmitigated scenarios represent highly conservative "worst-case" conditions where no response activities were assumed to occur throughout the 4-day model duration. These scenarios illustrate baseline conditions to determine the maximum extents of oil that could physically occur.

River Slough due to the White River releases would be patchy and discontinuous and occur only briefly in time (although the figures show cumulative maximum thickness over the 4-day model duration).

DHCs during both high and average river flow conditions were generally predicted to be transported downstream with the surface oil, extending in some cases farther than the floating slicks because surface floating oil may strand on shorelines, "hang" in back eddies, or be transported by wind. The water column processes of dissolution, dilution, volatilization (i.e., evaporation of soluble hydrocarbons from the water column), and degradation of lighter ends resulted in DHCs generally declining as oil was transported downstream within both the Bad and White Rivers. For the illustrative, unmitigated Bad River releases, DHC concentrations were predicted to decline with distance from >100 µg/L at upstream locations near the release location, corresponding with areas of heavy black oil) to between <1 µg/L and 25 µg/L at downstream locations near the Bad River Slough and Lake Superior, with only the FBR scenario under high flow conditions exceeding 100 µg/L at the downstream locations (Figure 4-5, Figure 4-9, Figure 4-16, Figure 4-20, Figure 4-27). For the unmitigated White River releases, DHCs near these downstream locations were predicted to be slightly greater than in the Bad River, with values ranging from >10 µg/L to >100 µg/L because the overall distance was shorter, and thicker surface oil was able to reach those locations, from which additional hydrocarbons continued to dissolve (Figure 4-57, Figure 4-61, Figure 4-69, Figure 4-73, Figure 4-80). DHCs were not generally predicted to enter the more stagnant Bad River Slough, for either the Bad River or White River release scenarios, as the majority of the river outflow was predicted to exit into Lake Superior.

Although there was complete ice coverage (100%) assumed under low river flow conditions, that prevented oil from reaching the surface and capped evaporation, the release volumes for entirely unmitigated FBR releases were large enough that the subsurface oil was still predicted to be transported downstream into the southern portions of the Reservation, before reaching equilibrium thickness (see Section 3.6) and effectively becoming trapped beneath the ice surface. Subsurface oil was predicted to strand on the underside of the ice reaching as far downstream in the Bad River as 43 km (27 mi, or approximately halfway to Lake Superior) and as far downstream in the White River as 32 km (20 mi. or nearly to the confluence of the Bad River), but did not extend north of Highway 2 in any scenario (Figure 4-12, Figure 4-23, Figure 4-64, Figure 4-76). Because of the smaller release volume in the HARV scenarios, oil trapped beneath the ice was predicted to stop within Copper Falls State Park for the Bad River scenarios and prior to the White River Boreal Forest for the White River, even without mitigation.

During low river flow, wintertime conditions, complete ice cover was predicted to cap evaporation leading to the highest magnitude concentrations of dissolved hydrocarbons in the water column. The soluble fraction of the oil (which would be able to evaporate under ice free conditions) was predicted to dissolve into the water column, being transported downstream toward and into Lake Superior within the 4-day modeled time period (Figure 4-13, Figure 4-24, Figure 4-65, Figure 4-77).

Due to the large amount of surface oil from the FBR and HARV releases that was predicted to transport downstream and strand on shorelines in these relatively narrow rivers, the resulting total hydrocarbon concentrations making contact with shorelines under high and average river flow conditions were predicted to exceed 500 g/m² for the majority of shore that was exposed to surface floating oil (Figure 4-6, Figure 4-10, Figure 4-17, Figure 4-21, Figure 4-28, Figure 4-58, Figure 4-62, Figure 4-70, Figure 4-74, Figure 4-81). Essentially, a large "slug" of oil was predicted to strand on both shorelines up to their holding capacity as the oil was transported downstream. Farther downstream, in areas that were predicted to be contacted by sheens of rainbow or dull brown color, the shoreline oil was predicted to be patchy and discontinuous, with concentrations less than 500 g/m². For the smaller volume releases, these sheens were reached in shorter

distances, and the total length of shoreline oiled was predicted to be far less than the FBR releases. Note that in low river flow conditions, very little (<0.1%) of the total release volume was predicted to strand on shorelines, as the release was trapped beneath the ice and the banks were assumed to be frozen over with ice.

Concentrations of total predicted hydrocarbons in the sediment varied between scenarios, but patchy concentrations up to 0.5 g/m^2 were predicted in some scenarios, notably for the FBR releases and high river flow conditions that had correspondingly high TSS values within the water column (Figure 4-6, Figure 4-10, Figure 4-17, Figure 4-21, Figure 4-28, Figure 4-58, Figure 4-62, Figure 4-70, Figure 4-74, Figure 4-81). There was significant entrainment and resulting interactions of oil with suspended sediments within the water column at Copper Falls, resulting in sedimentation of oil in downstream reaches of the Bad River. In general, less than 15 bbl of oil was predicted to settle across the suite of Bad River scenarios due to the greater overall current velocities which were above the depositional threshold. In the White River, up to 70 bbl of the HARV release and 350 bbl of the FBR release were predicted to settle. These maximum amounts of sediment oil were predicted in the White River under high river flow conditions because there was higher sediment load in the water column (191 mg/L), yet current speeds were still slow enough to fall below the depositional threshold and allow for sediment deposition. In the Bad River, the current speeds (and resulting turbulence) were generally sufficient to result in most sediments remaining within the water column. Under low river flow conditions, sediment load was very low (4 mg/L) resulting in very limited deposition (<0.1% of the total release volume, consistently around 0.01 g/m^2; not depicted in figures as predicted shoreline and sediment oil were both near zero).

Response Mitigated Trajectory and Fate

Representative response-mitigated scenarios were modeled for the same FBR, HARV, and RARV volumes to compare with the unmitigated release scenarios and illustrate outcomes for a more realistic spill response. Response mitigated scenarios were predicted to have approximately 27-35% and 42-57% of the oil collected under high and average river flow conditions, respectively, resulting in nearly all of the surface oil being collected within the modeled time frame (<0.1% of surface oil remaining; Table 4-3, Table 4-4). This mitigation targeted the containment and collection of surface oil, which also resulted in slightly smaller fractions of oil predicted to evaporate (32-36% under high river flow conditions, 38-44% under average river flow conditions), when compared to unmitigated scenarios. Because the surface oil was being actively removed, the fractions of oil predicted to strand on shorelines were, in most cases, much smaller than unmitigated scenarios (29-34% under high river flow conditions, 3-12% under average river flow conditions). However, for the HARV release in the White River under high river flow conditions, only 0.1% of the oil was mitigated and 64% was predicted to strand ashore, where it would be subsequently targeted by Enbridge's SCAT program (Enbridge, 2016). In this scenario large quantities of oil were predicted to accumulate on the vegetated banks (with higher holding capacity) upstream of the MCPs (i.e., prior to reaching the MCP). In a real-world release, CPs would be set up at locations that would best target the oil at the specific time of response and removal activities would be undertaken along oiled shorelines. The relative amounts of oil predicted to strand on shorelines varied significantly based on the size of the simulated release and the containment and collection capacity of each successive downstream control point. Under low river flow conditions, nearly all oil was predicted to be collected because sufficient time was available after CP activation to recover the oil under the assumed winter response conditions. Should a release occur under wintertime conditions, it is unlikely that all of the oil would be collected. The model predictions are influenced by several assumptions including the complete prevention of evaporation and all whole oil stranding under the ice (as opposed to portions frozen within the ice, carried downstream, or

migrating upward through the ice and pooling on the surface). While complete collection under winter conditions would be unlikely, substantial mitigation may be achieved under wintertime conditions. As described in Section 2.1.2 of the Oil Spill Report, emergency response efforts can be limited at any time of the year (including winter) based upon location-specific and environmental condition-specific limitations, such as weather conditions causing temporary work stoppage, or equipment issues or maintenance needs. To account for this, RPS modeled conservatively-based recovery rates and timing to reflect such conditions (and acknowledging that snow and ice can also significantly or completely reduce the volume of oil ever reaching the waterway in the first place), recognizing that complete removal of oil may not be possible at all CPs under all conditions.

In general, less oil was predicted to be on the surface, evaporated to the atmosphere, or stranded on shorelines in the mitigated scenarios because it had been contained before further downstream transport and removed from the environment. In particular, mitigation activities reduced the percentage of oil on the surface from as much as 40% to <0.1% of the release volume within the modeled timeframe. This resulted in a reduction of oil stranding on shorelines by nearly 50-90% for the average and high river flow Bad River scenarios, which resulted in final shoreline quantities that were predicted to be less than one third of the total release volume. In the White River, mitigation activities had a similar effect on reducing shoreline oil (by as much as 78%). It is also notable that mitigation activities substantially reduced the amount of oil that was predicted to enter Lake Superior to less than 0.1% of the total release volume.

For the mitigated scenarios under most conditions, released oil was not predicted to reach the most downstream portions of the Bad River (north of Highway 2), including the wild rice areas and Bad River Slough. However, for the two FBR scenarios in the Bad River under average and high river flow conditions, sufficient oil volume was released that a small amount of surface oil (<1 bbl in total) was predicted to reach the area closest to the Bad River Slough and Lake Superior, at levels that were never greater than patchy and discontinuous dull brown or rainbow sheens (<10 µm) for brief periods of time (i.e., less than a few hours). The cumulative maximum figures (Figure 4-30, Figure 4-34) depict the thickest oil that occurred at any point over the 4-day simulation, but the thicknesses at those locations would at all other times be less than the reported maximum, as the oil slug passed through, and zero for the majority of the simulated time frame. Further, it is notable that the mitigation modeled herein was limited to only containment boom and skimmer resources at the seven Bad River MCPs and five White River MCPs defined in Section 3.10. In an actual response, substantial additional resources would be deployed at an additional barrier downstream of Highway 2, as well as additional tactics at the CPs (e.g., X-Tex fabric, pom-pom snares, and sorbent booms) that could minimize sheens and help capture submerged oil droplets downstream of turbulent waters. Predicted maximum surface oil thicknesses for each response mitigated scenario are depicted in Figure 4-30, Figure 4-34, Figure 4-38, Figure 4-41, Figure 4-45, Figure 4-49, Figure 4-52, Figure 4-83, Figure 4-87, Figure 4-91, Figure 4-94, Figure 4-98, Figure 4-102, Figure 4-105.

In each mitigated scenario, heavy black oil on the surface (>1,000 µm) was predicted to be transported downstream to the point that collection efforts and oil stranding on shorelines reduced thickness appreciably. In the Bad River, these slicks were predicted to extend approximately 8 to 30 km (5 to 19 mi.) downstream, reaching locations somewhere between MCP BROR01 and MCP SURCP0800, primarily based on the volume of oil released. In the White River, these slicks were predicted to extend approximately 8 to 17 km (5-11 mi.) downstream, reaching MCPs WROR01, WR01, or WROR02 depending on the volume of oil released and simulated river flow conditions.

DHCs for the mitigated scenarios had similar extents to the unmitigated scenarios. Generally, concentrations within the water column decreased with distance from >100 µg/L at upstream locations near the release location

(corresponding with areas of heavy black oil), to between <1 µg/L and 25 µg/L at downstream locations near the Bad River Slough and Lake Superior. In some scenarios, downstream concentrations were predicted to be partially reduced due to mitigation efforts removing surface oil. However, much of the dissolution was predicted to occur when fresh oil with high soluble content entered the water column upstream of the MCPs. Dissolved hydrocarbons are transported downstream without being affected by mitigation efforts, as the boom and skimmer response equipment targets surface floating oil and not contaminants within the water. Predicted maximum DHCs for each response mitigated scenario are depicted in Figure 4-31, Figure 4-35, Figure 4-39, Figure 4-42, Figure 4-46, Figure 4-50, Figure 4-53, Figure 4-84, Figure 4-88, Figure 4-92,

Figure 4-95, Figure 4-99, Figure 4-103, Figure 4-106.

Similar to the unmitigated scenarios, shoreline concentrations for the response mitigated scenarios were predicted to exceed 500 g/m^2 for the majority of shorelines that were exposed to heavy black oil. However, because the extent of heavy black oil was shorter than in unmitigated scenarios, the resulting shoreline extents above 500 g/m^2 were generally limited to 10-40 km (7-25 mi.) downstream of the release point for the FBR scenarios and less than 10 km (6 mi.) downstream of the release point for the HARV scenarios. Response efforts were predicted to reduce shoreline oiling by approximately 40-90%. However, under high river flow conditions for the FBR and HARV releases, as much as 2,930 bbl and 1,230 bbl (respectively) may still strand on shorelines due primarily to heavy black oil predicted to contact high oil capacity vegetated regions upstream of the MCPs (Table 4-3, Table 4-4). Regardless of release volume (FBR, HARV, or RARV), for both the Bad River and White River releases, shoreline oil was generally not predicted to reach the wild rice habitats and slough areas, north of Highway 2. Similar to the unmitigated scenarios, significant sediment oiling was not predicted in the Bad River and was limited to tens of barrels (averaging <2.4% of release volumes) over the White River channel at levels typically <0.5 g/m^2. Predicted maximum shoreline and sediment concentrations are depicted in Figure 4-32, Figure 4-36, Figure 4-43, Figure 4-47, Figure 4-54, Figure 4-85, Figure 4-89, Figure 4-96, Figure 4-100, Figure 4-107).

Table 4-1. Time any oil contamination was predicted to reach each downstream AOI for the modeled river flow conditions in the Bad River. The number of days, hours, and minutes following the initial release are provided as Days HH:mm.

Downstream Times to AOIs				
River Flow Conditions	**Copper Falls**	**Reservation Boundary**	**Hwy. 2 Crossing**	**Lake Superior**
High River Flow	0 days 05:30	0 days 11:25	1 day 20:17	2 days 04:43
Average River Flow	0 days 09:14	0 days 17:44	3 days 02:51	3 days 08:27
Low River Flow	0 days 13:11	1 day 00:30	3 days 15:26	3 days 23:58

Note, this analysis includes the assessment of any quantity of oil contamination (i.e., binary presence/absence), be it whole oil or the soluble fraction (i.e., dissolved).

Table 4-2. Time any oil contamination was predicted to reach each downstream AOI for the modeled river flow conditions in the White River. The number of days, hours, and minutes following the initial release are provided as Days HH:mm.

Downstream Times to AOIs					
River Flow Conditions	**Hwy 13 Crossing**	**Reservation Boundary**	**Bad River**	**Hwy. 2 Crossing**	**Lake Superior**
High River Flow	0 days 12:58	0 days 23:22	2 days 11:39	2 days 02:55	2 days 16:31
Average River Flow	0 days 16:30	1 day 04:04	2 days 20:43	2 days 23:15	3 days 06:25
Low River Flow	0 days 22:00	1 day 11:20	3 days 09:20	3 days 11:17	3 days 22:02

Note, this analysis includes the assessment of any quantity of oil contamination (i.e., binary presence/absence), be it whole oil or the soluble fraction (i.e., dissolved).

Table 4-3. Summary of predicted mass balance information for the Bad River scenarios at the end of each four-day simulation. All values represent a percent of the total volume of spilled oil at the last modeled time step.

Scenario	Surface*	Evaporated	Entrained	Sediment	Ashore	Degraded	Out of Model Domain*	Removed
Bad River Unmitigated								
FBR (9,874 bbl) High River Flow	<0.1	39.4	<0.1	<0.1	60.2	0.3	<0.1	NA
FBR (9,874 bbl) Average River Flow	39.4	51.1	0.1	<0.1	9.1	0.3	<0.1	NA
FBR (9,874 bbl)¥ Low River Flow	<0.1	<0.1	98.9	<0.1	<0.1	1.0	<0.1	NA
HARV (1,911 bbl) High River Flow	<0.1	35.7	<0.1	<0.1	63.9	0.3	<0.1	NA
HARV (1,911 bbl) Average River Flow	16.6	48.6	<0.1	<0.1	34.5	0.3	<0.1	NA
HARV (1,911 bbl)¥ Low River Flow	<0.1	<0.1	98.6	<0.1	<0.1	1.0	<0.1	NA
RARV (334 bbl) Average River Flow	<0.1	44.4	<0.1	<0.1	55.2	0.3	<0.1	NA
Bad River Mitigated								
Mitigated **FBR (9,874 bbl) High River Flow**	<0.1	36.4	<0.1	<0.1	28.8	0.2	<0.1	34.6
Mitigated **FBR (9,874 bbl) Average River Flow**	<0.1	41.8	<0.1	<0.1	3.4	0.1	<0.1	54.5
Mitigated **FBR (9,874 bbl)¥ Low River Flow**	<0.1	<0.1	<0.1	<0.1	<0.1	0.1	<0.1	99.9
Mitigated **HARV (1,911 bbl) High River Flow**	<0.1	34.0	<0.1	<0.1	32.3	0.2	<0.1	33.4
Mitigated **HARV (1,911 bbl) Average River Flow**	<0.1	38.7	<0.1	<0.1	3.8	0.1	<0.1	57.4
Mitigated **HARV (1,911 bbl)¥ Low River Flow**	<0.1	<0.1	<0.1	<0.1	<0.1	0.1	<0.1	99.9
Mitigated **RARV (334 bbl) Average River Flow**	<0.1	37.7	<0.1	<0.1	10.7	<0.1	<0.1	51.4

¥ For the low flow scenario, entrained oil includes both subsurface oil trapped under the ice and oil entrained or dissolved into the water column. Additionally, the assumed 100% ice cover was simulated to prevent any evaporation of the volatile fraction of the oil.

* Oil outside of the model domain is in Lake Superior. However, there is water near the edge of the model domain that is contained within Lake Superior; therefore, portions of the surface oil may be located within the Bad River and within Lake Superior near the mouth of the Bad River.

www.rpsgroup.com

Table 4-4. Summary of predicted mass balance information for the White River scenarios at the end of each four-day simulation. All values represent a percent of the total volume of spilled oil at the last modeled time step.

Scenario	Surface*	Evaporated	Entrained	Sediment	Ashore	Degraded	Out of Model Domain*	Removed
White River Unmitigated								
FBR (8,517 bbl) High River Flow	<0.1	36.4	<0.1	3.8	59.5	0.3	<0.1	NA
FBR (8,517 bbl) Average River Flow	12.2	49.2	<0.1	0.4	15.6	0.2	22.3	NA
FBR (8,517 bbl)¥ Low River Flow	<0.1	<0.1	98.9	<0.1	<0.1	1.0	<0.1	NA
HARV (1,911 bbl) High River Flow	<0.1	32.2	<0.1	3.5	63.9	0.3	<0.1	NA
HARV (1,911 bbl) Average River Flow	1.6	45.5	<0.1	3.5	46.5	0.3	2.6	NA
HARV (1,911 bbl)¥ Low River Flow	<0.1	<0.1	98.9	<0.1	<0.1	1.0	<0.1	NA
RARV (334 bbl) Average River Flow	<0.1	44.1	0.1	3.7	51.8	0.3	<0.1	NA
White River Mitigated								
Mitigated **FBR (8,517 bbl) High River Flow**	<0.1	36.1	<0.1	2.5	34.4	0.2	<0.1	26.7
Mitigated **FBR (8,517 bbl) Average River Flow**	<0.1	44.2	<0.1	0.4	4.3	0.1	<0.1	50.9
Mitigated **FBR (8,517 bbl)¥ Low River Flow**	<0.1	<0.1	<0.1	<0.1	<0.1	0.1	<0.1	99.9
Mitigated **HARV (1,911 bbl) High River Flow**	<0.1	32.4	<0.1	3.1	63.8	0.3	<0.1	0.1
Mitigated **HARV (1,911 bbl) Average River Flow**	<0.1	43.2	<0.1	4.8	10.0	0.1	<0.1	41.8
Mitigated **HARV (1,911 bbl)¥ Low River Flow**	<0.1	<0.1	<0.1	<0.1	<0.1	0.1	<0.1	99.9
Mitigated **RARV (334 bbl) Average River Flow**	<0.1	40.2	0.2	6.0	11.8	0.1	<0.1	41.6

¥ For the low flow scenario, entrained oil includes both subsurface oil trapped under the ice and oil entrained or dissolved into the water column. Additionally, the assumed 100% ice cover was simulated to prevent any evaporation of the volatile fraction of the oil.

* Oil outside of the model domain is in Lake Superior. However, there is water near the edge of the model domain that is contained within Lake Superior; therefore, portions of the surface oil may be located within the Bad River and within Lake Superior near the mouth of the Bad River.

Table 4-5. Predicted amount of oil removal at each MCP for the emergency response mitigated scenarios in the Bad River.

Control Point		1 SURCP0795	2 BROR01	3 BROR02	4 SURCP0796	5 SURCP0795	6 SURCP0797	7 SURCP0800	8 SURCP0801
Mitigated FBR (9,874 bbl) High River Flow Bad River Channel	Oil Removed (MT)	25.512	51.883	39.119	31.248	232.176	62.364	9.327	0.298
	Oil/Water Emulsion Removed (m^3)	28.8	56.036	39.119	31.248	232.176	62.364	9.327	0.298
Mitigated FBR (9,874 bbl) Average River Flow Bad River Channel	Oil Removed (MT)	44.69	104.883	52.57	41.067	303.385	76.649	72.231	5.673
	Oil/Water Emulsion Removed (m^3)	50.877	113.912	52.57	41.067	303.385	76.649	72.231	5.673
Mitigated FBR (9,874 bbl) Low River Flow Bad River Channel	Oil Removed (MT)	>99% of whole oil*					NA	NA	NA
	Oil/Water Emulsion Removed (m^3)	NA	NA	NA	NA	NA	NA	NA	NA
Mitigated HARV (1,911 bbl) High River Flow Bad River Channel	Oil Removed (MT)	5.183	30.64	16.453	12.181	19.095	0.33	0.009	0.029
	Oil/Water Emulsion Removed (m^3)	5.881	33.12	16.453	12.181	19.095	0.33	0.009	0.029
Mitigated HARV (1,911 bbl) Average River Flow Bad River Channel	Oil Removed (MT)	25.515	60.431	21.016	16.107	19.648	0.416	0.035	0
	Oil/Water Emulsion Removed (m^3)	29.094	65.837	21.016	16.107	19.648	0.416	0.035	0
Mitigated HARV (1,911 bbl) Low River Flow Bad River Channel	Oil Removed (MT)	>99% of whole oil*		NA	NA	NA	NA	NA	NA
	Oil/Water Emulsion Removed (m^3)	NA	NA	NA	NA	NA	NA	NA	NA
Mitigated RARV (334 bbl) Avg River Flow Bad River Channel	Oil Removed (MT)	6.721	15.378	0.154	0.081	0.068	0	0	0
	Oil/Water Emulsion Removed (m^3)	7.651	16.962	0.154	0.081	0.068	0	0	0

* Recovery under low river flow, 100% ice-covered conditions would occur under the ice at points throughout the river channel, not solely at the MCP.

Table 4-6. Predicted amount of oil removal at each MCP for the emergency response mitigated scenarios in the White River.

Control Point		1 WROR01	2 WR01	3 WROR02	4 WROR03	5 WROR04	6 WR02
Mitigated FBR (8,517 bbl) High River Flow White River Channel	Oil Removed (MT)	0	259.518	39.49	0	0	0
	Oil/Water Emulsion Removed (m³)	0	267.153	39.49	0	0	0
Mitigated FBR (8,517 bbl) Average River Flow White River Channel	Oil Removed (MT)	0	422.44	63.284	80.148	0	0
	Oil/Water Emulsion Removed (m³)	0	435.541	63.284	0	0	0
Mitigated FBR (8,517 bbl) Low River Flow White River Channel	Oil Removed (MT)	>99% of whole oil*		NA	NA	NA	NA
	Oil/Water Emulsion Removed (m³)	NA	NA	NA	NA	NA	NA
Mitigated HARV (1,911 bbl) High River Flow White River Channel	Oil Removed (MT)	0	0.343	0	0.006	0	0
	Oil/Water Emulsion Removed (m³)	0	0.37	0	0	0	0
Mitigated HARV (1,911 bbl) Average River Flow White River Channel	Oil Removed (MT)	0	104.183	0	0	0	0
	Oil/Water Emulsion Removed (m³)	0	112.095	0	0	0	0
Mitigated HARV (1,911 bbl) Low River Flow White River Channel	Oil Removed (MT)	>99% of whole oil*	NA	NA	NA	NA	NA
	Oil/Water Emulsion Removed (m³)	NA	NA	NA	NA	NA	NA
Mitigated RARV (334 bbl) Avg River Flow White River Channel	Oil Removed (MT)	0	18.415	0	0	0	0
	Oil/Water Emulsion Removed (m³)	0	20.516	0	0	0	0

* Recovery under low river flow, 100% ice-covered conditions would occur under the ice at points throughout the river channel, not solely at the MCP.

4.1.1 Bad River Releases

4.1.1.1 FBR (9,874 bbl), High River Flow, Bad River Channel Release

Figure 4-3. Oil mass balance graph for the unmitigated FBR scenario in high river flow conditions modeled in April at the Bad River channel location.

Figure 4-4. Composite of maximum surface oil thickness over 4 days for the unmitigated FBR scenario in high river flow conditions modeled in April at the Bad River channel location. This represents the maximum thickness of surface oil that was predicted for each location. The maximum levels of coverage would not be observed at each location simultaneously.

Figure 4-5. Composite of maximum total dissolved hydrocarbon concentration over 4 days for the unmitigated FBR scenario in high river flow conditions modeled in April at the Bad River channel location. This represents the maximum in-water contamination that was predicted for each location.

Figure 4-6. Maximum total hydrocarbon mass on the shore and on sediments after 4 days for the unmitigated FBR scenario in high river flow conditions modeled in April at the Bad River channel location.

4.1.1.2 FBR (9,874 bbl), Average River Flow, Bad River Channel Release

Figure 4-7. Oil mass balance graph for the unmitigated FBR scenario in average river flow conditions modeled in June at the Bad River channel location.

Figure 4-8. Composite of maximum surface oil thickness over 4 days for the unmitigated FBR scenario in average river flow conditions modeled in June at the Bad River channel location. This represents the maximum thickness of surface oil that was predicted for each location. The maximum levels of coverage would not be observed at each location simultaneously.

Figure 4-9. Composite of maximum total dissolved hydrocarbon concentration over 4 days for the unmitigated FBR scenario in average river flow conditions modeled in June at the Bad River channel location. This represents the maximum in-water contamination that was predicted for each location.

Figure 4-10. Maximum total hydrocarbon mass on the shore and on sediments after 4 days for the unmitigated FBR scenario in average river flow conditions modeled in June at the Bad River channel location.

4.1.1.3 FBR (9,874 bbl), Low River Flow, Bad River Channel Release
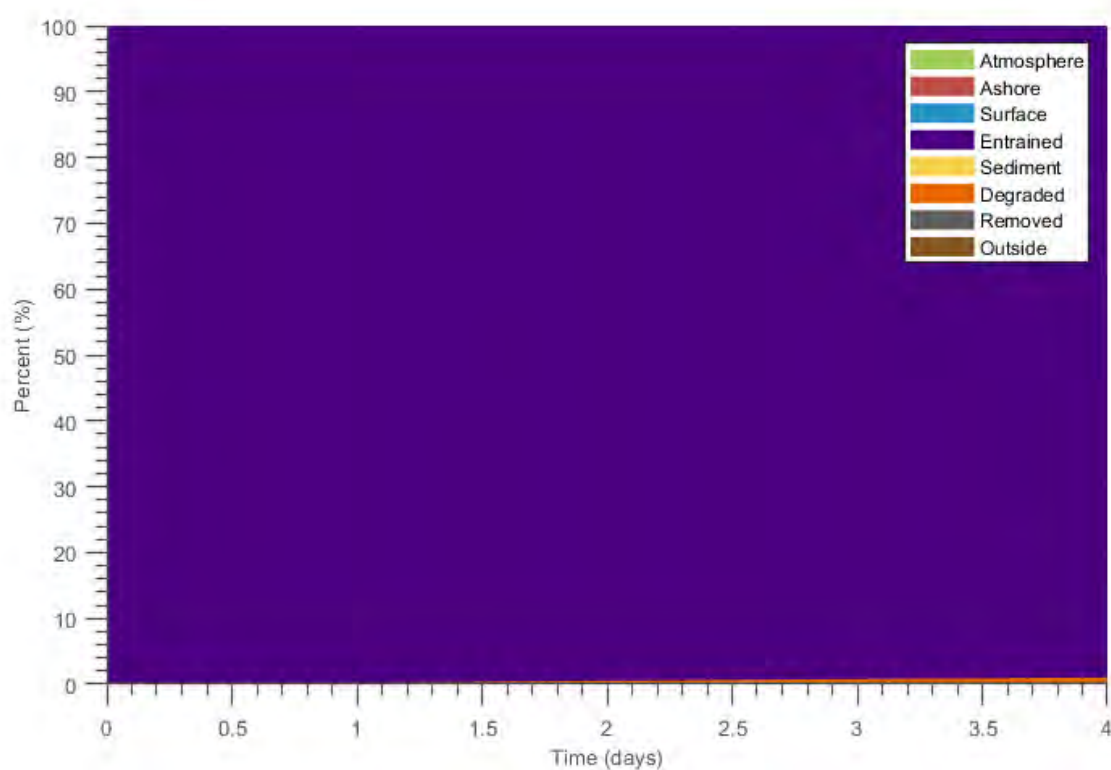
Figure 4-11. Oil mass balance graph for the unmitigated FBR scenario in low river flow conditions modeled in January at the Bad River channel location.
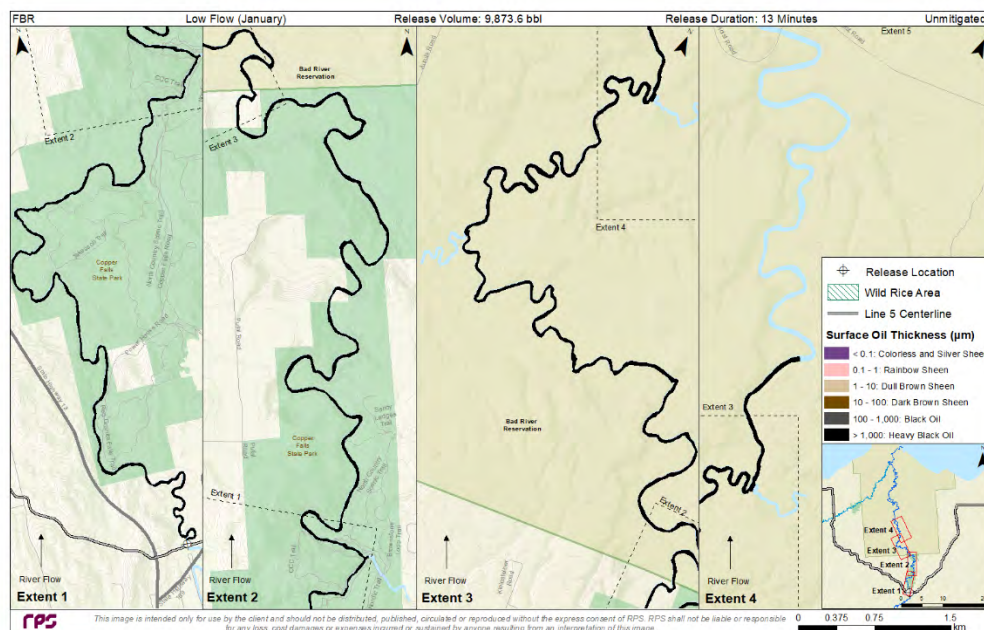
Panel intentionally left blank.

Downstream extents 5-8 not displayed because no oil was predicted there.

Figure 4-12. Composite of maximum subsurface oil thickness (beneath ice) for the unmitigated FBR scenario in low river flow conditions modeled in January at the Bad River channel location. This represents the maximum thickness of oil that was predicted for each location. The maximum levels of coverage would not be observed at each location simultaneously.
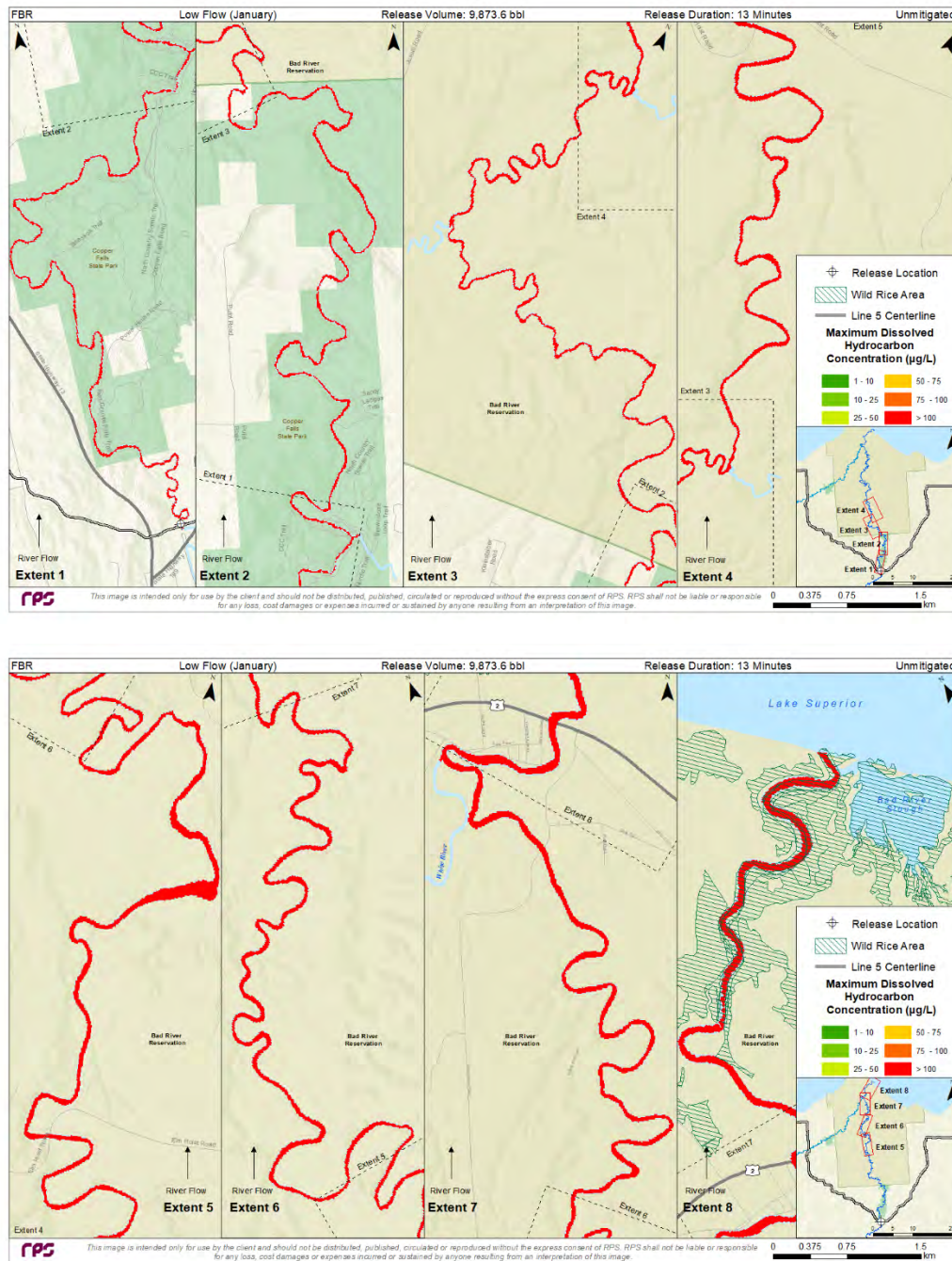
Figure 4-13. Composite of maximum total dissolved hydrocarbon concentration for the unmitigated FBR scenario in low river flow conditions modeled in January at the Bad River channel location. This represents the maximum in-water contamination that was predicted for each location.

4.1.1.4 HARV (1,911 bbl), High River Flow, Bad River Channel Release
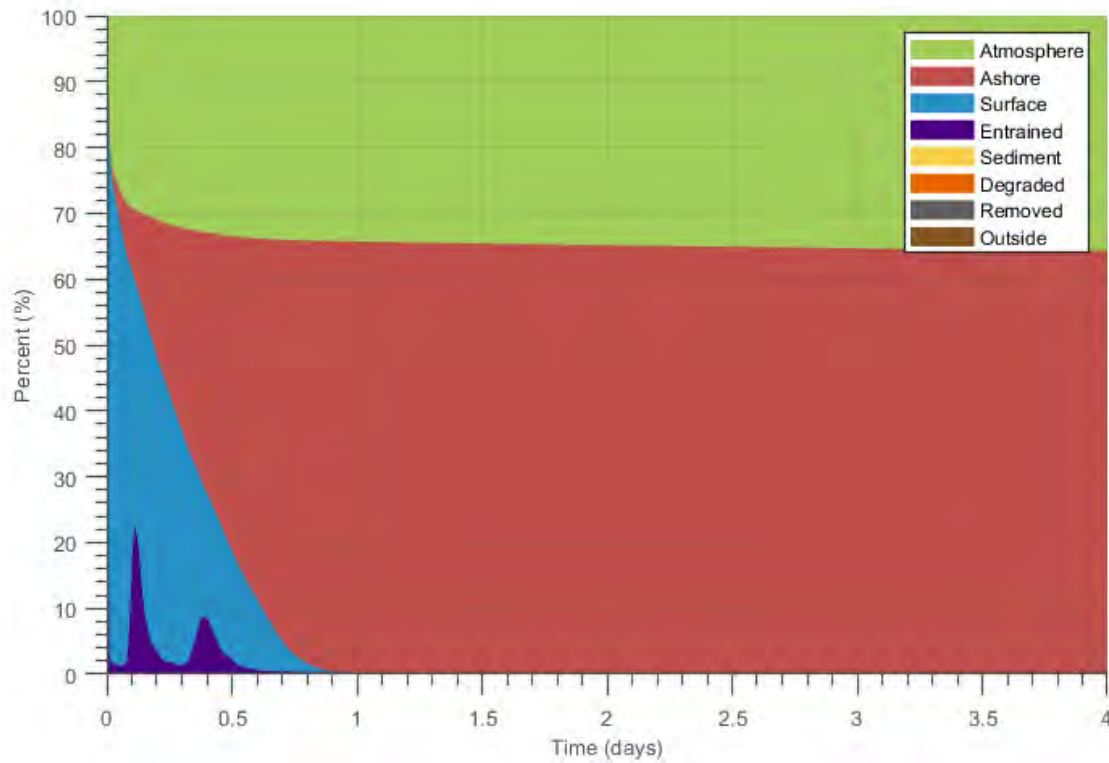
Figure 4-14. Oil mass balance graph for the unmitigated HARV scenario in high river flow conditions modeled in April at the Bad River channel location.
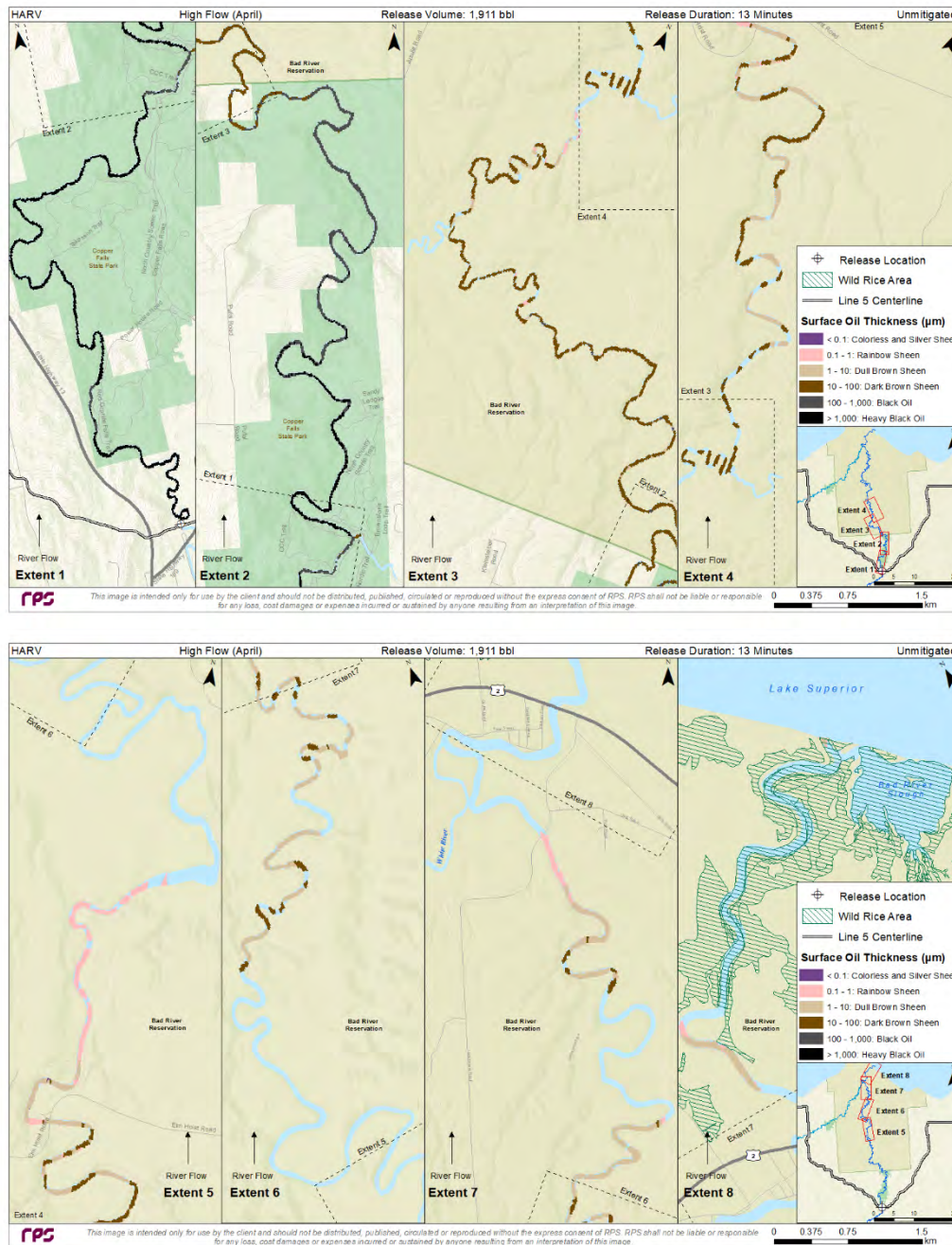
Figure 4-15. Composite of maximum surface oil thickness over 4 days for the unmitigated HARV scenario in high river flow conditions modeled in April at the Bad River channel location. This represents the maximum thickness of surface oil that was predicted for each location. The maximum levels of coverage would not be observed at each location simultaneously.

Figure 4-16. Composite of maximum total dissolved hydrocarbon concentration over 4 days for the unmitigated HARV scenario in high river flow conditions modeled in April at the Bad River channel location. This represents the maximum in-water contamination that was predicted for each location.

Figure 4-17. Maximum total hydrocarbon mass on the shore and on sediments after 4 days for the unmitigated HARV scenario in high river flow conditions modeled in April at the Bad River channel location.

4.1.1.5 HARV (1,911 bbl), Average River Flow, Bad River Channel Release
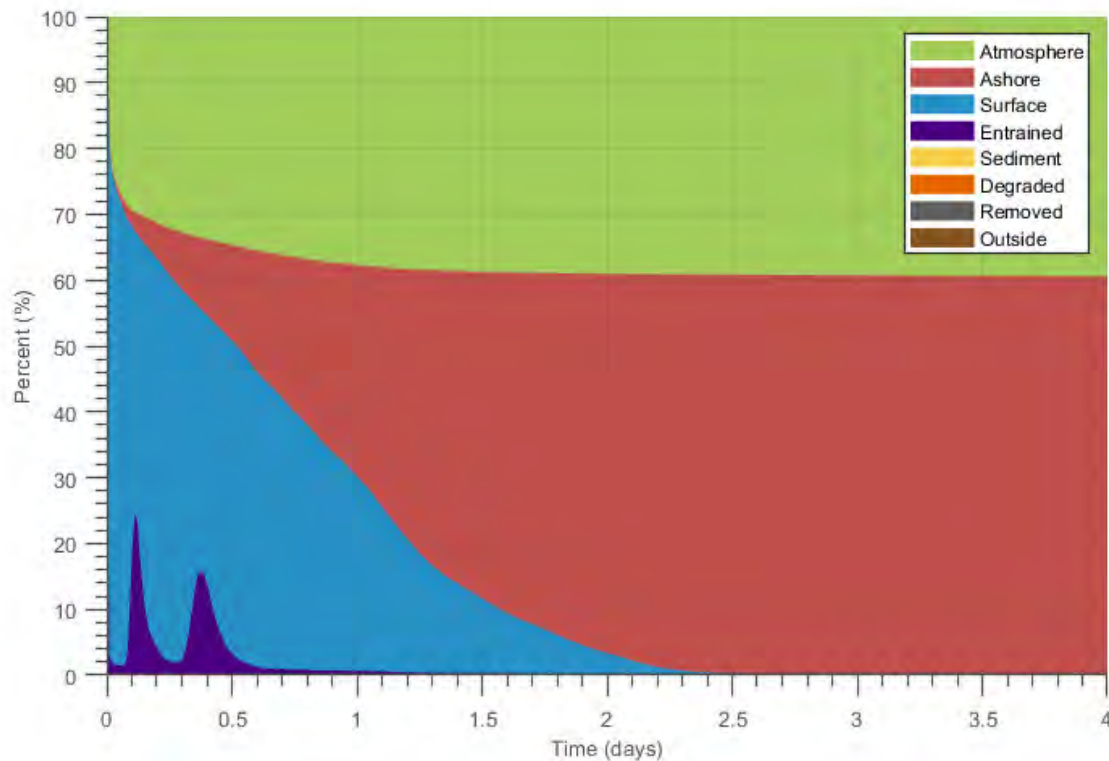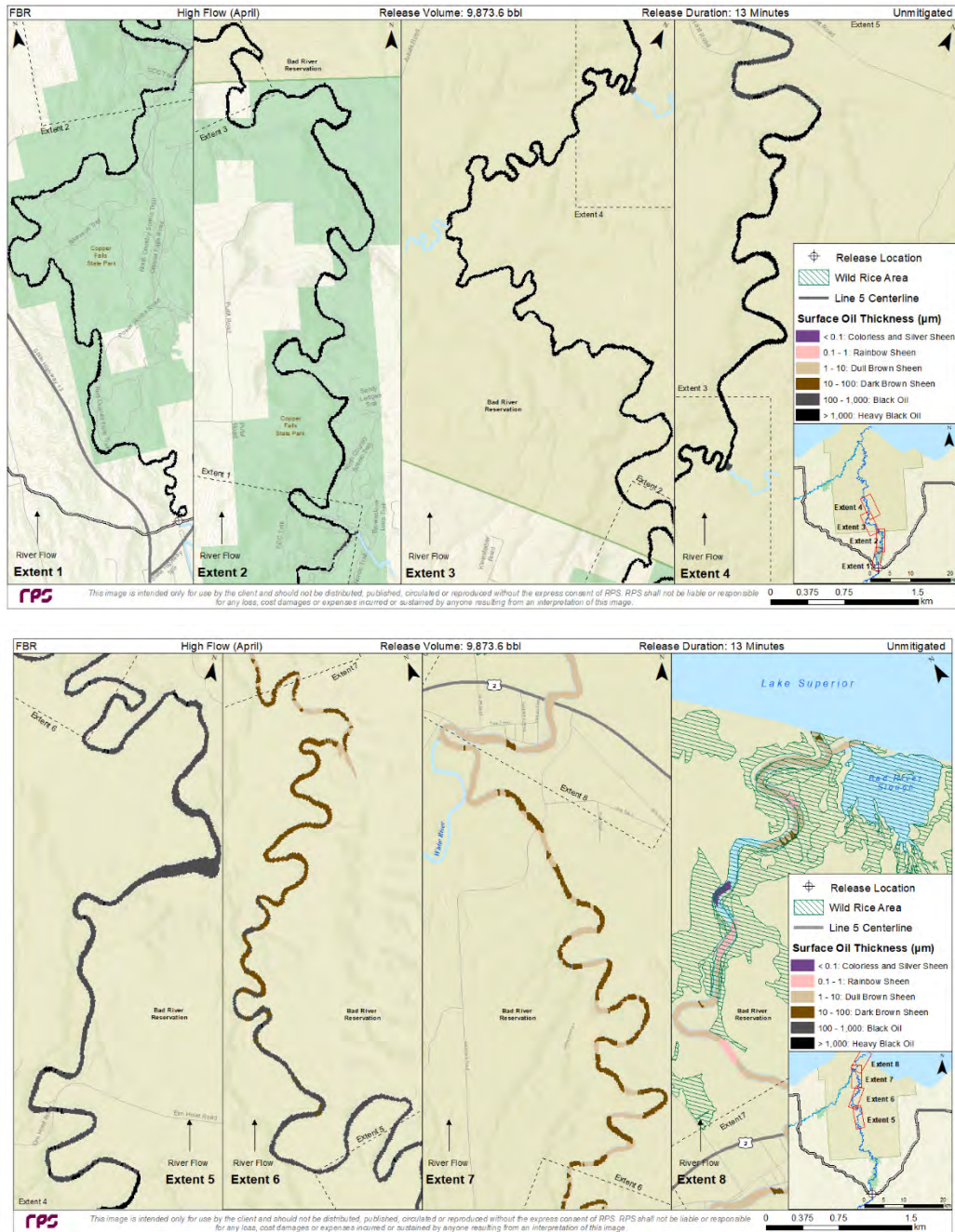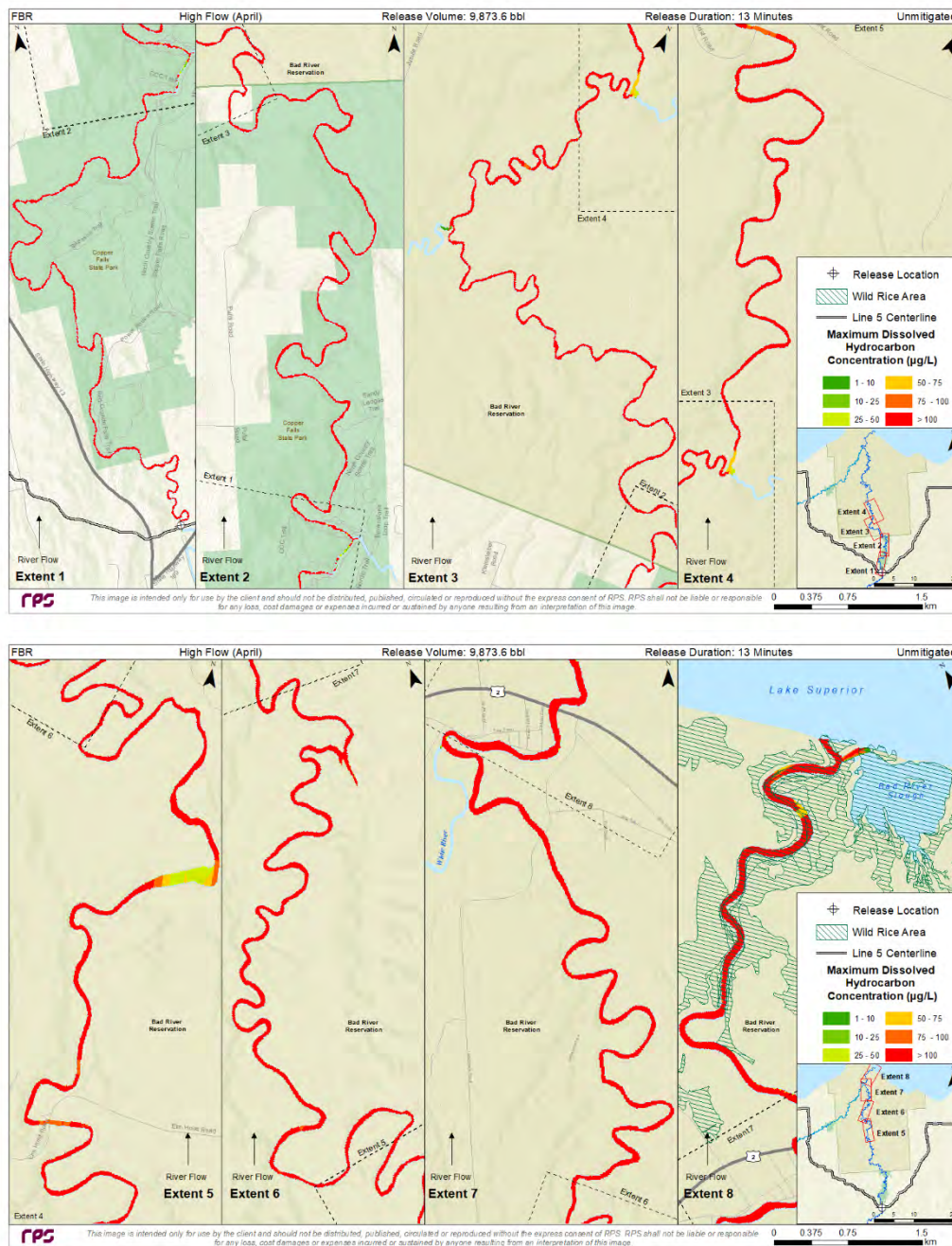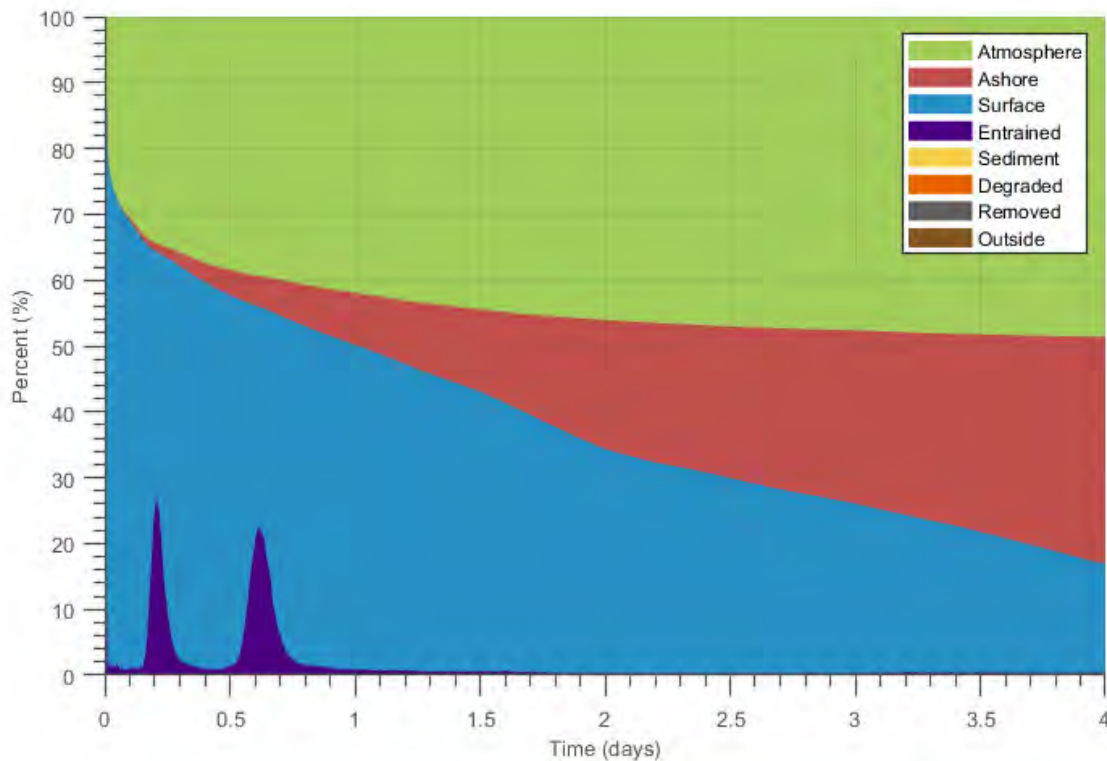

Figure 4-18. Oil mass balance graph for the unmitigated HARV scenario in average river flow conditions modeled in June at the Bad River channel location.
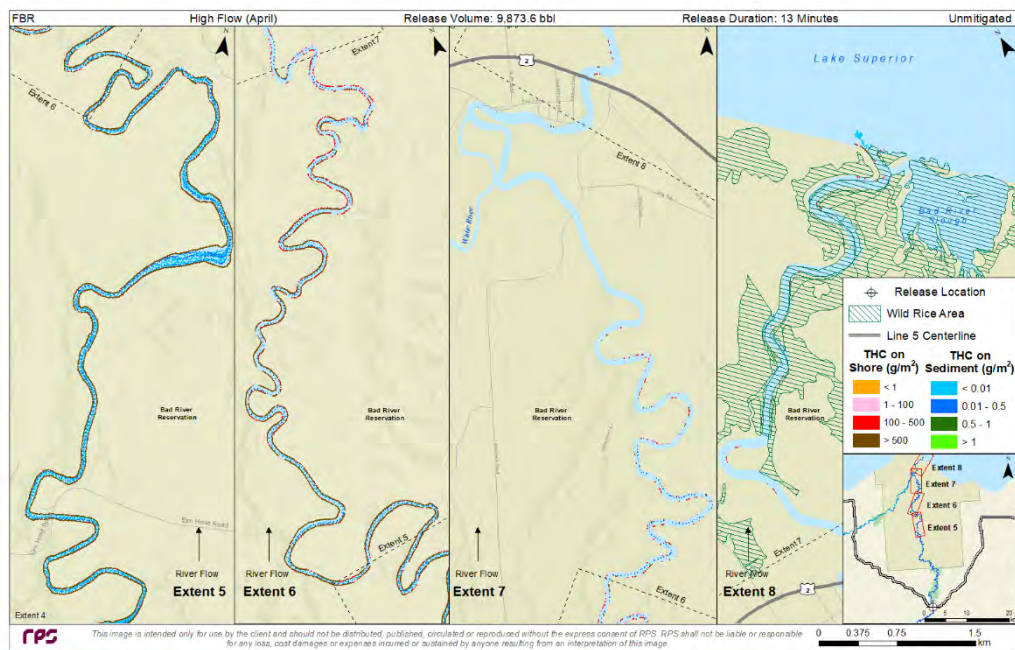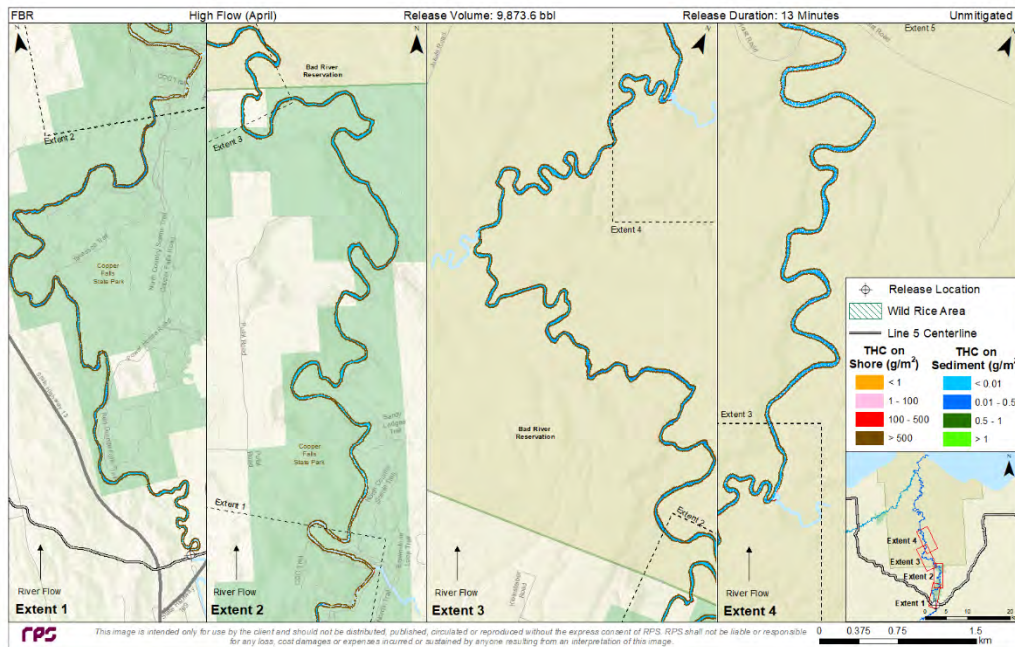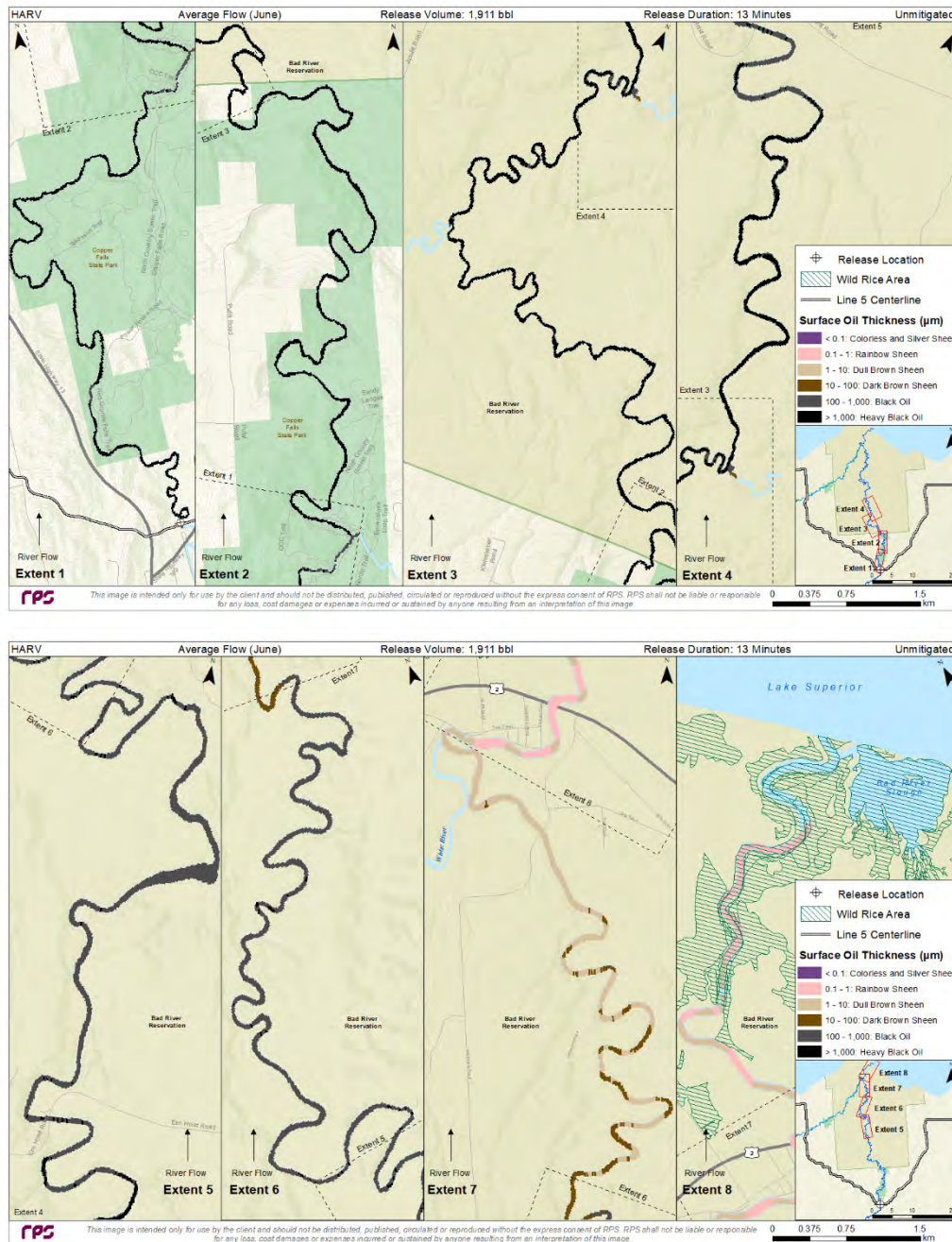
Figure 4-19. Composite of maximum surface oil thickness over 4 days for the unmitigated HARV scenario in average river flow conditions modeled in June at the Bad River channel location. This represents the maximum thickness of surface oil that was predicted for each location. The maximum levels of coverage would not be observed at each location simultaneously.

Figure 4-20. Composite of maximum total dissolved hydrocarbon concentration over 4 days for the unmitigated HARV scenario in average river flow conditions modeled in June at the Bad River channel location. This represents the maximum in-water contamination that was predicted for each location.

Figure 4-21. Maximum total hydrocarbon mass on the shore and on sediments after 4 days for the unmitigated HARV scenario in average river flow conditions modeled in June at the Bad River channel location.

4.1.1.6 HARV (1,911 bbl), Low River Flow, Bad River Channel Release
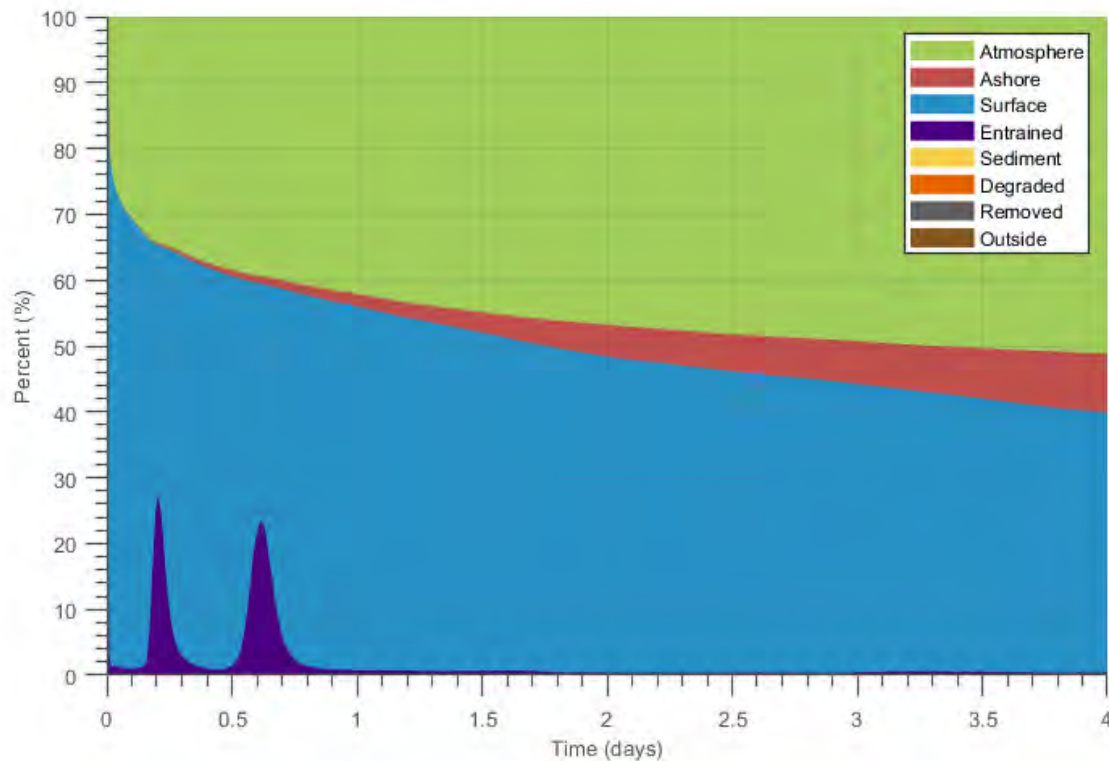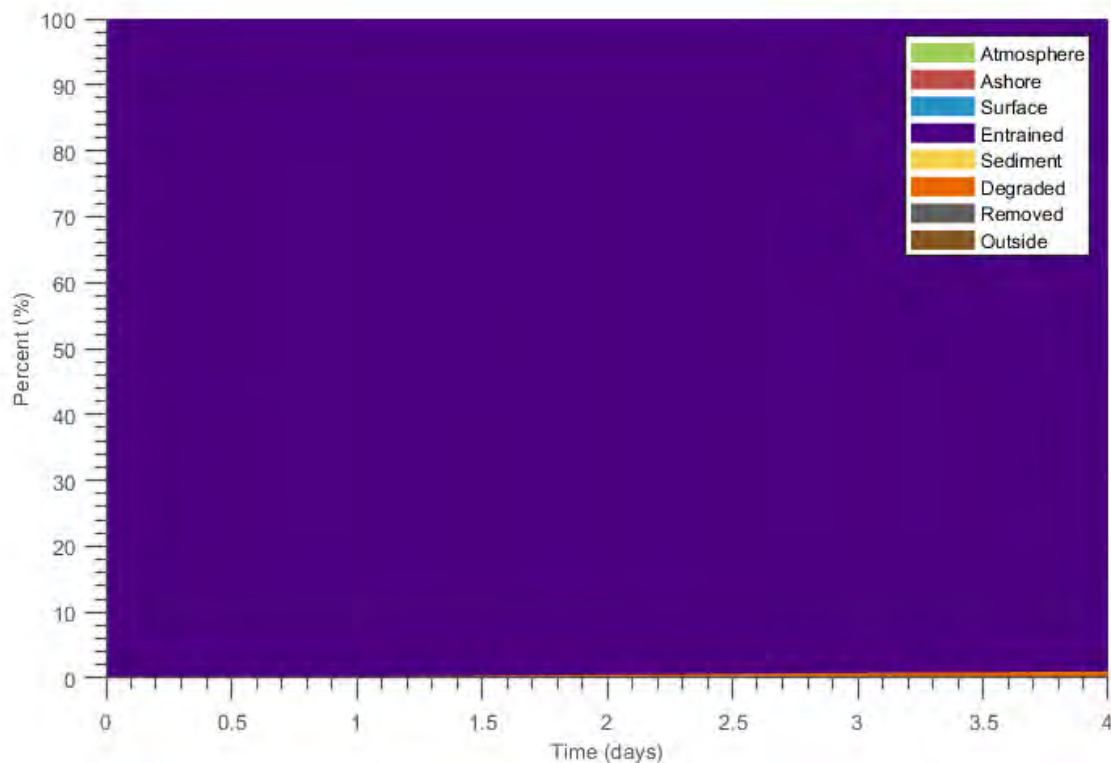

Figure 4-22. Oil mass balance graph for the unmitigated HARV scenario in low river flow conditions modeled in January at the Bad River channel location.
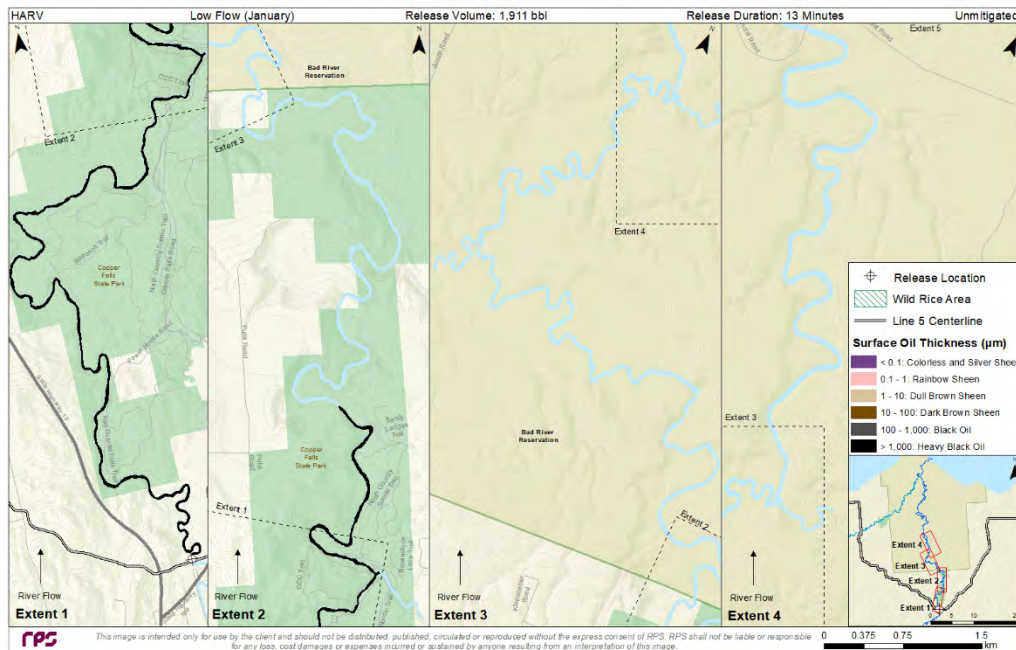
Panel intentionally left blank.

Downstream extents 5-8 not displayed because no oil was predicted there.

Figure 4-23. Composite of maximum subsurface oil thickness (beneath ice) for the unmitigated HARV scenario in low river flow conditions modeled in January at the Bad River channel location. This represents the maximum thickness of oil that was predicted for each location. The maximum levels of coverage would not be observed at each location simultaneously.

Figure intentionally left blank.

Cumulative maximum DHCs were predicted to exceed 100 µg/L

from the release location down to Lake Superior. See Figure 4-13.

Figure 4-24. Composite of maximum total dissolved hydrocarbon concentration for the unmitigated HARV scenario in low river flow conditions modeled in January at the Bad River channel location. This represents the maximum in-water contamination that was predicted for each location.

4.1.1.7 RARV (334 bbl), Average River Flow, Bad River Channel Release

Figure 4-25. Oil mass balance graph for the unmitigated RARV scenario in average river flow conditions modeled in June at the Bad River channel location.
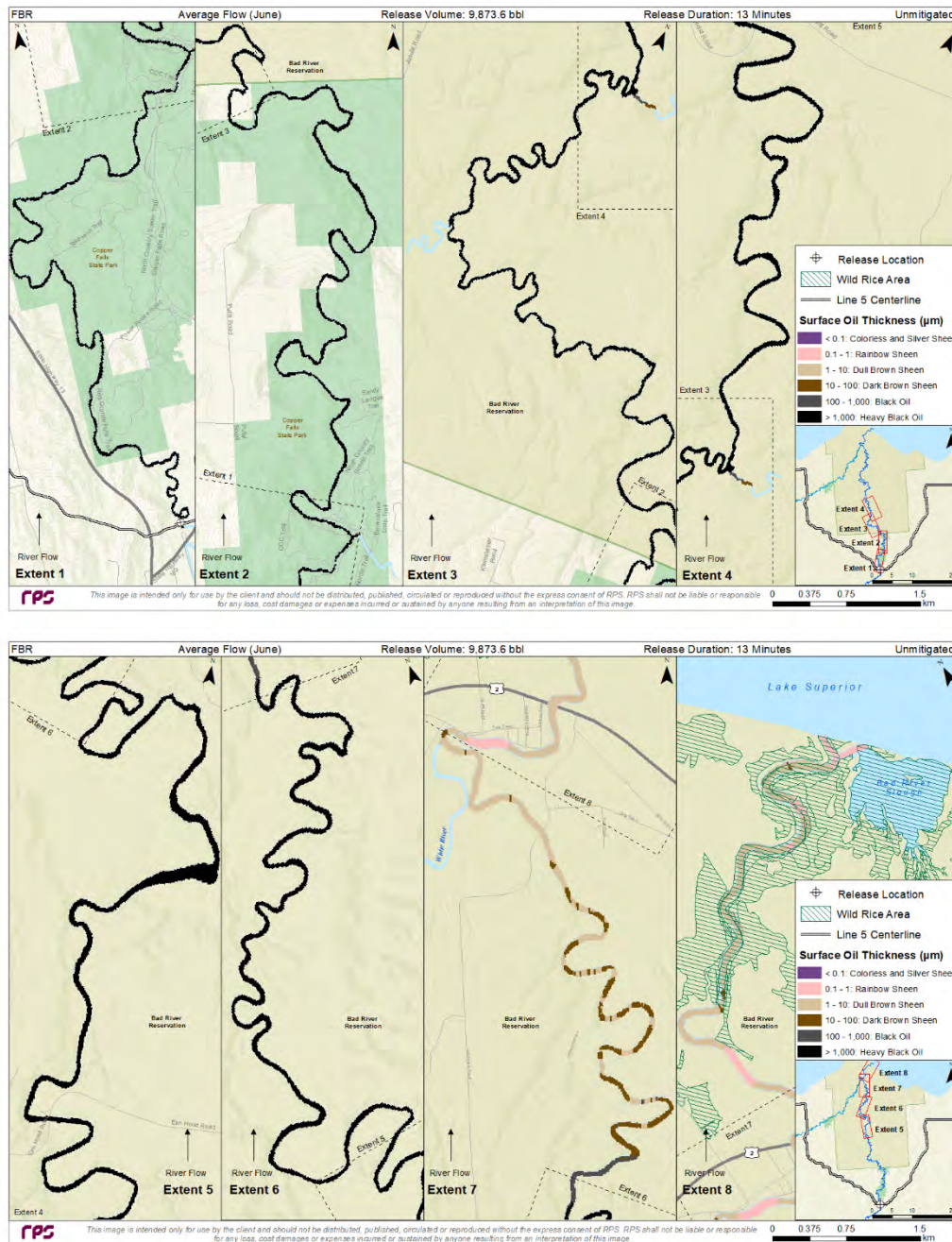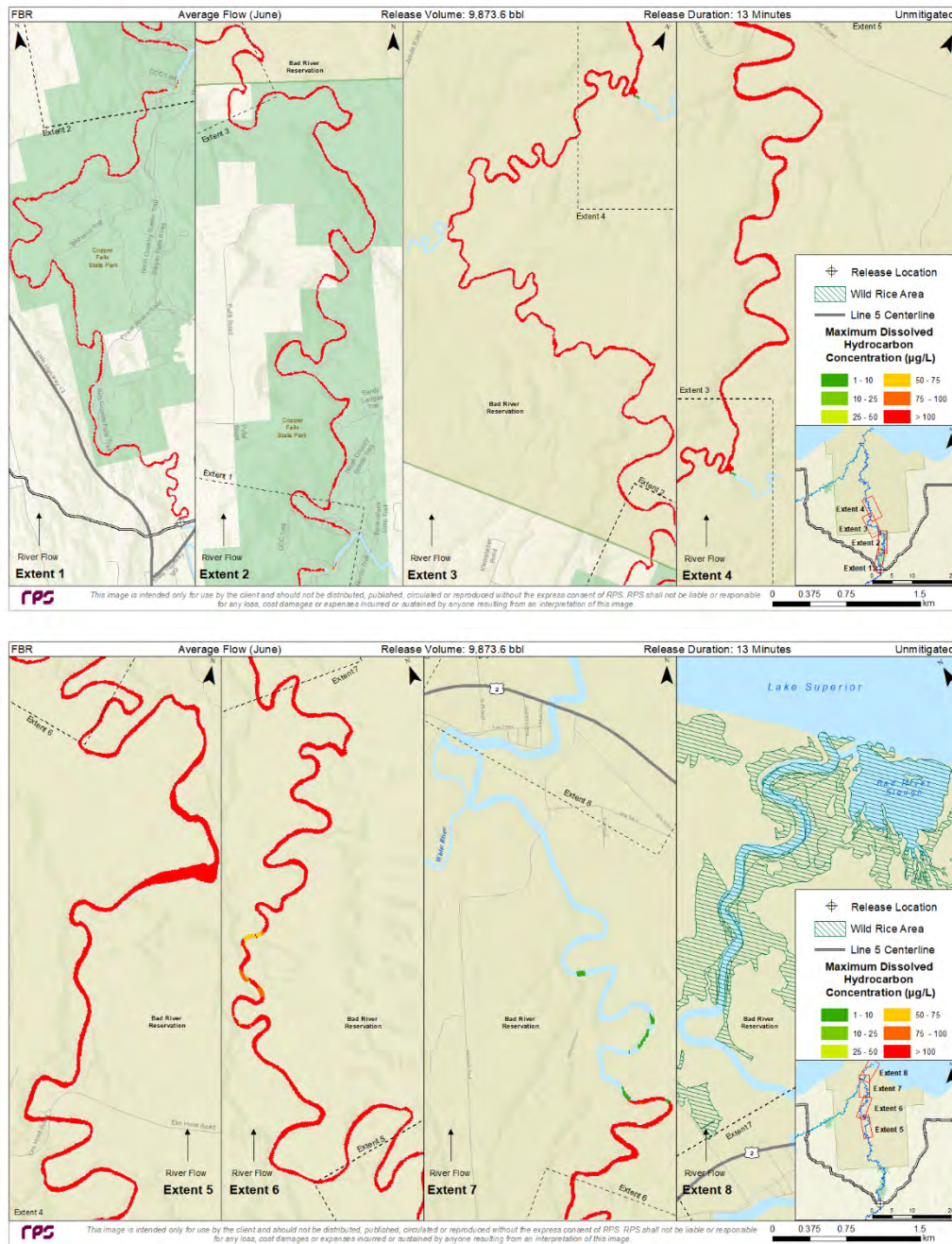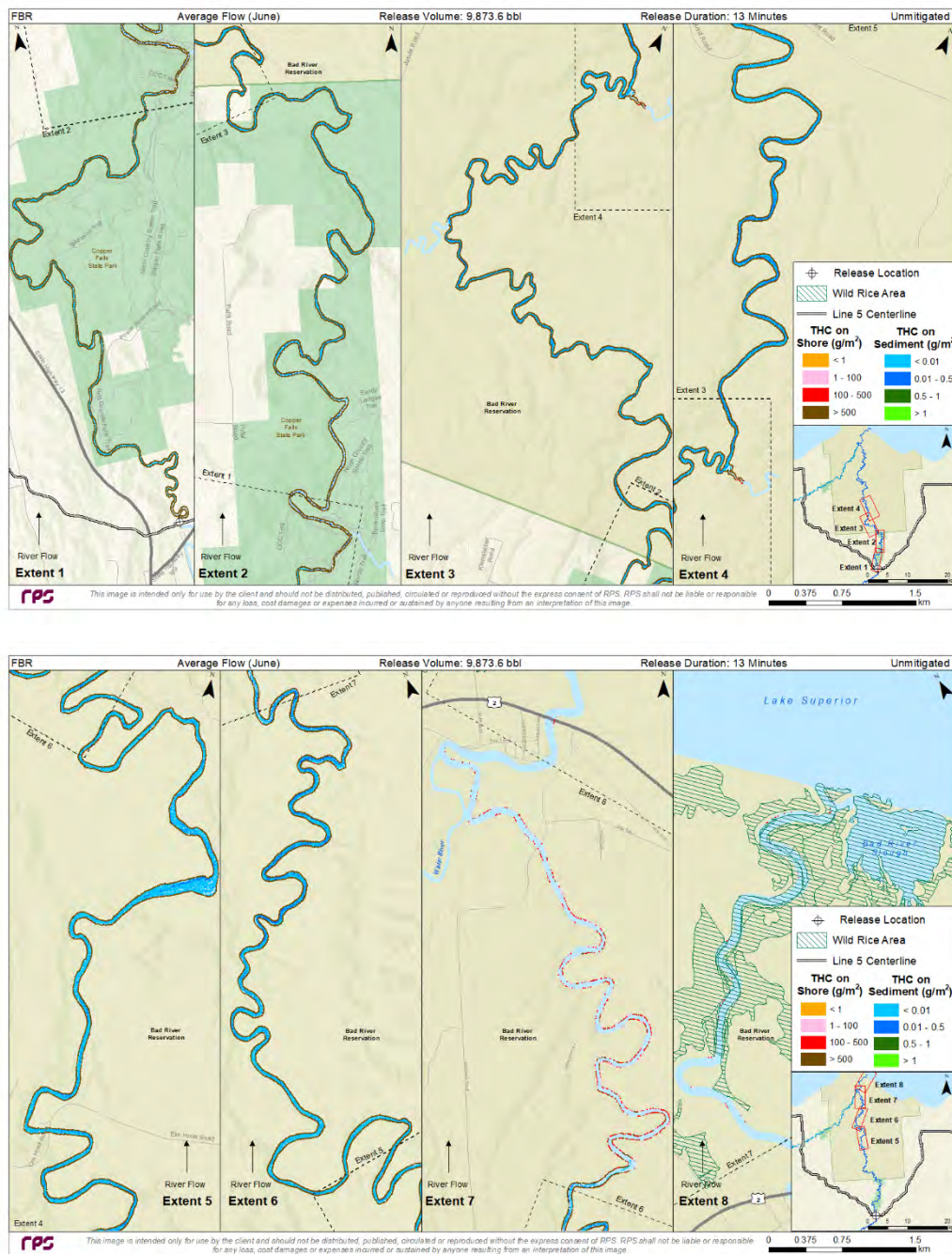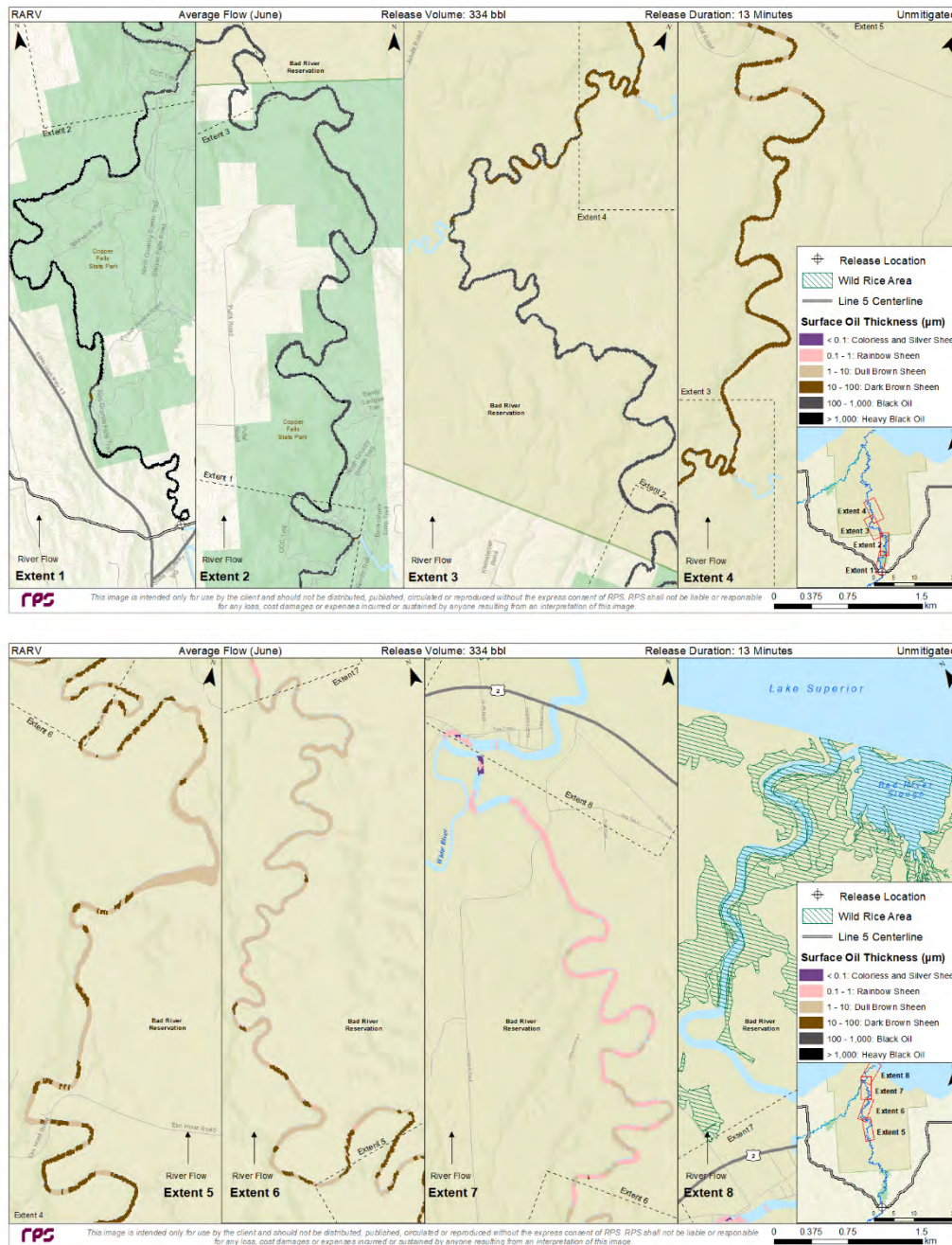
Figure 4-26. Composite of maximum surface oil thickness over 4 days for the unmitigated RARV scenario in average river flow conditions modeled in June at the Bad River channel location. This represents the maximum thickness of surface oil that was predicted for each location. The maximum levels of coverage would not be observed at each location simultaneously.
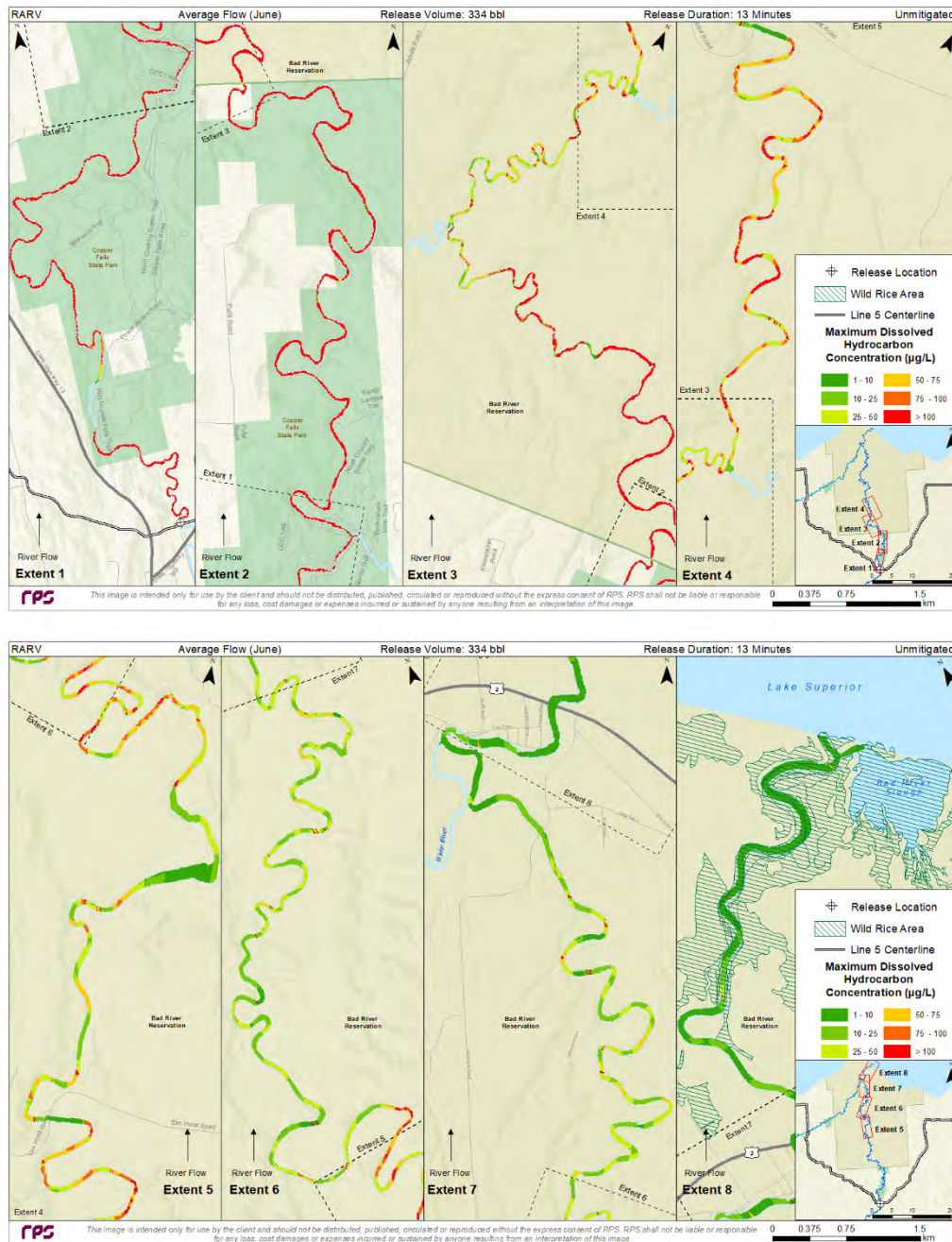
Figure 4-27. Composite of maximum total dissolved hydrocarbon concentration over 4 days for the unmitigated RARV scenario in average river flow conditions modeled in June at the Bad River channel location. This represents the maximum in-water contamination that was predicted for each location.

Figure 4-28. Maximum total hydrocarbon mass on the shore and on sediments after 4 days for the unmitigated RARV scenario in average river flow conditions modeled in June at the Bad River channel location.
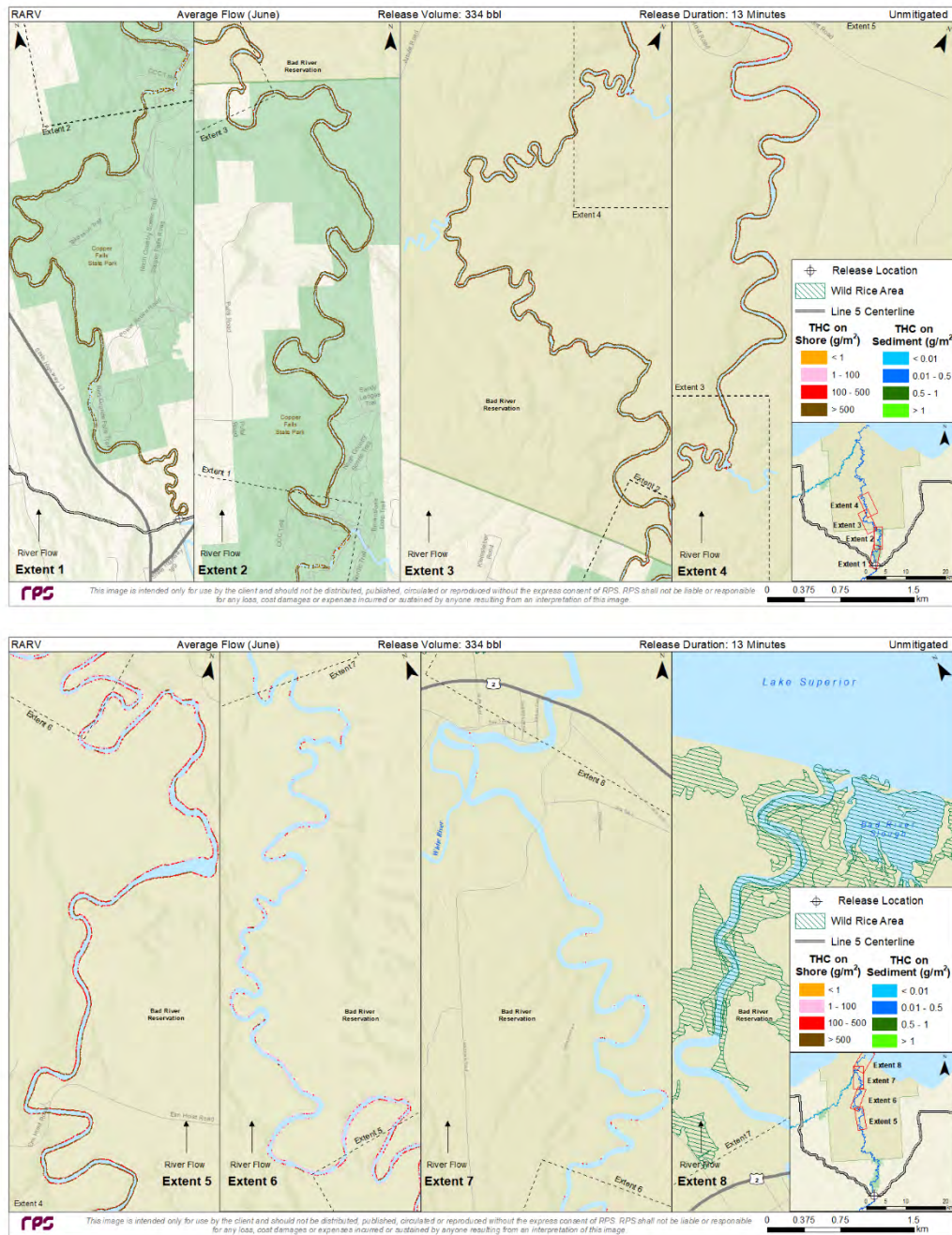
### 4.1.1.8   Mitigated FBR (9,874 bbl), High River Flow, Bad River Channel Release

Figure 4-29. Oil mass balance graph for the mitigated FBR scenario in high river flow conditions modeled in April at the Bad River channel location.

Figure 4-30. Composite of maximum surface oil thickness over 4 days for the mitigated FBR scenario in high river flow conditions modeled in April at the Bad River channel location. This represents the maximum thickness of surface oil that was predicted for each location. An additional barrier was not modeled. Small amounts of oil (e.g., sheens <1/1,000[th] the thickness of heavy black oil) are not likely to be transported beyond this point.

Figure 4-31. Composite of maximum total dissolved hydrocarbon concentration over 4 days for the mitigated FBR scenario in high river flow conditions modeled in April at the Bad River channel location. This represents the maximum in-water contamination that was predicted for each location.
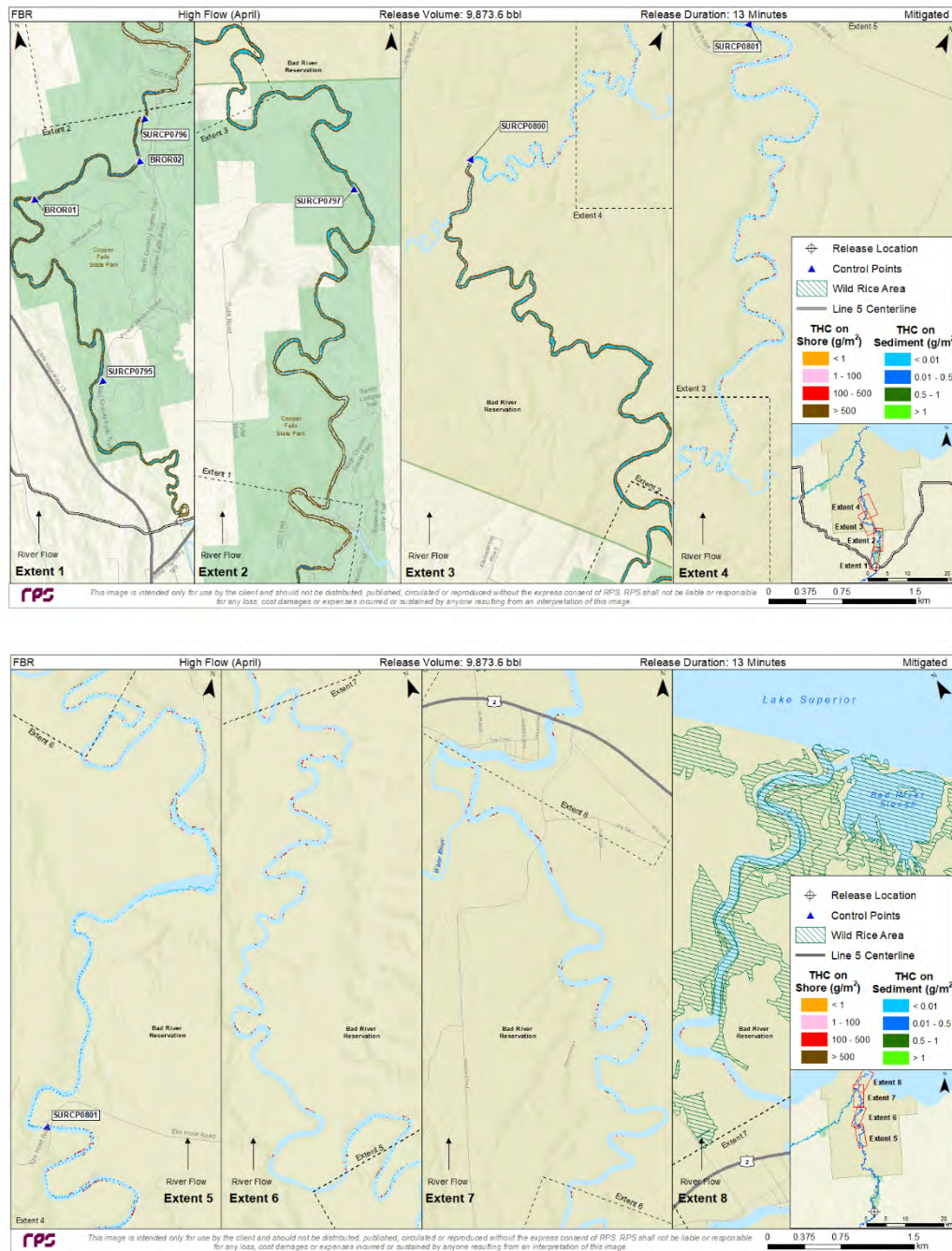
Figure 4-32. Maximum total hydrocarbon mass on the shore and on sediments after 4 days for the mitigated FBR scenario in high river flow conditions modeled in April at the Bad River channel location.

## 4.1.1.9 Mitigated FBR (9,874 bbl), Average River Flow, Bad River Channel Release
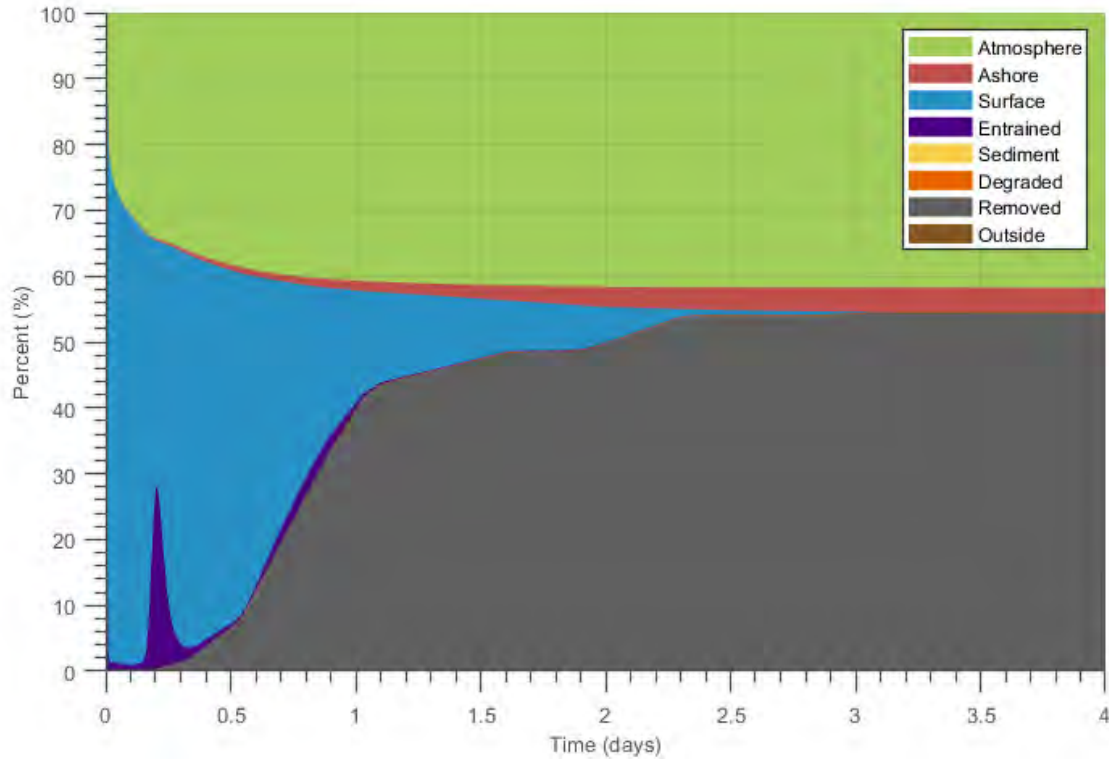
Figure 4-33. Oil mass balance graph for the mitigated FBR scenario in average river flow conditions modeled in June at the Bad River channel location.

Figure 4-34. Composite of maximum surface oil thickness over 4 days for the mitigated FBR scenario in average river flow conditions modeled in June at the Bad River channel location. This represents the maximum thickness of surface oil that was predicted for each location. An additional barrier was not modeled. Small amounts of oil (e.g., sheens <1/1,000th the thickness of heavy black oil) are not likely to be transported beyond this point.
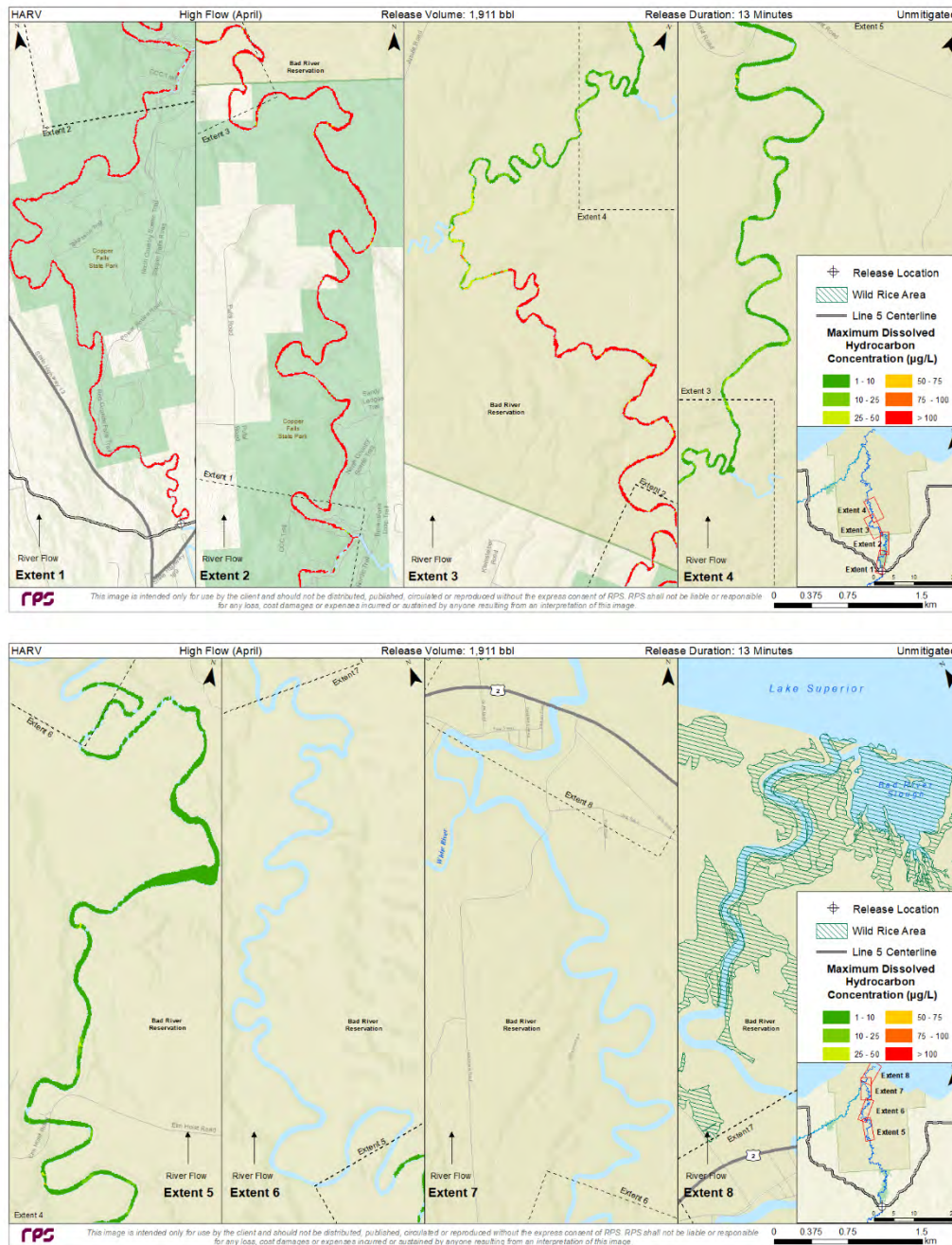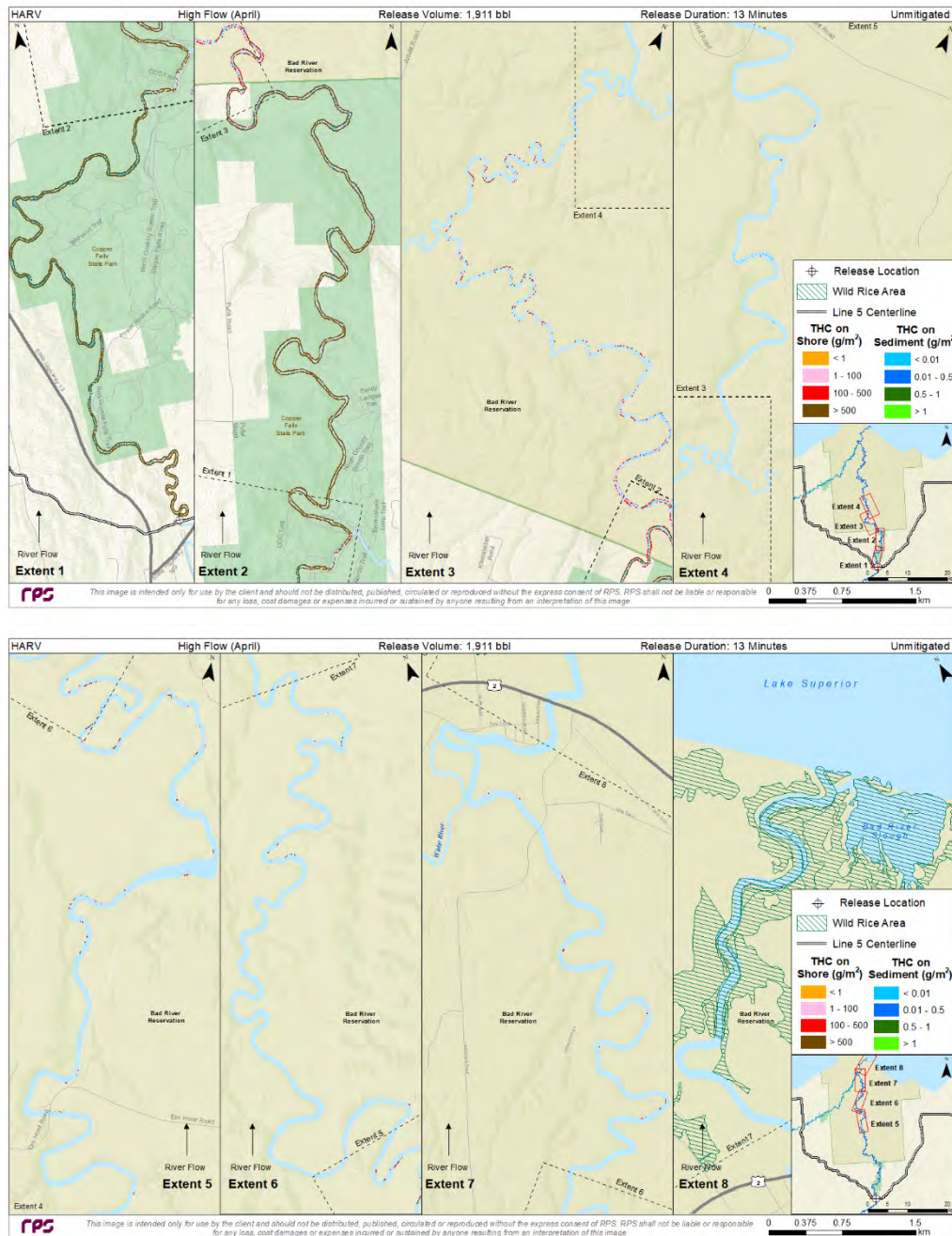
Figure 4-35. Composite of maximum total dissolved hydrocarbon concentration over 4 days for the mitigated FBR scenario in average river flow conditions modeled in June at the Bad River channel location. This represents the maximum in-water contamination that was predicted for each location.

Figure 4-36. Maximum total hydrocarbon mass on the shore and on sediments after 4 days for the FBR scenario in average river flow conditions modeled in June at the Bad River channel location.

## 4.1.1.10 Mitigated FBR (9,874 bbl), Low River Flow, Bad River Channel Release

Figure 4-37. Oil mass balance graph for the mitigated FBR scenario in low river flow conditions modeled in January at the Bad River channel location.
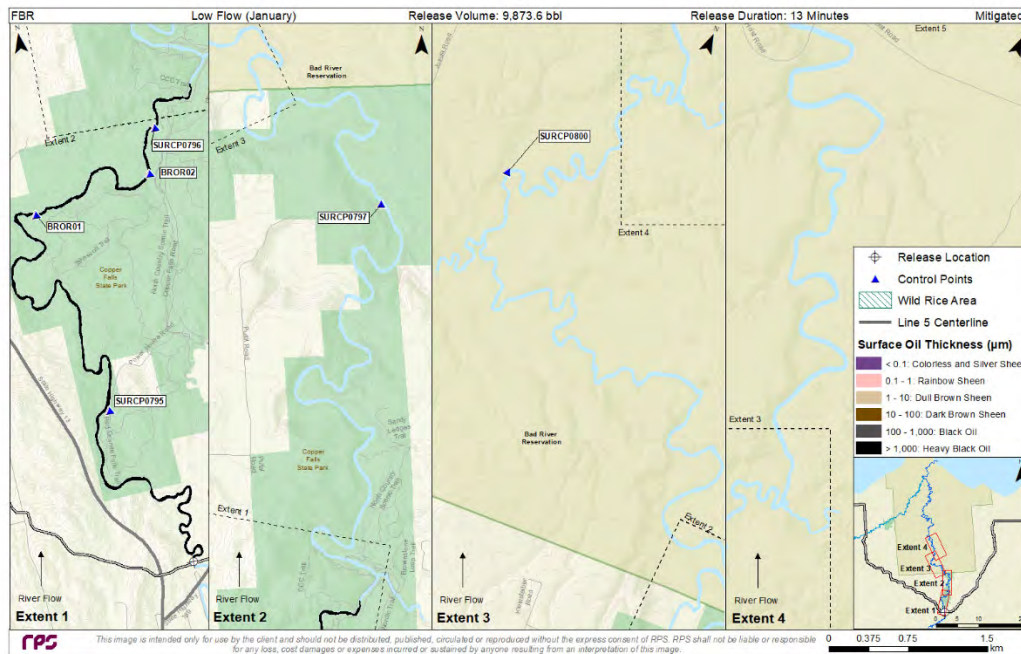
Panel intentionally left blank.

Downstream extents 5-8 not displayed because no oil was predicted there.

Figure 4-38. Composite of maximum subsurface oil thickness (beneath ice) for the mitigated FBR scenario in low river flow conditions modeled in January at the Bad River channel location. This represents the maximum thickness of oil that was predicted for each location. The maximum levels of coverage would not be observed at each location simultaneously.

Figure intentionally left blank.

Cumulative maximum DHCs were predicted to exceed 100 µg/L

from the release location down to Lake Superior. See Figure 4-13.

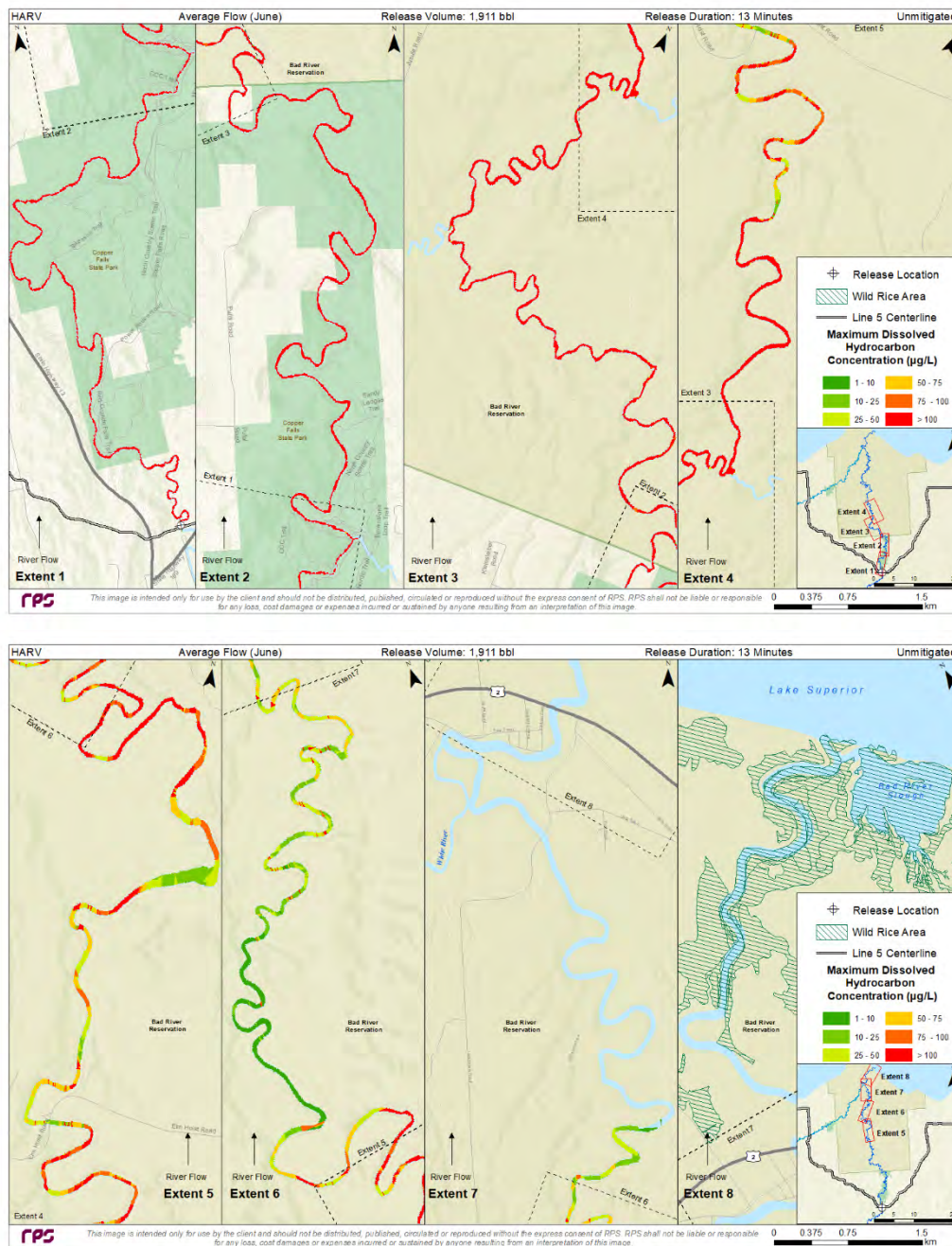**Figure 4-39. Composite of maximum total dissolved hydrocarbon concentration for the mitigated FBR scenario in low river flow conditions modeled in January at the Bad River channel location. This represents the maximum in-water contamination that was predicted for each location.**

4.1.1.11 Mitigated HARV (1,911 bbl), High River Flow, Bad River Channel Release
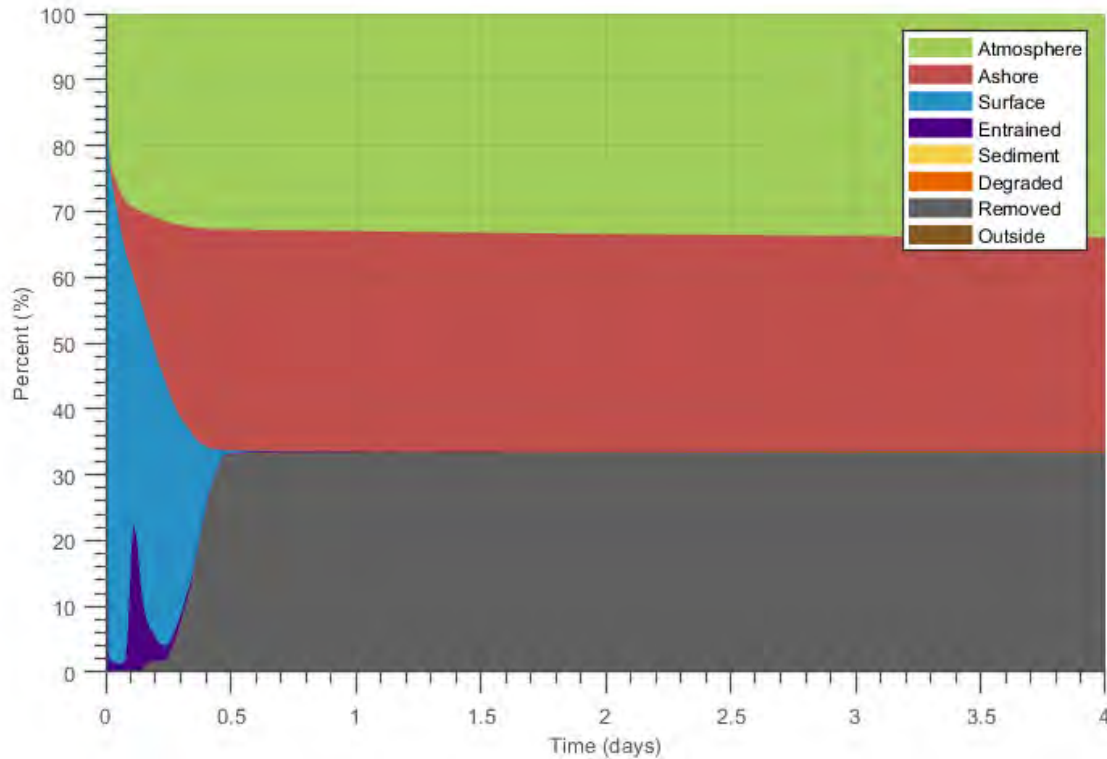
Figure 4-40. Oil mass balance graph for the mitigated HARV scenario in high river flow conditions modeled in April at the Bad River channel location.

Figure 4-41. Composite of maximum surface oil thickness over 4 days for the mitigated HARV scenario in high river flow conditions modeled in April at the Bad River channel location. This represents the maximum thickness of surface oil that was predicted for each location. An additional barrier was not modeled. Small amounts of oil (e.g., sheens <1/1,000th the thickness of heavy black oil) are not likely to be transported beyond this point.

Figure 4-42. Composite of maximum total dissolved hydrocarbon concentration over 4 days for the mitigated HARV scenario in high river flow conditions modeled in April at the Bad River channel location. This represents the maximum in-water contamination that was predicted for each location.
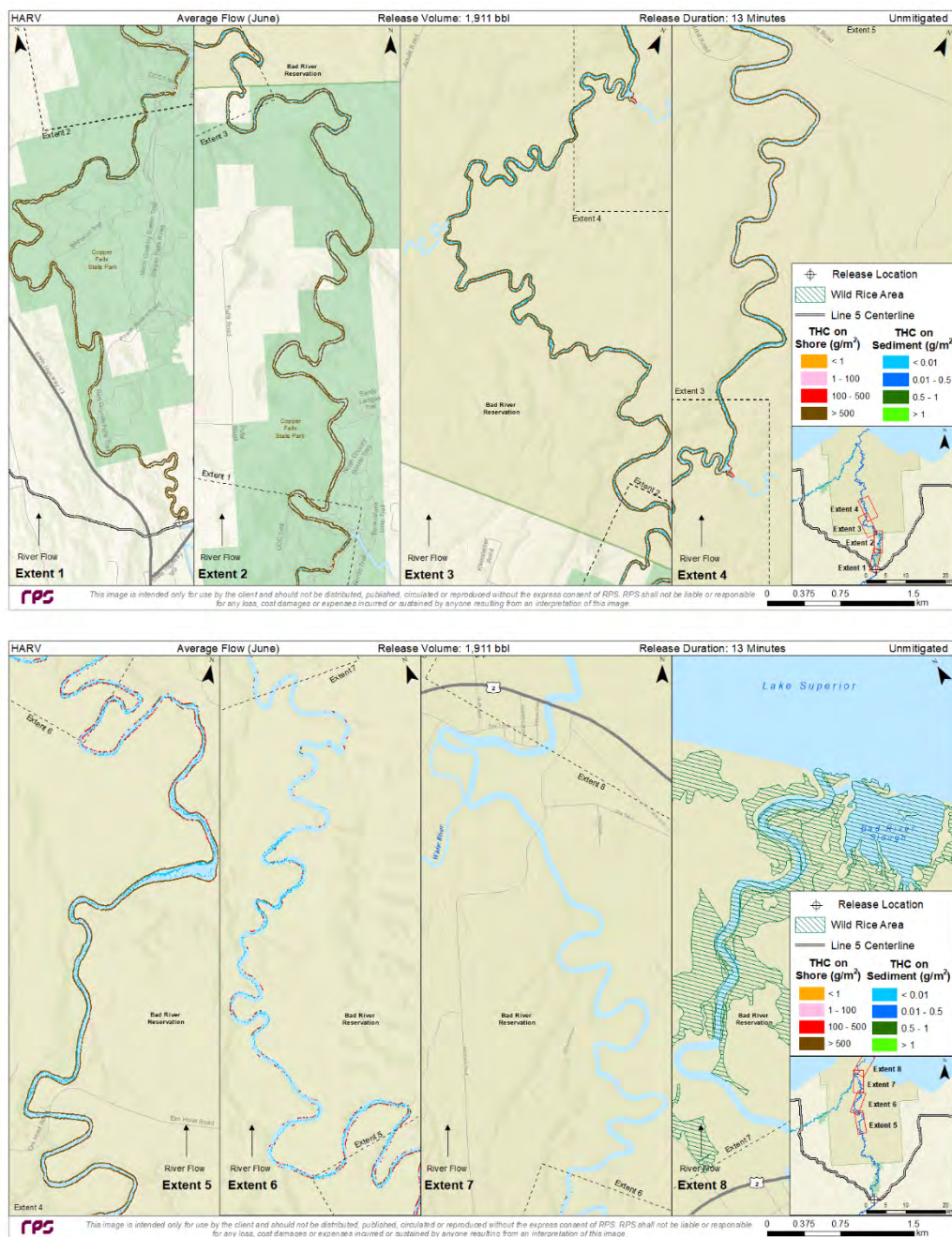
Figure 4-43. Maximum total hydrocarbon mass on the shore and on sediments after 4 days for the mitigated HARV scenario in high river flow conditions modeled in April at the Bad River channel location.

### 4.1.1.12 Mitigated HARV (1,911 bbl), Average River Flow, Bad River Channel Release
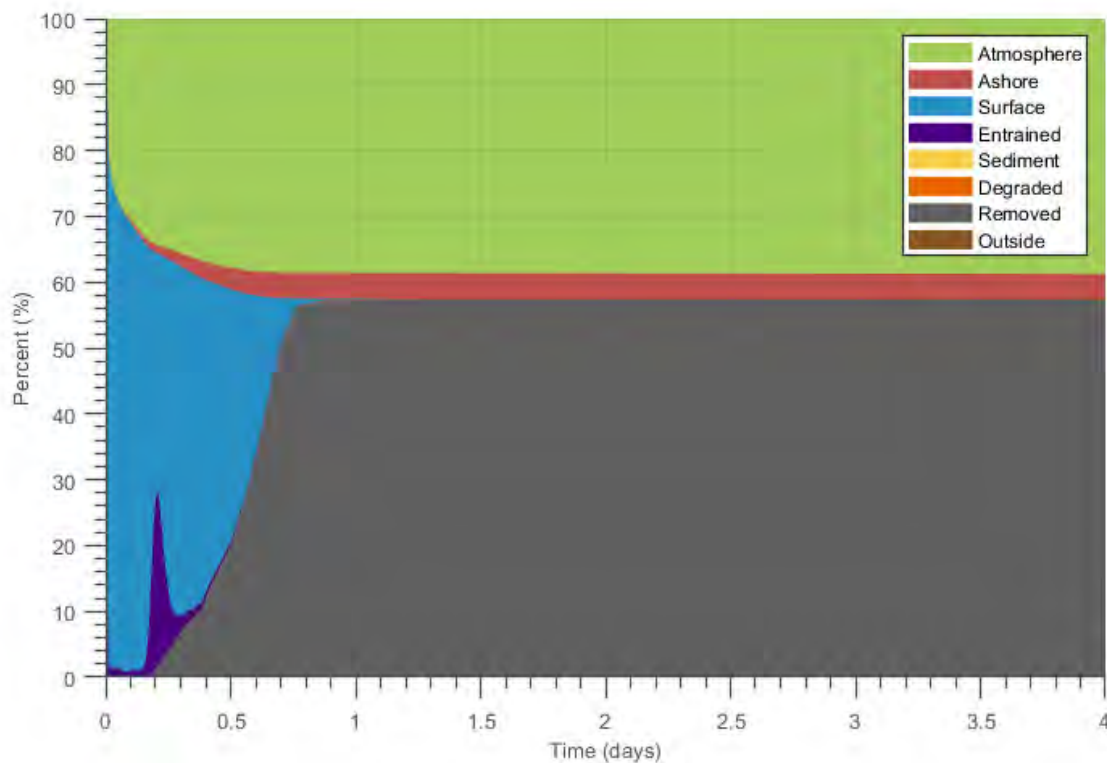
Figure 4-44. Oil mass balance graph for the mitigated HARV scenario in average river flow conditions modeled in June at the Bad River channel location.
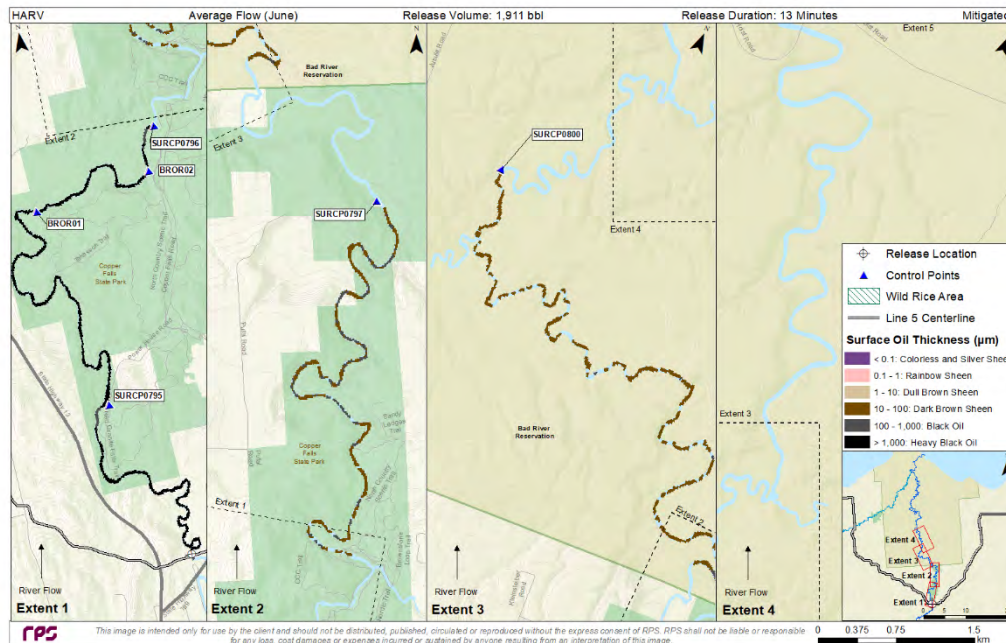
Panel intentionally left blank.

Downstream extents 5-8 not displayed because no oil was predicted there.

Figure 4-45. Composite of maximum surface oil thickness over 4 days for the mitigated HARV scenario in average river flow conditions modeled in June at the Bad River channel location. This represents the maximum thickness of surface oil that was predicted for each location. The maximum levels of coverage would not be observed at each location simultaneously.

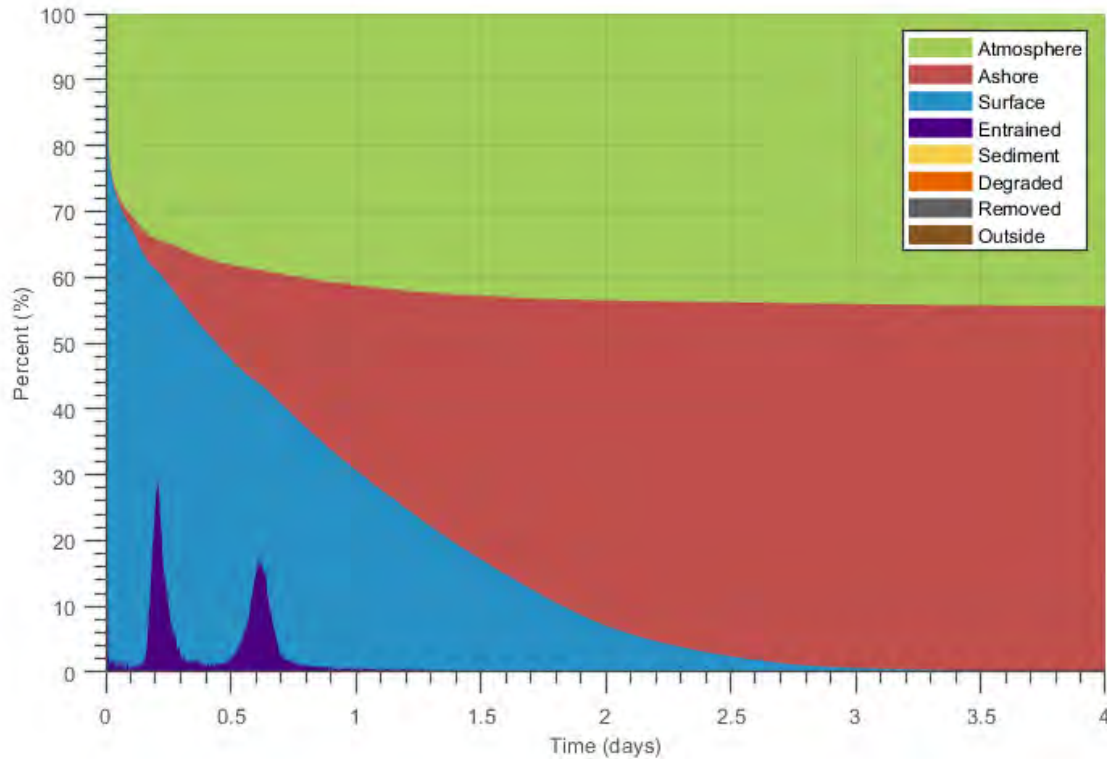**Figure 4-46. Composite of maximum total dissolved hydrocarbon concentration over 4 days for the mitigated HARV scenario in average river flow conditions modeled in June at the Bad River channel location. This represents the maximum in-water contamination that was predicted for each location.**

Panel intentionally left blank.

Downstream extents 5-8 not displayed because no oil was predicted there.

Figure 4-47. Maximum total hydrocarbon mass on the shore and on sediments after 4 days for the mitigated HARV scenario in average river flow conditions modeled in June at the Bad River channel location.

4.1.1.13 Mitigated HARV (1,911 bbl), Low River Flow, Bad River Channel Release

Figure 4-48. Oil mass balance graph for the mitigated HARV scenario in low river flow conditions modeled in January at the Bad River channel location.
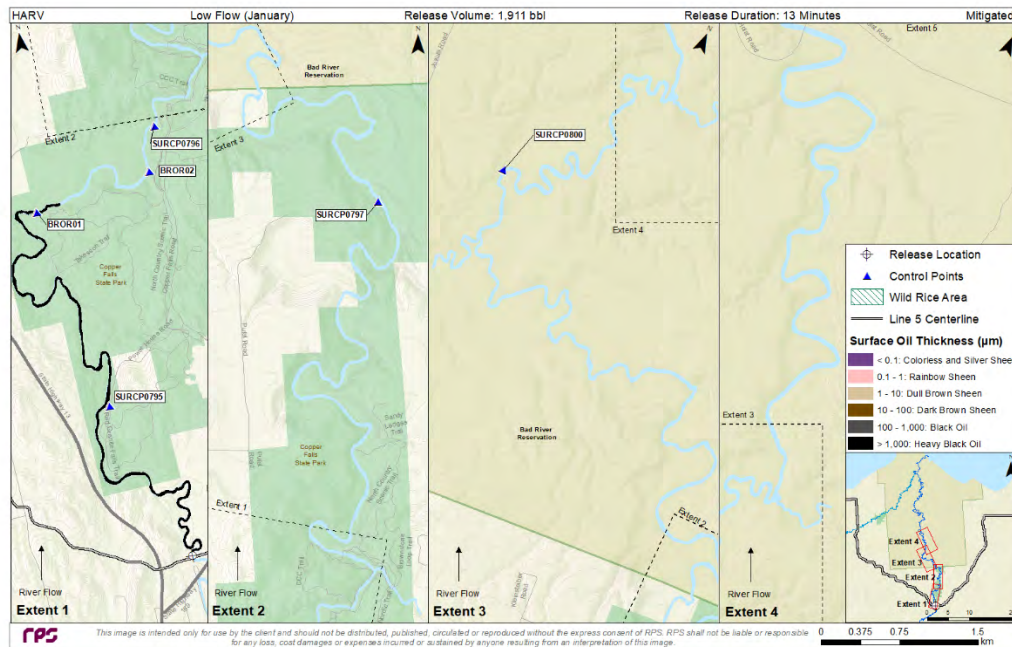
Panel intentionally left blank.

Downstream extents 5-8 not displayed because no oil was predicted there.

Figure 4-49. Composite of maximum subsurface oil thickness (beneath ice) for the mitigated HARV scenario in low river flow conditions modeled in January at the Bad River channel location. This represents the maximum thickness of oil that was predicted for each location. The maximum levels of coverage would not be observed at each location simultaneously.

Figure intentionally left blank.

Cumulative maximum DHCs were predicted to exceed 100 µg/L

from the release location down to Lake Superior. See Figure 4-13.

Figure 4-50. Composite of maximum total dissolved hydrocarbon concentration for the mitigated HARV scenario in low river flow conditions modeled in January at the Bad River channel location. This represents the maximum in-water contamination that was predicted for each location.

4.1.1.14 Mitigated RARV (334 bbl), Average River Flow, Bad River Channel Release
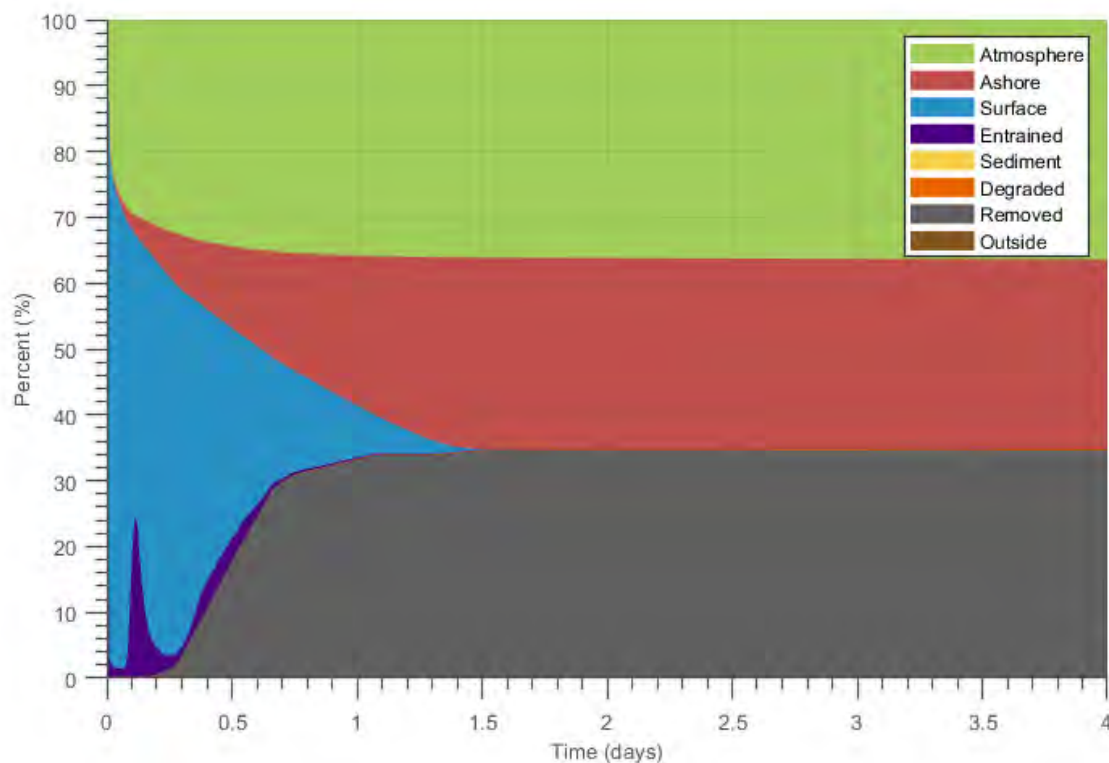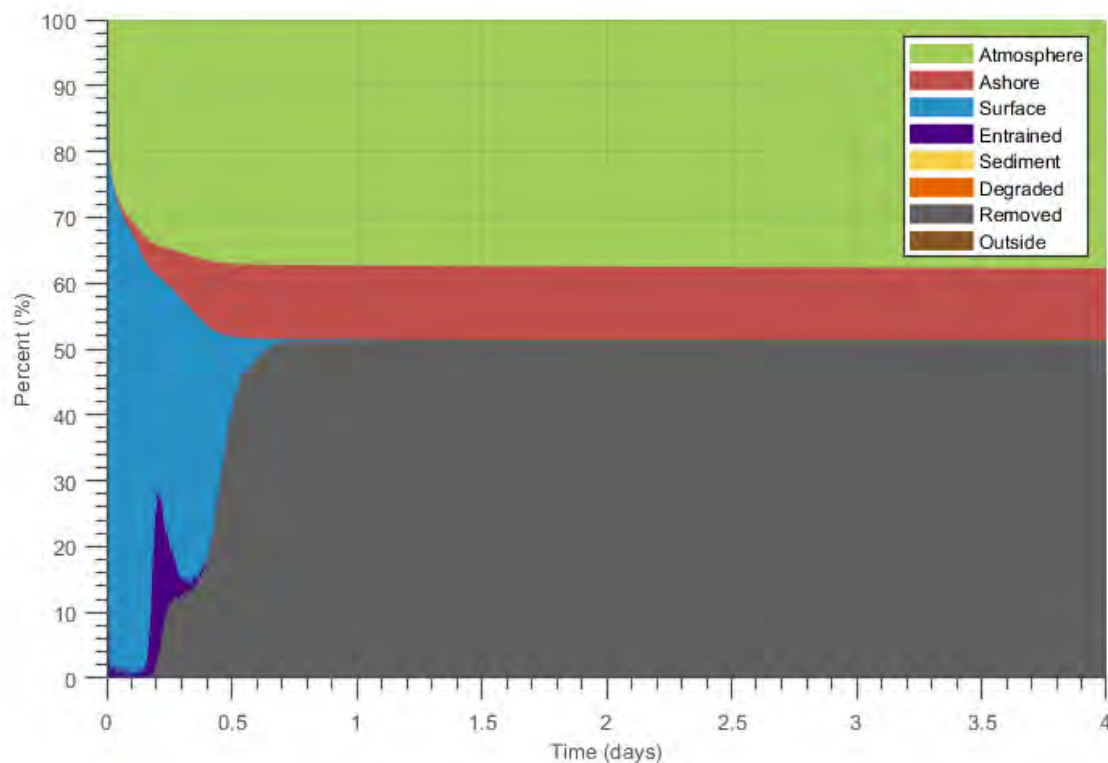

Figure 4-51. Oil mass balance graph for the mitigated RARV scenario in average river flow conditions modeled in June at the Bad River channel location.
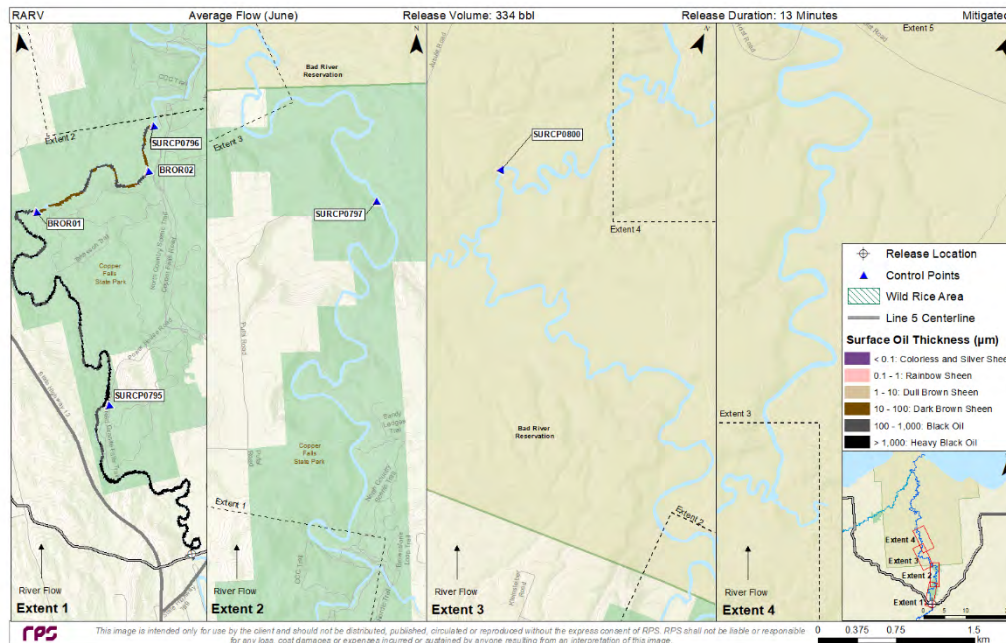
Panel intentionally left blank.

Downstream extents 5-8 not displayed because no oil was predicted there.
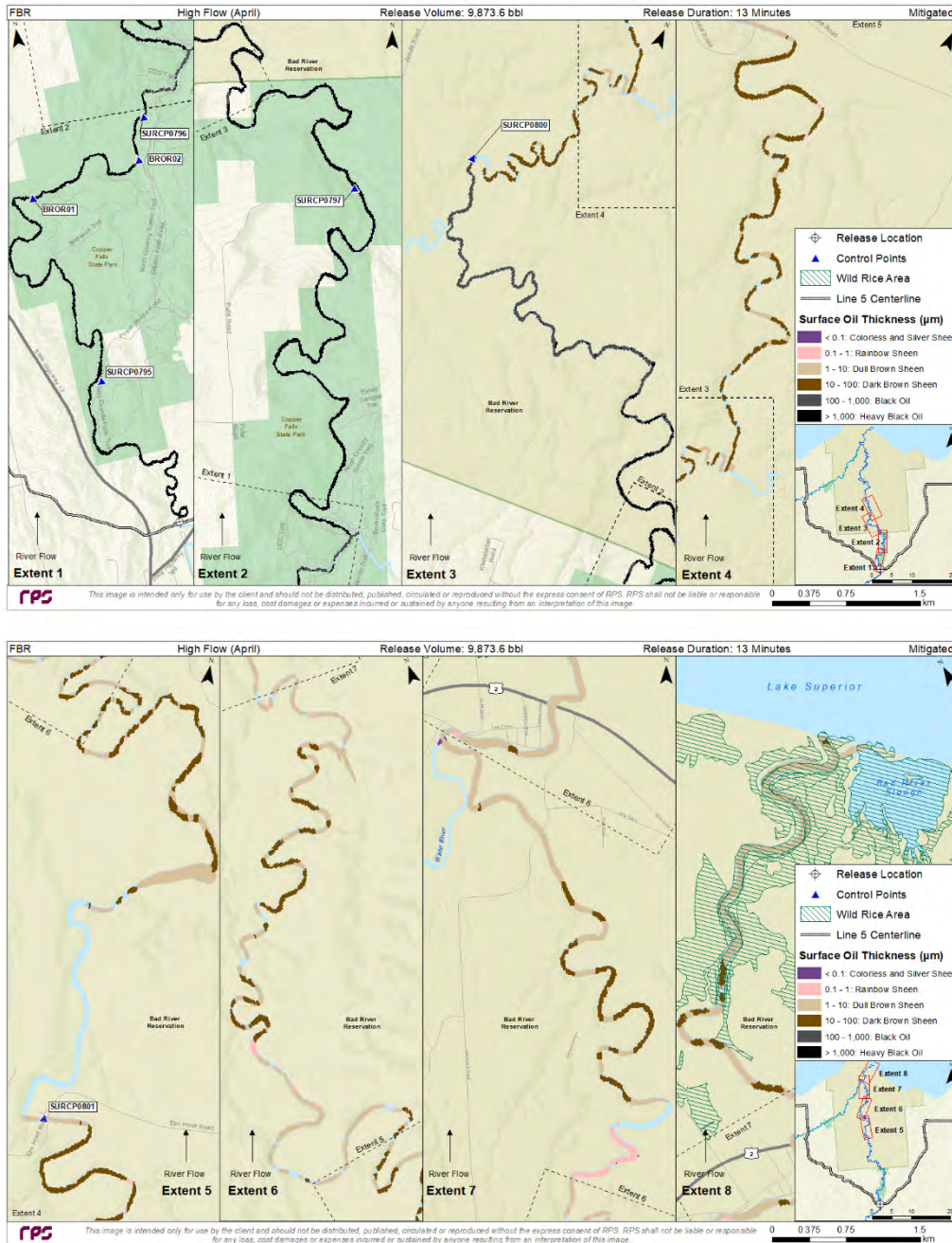
Figure 4-52. Composite of maximum surface oil thickness over 4 days for the mitigated RARV scenario in average river flow conditions modeled in June at the Bad River channel location. This represents the maximum thickness of surface oil that was predicted for each location. The maximum levels of coverage would not be observed at each location simultaneously.
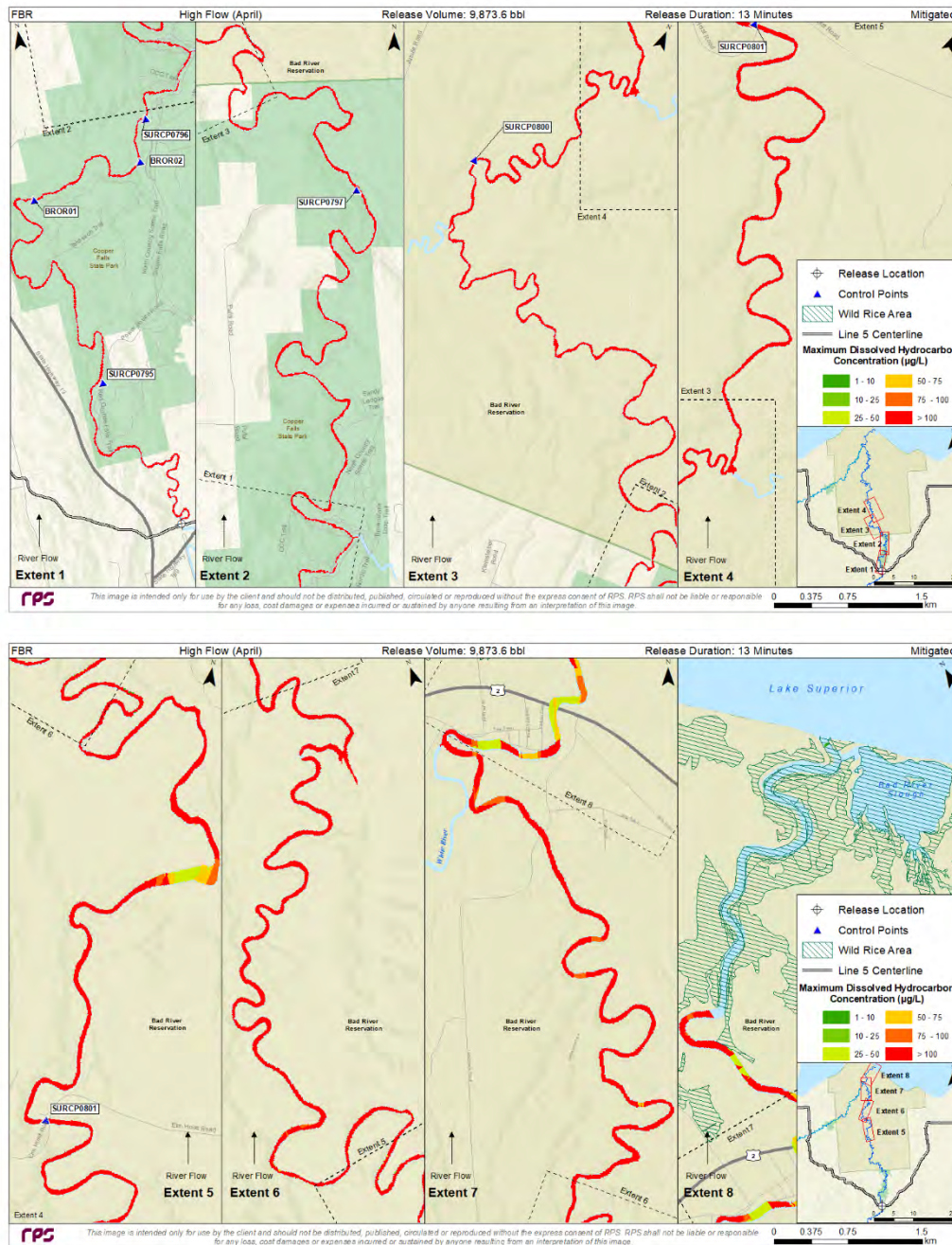
Figure 4-53. Composite of maximum total dissolved hydrocarbon concentration over 4 days for the mitigated RARV scenario in average river flow conditions modeled in June at the Bad River channel location. This represents the maximum in-water contamination that was predicted for each location.

Panel intentionally left blank.

Downstream extents 5-8 not displayed because no oil was predicted there.

Figure 4-54. Maximum total hydrocarbon mass on the shore and on sediments after 4 days for the mitigated RARV scenario in average river flow conditions modeled in June at the Bad River channel location.

4.1.2   White River Releases

4.1.2.1   FBR (8,517 bbl), High River Flow, White River Channel Release

Figure 4-55. Oil mass balance graph for the unmitigated FBR scenario in high river flow conditions modeled in April at the White River channel location.

Panel intentionally left blank.

Downstream extents 5-8 not displayed because no oil was predicted there.

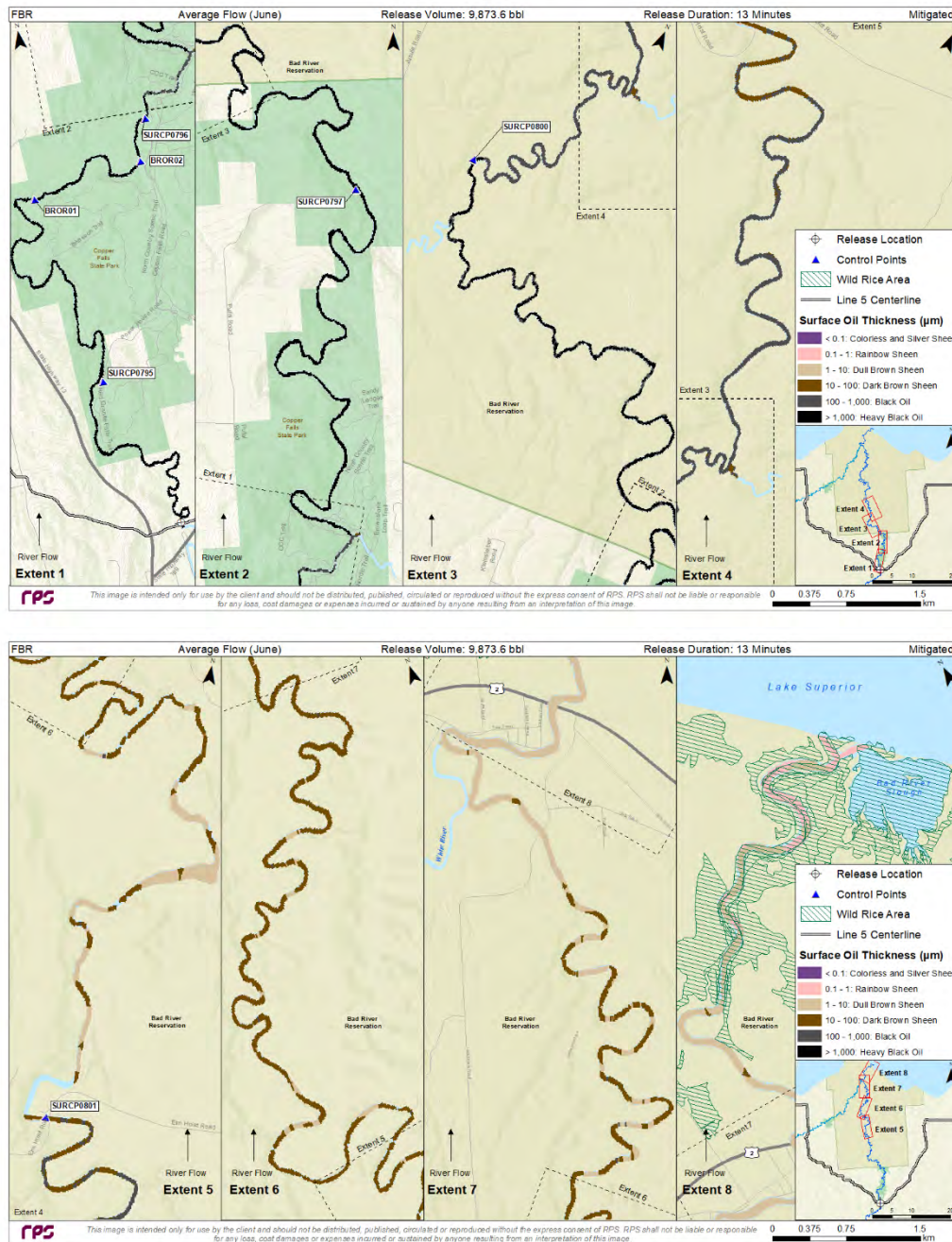**Figure 4-56. Composite of maximum surface oil thickness over 4 days for the unmitigated FBR scenario in high river flow conditions modeled in April at the White River channel location. This represents the maximum thickness of surface oil that was predicted for each location. The maximum levels of coverage would not be observed at each location simultaneously.**
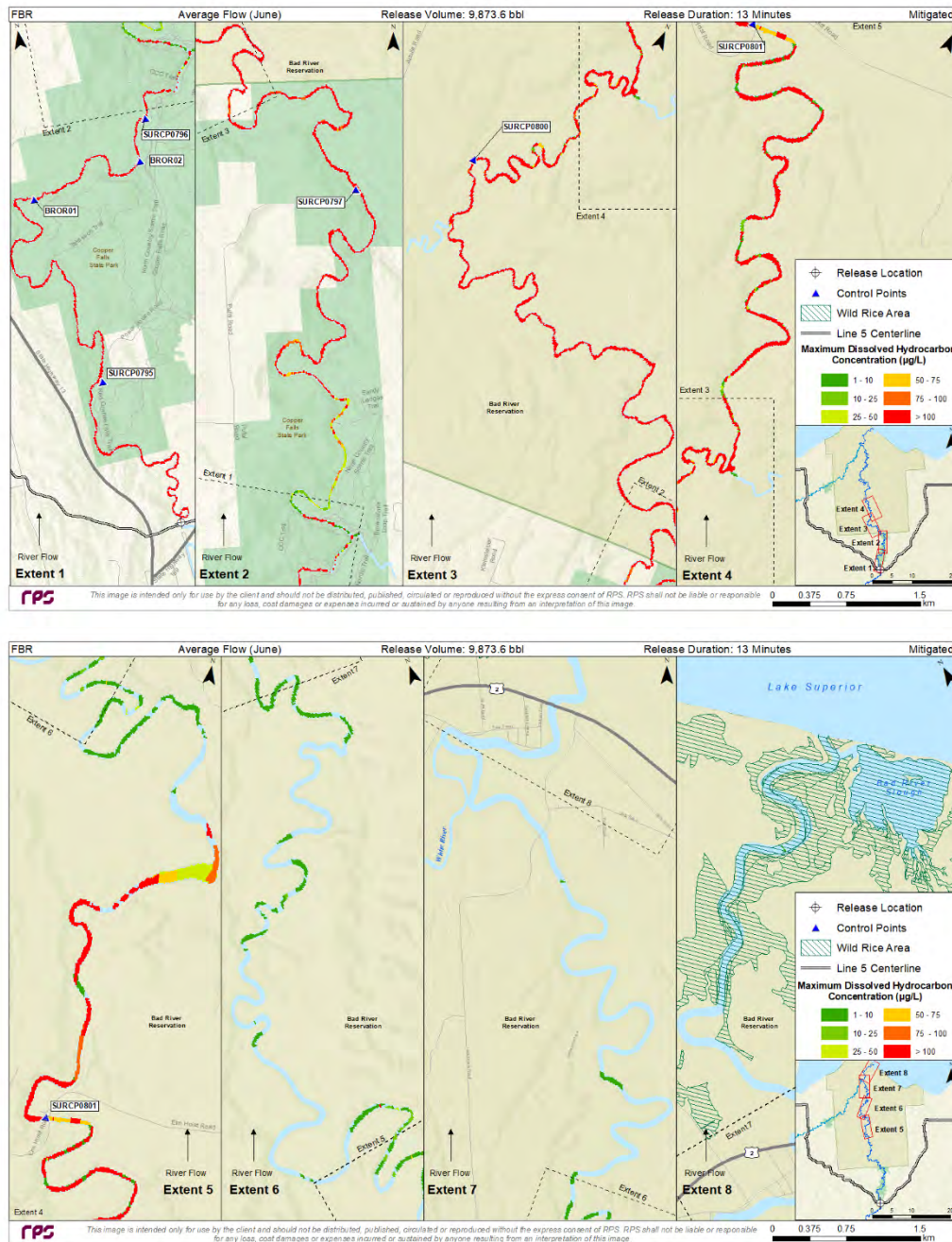
Figure 4-57. Composite of maximum total dissolved hydrocarbon concentration over 4 days for the unmitigated FBR scenario in high river flow conditions modeled in April at the White River channel location. This represents the maximum in-water contamination that was predicted for each location.

Figure 4-58. Maximum total hydrocarbon mass on the shore and on sediments after 4 days for the unmitigated FBR scenario in high river flow conditions modeled in April at the White River channel location.

4.1.2.2 FBR (8,517 bbl), Average River Flow, White River Channel Release

Figure 4-59. Oil mass balance graph for the unmitigated FBR scenario in average river flow conditions modeled in June at the White River channel location.
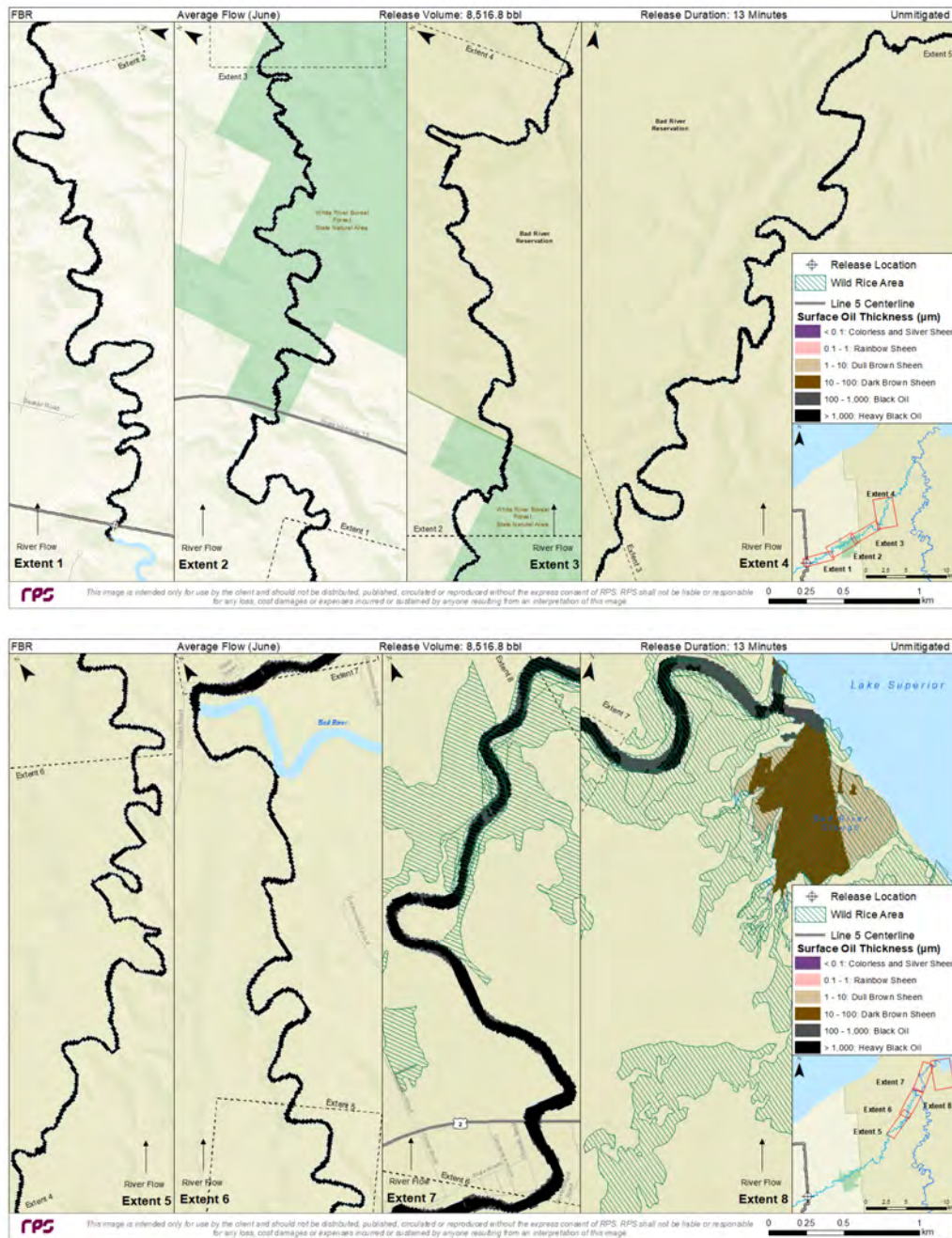
Figure 4-60. Composite of maximum surface oil thickness over 4 days for the unmitigated FBR scenario in average river flow conditions modeled in June at the White River channel location. This represents the maximum thickness of surface oil that was predicted for each location. The maximum levels of coverage would not be observed at each location simultaneously.
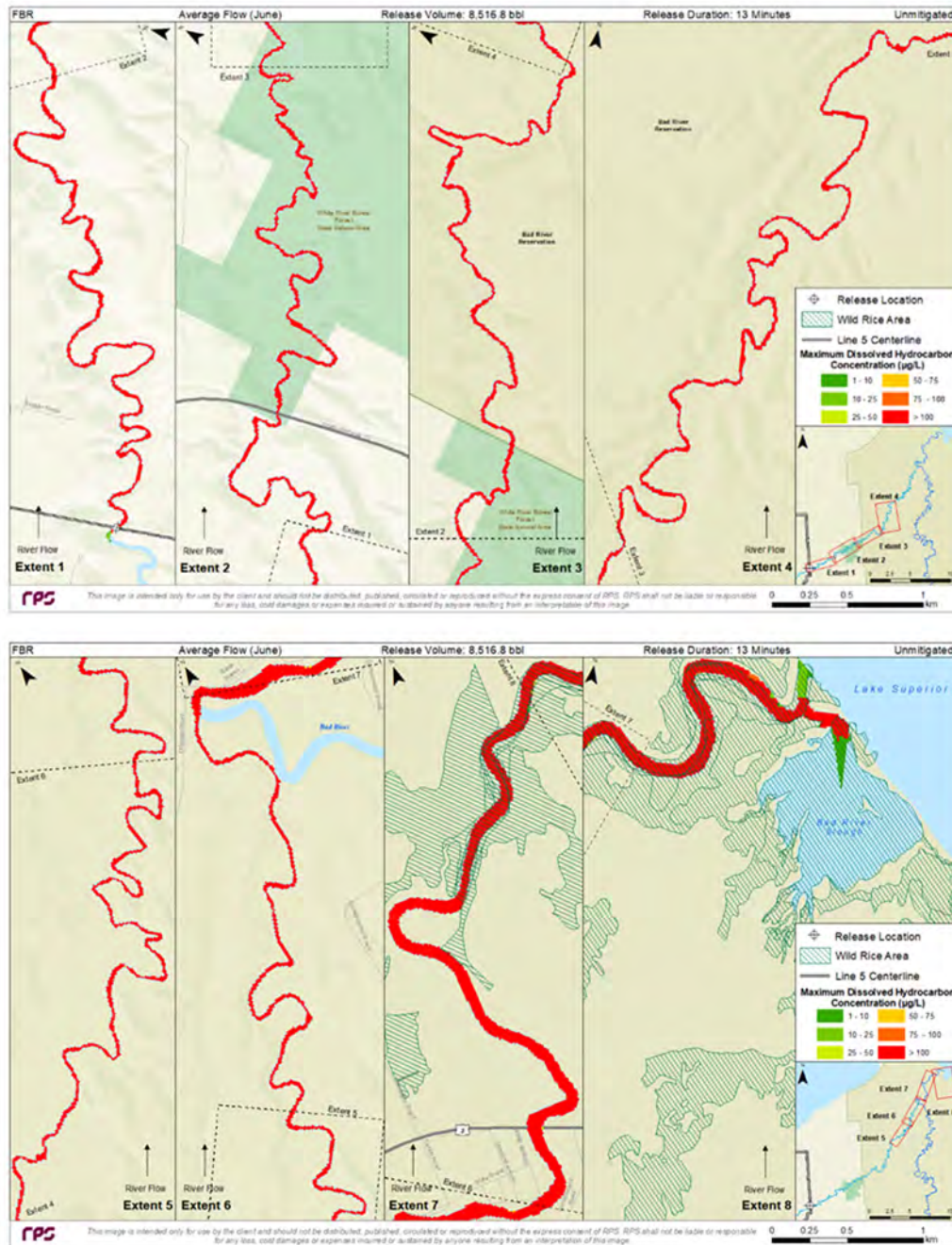
Figure 4-61. Composite of maximum total dissolved hydrocarbon concentration over 4 days for the unmitigated FBR scenario in average river flow conditions modeled in June at the White River channel location. This represents the maximum in-water contamination that was predicted for each location.
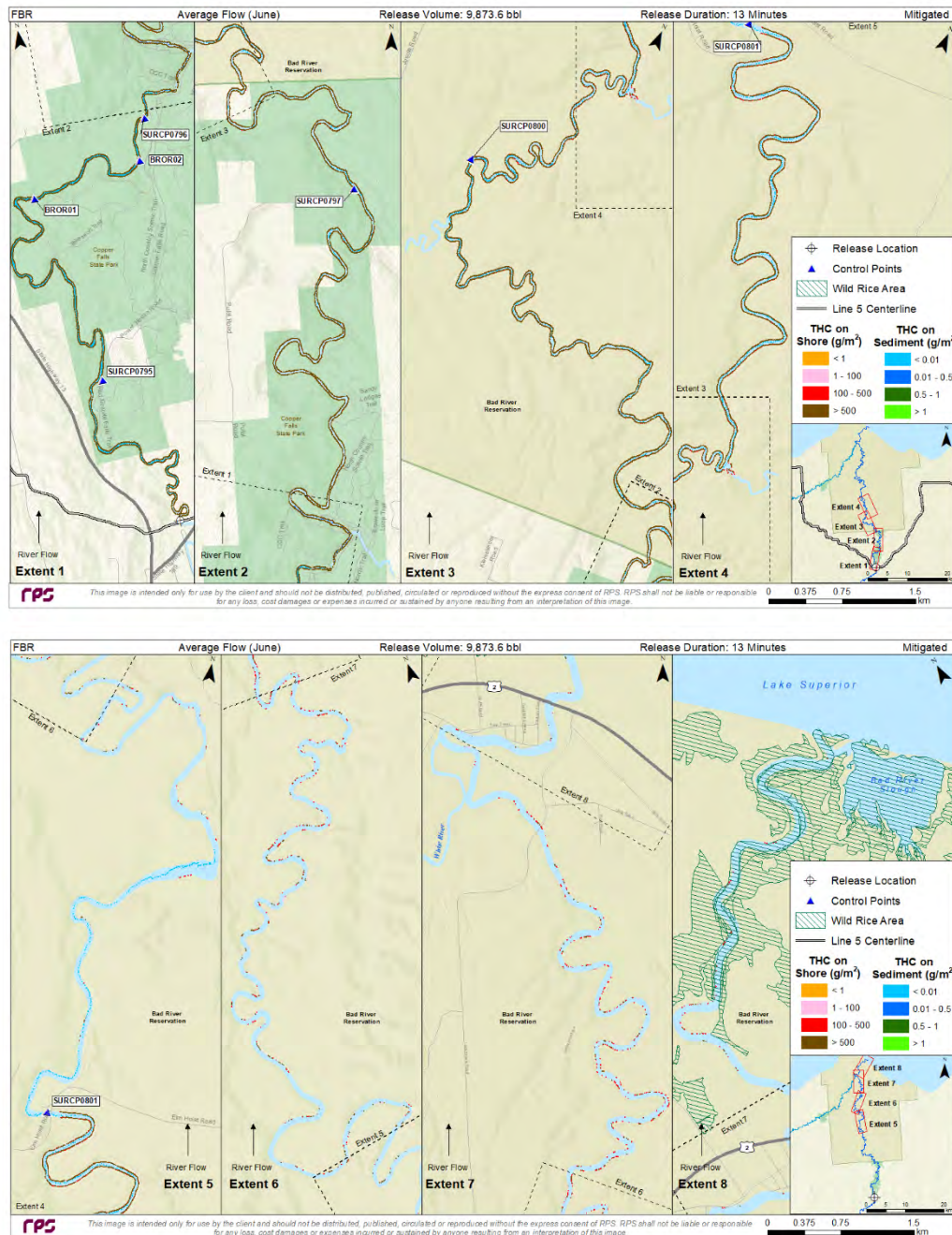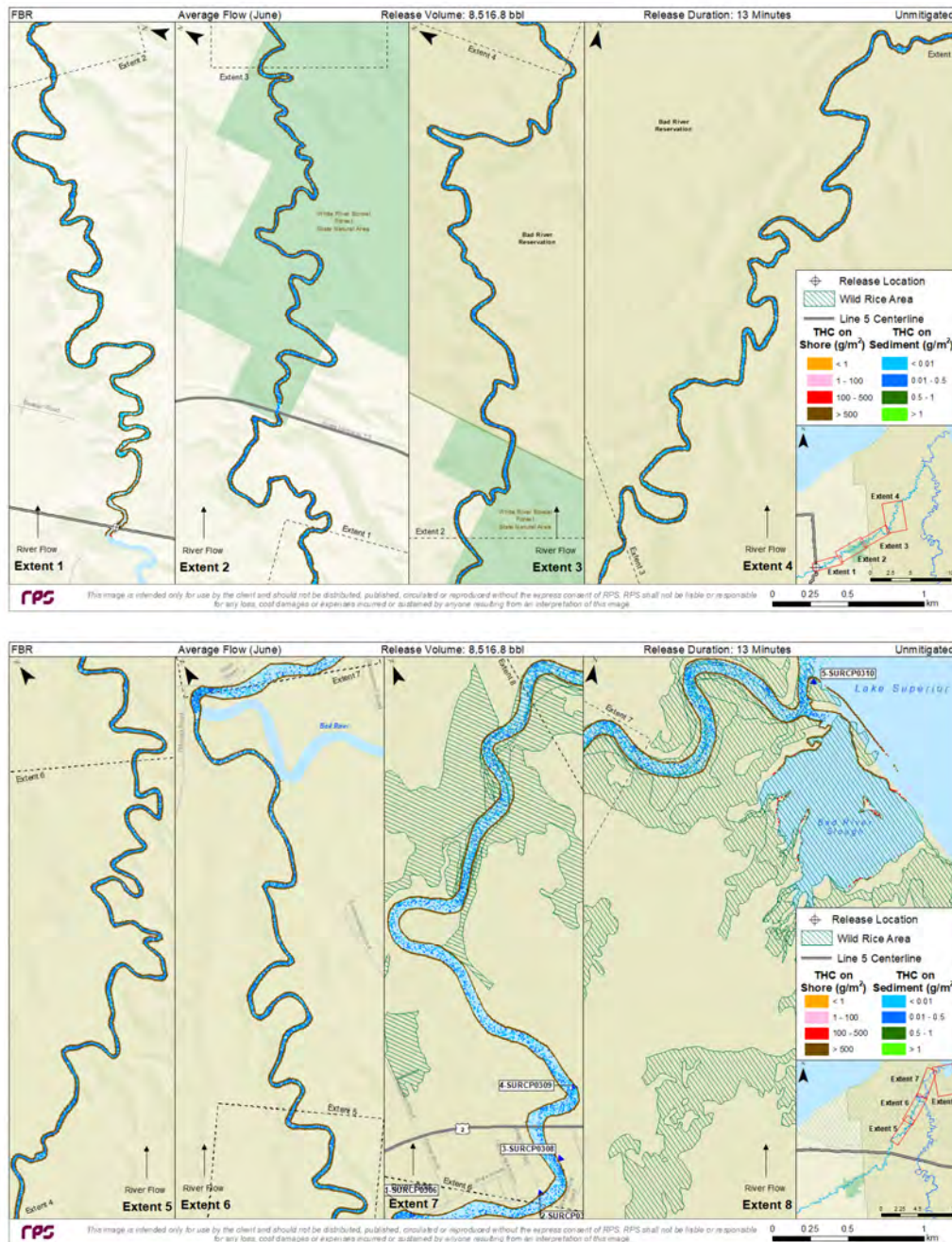
Figure 4-62. Maximum total hydrocarbon mass on the shore and on sediments after 4 days for the unmitigated FBR scenario in average river flow conditions modeled in June at the White River channel location.

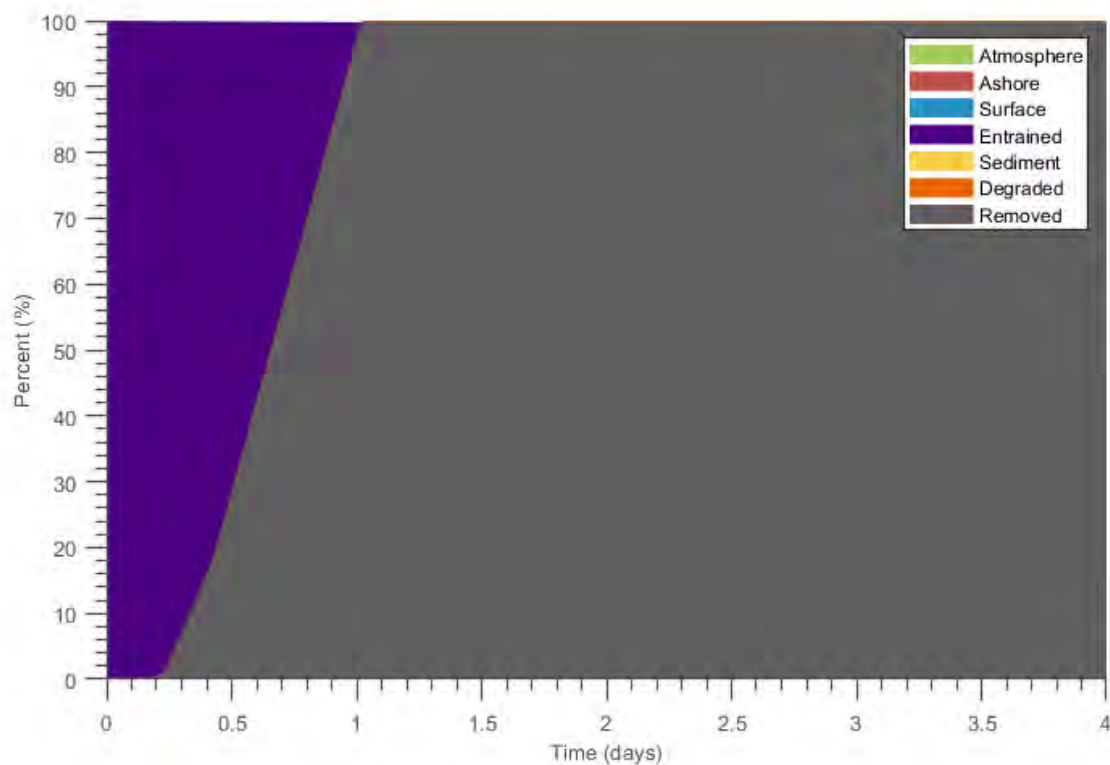### 4.1.2.3 FBR (8,517 bbl), Low River Flow, White River Channel Release
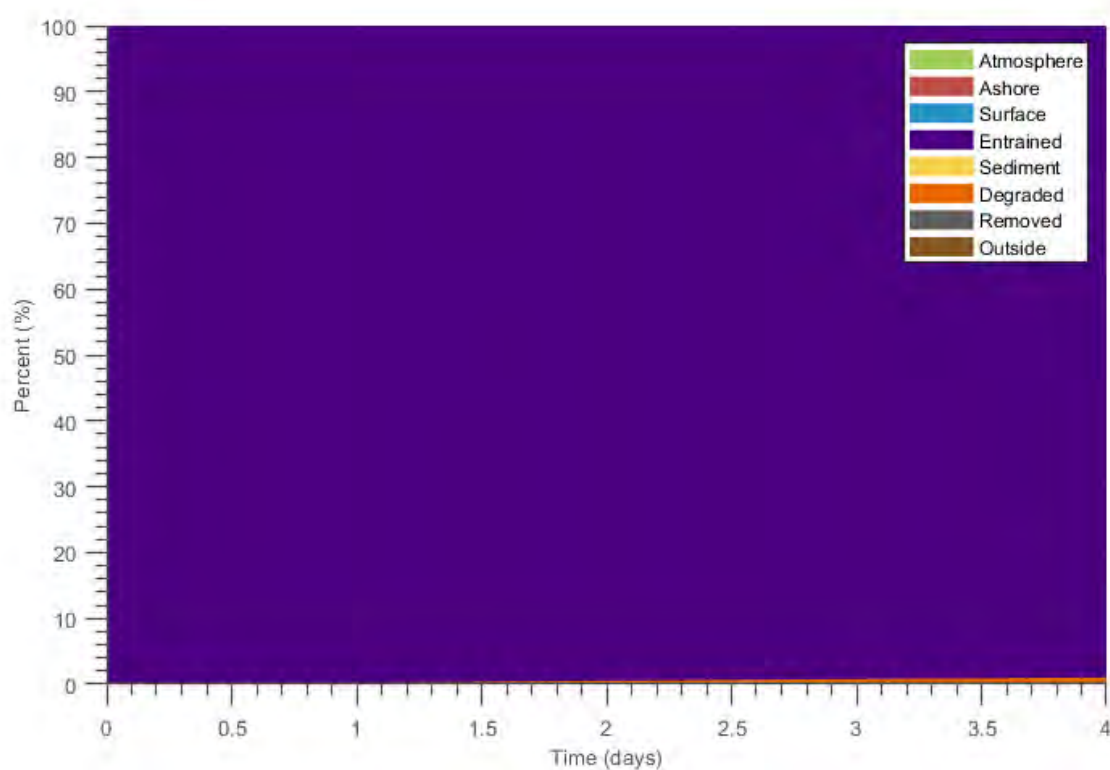
Figure 4-63. Oil mass balance graph for the unmitigated FBR scenario in low river flow conditions modeled in January at the White River channel location.
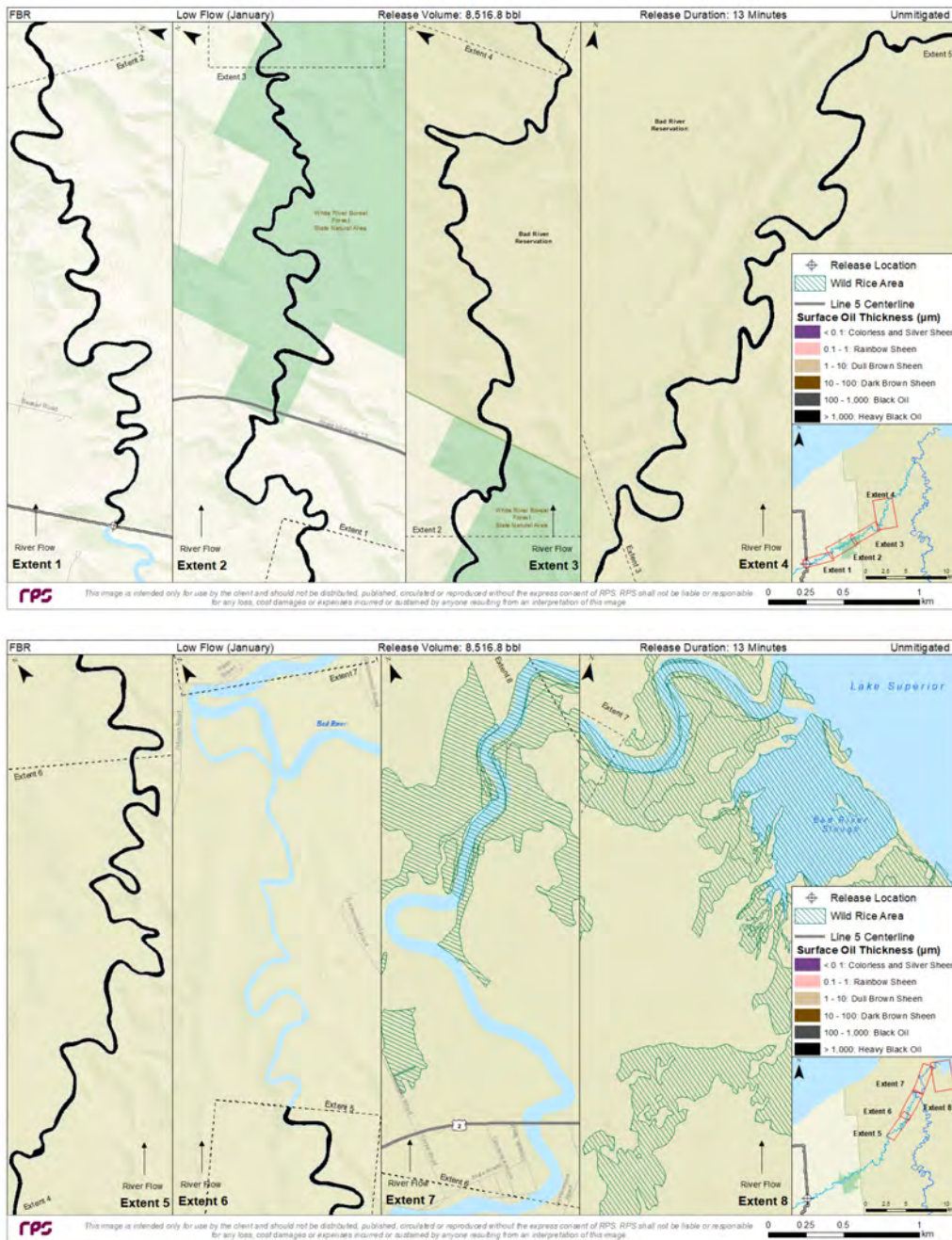
Figure 4-64. Composite of maximum subsurface oil thickness (beneath ice) for the unmitigated FBR scenario in low river flow conditions modeled in January at the White River channel location. This represents the maximum thickness of oil that was predicted for each location. The maximum levels of coverage would not be observed at each location simultaneously.

Figure 4-65. Composite of maximum total dissolved hydrocarbon concentration for the unmitigated FBR scenario in low river flow conditions modeled in January at the White River channel location. This represents the maximum in-water contamination that was predicted for each location.

Figure 4-66. Maximum total hydrocarbon mass on the shore and on sediments after 4 days for the unmitigated FBR scenario in low river flow conditions modeled in January at the White River channel location

4.1.2.4 HARV (1,911 bbl), High River Flow, White River Channel Release

Figure 4-67. Oil mass balance graph for the unmitigated HARV scenario in high river flow conditions modeled in April at the White River channel location.

Panel intentionally left blank.

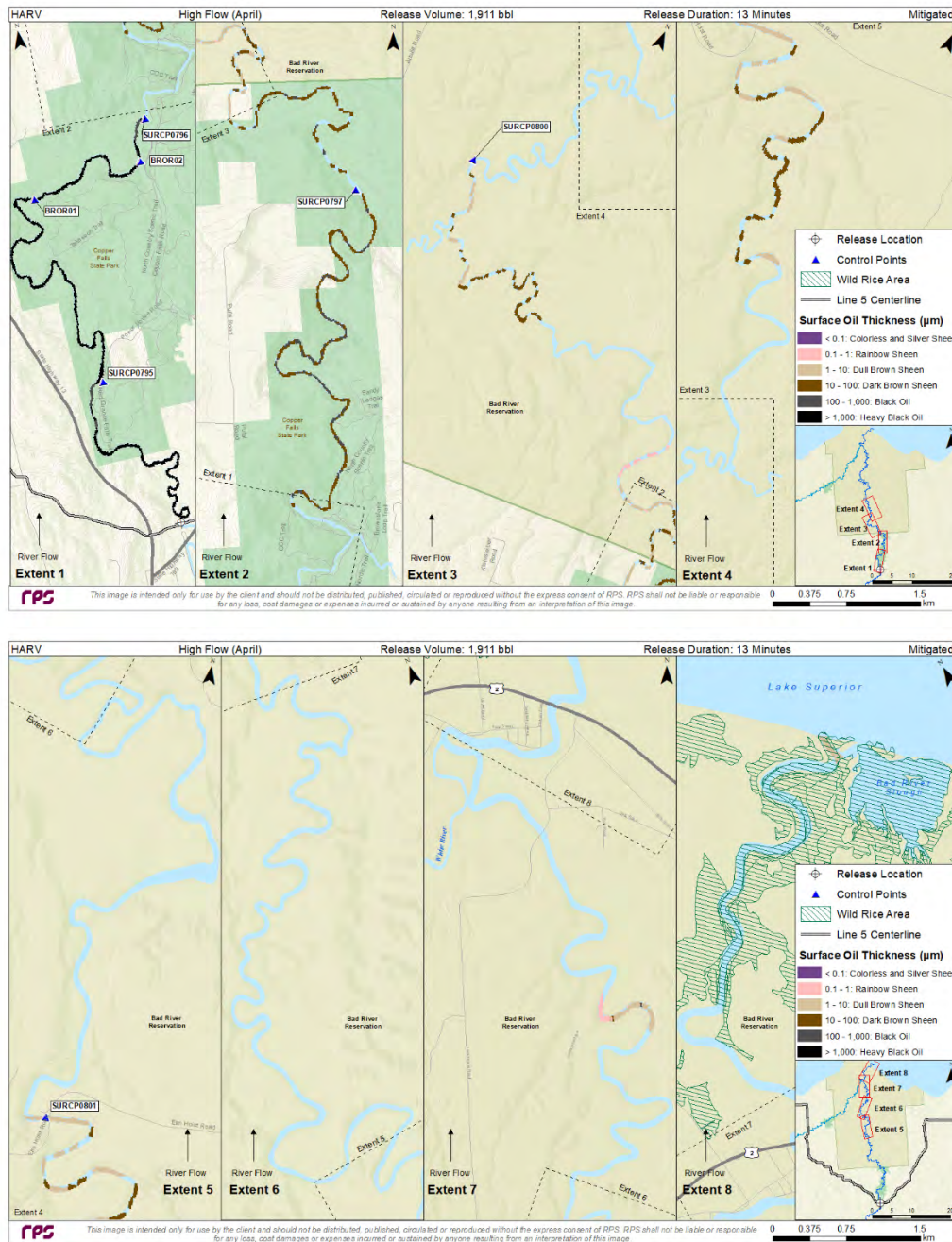Downstream extents 5-8 not displayed because no oil was predicted there.

Figure 4-68. Composite of maximum surface oil thickness over 4 days for the unmitigated HARV scenario in high river flow conditions modeled in April at the White River channel location. This represents the maximum thickness of surface oil that was predicted for each location. The maximum levels of coverage would not be observed at each location simultaneously.
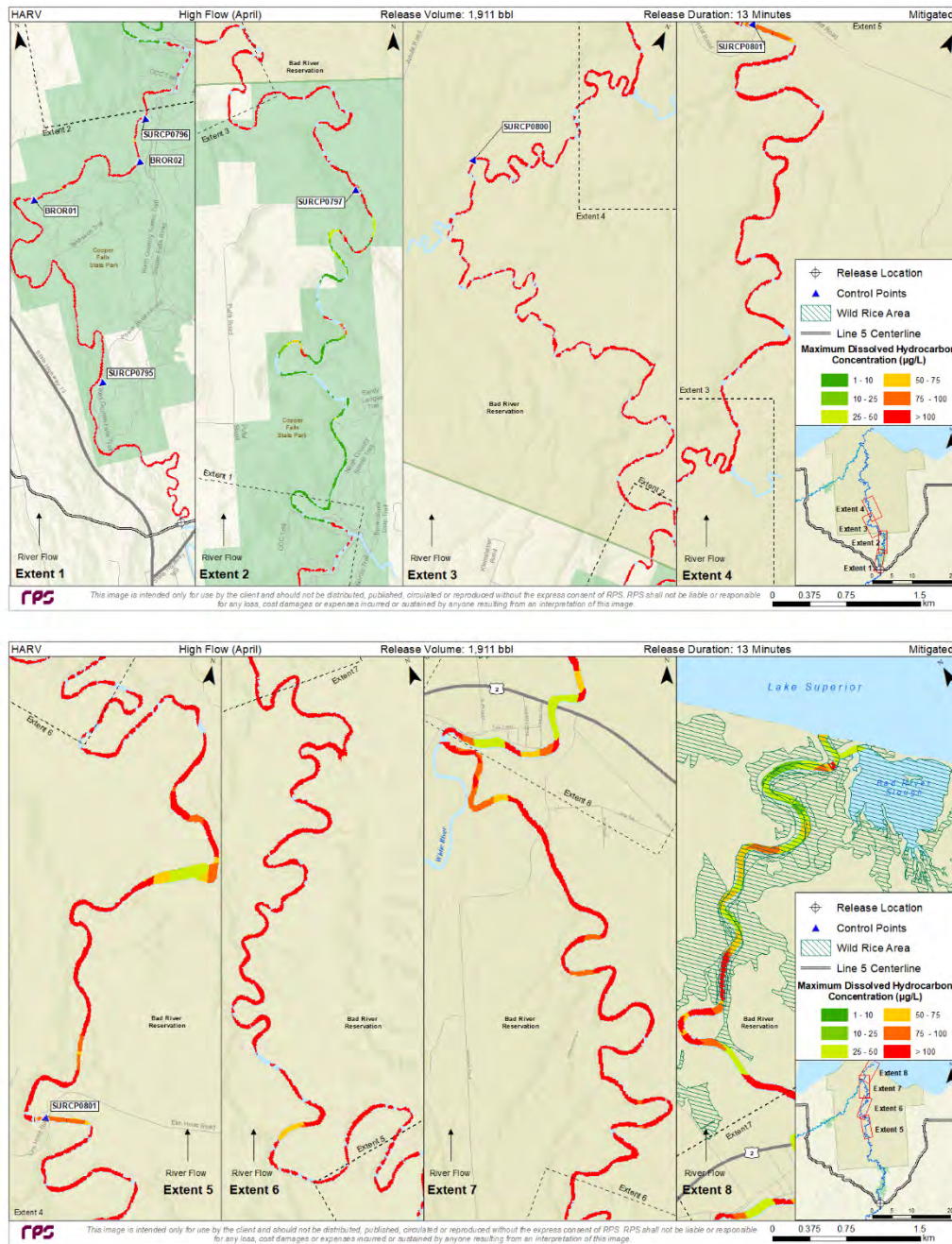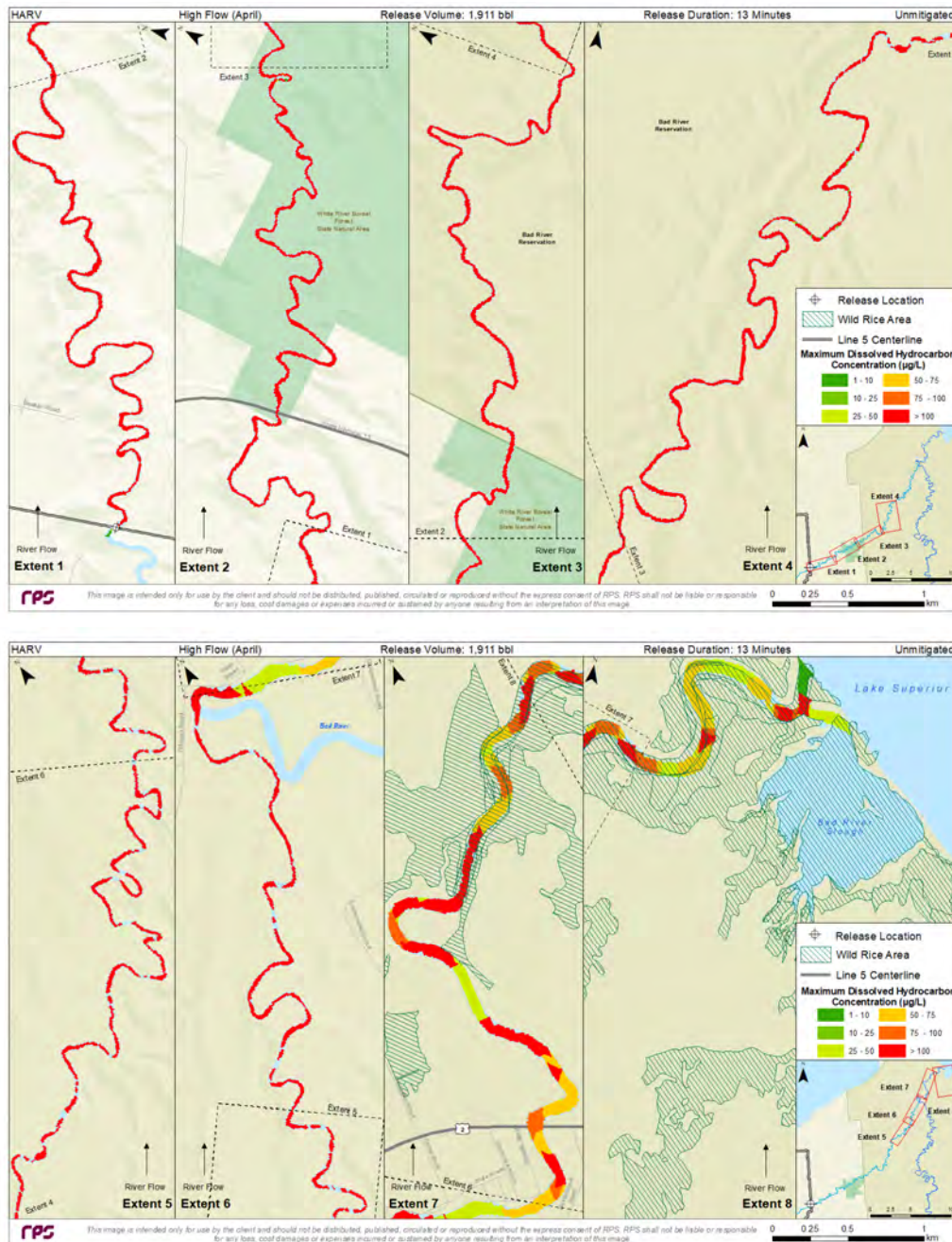
Figure 4-69. Composite of maximum total dissolved hydrocarbon concentration over 4 days for the unmitigated HARV scenario in high river flow conditions modeled in April at the White River channel location. This represents the maximum in-water contamination that was predicted for each location.
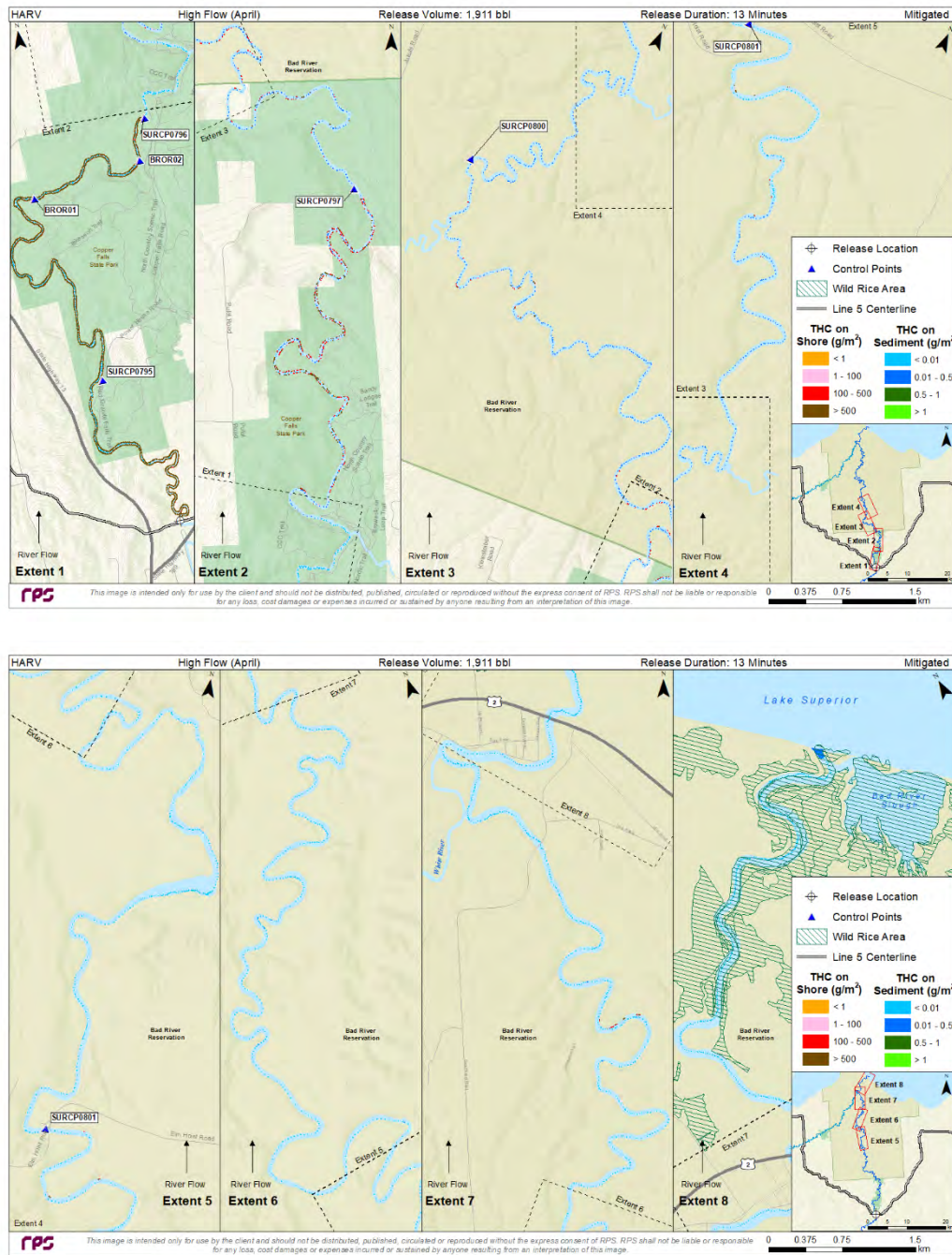
Figure 4-70. Maximum total hydrocarbon mass on the shore and on sediments after 4 days for the unmitigated HARV scenario in high river flow conditions modeled in April at the White River channel location.

4.1.2.5 HARV (1,911 bbl), Average River Flow, White River Channel Release

Figure 4-71. Oil mass balance graph for the unmitigated HARV scenario in average river flow conditions modeled in June at the White River channel location.

Figure 4-72. Composite of maximum surface oil thickness over 4 days for the unmitigated HARV scenario in average river flow conditions modeled in June at the White River channel location. This represents the maximum thickness of surface oil that was predicted for each location. The maximum levels of coverage would not be observed at each location simultaneously.
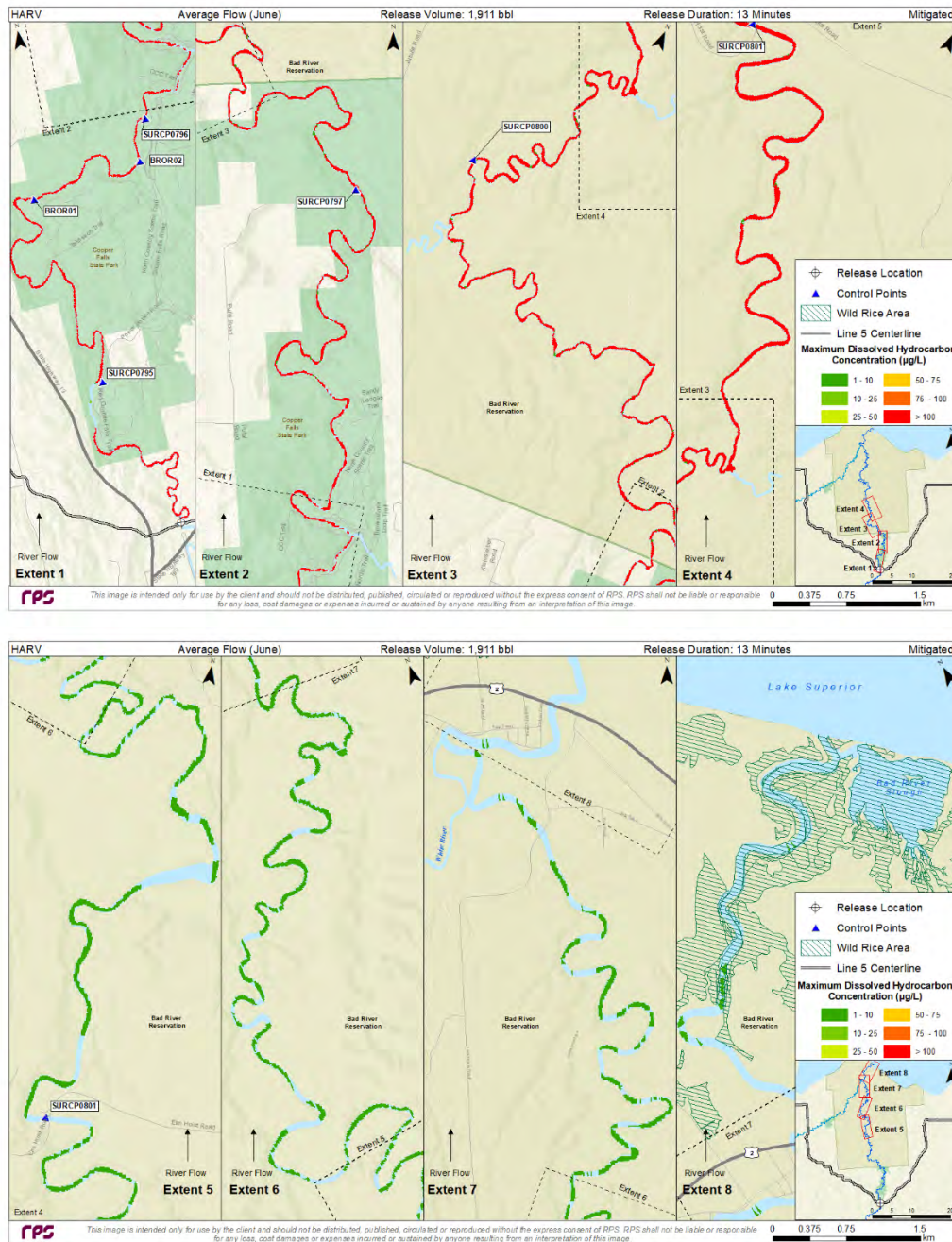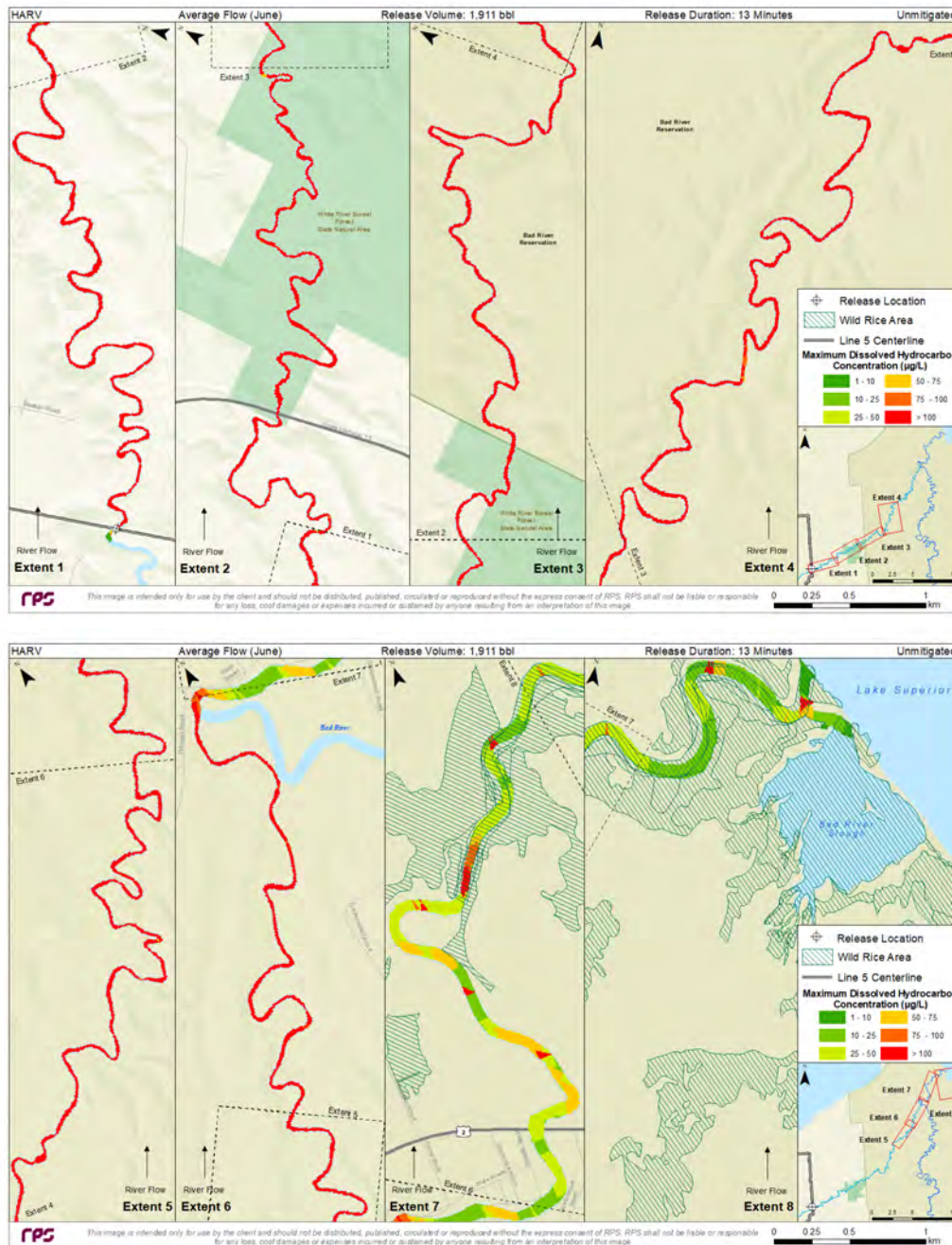
Figure 4-73. Composite of maximum total dissolved hydrocarbon concentration over 4 days for the unmitigated HARV scenario in average river flow conditions modeled in June at the White River channel location. This represents the maximum in-water contamination that was predicted for each location.

Figure 4-74. Maximum total hydrocarbon mass on the shore and on sediments after 4 days for the unmitigated HARV scenario in average river flow conditions modeled in June at the White River channel location.

4.1.2.6 HARV (1,911 bbl), Low River Flow, White River Channel Release
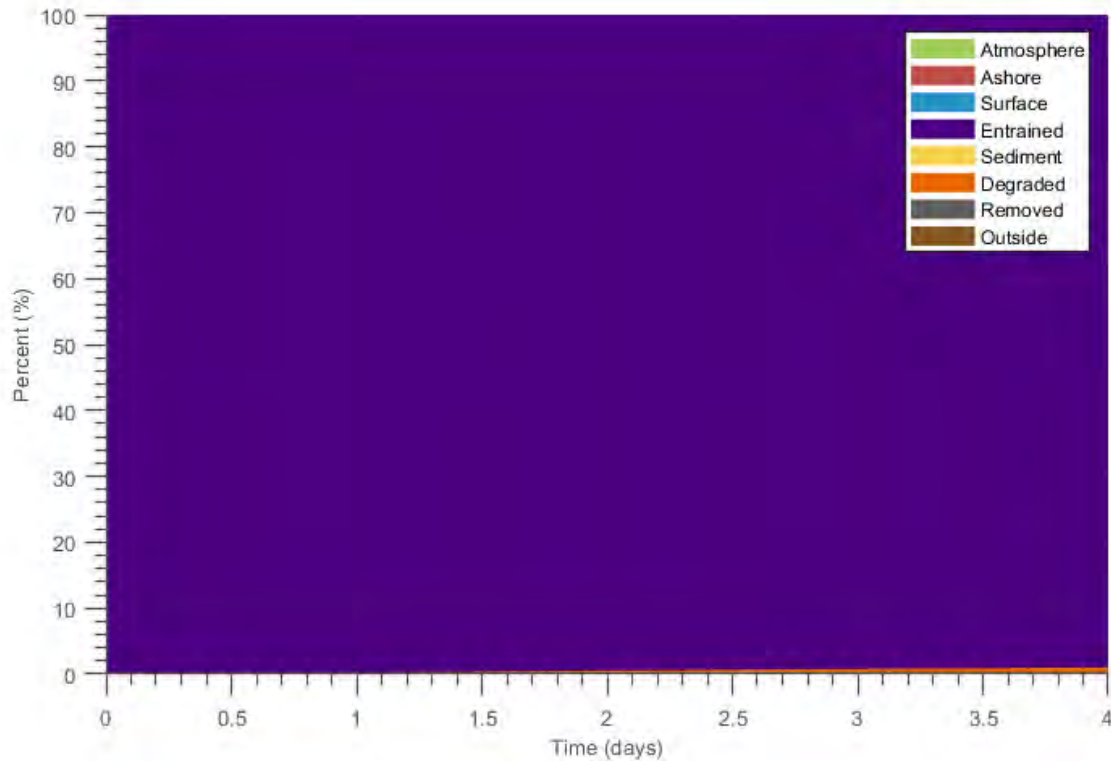
Figure 4-75. Oil mass balance graph for the unmitigated HARV scenario in low river flow conditions modeled in January at the White River channel location.
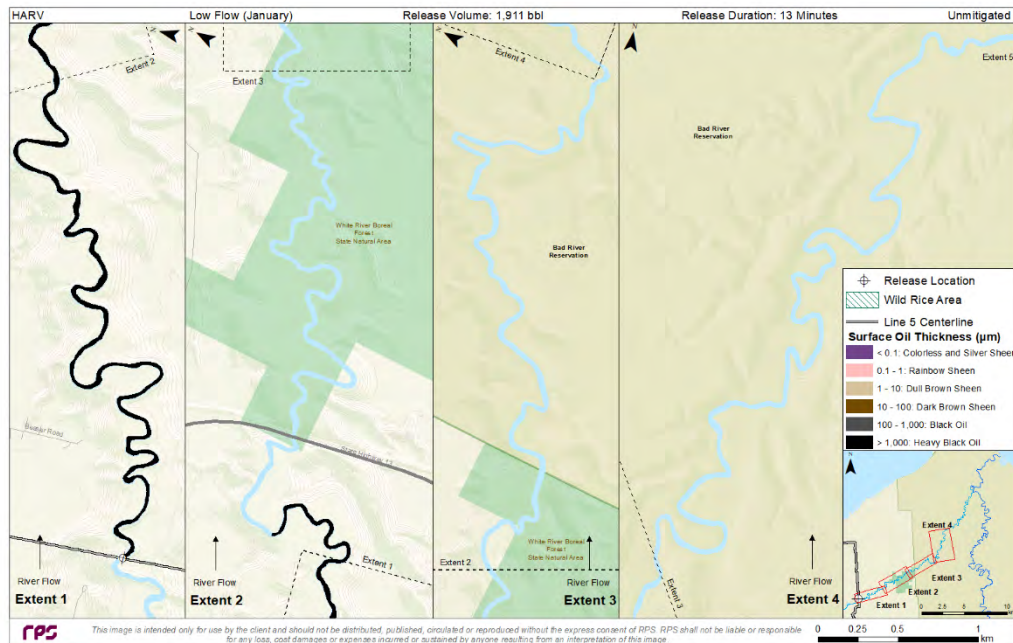
Panel intentionally left blank.

Downstream extents 5-8 not displayed because no oil was predicted there.

Figure 4-76. Composite of maximum subsurface oil thickness (beneath ice) for the unmitigated HARV scenario in low river flow conditions modeled in January at the White River channel location. This represents the maximum thickness of oil that was predicted for each location. The maximum levels of coverage would not be observed at each location simultaneously.
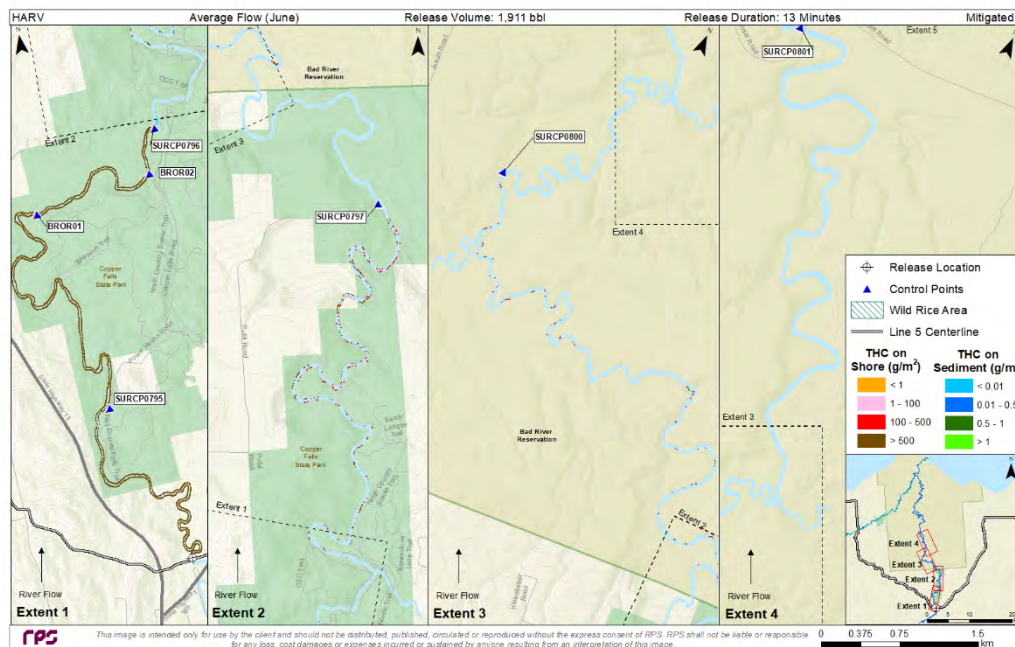
Figure intentionally left blank.

Cumulative maximum DHCs were predicted to exceed 100 µg/L

from the release location down to Lake Superior. See Figure 4-65.

Figure 4-77. Composite of maximum total dissolved hydrocarbon concentration for the unmitigated HARV scenario in low river flow conditions modeled in January at the White River channel location. This represents the maximum in-water contamination that was predicted for each location.

4.1.2.7 RARV (334 bbl), Average River Flow, White River Channel Release
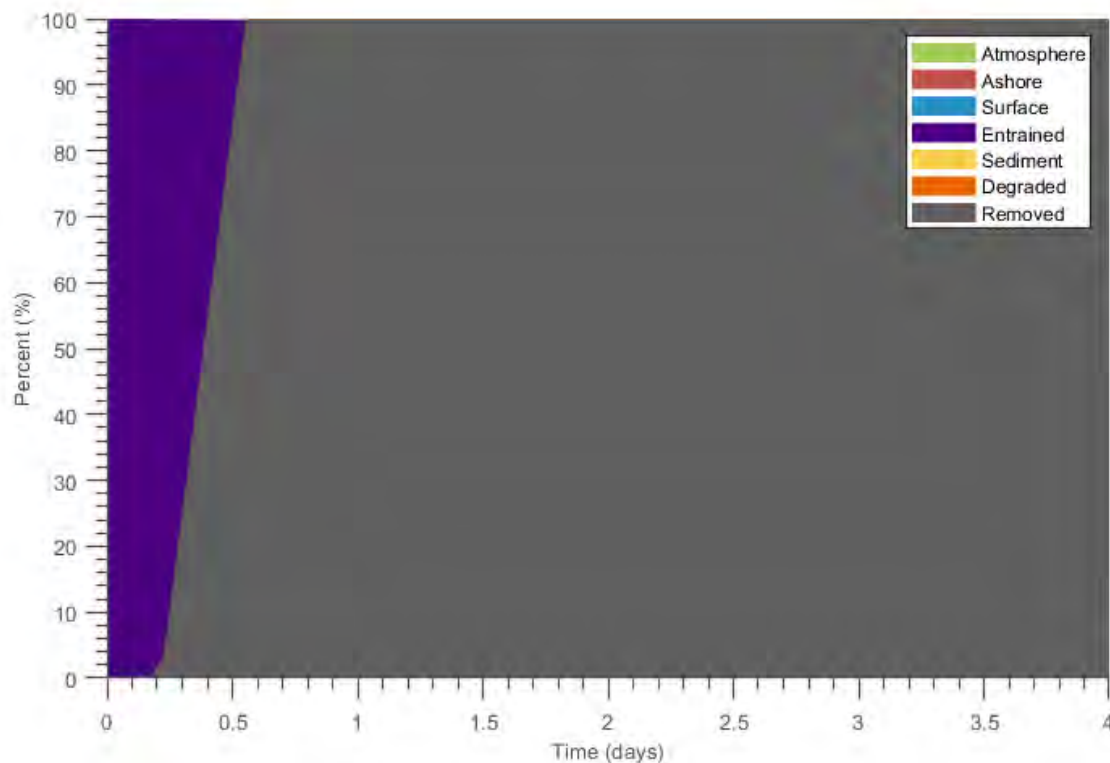

Figure 4-78. Oil mass balance graph for the unmitigated RARV scenario in average river flow conditions modeled in June at the White River channel location.
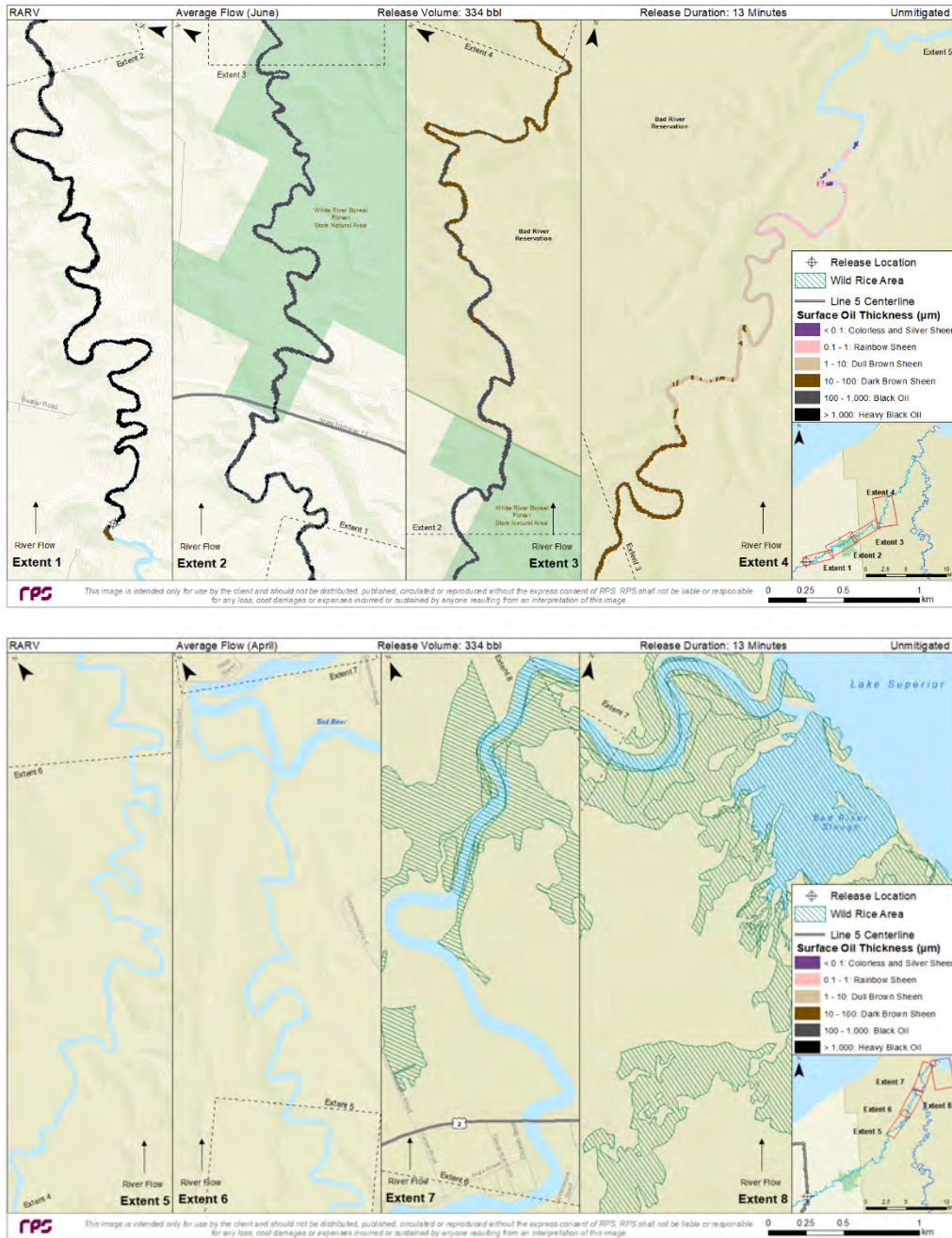
Figure 4-79. Composite of maximum surface oil thickness over 4 days for the unmitigated RARV scenario in average river flow conditions modeled in June at the White River channel location. This represents the maximum thickness of surface oil that was predicted for each location. The maximum levels of coverage would not be observed at each location simultaneously.
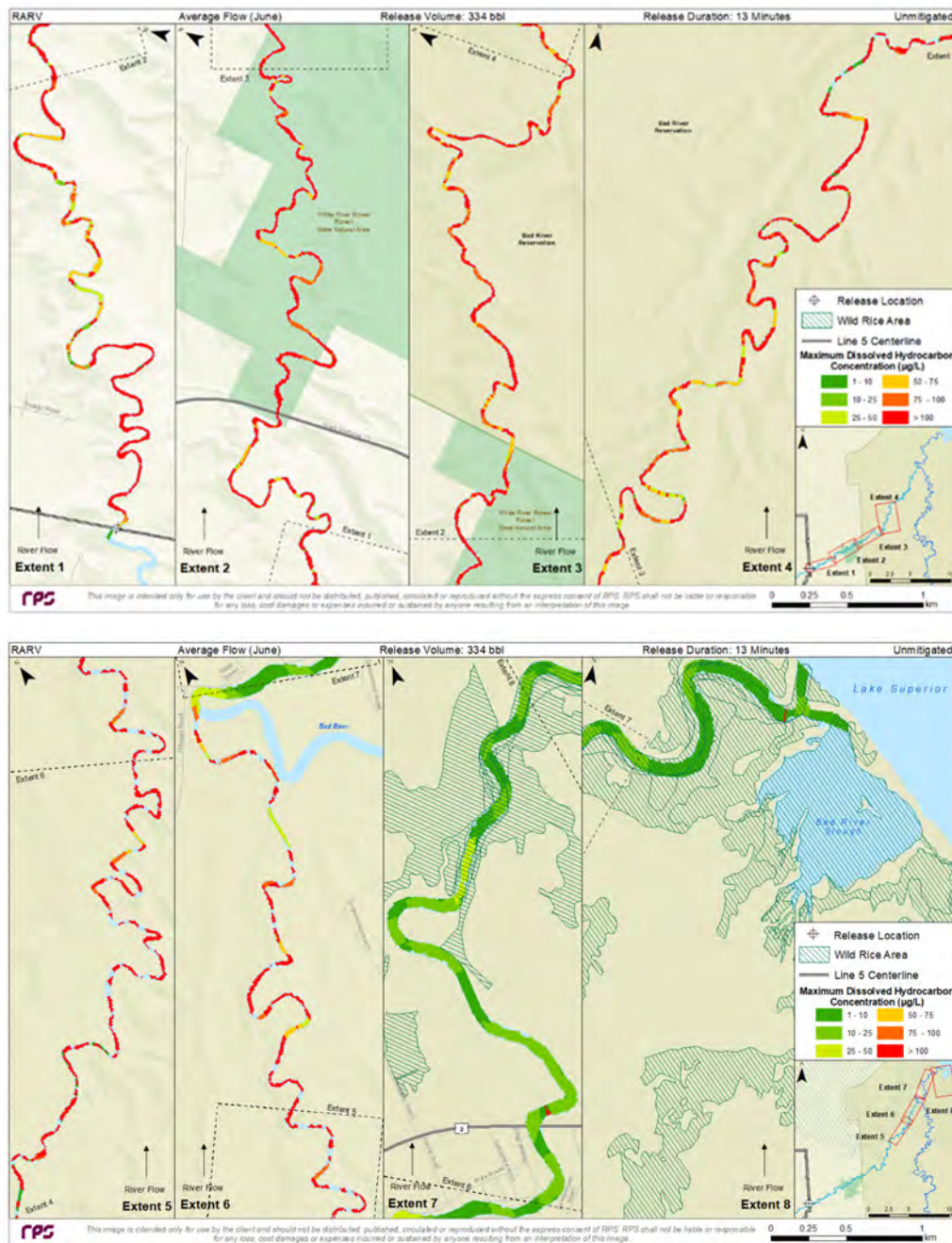
Figure 4-80. Composite of maximum total dissolved hydrocarbon concentration over 4 days for the unmitigated RARV scenario in average river flow conditions modeled in June at the White River channel location. This represents the maximum in-water contamination that was predicted for each location.
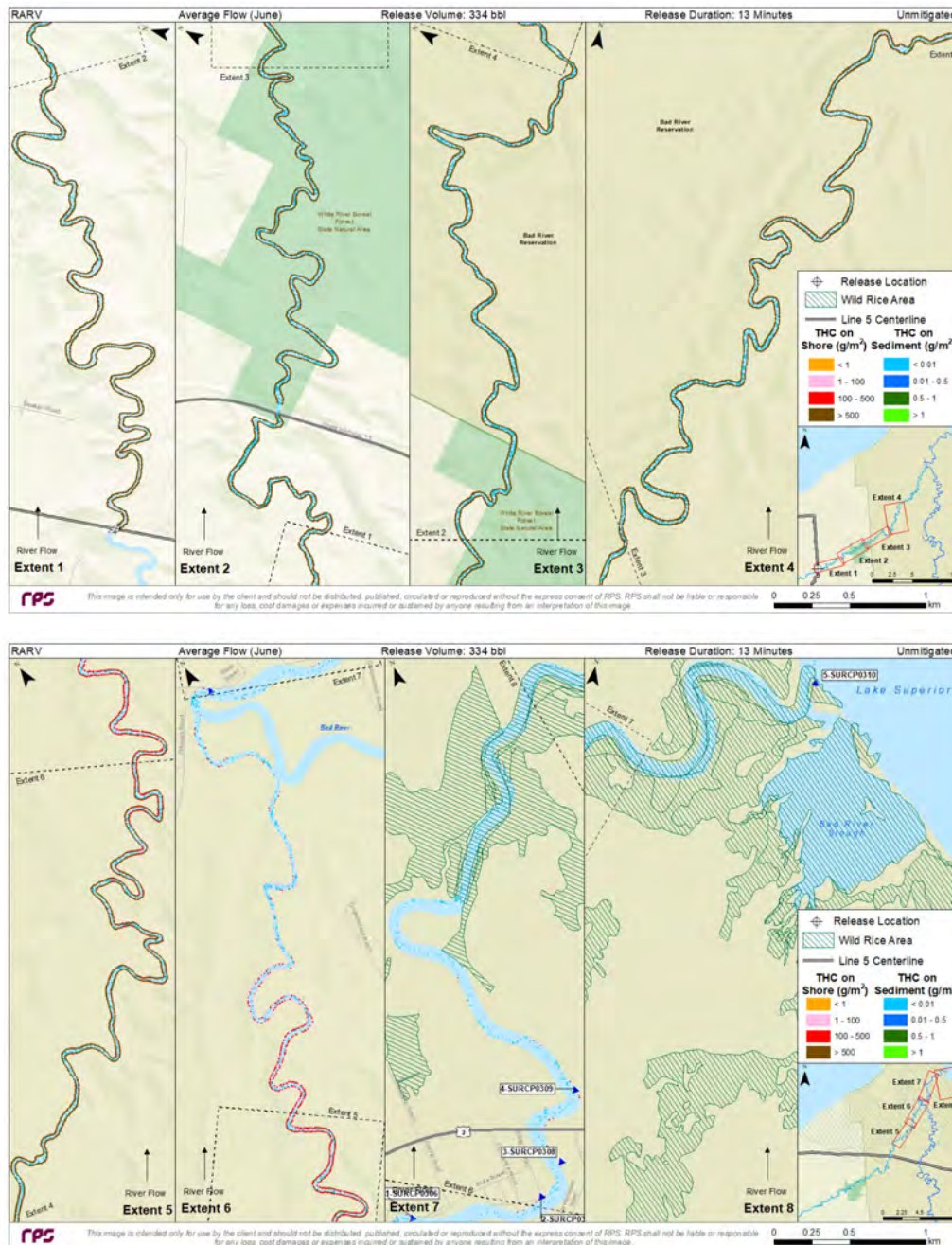
Figure 4-81. Maximum total hydrocarbon mass on the shore and on sediments after 4 days for the unmitigated RARV scenario in average river flow conditions modeled in June at the White River channel location.

## 4.1.2.8 Mitigated FBR (8,517 bbl), High River Flow, White River Channel Release
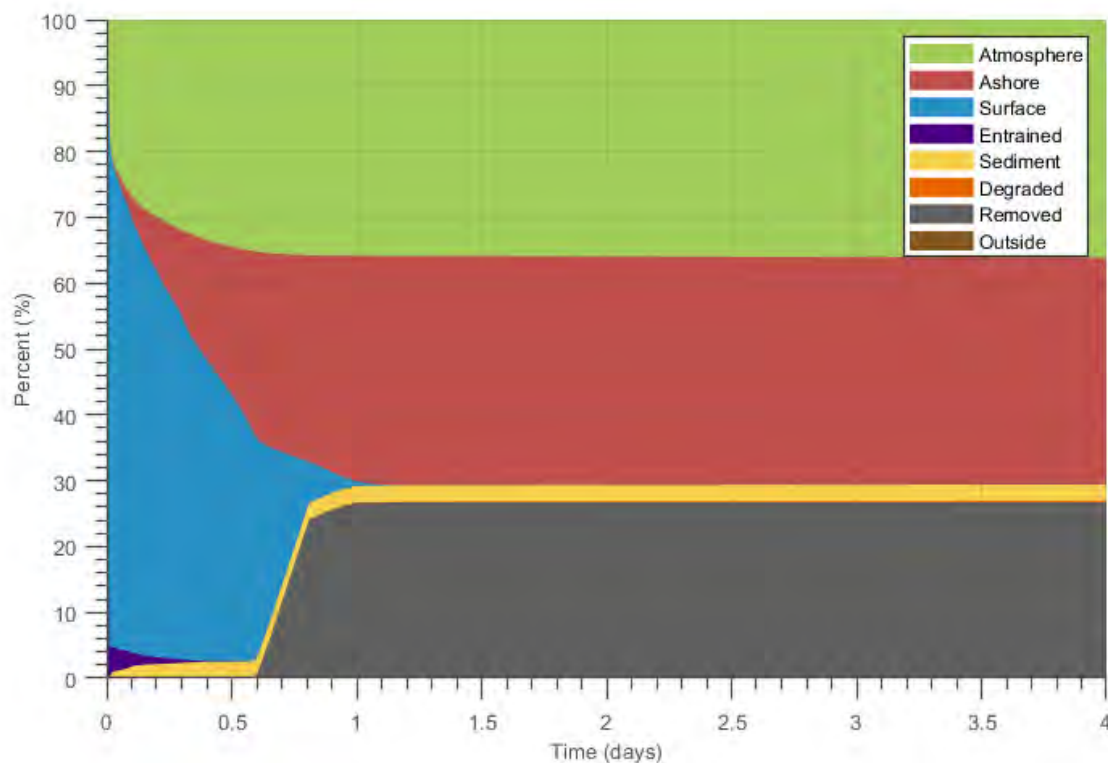
Figure 4-82. Oil mass balance graph for the mitigated FBR scenario in high river flow conditions modeled in April at the White River channel location.
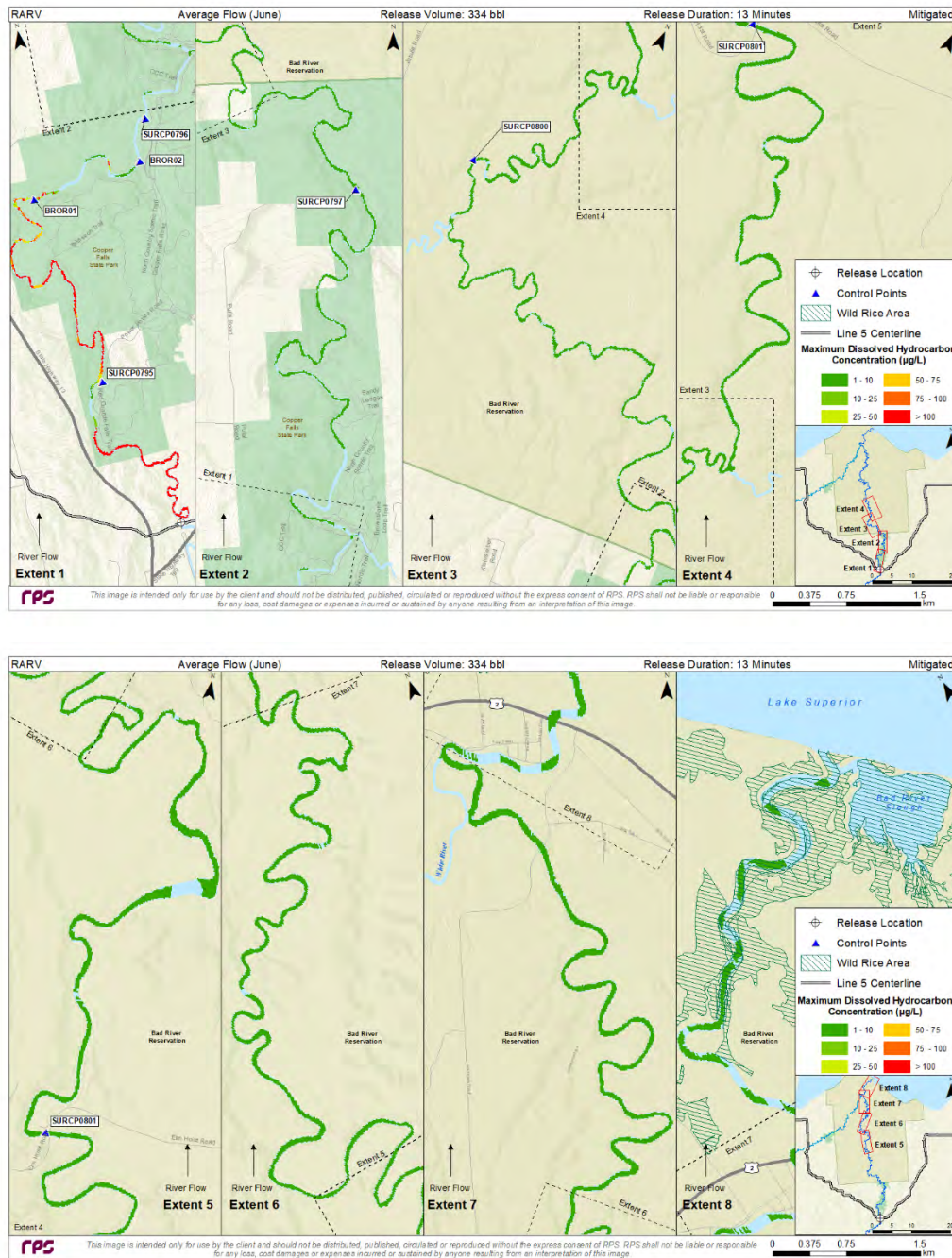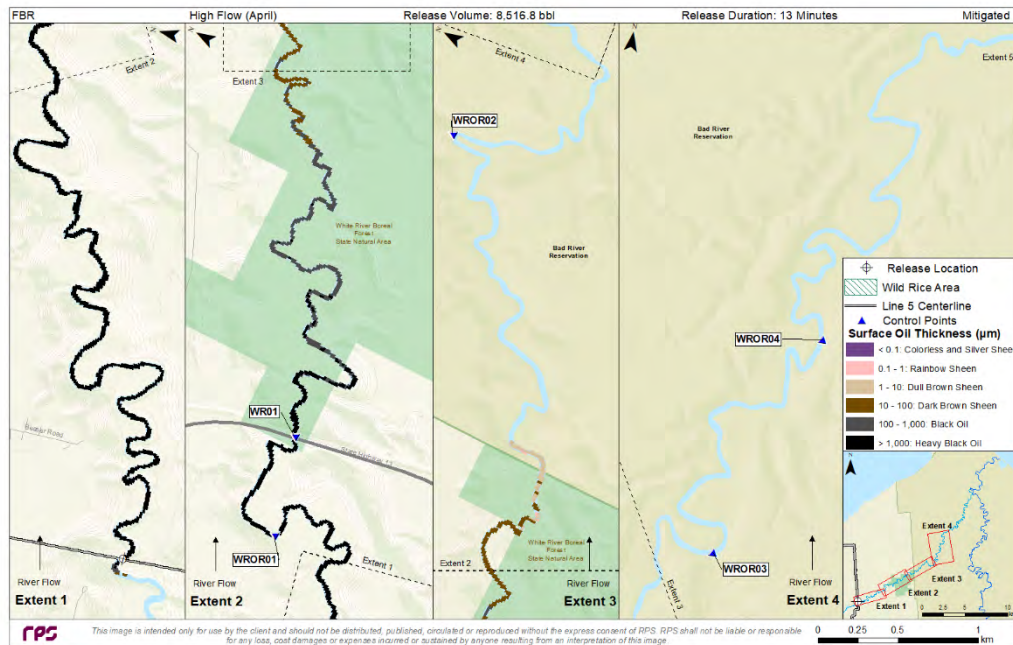
Panel intentionally left blank.

Downstream extents 5-8 not displayed because no oil was predicted there.

Figure 4-83. Composite of maximum surface oil thickness over 4 days for the mitigated FBR scenario in high river flow conditions modeled in April at the White River channel location. This represents the maximum thickness of surface oil that was predicted for each location. The maximum levels of coverage would not be observed at each location simultaneously.
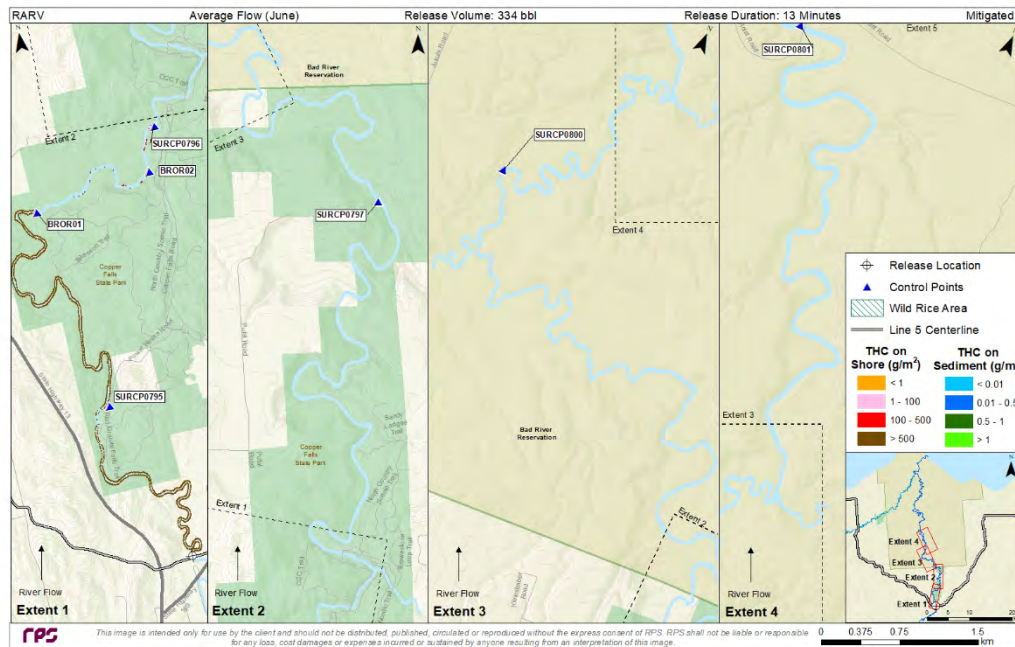
Panel intentionally left blank.

Downstream extents 5-8 not displayed because no oil was predicted there.

Figure 4-84. Composite of maximum total dissolved hydrocarbon concentration over 4 days for the mitigated FBR scenario in high river flow conditions modeled in April at the White River channel location. This represents the maximum in-water contamination that was predicted for each location.

Panel intentionally left blank.

Downstream extents 5-8 not displayed because no oil was predicted there.

Figure 4-85. Maximum total hydrocarbon mass on the shore and on sediments after 4 days for the mitigated FBR scenario in high river flow conditions modeled in April at the White River channel location.

4.1.2.9 Mitigated FBR (8,517 bbl), Average River Flow, White River Channel Release
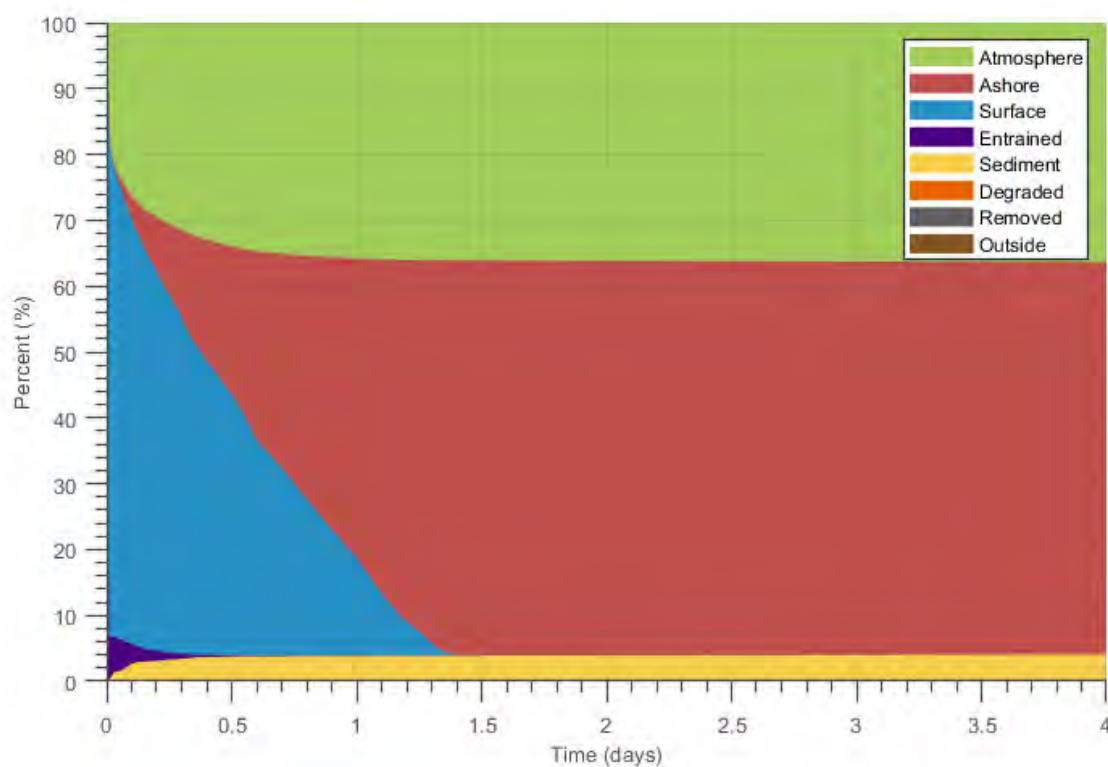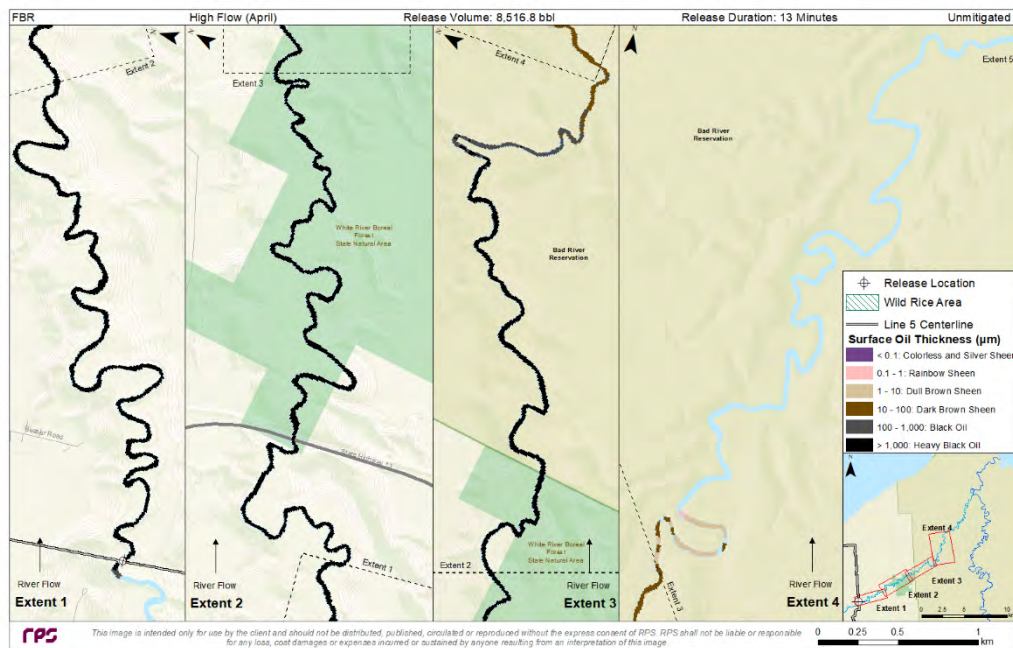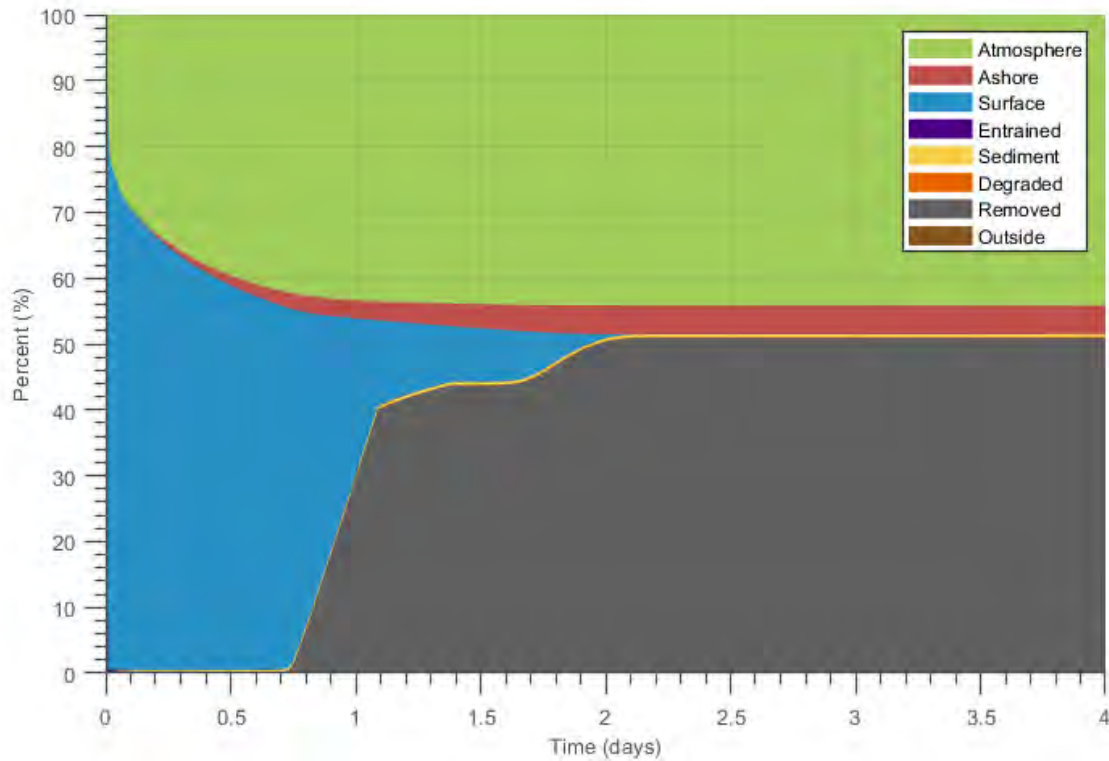

Figure 4-86. Oil mass balance graph for the mitigated FBR scenario in average river flow conditions modeled in June at the White River channel location.
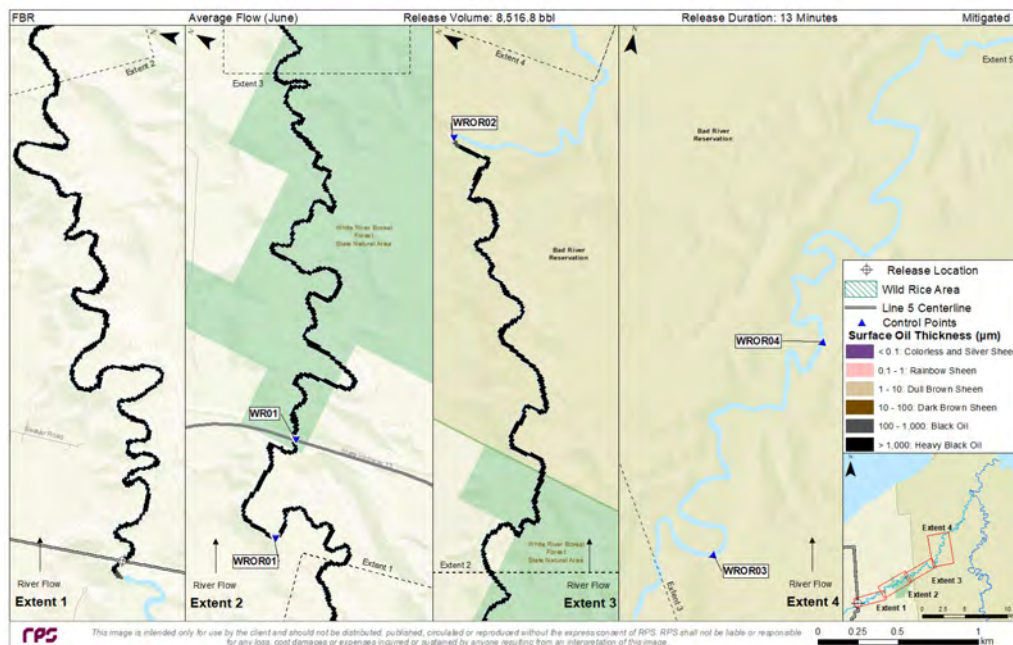
Panel intentionally left blank.

Downstream extents 5-8 not displayed because no oil was predicted there.

Figure 4-87. Composite of maximum surface oil thickness over 4 days for the mitigated FBR scenario in average river flow conditions modeled in June at the White River channel location. This represents the maximum thickness of surface oil that was predicted for each location. The maximum levels of coverage would not be observed at each location simultaneously.
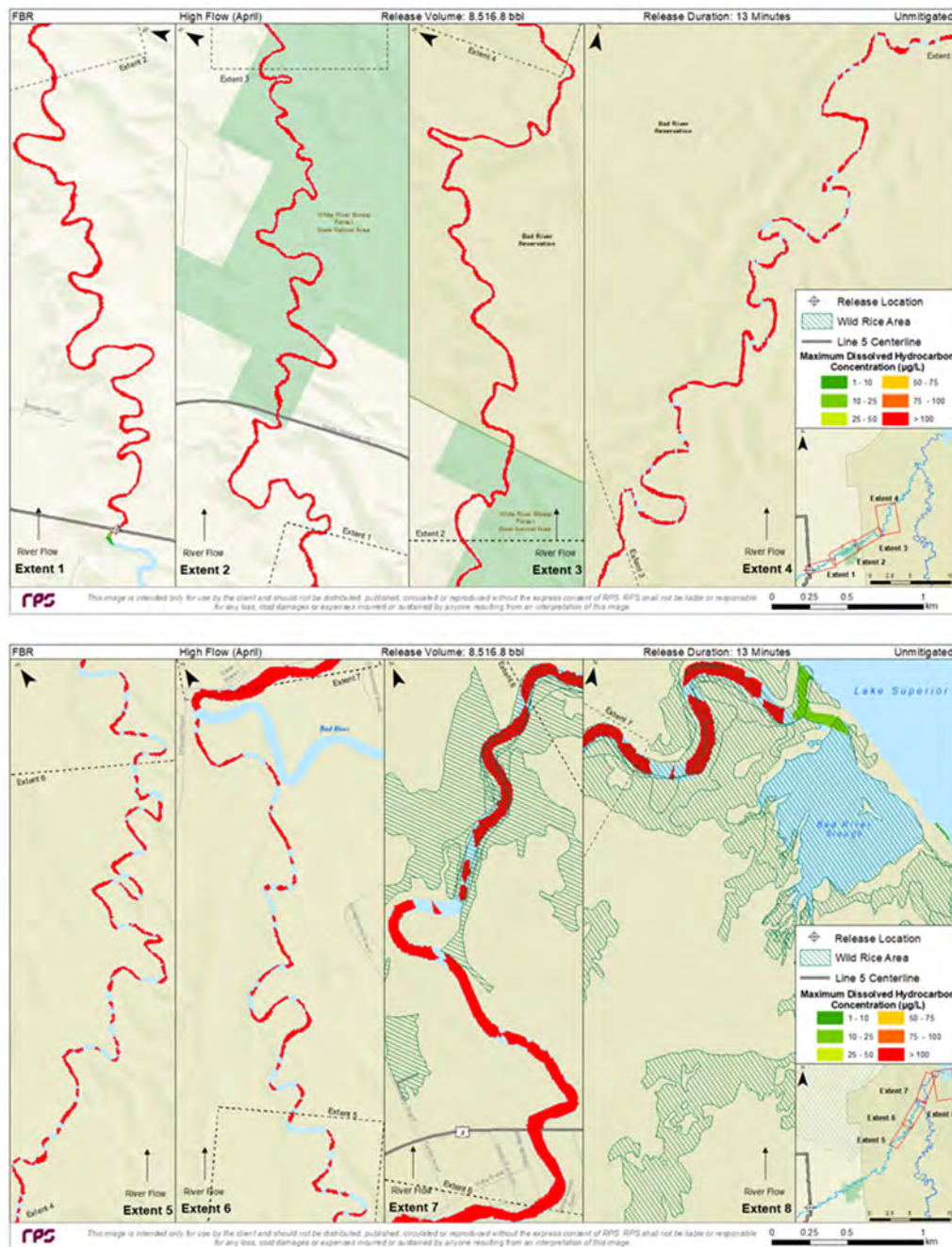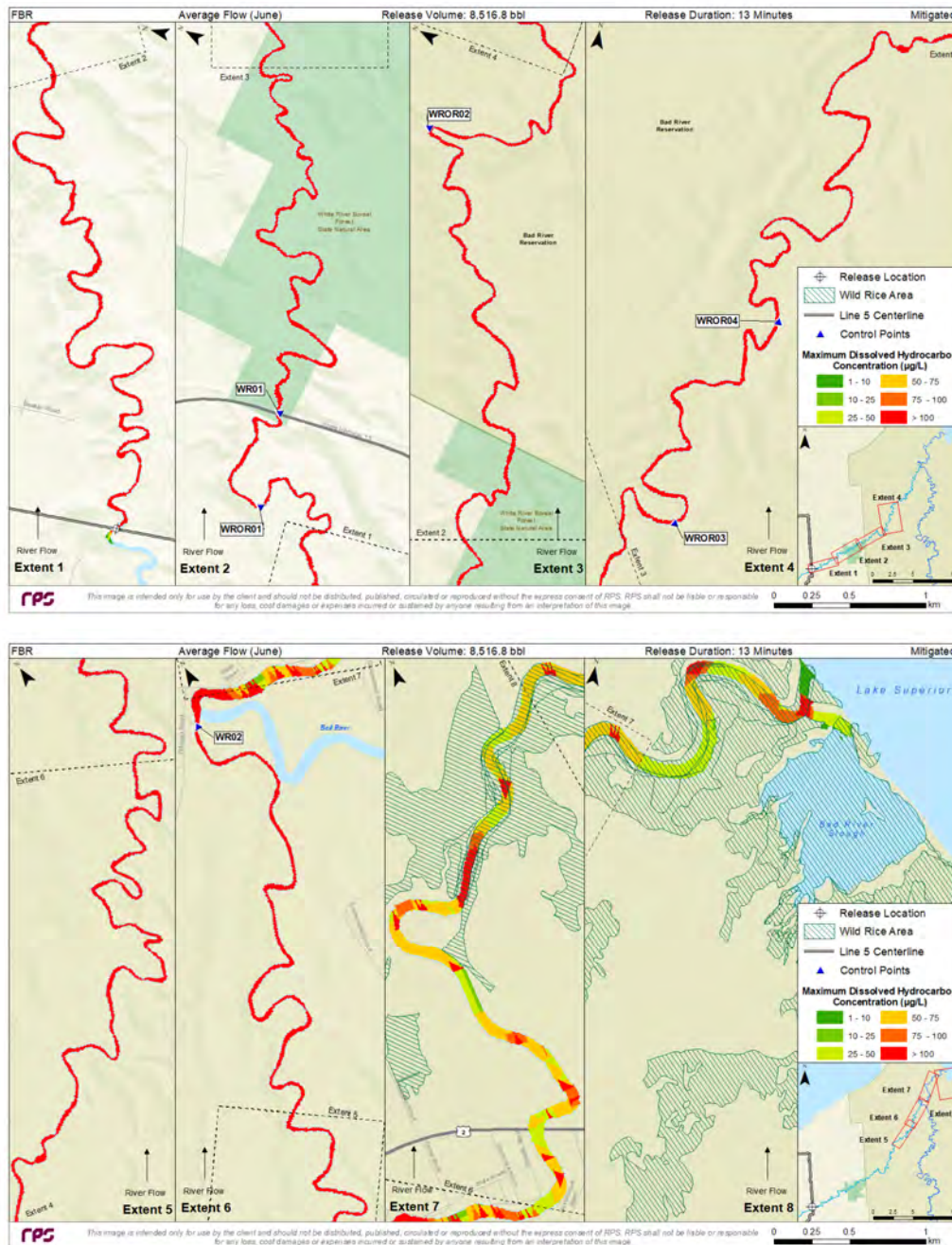
Figure 4-88. Composite of maximum total dissolved hydrocarbon concentration over 4 days for the mitigated FBR scenario in average river flow conditions modeled in June at the White River channel location. This represents the maximum in-water contamination that was predicted for each location.
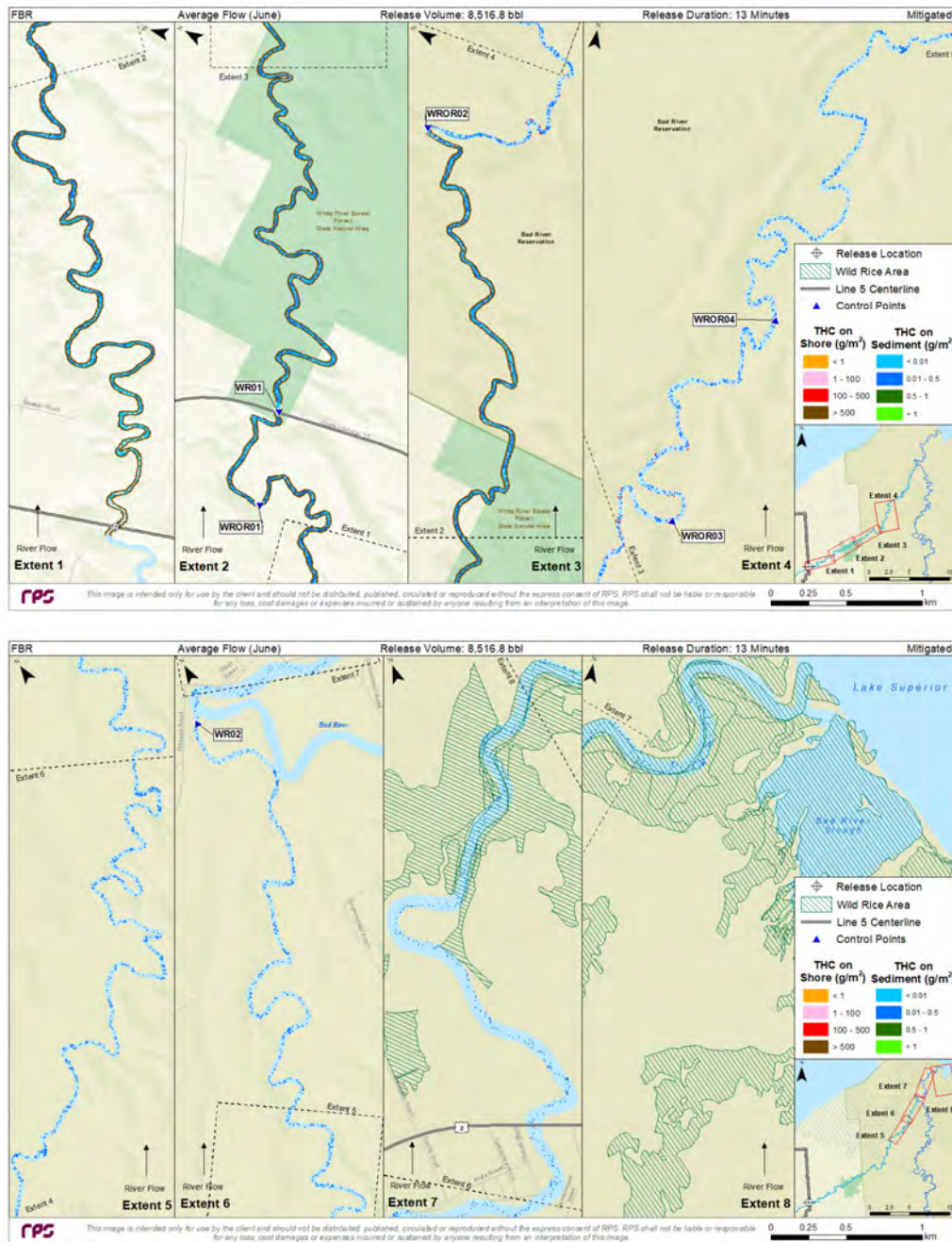
Figure 4-89. Maximum total hydrocarbon mass on the shore and on sediments after 4 days for the mitigated FBR scenario in average river flow conditions modeled in June at the White River channel location.

4.1.2.10 Mitigated FBR (8,517 bbl), Low River Flow, White River Channel Release
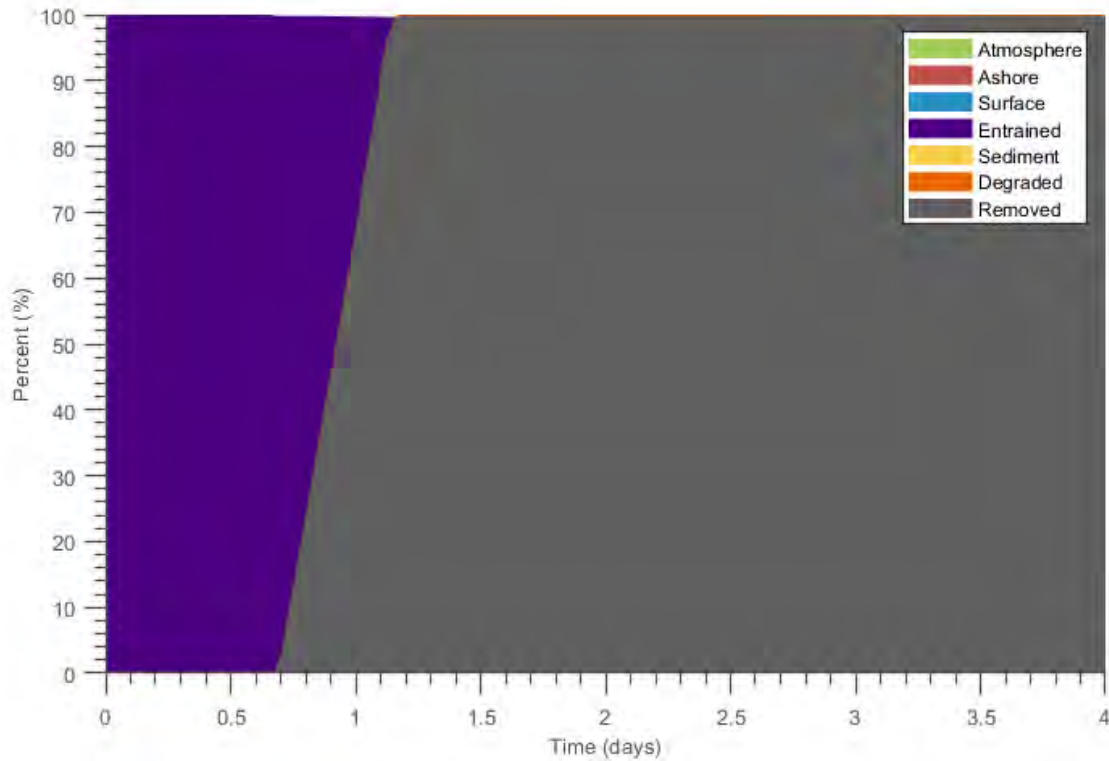
Figure 4-90. Oil mass balance graph for the mitigated FBR scenario in low river flow conditions modeled in January at the White River channel location.
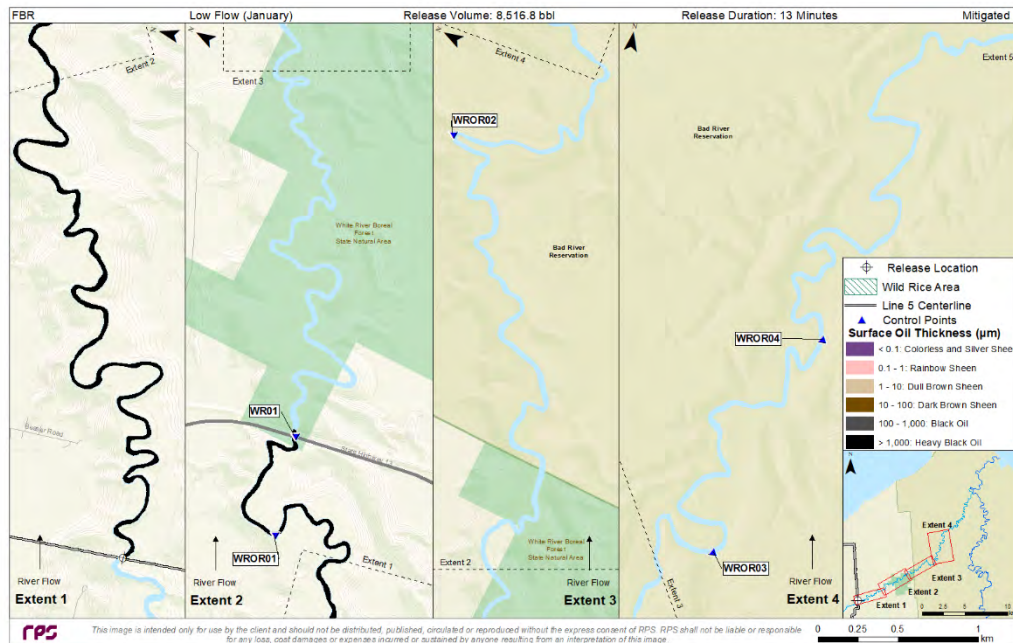
Panel intentionally left blank.

Downstream extents 5-8 not displayed because no oil was predicted there.

Figure 4-91. Composite of maximum subsurface oil thickness (beneath ice) for the mitigated FBR scenario in low river flow conditions modeled in January at the White River channel location. This represents the maximum thickness of oil that was predicted for each location. The maximum levels of coverage would not be observed at each location simultaneously.

Figure intentionally left blank.

Cumulative maximum DHCs were predicted to exceed 100 µg/L

from the release location down to Lake Superior. See Figure 4-65.

Figure 4-92. Composite of maximum total dissolved hydrocarbon concentration for the mitigated FBR scenario in low river flow conditions modeled in January at the White River channel location. This represents the maximum in-water contamination that was predicted for each location.
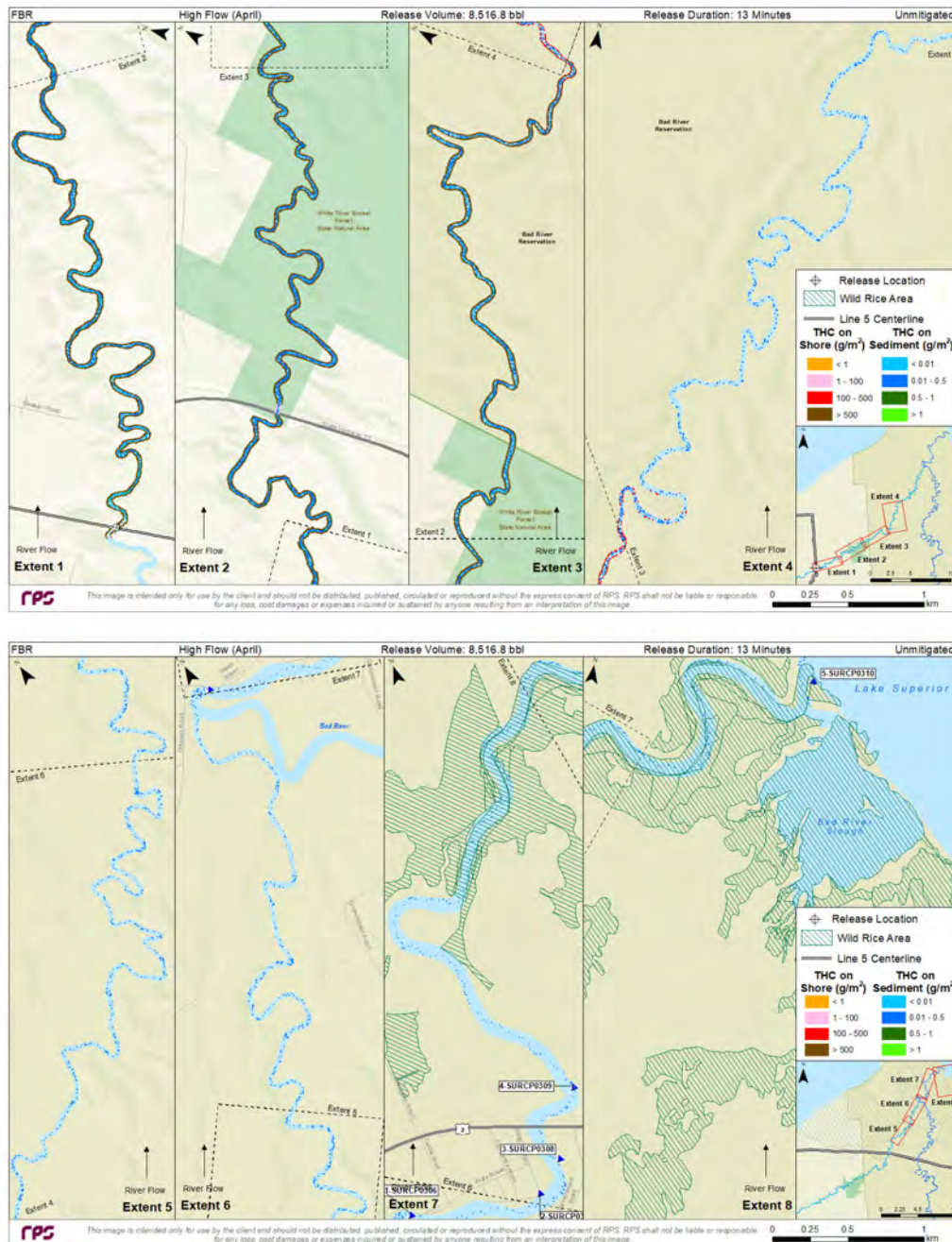
4.1.2.11 Mitigated HARV (1,911 bbl), High River Flow, White River Channel Release
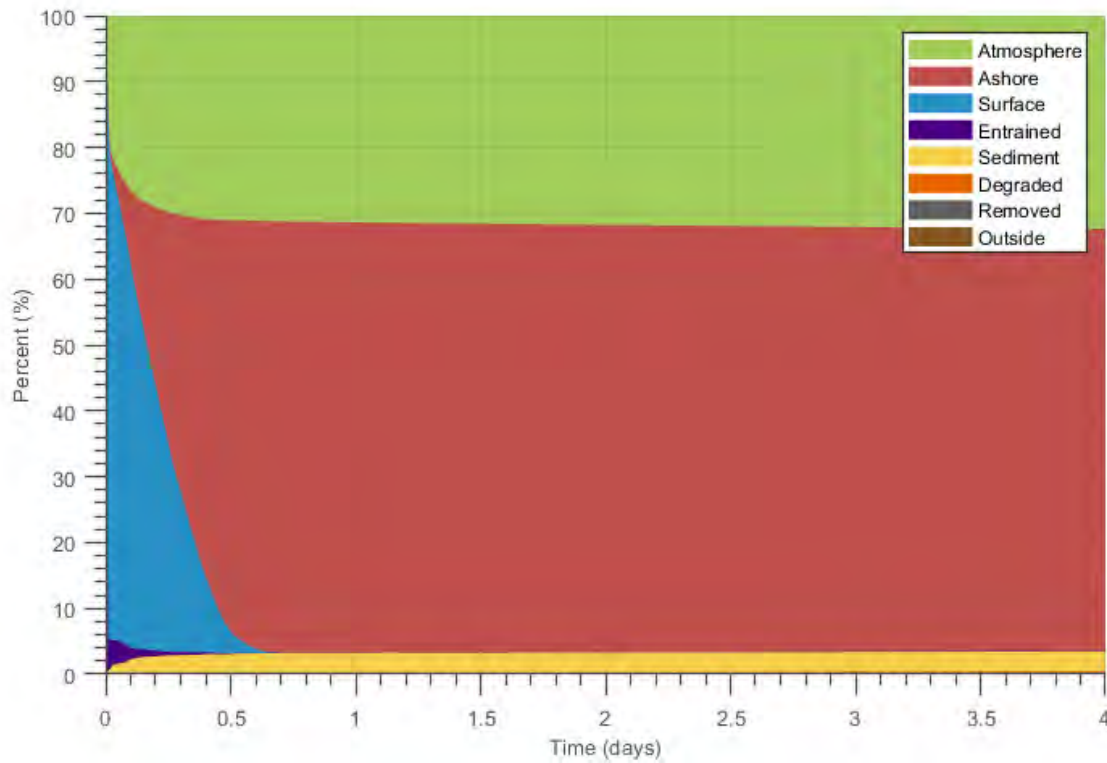
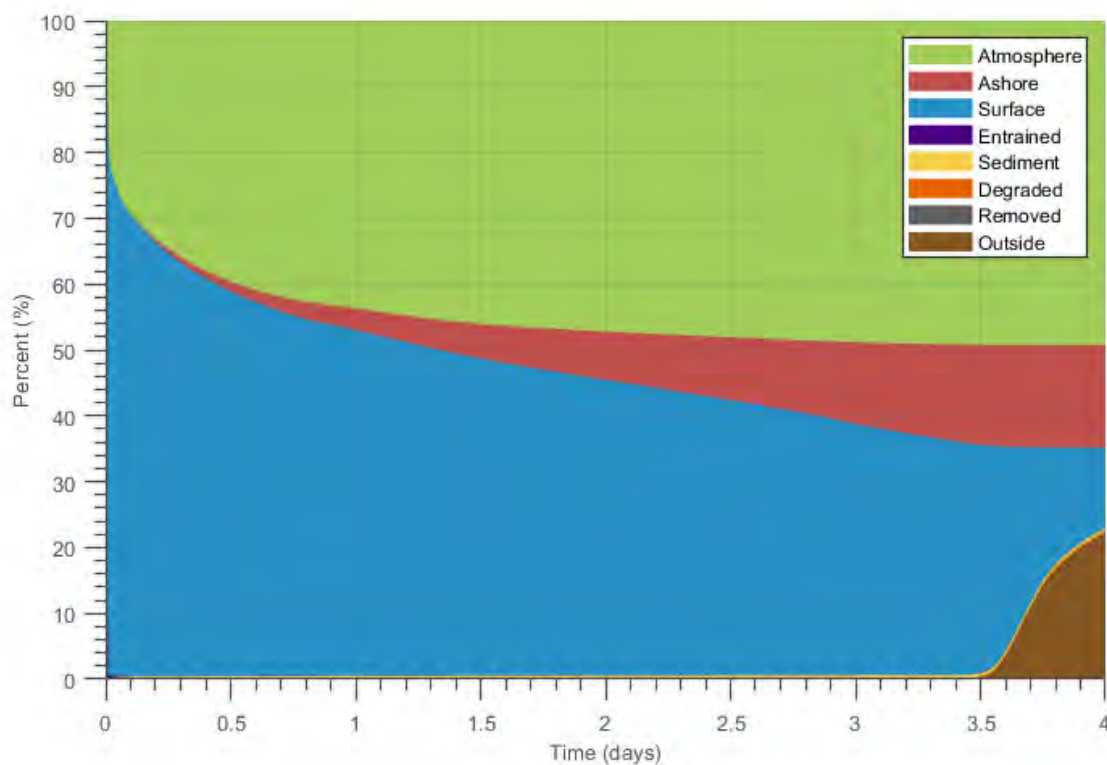**Figure 4-93. Oil mass balance graph for the mitigated HARV scenario in high river flow conditions modeled in April at the White River channel location.**
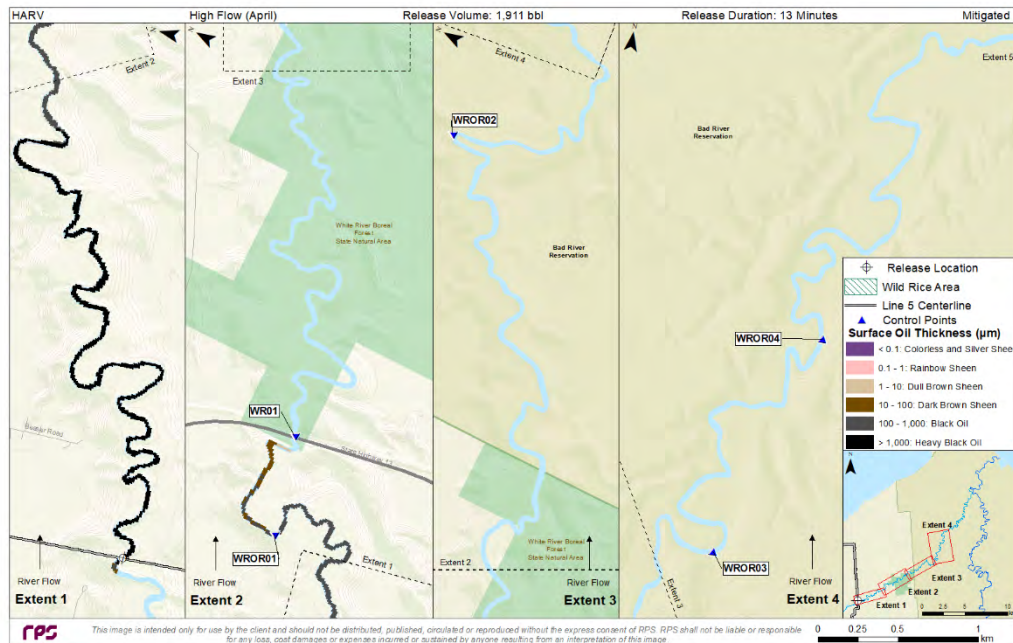
Panel intentionally left blank.

Downstream extents 5-8 not displayed because no oil was predicted there.

Figure 4-94. Composite of maximum surface oil thickness over 4 days for the mitigated HARV scenario in high river flow conditions modeled in April at the White River channel location. This represents the maximum thickness of surface oil that was predicted for each location. The maximum levels of coverage would not be observed at each location simultaneously.

Panel intentionally left blank.

Downstream extents 5-8 not displayed because no oil was predicted there.

Figure 4-95. Composite of maximum total dissolved hydrocarbon concentration over 4 days for the mitigated HARV scenario in high river flow conditions modeled in April at the White River channel location. This represents the maximum in-water contamination that was predicted for each location.
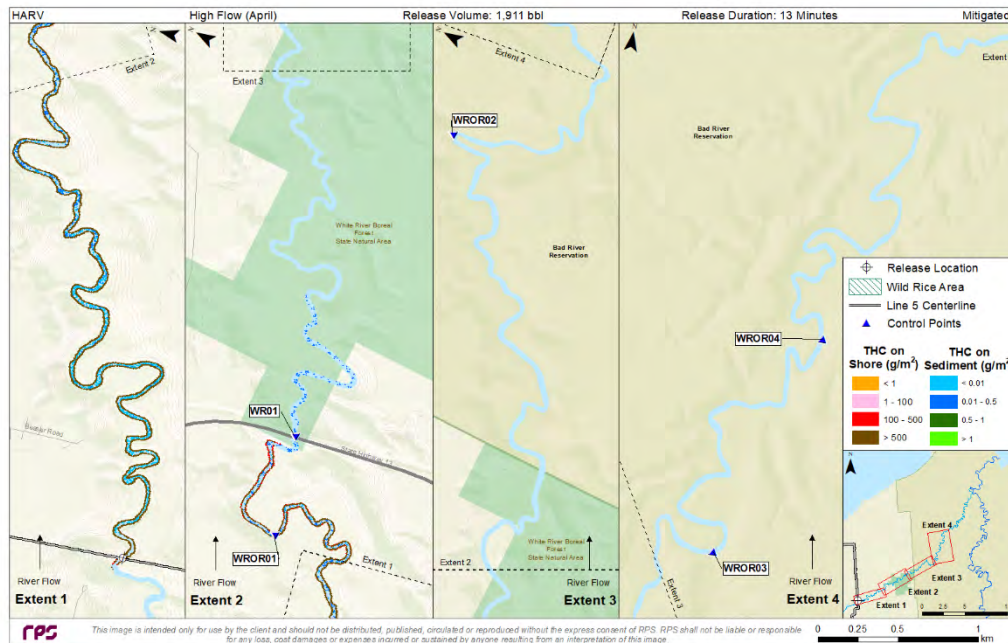
Panel intentionally left blank.

Downstream extents 5-8 not displayed because no oil was predicted there.

Figure 4-96. Maximum total hydrocarbon mass on the shore and on sediments after 4 days for the mitigated HARV scenario in high river flow conditions modeled in April at the White River channel location.

### 4.1.2.12 Mitigated HARV (1,911 bbl), Average River Flow, White River Channel Release
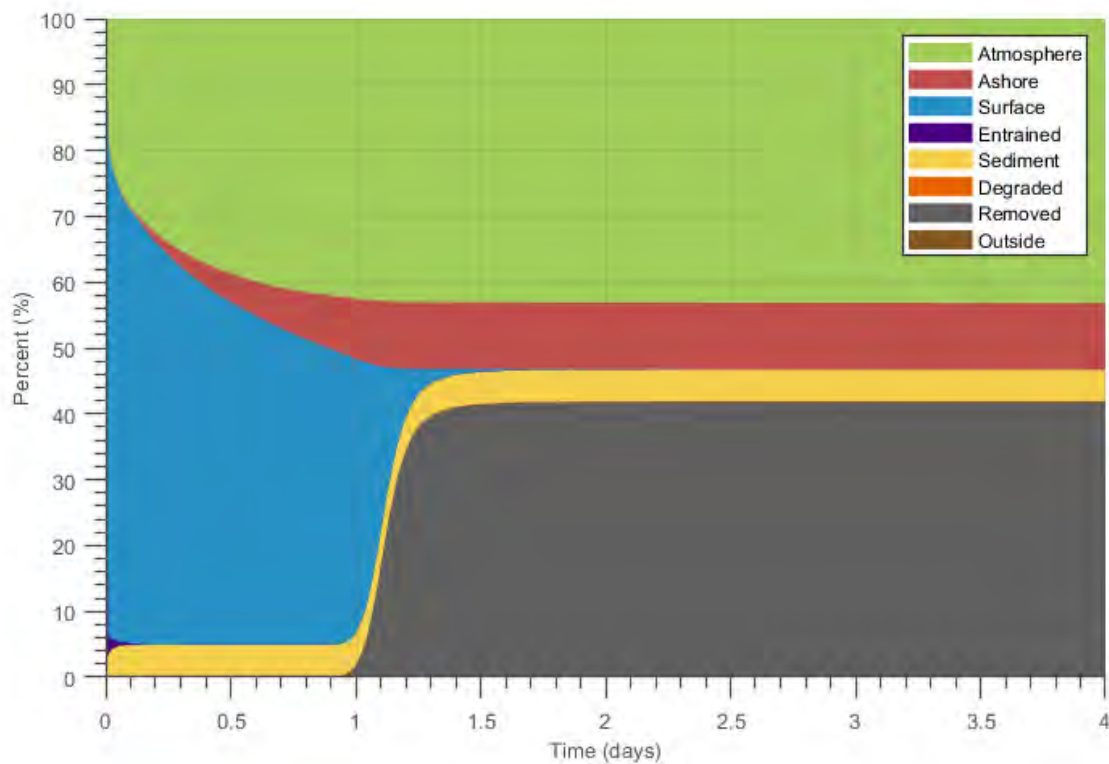
Figure 4-97. Oil mass balance graph for the mitigated HARV scenario in average river flow conditions modeled in June at the White River channel location.
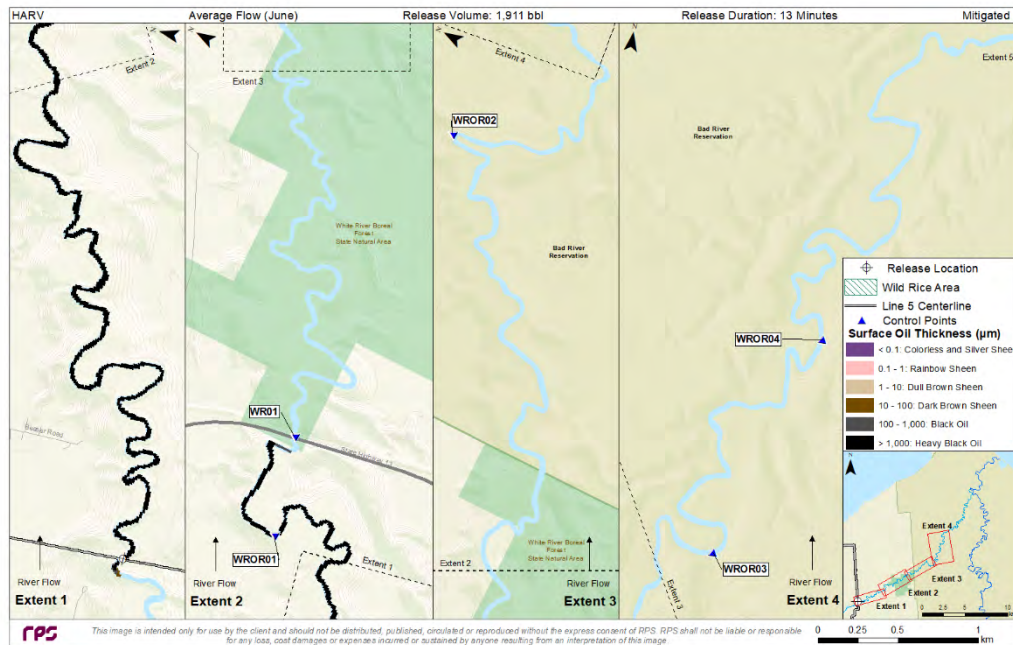
Panel intentionally left blank.

Downstream extents 5-8 not displayed because no oil was predicted there.

Figure 4-98. Composite of maximum surface oil thickness over 4 days for the mitigated HARV scenario in average river flow conditions modeled in June at the White River channel location. This represents the maximum thickness of surface oil that was predicted for each location. The maximum levels of coverage would not be observed at each location simultaneously.
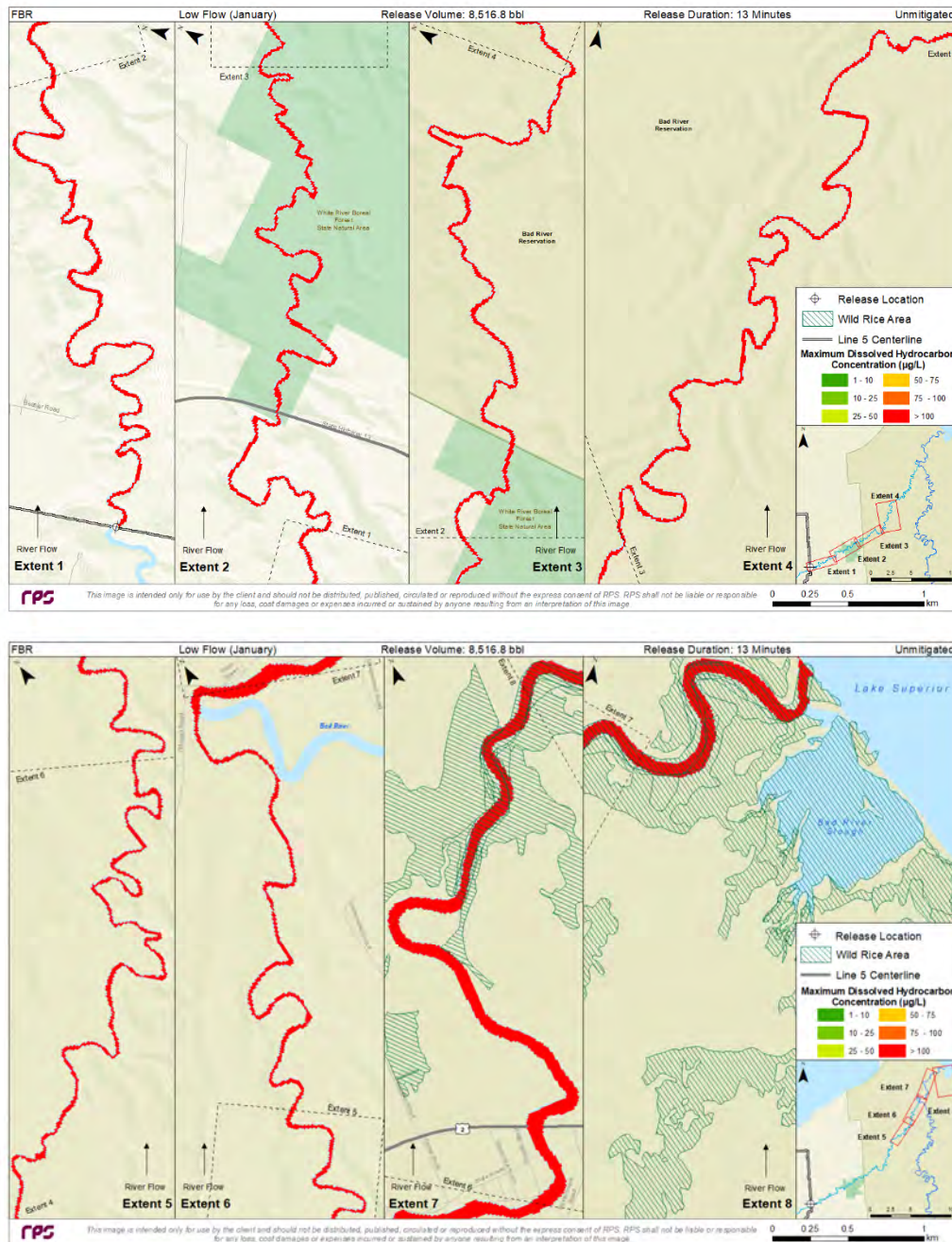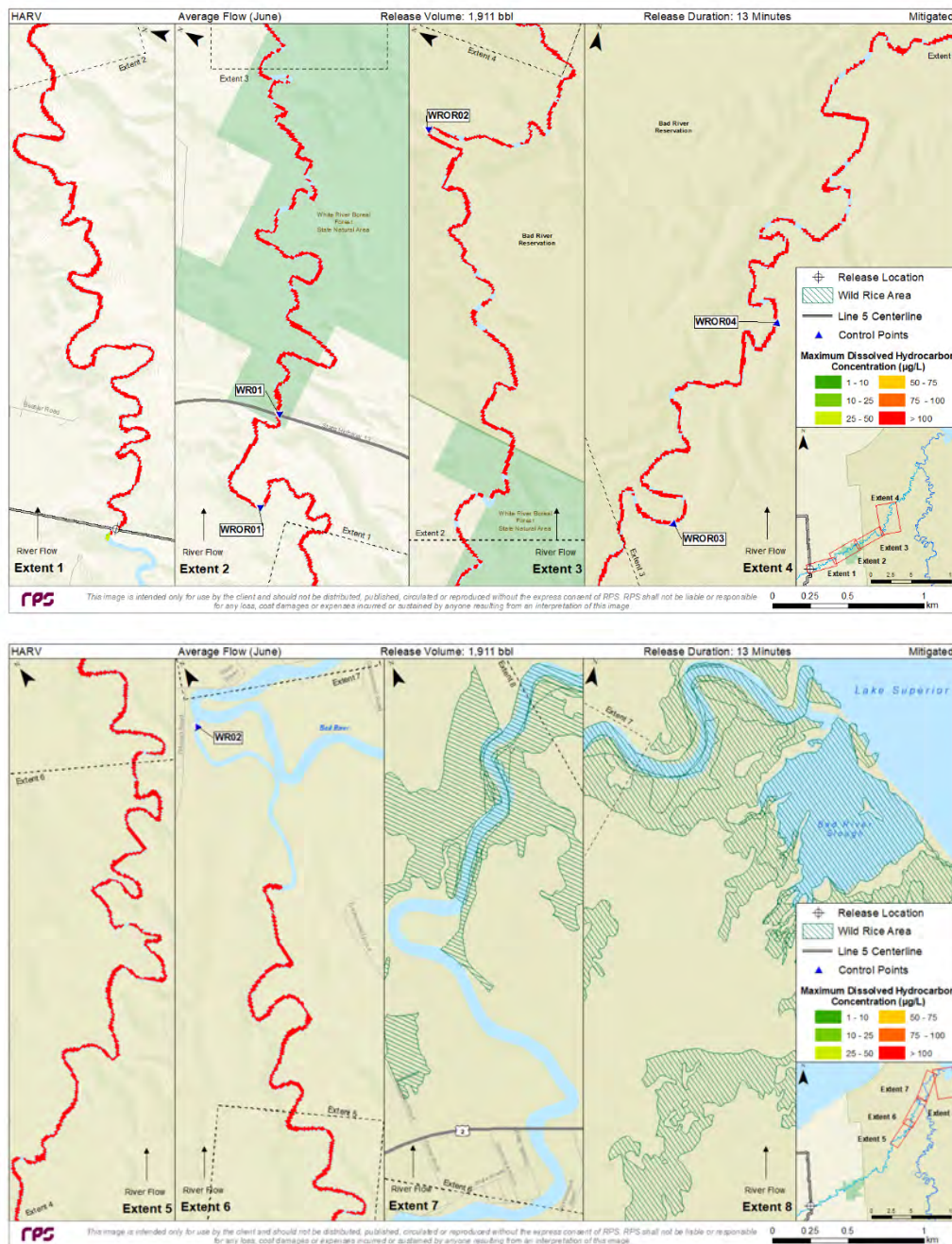
Figure 4-99. Composite of maximum total dissolved hydrocarbon concentration over 4 days for the mitigated HARV scenario in average river flow conditions modeled in June at the White River channel location. This represents the maximum in-water contamination that was predicted for each location.
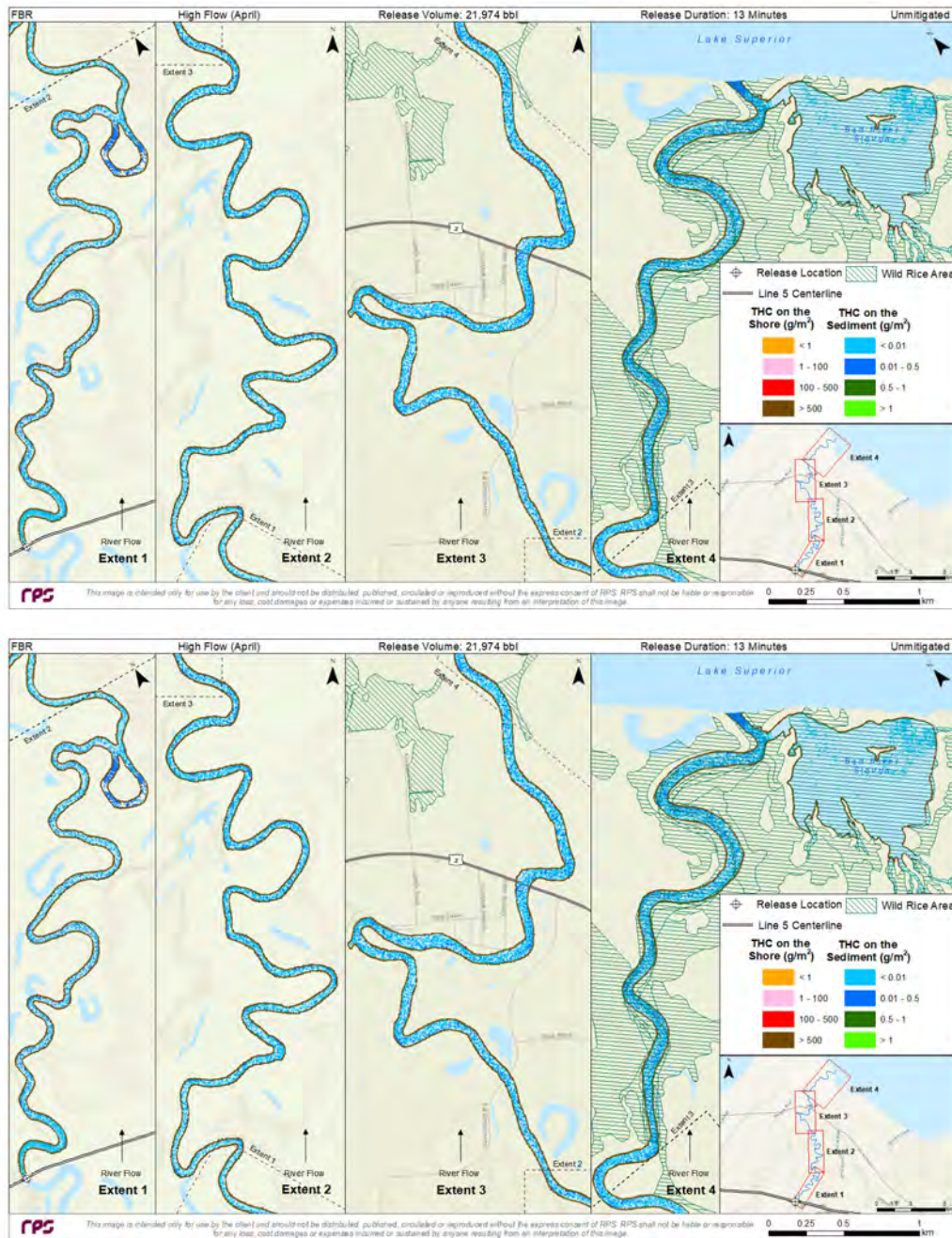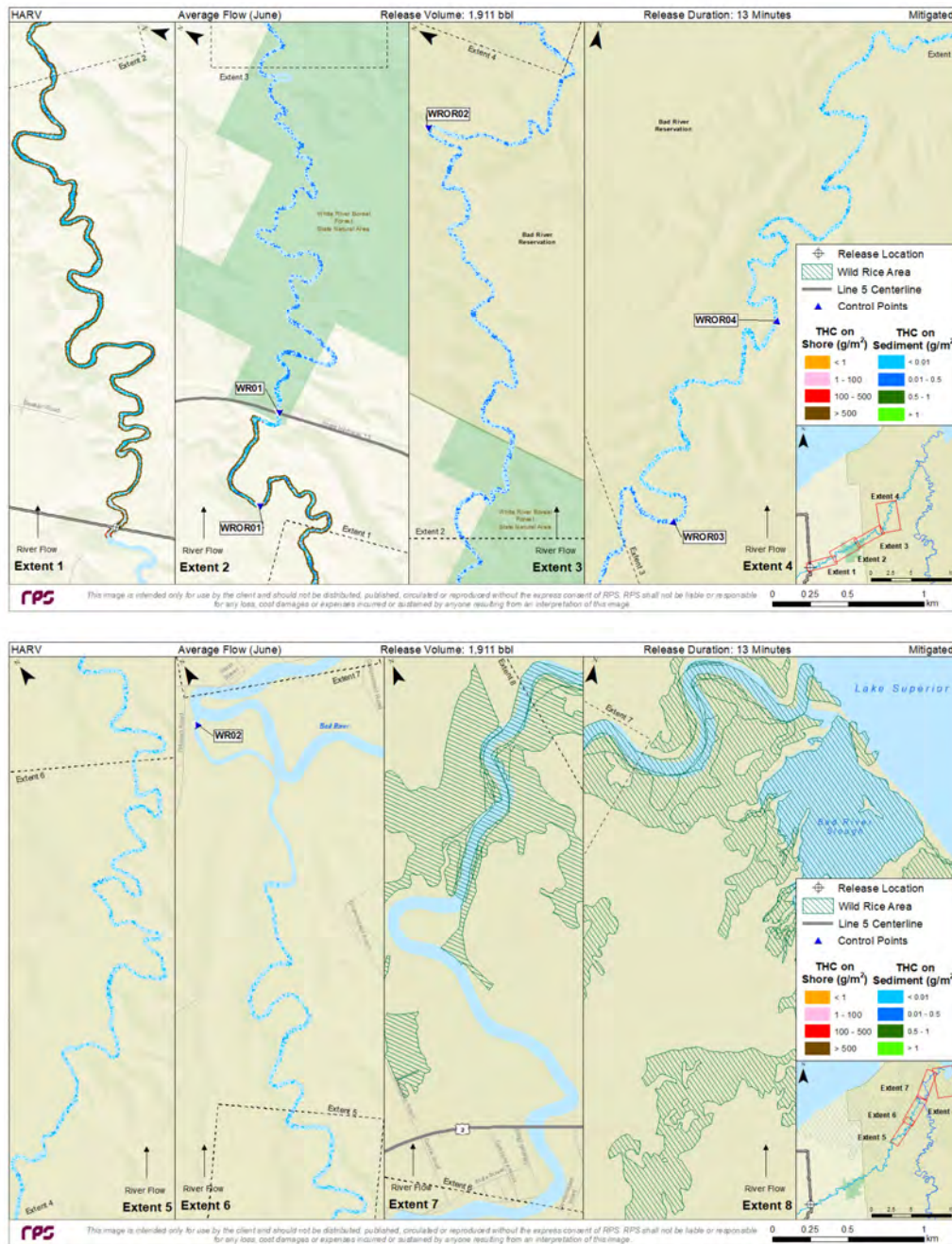
Figure 4-100. Maximum total hydrocarbon mass on the shore and on sediments after 4 days for the mitigated HARV scenario in average river flow conditions modeled in June at the White River channel location.

4.1.2.13 Mitigated HARV (1,911 bbl), Low River Flow, White River Channel Release
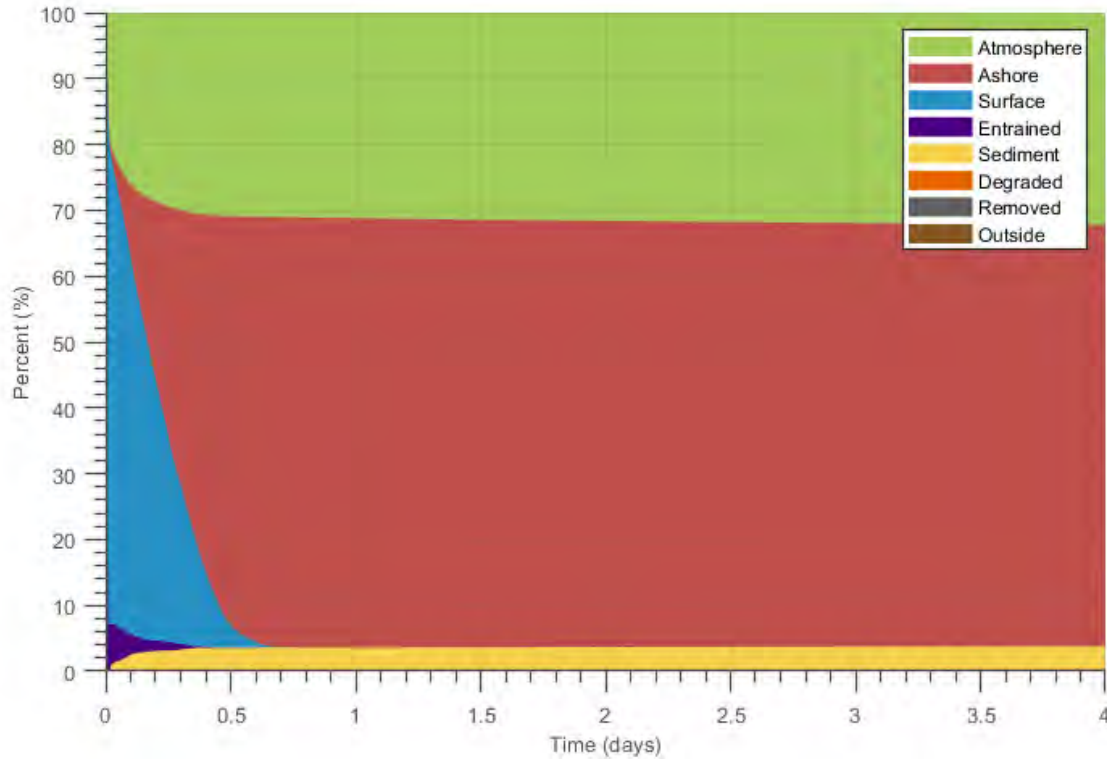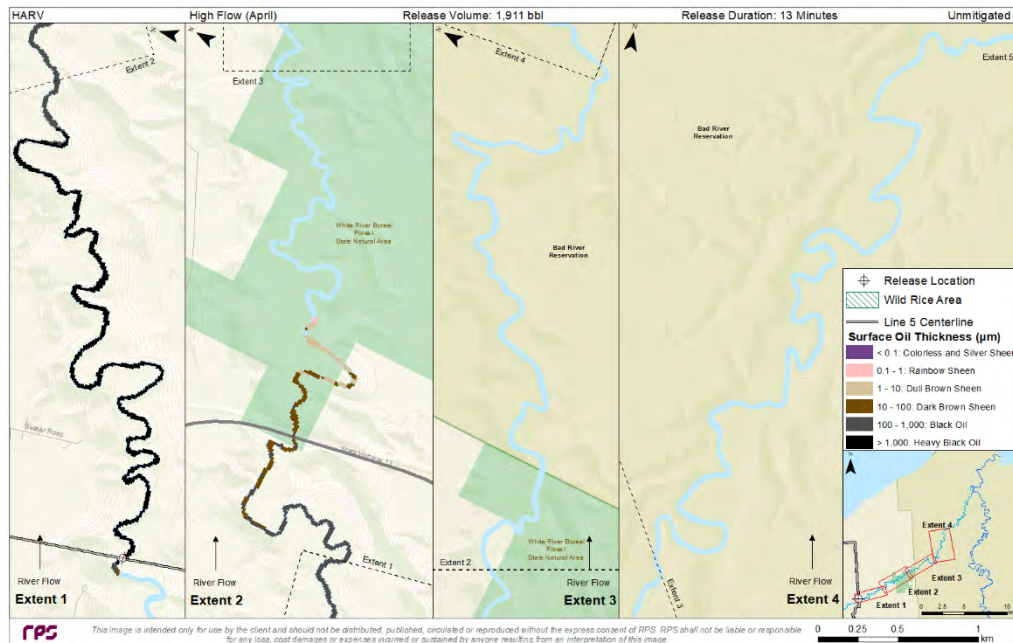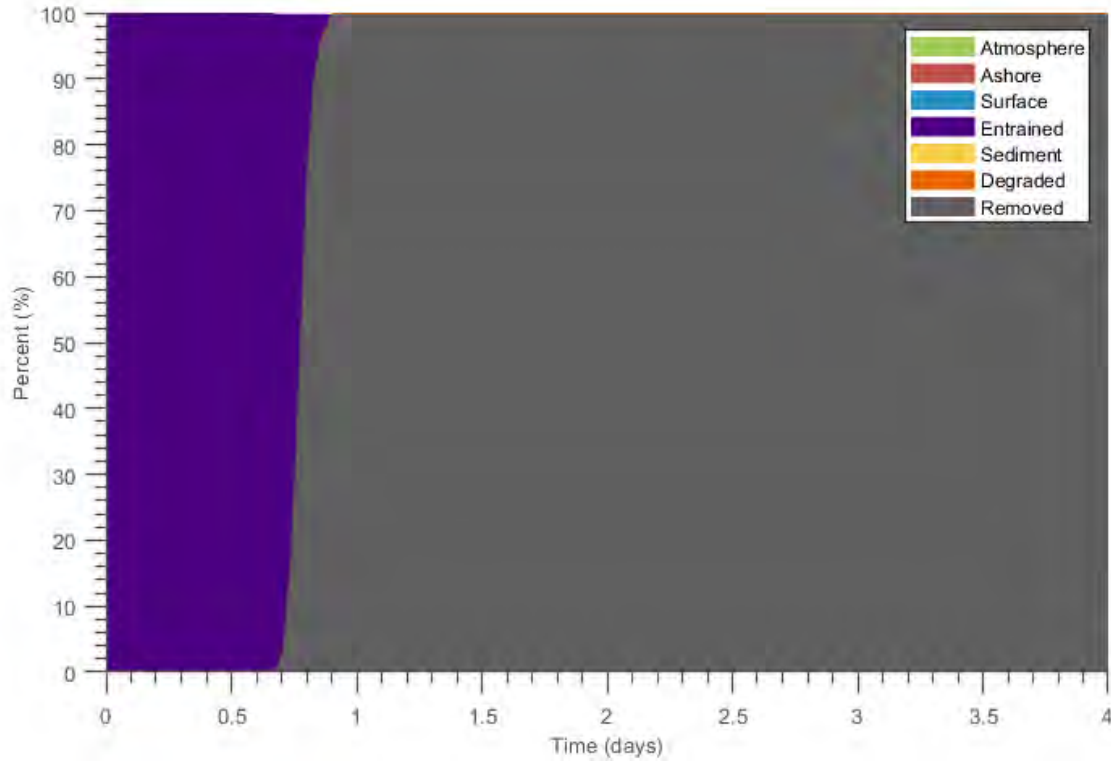

Figure 4-101. Oil mass balance graph for the mitigated HARV scenario in low river flow conditions modeled in January at the White River channel location.
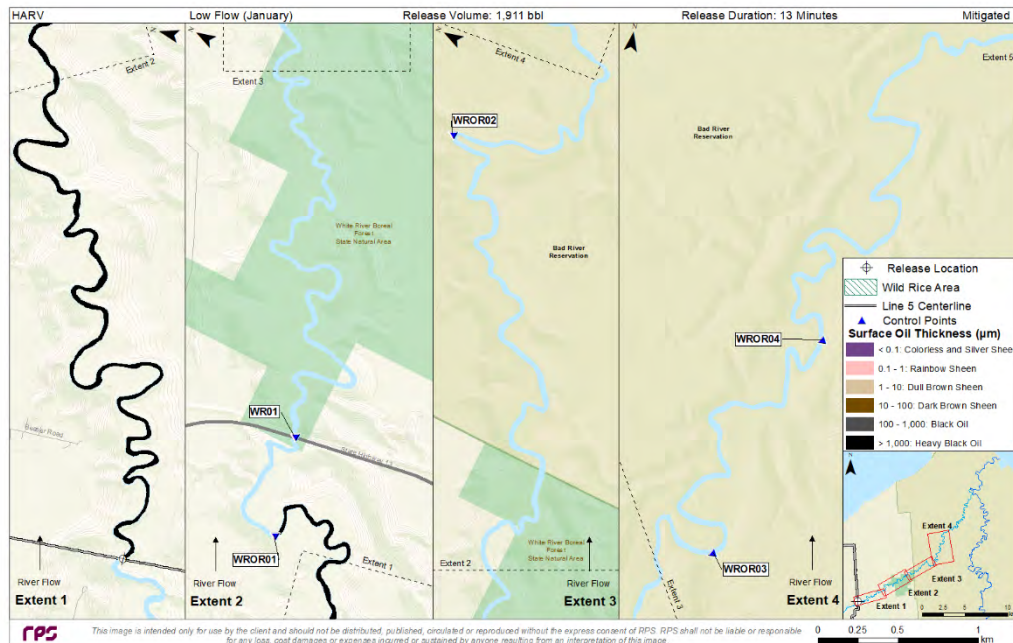
Panel intentionally left blank.

Downstream extents 5-8 not displayed because no oil was predicted there.

Figure 4-102. Composite of maximum subsurface oil thickness (beneath ice) for the mitigated HARV scenario in low river flow conditions modeled in January at the White River channel location. This represents the maximum thickness of oil that was predicted for each location. The maximum levels of coverage would not be observed at each location simultaneously.

Figure intentionally left blank.

Cumulative maximum DHCs were predicted to exceed 100 μg/L

from the release location down to Lake Superior. See Figure 4-65.

Figure 4-103. Composite of maximum total dissolved hydrocarbon concentration for the mitigated HARV scenario in low river flow conditions modeled in January at the White River channel location. This represents the maximum in-water contamination that was predicted for each location.
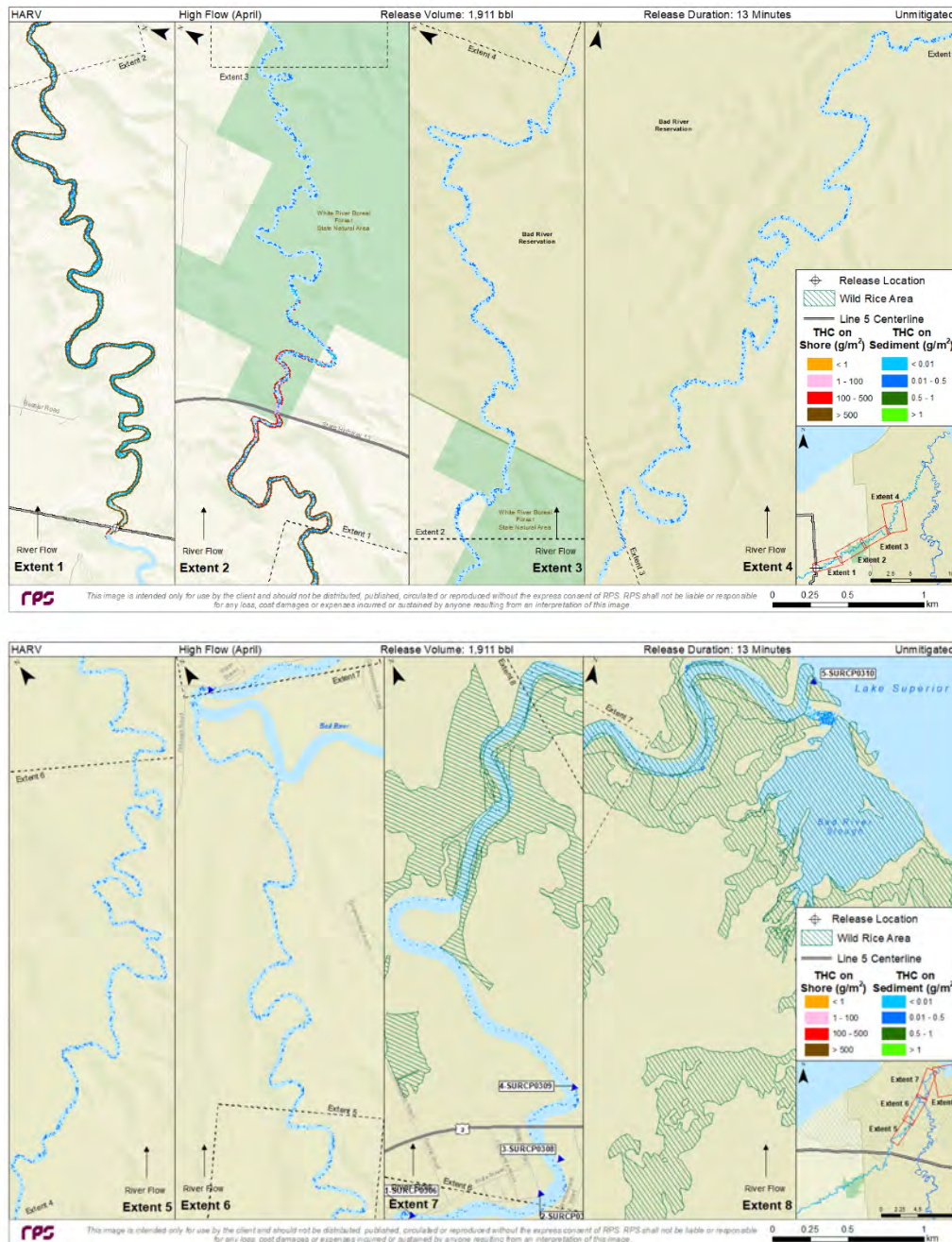
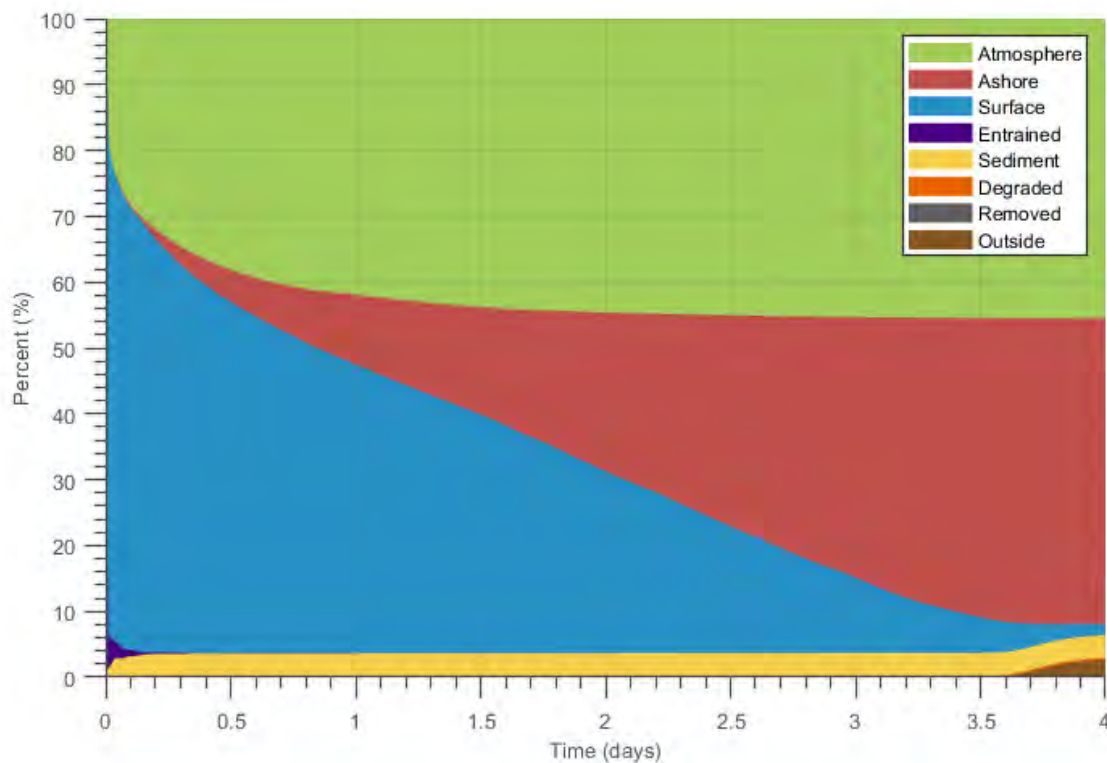### 4.1.2.14 Mitigated RARV (334 bbl), Average River Flow, White River Channel Release
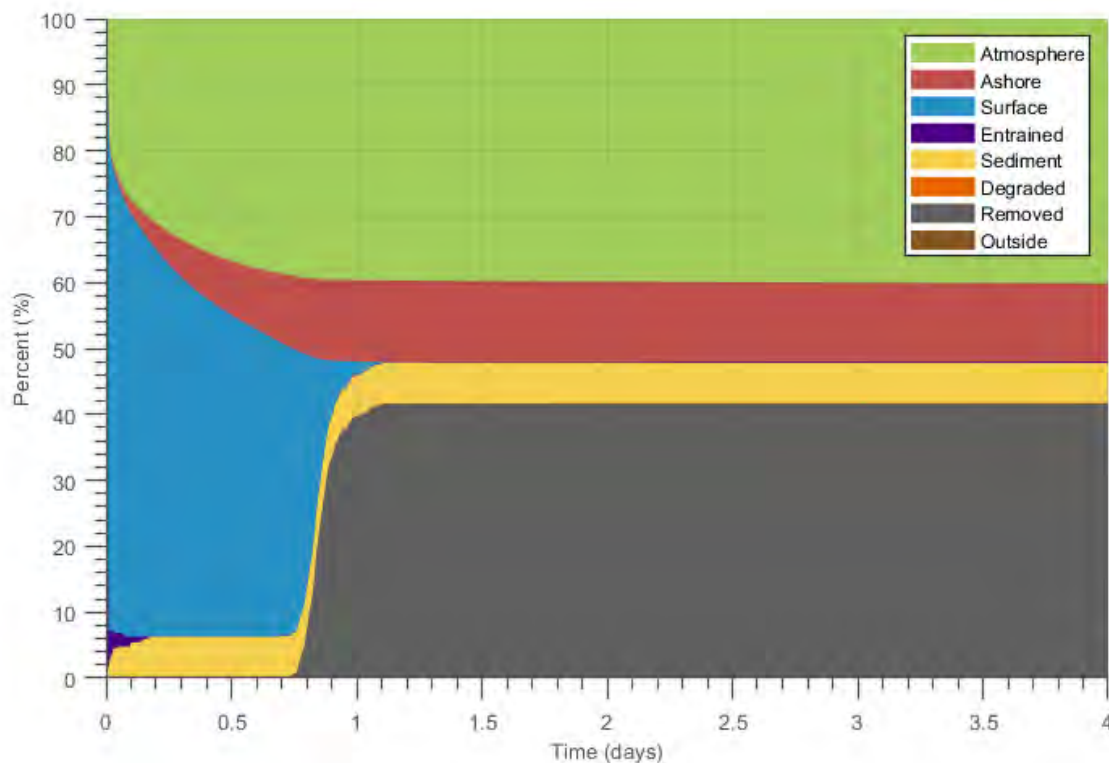
Figure 4-104. Oil mass balance graph for the mitigated RARV scenario in average river flow conditions modeled in June at the White River channel location.
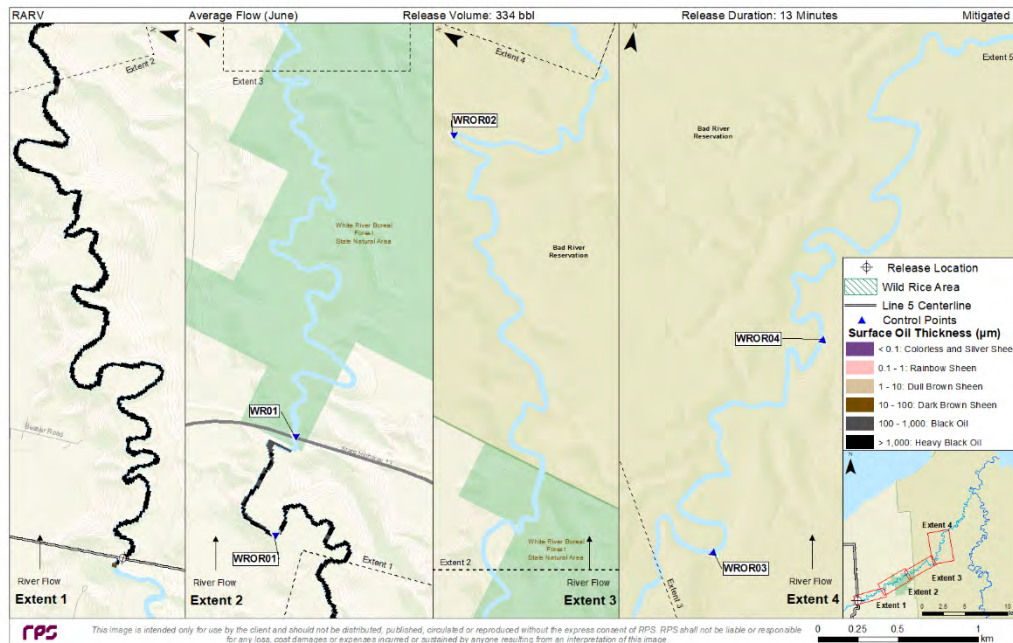
Panel intentionally left blank.

Downstream extents 5-8 not displayed because no oil was predicted there.
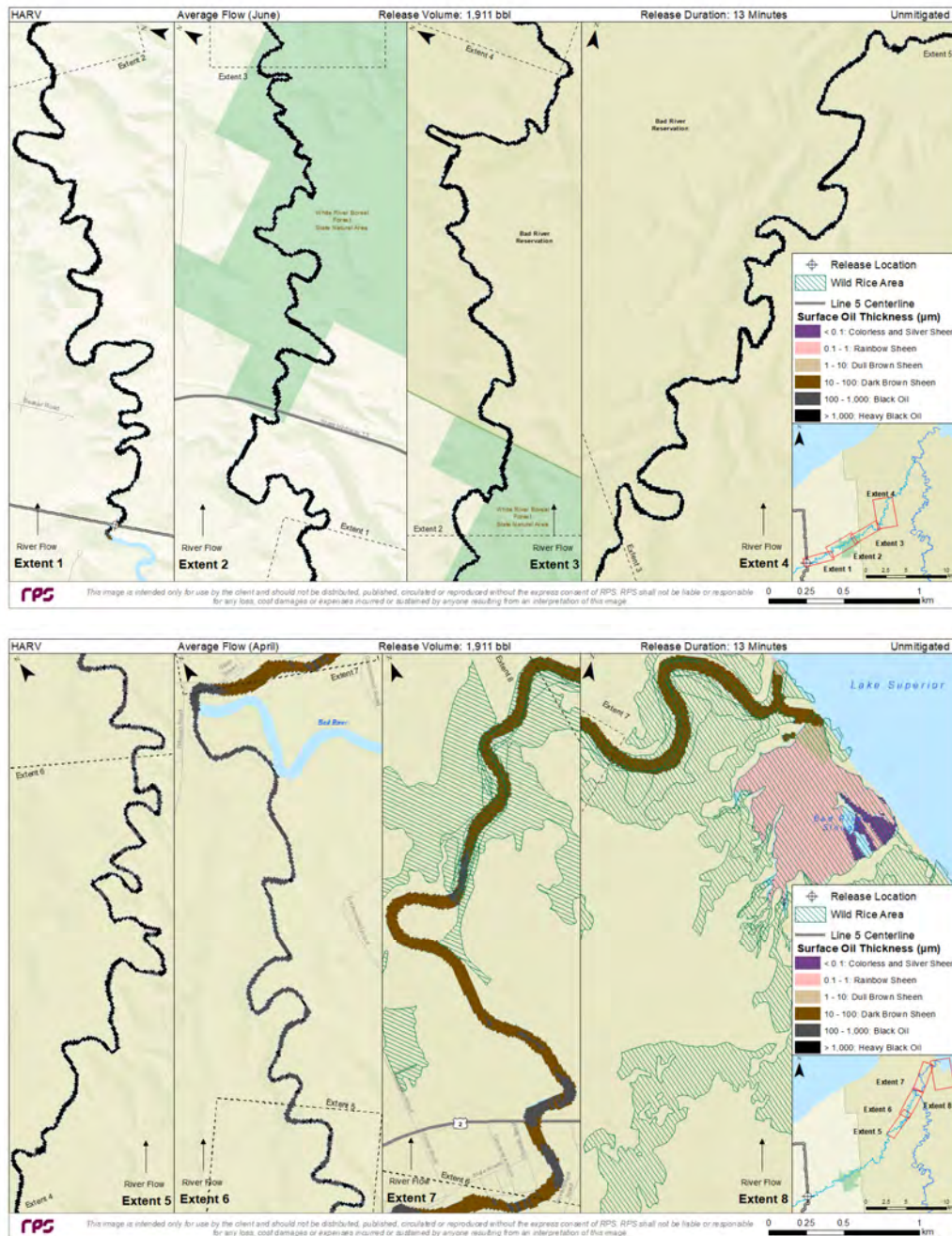
Figure 4-105. Composite of maximum subsurface oil thickness (beneath ice) for the mitigated RARV scenario in average river flow conditions modeled in June at the White River channel location. This represents the maximum thickness of oil that was predicted for each location. The maximum levels of coverage would not be observed at each location simultaneously.
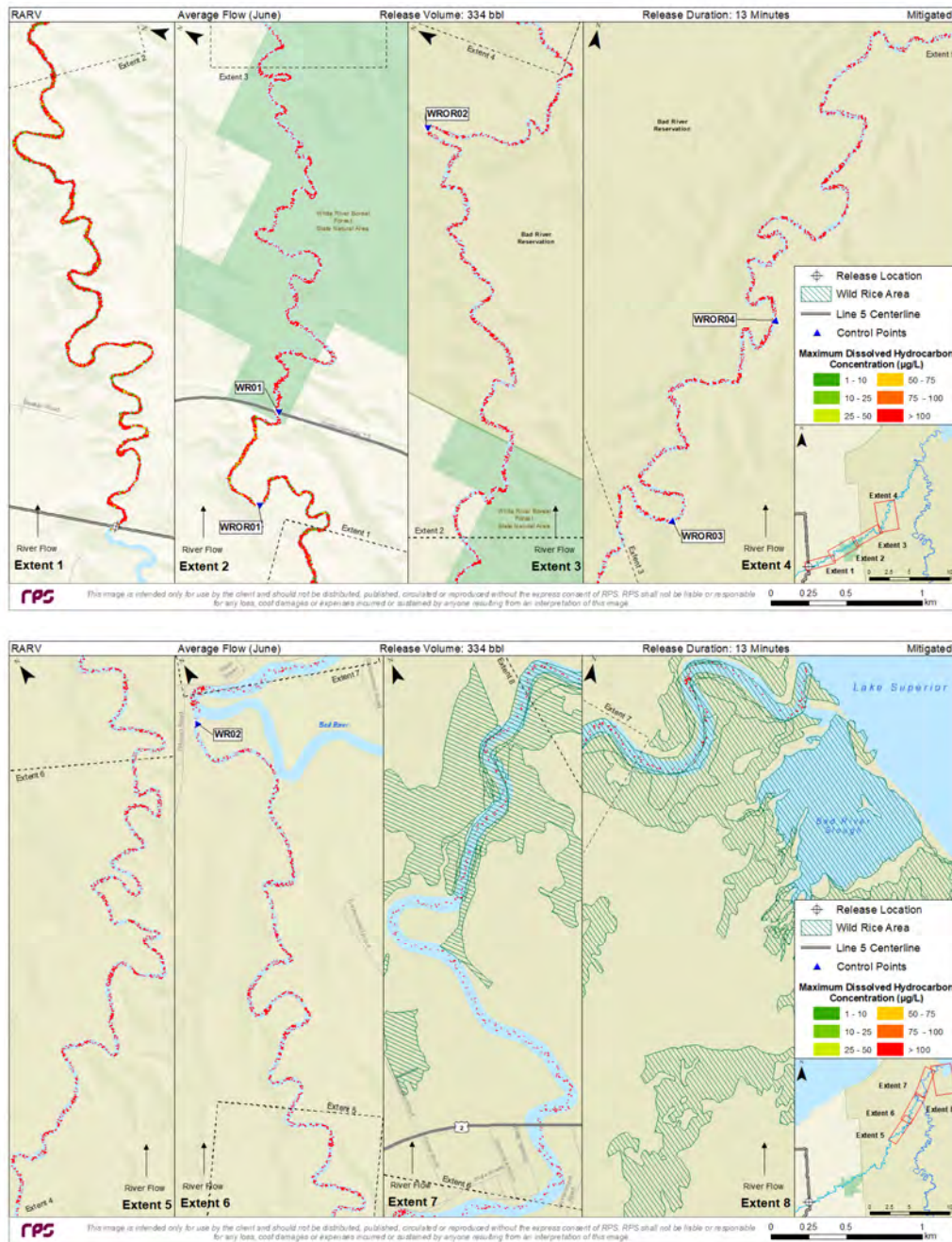
Figure 4-106. Composite of maximum total dissolved hydrocarbon concentration for the mitigated RARV scenario in average river flow conditions modeled in June at the White River channel location. This represents the maximum in-water contamination that was predicted for each location.
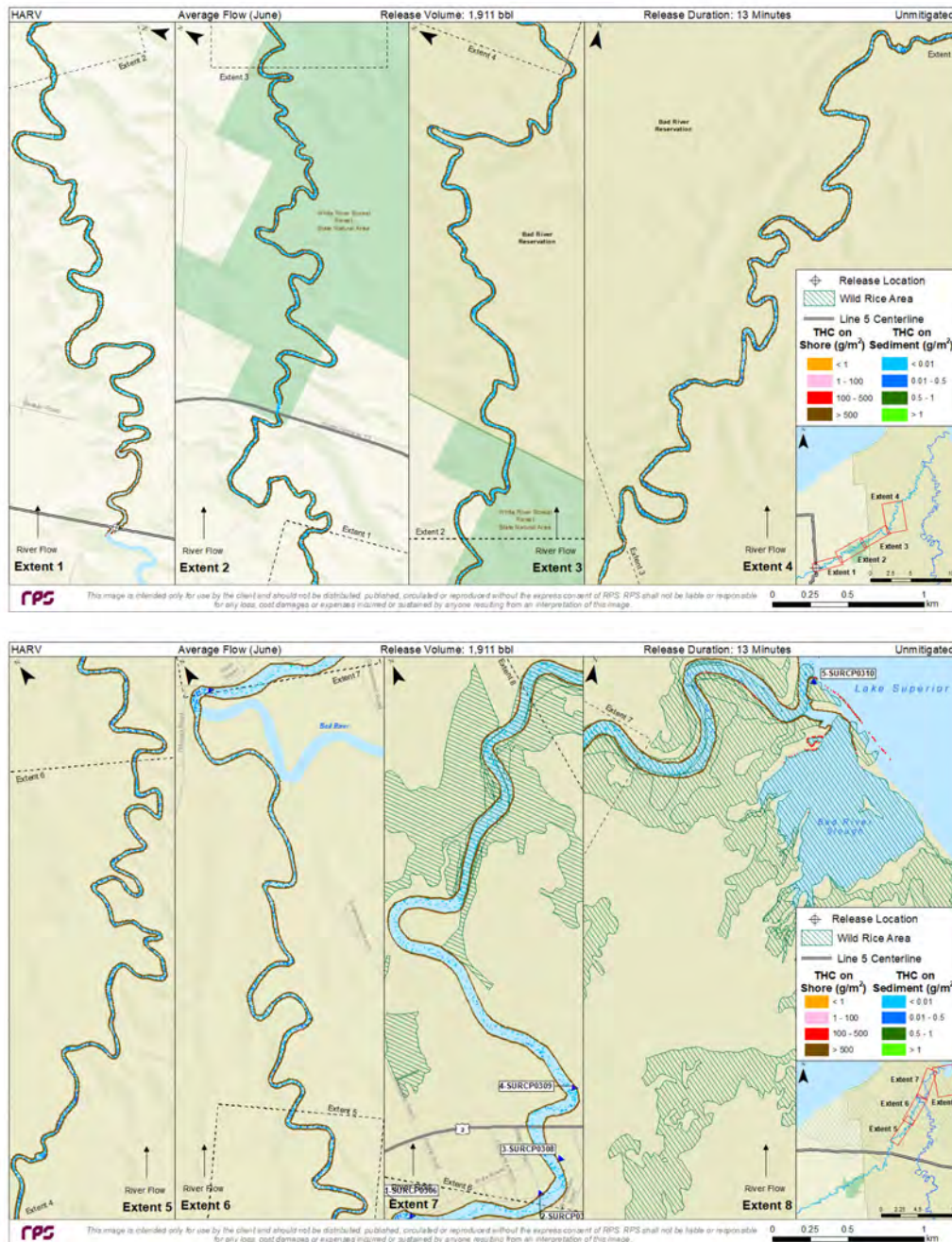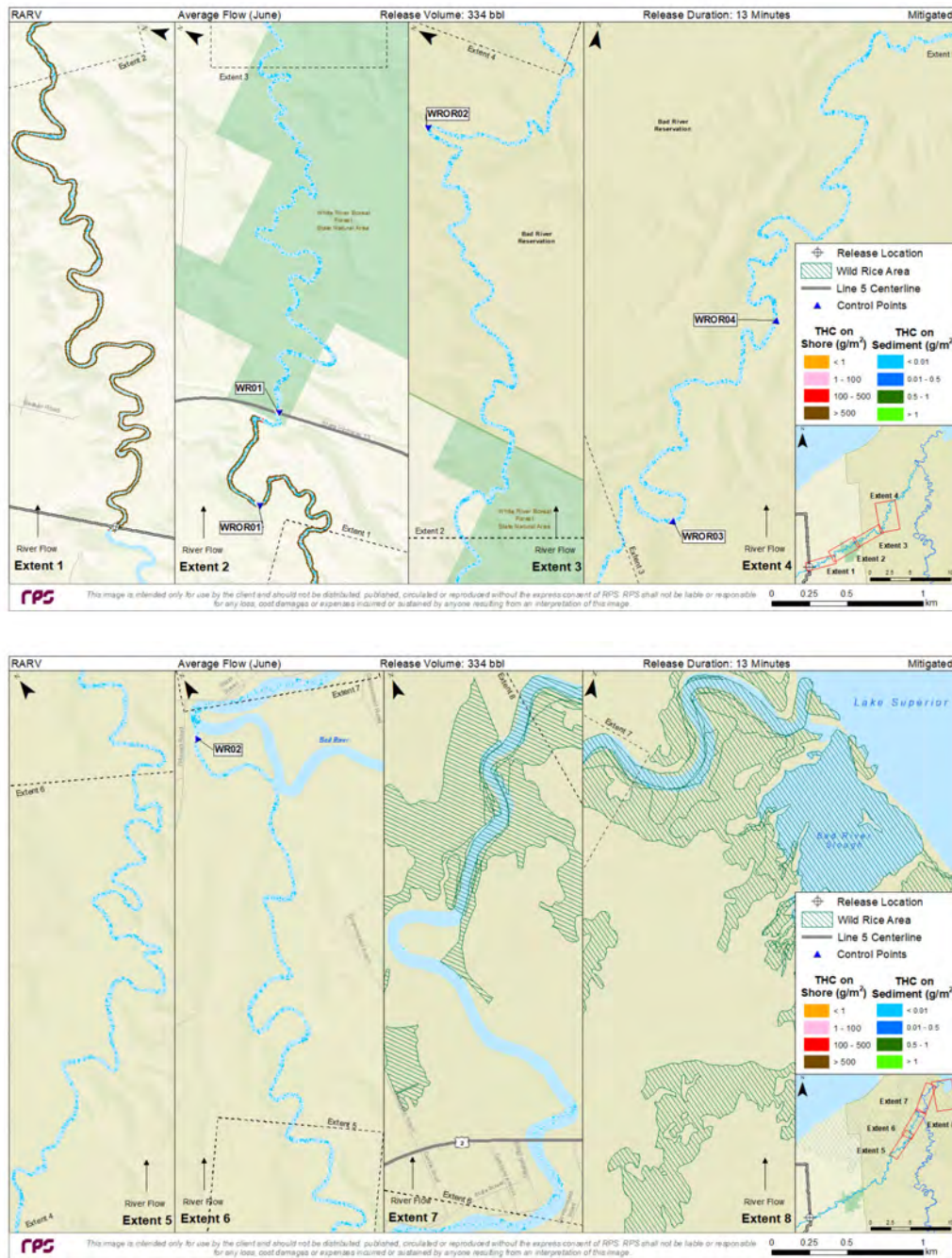
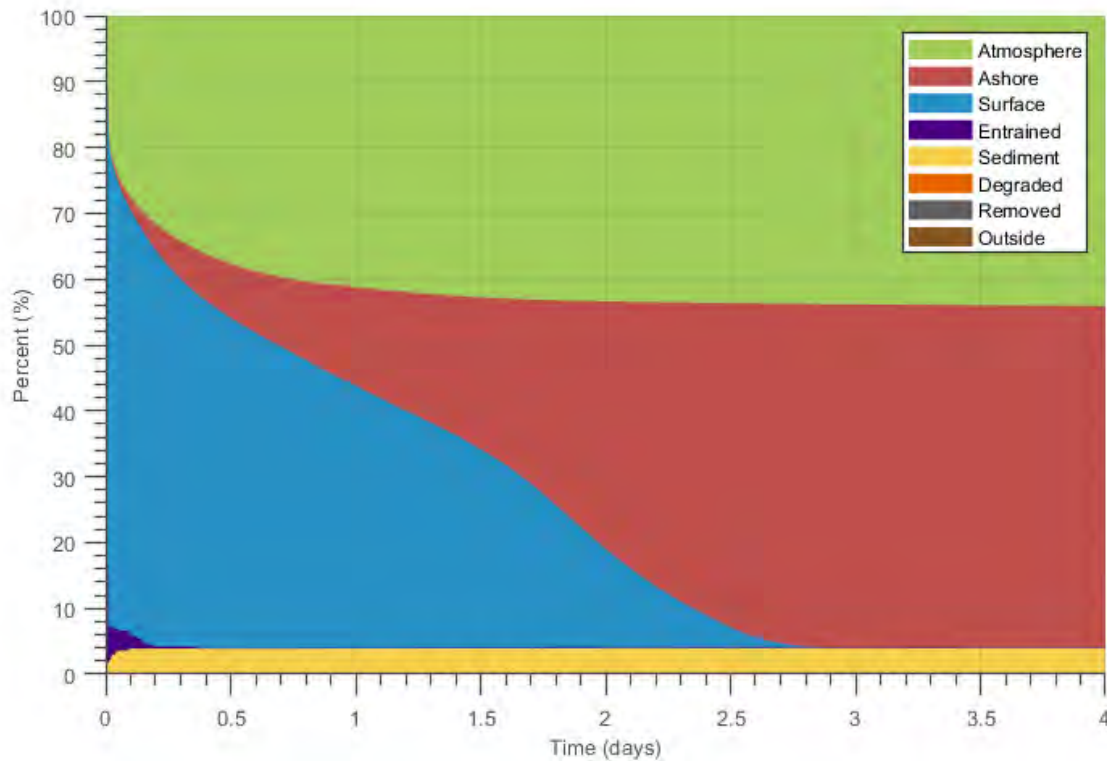**Figure 4-107. Maximum total hydrocarbon mass on the shore and on sediments after 4 days for the mitigated RARV scenario in average river flow conditions modeled in June at the White River channel location.**

4.2 Effects Modeling Results and Discussion

The SIMAP trajectory and fate modeling results were used to conduct a biological effects assessment. The assessment estimated the potential short-term (i.e., acute) exposure of biota to floating oil and subsurface oil contamination (in-water and on sediments) and predicted the resulting percent mortality. Values were derived based on the calculated river area affected within each grid cell based upon the concentration and duration of exposure, relative to the sensitivity being assessed. The results predicted from the biological effects assessment assumed that organisms were present within each grid cell.[2]

Acute mortality was evaluated for generic behavior groups of both pelagic and demersal species, benthic and planktonic organisms, and other avian, wildlife, and mammalian receptors. Therefore, while species-specific effects were not simulated, broad behavior groups were assessed and predicted effects would be applicable to all species of that behavior group if they were present. Local examples of species that would fall under the assessed groups include: dabbling waterfowl (e.g., Canada geese), wetland wildlife (e.g., great blue heron), terrestrial wildlife (e.g., black bear), fur-bearing mammals (e.g., beavers and muskrat), raptors (e.g., bald eagle), demersal fish (e.g., walleye), small pelagic fish/inverts (e.g., small mouth bass), large pelagic fish (e.g., northern pike), benthic - in sediments (e.g., worms), demersal - stationary (clams/mussels), and planktonic (e.g., phytoplankton and ichthyoplankton).

4.2.1 Guidance for Interpreting Results

The results of the biological exposure model were presented as the "Equivalent Area (in km^2) of 100-percent mortality" (EA-100) by organism behavior group. Estimates were separately calculated for the surface, shoreline, and water column. Exposure to oil often results in less than 100-percent mortality, and the percent mortality often varies by area. Therefore, to enable comparison between the overall effects among release scenarios, Equivalent Areas of 100-percent predicted mortality were estimated. For example, the EA-100 for fur-bearing mammals would be the same (1 km^2) for a release that resulted in 100-percent mortality over 1 km^2, 1-percent mortality over 100 km^2, or 20-percent mortality over 5 km^2.

The results of the biological exposure model were also presented as the cumulative percentage of the modeled habitat that was predicted to experience 100% mortality. Returning to the example above, if the fur-bearing mammals had a total habitat of 25 km^2, then the scenarios would result in cumulatively 4% (1 km^2 / 25 km^2) of the habitat experiencing 100% mortality.

Acute toxicity for the water surface was calculated based on the area swept by surface oil over a 10 μm threshold thickness for acute toxic effects. Acute toxicity for the shoreline was calculated based on the length of shoreline oiled over a 100 μm threshold thickness. Biota potentially affected by surface and shoreline oiling include waterfowl, aerial and diving birds, wetland and terrestrial wildlife, and fur-bearing marine mammals.

---

[2] In each grid cell, acute toxicity to aquatic biota in water column (for pelagic organisms) and demersal (bottom 1 m or 3.3 ft of the water immediately above the sediments) habitats were evaluated by tracking exposure for these different behavior groups. In rivers, such as this, where water depths would be less than 1 m (3.3 ft), the affected areas for water column and demersal biota were equal.

Acute toxicity for in-water effects was based upon sensitivities of 5 µg/L for sensitive species and 50 µg/L for average-sensitivity species. All organisms were assumed to have either a high (5 µg/L) or average (50 µg/L) sensitivity threshold, which was protective of 97.5% and 50% of all species, respectively (Section 2.1.6). Therefore, the sensitive species results bound the conservative upper-end of predicted in-water effects (i.e., worst-case), while the average sensitivity species results provide a more realistic assessment of likely effects. Biota potentially affected by water column toxicity included bottom-dwelling fish and invertebrates, swimming fish and invertebrates, large swimming fish, benthic organisms residing within the bottom sediments, and plankton that drift with the currents. Examples of sensitive organisms include fish eggs, larvae, and fry, while average sensitivity organisms include adult catfish, sunfish, and walleye. Note that the equivalent areas of predicted mortality above the stated thresholds would only occur if the organisms were present in the areas affected by spilled oil, aligning in both space and time. A full description of the acute biological effects modeling, including selection of thresholds of concern and validation, is provided in Section 2.1.6.

Note that the maps in this report depict instantaneous maximum concentrations. Therefore, areas depicting 5 µg/L do *not* correlate with 50% predicted mortality for sensitive species, because the exposure duration would need to be sufficiently long (days) for these predicted mortality rates to occur. For the short durations of exposure (i.e., minutes to hours) that were predicted in this modeling, instantaneous concentrations would need to be much higher than the identified threshold (LC_{50}) to result in acute mortality.

In order to calculate the percentages of the habitats experiencing 100% mortality, it was important to understand how the length and area of habitat changed under different river flow conditions. The extent of the model domain evaluated in the Bad River (including the Bad River Slough) was approximately 14.24 km^2 with a total shoreline length of approximately 274 km (170 mi.). Under high and average river flow conditions, 47 km (29 mi.) and 6 km (3.7 mi.) of this shoreline was classified as vegetated, respectively. During low river flow, the model domain was assumed to be covered in snow and ice, thus 100% of the shoreline (274 km) was classified as ice-edge (Table 4-7 and able 4-8). The extent of the model domain evaluated in the White River (including the subsequent downstream Bad River and Bad River Slough) was approximately 5.9 km^2 with a total shoreline length of approximately 138 km (86 mi.). Under high and average river flow conditions, 81 km (50 mi.) and 11 km (6.8 mi.) of this shoreline was classified as vegetated, respectively. Although a portion of the discharged oil had the potential to enter Lake Superior (specifically for the unmitigated, larger [FBR and HARV] releases under average river flow conditions), biological effects were not assessed in areas within the Lake. The unmitigated scenarios were modeled to illustrate baseline conditions and determine the maximum extents of oil that could physically occur, and therefore were not considered realistic scenarios for potential effects within Lake Superior (i.e., where no response was conducted within the rivers or Lake Superior for the full 4-day model duration).

Table 4-7. Length (white) and proportion (grey) of different shoreline habitats (as percent of total shoreline length within the habitat grid of each model domain) for the seasons modeled in the Bad River.

Seasonal Condition	Amount of Shoreline Types	Bad River - Shoreline Types by Seasonal Condition									
		Rocky Shore	Gravel Beach	Sand / Mud Beach	Mudflat	Wetland	Grass Banks	Forests	Ice Edge	Artificial / Manmade	Total
High River Flow	Total Length (km)	<1	3	72	152	47	0	0	0	0	274
	Total Length (mi)	<1	2	45	94	29	0	0	0	0	170
	Percent of Shoreline by Habitat Type	<1	1%	26%	55%	17%	0%	0%	0%	0%	100%
Average River Flow	Total Length (km)	<1	3	89	175	6	0	0	0	0	274
	Total Length (mi)	<1	2	55	109	4	0	0	0	0	170
	Percent of Shoreline by Habitat Type	<1	1%	32%	64%	2%	0%	0%	0%	0%	99%
Low River Flow	Total Length (km)	0	0	0	0	0	0	0	274	0	274
	Total Length (mi)	0	0	0	0	0	0	0	170	0	170
	Percent of Shoreline by Habitat Type	0	0%	0%	0%	0%	0%	0%	100%	0%	100%

Table 4-8. Length (white) and proportion (grey) of different shoreline habitats (as percent of total shoreline length within the habitat grid of each model domain) for the seasons modeled in the White River.

Seasonal Condition	Amount of Shoreline Types	White River - Shoreline Types by Seasonal Condition									
		Rocky Shore	Gravel Beach	Sand / Mud Beach	Mudflat	Wetland	Grass Banks	Forests	Ice Edge	Artificial / Manmade	Total
High River Flow	Total Length (km)	3	0	53	1	81	0	0	0	0	138
	Total Length (mi)	2	0	33	0	50	0	0	0	0	86
	Percent of Shoreline by Habitat Type	0	0%	39%	1%	59%	0%	0%	0%	0%	100%
Average River Flow	Total Length (km)	3	0	117	7	11	0	0	0	0	138
	Total Length (mi)	2	0	73	4	7	0	0	0	0	86
	Percent of Shoreline by Habitat Type	0	0%	85%	5%	8%	0%	0%	0%	0%	100%
Low River Flow	Total Length (km)	0	0	0	0	0	0	0	138	0	138
	Total Length (mi)	0	0	0	0	0	0	0	86	0	86
	Percent of Shoreline by Habitat Type	0%	0%	0%	0%	0%	0%	0%	100%	0%	100%

4.2.2 Results

4.2.2.1 Surface Effects

Potential effects on wildlife were presented as the EA-100 (in km^2) of the river that was covered by surface oil above the thickness threshold for acute effects (10 µm) at any time during the FBR, HARV, and RARV releases in the Bad River (Table 4-9) and White River (Table 4-10). The percent habitat mortality was also presented, which represents the fraction of the total habitat area occupied by each behavior group that was predicted to be affected for each release case. In general, the larger FBR release cases were predicted to result in the largest surface areas (and percentages of each habitat) of acute mortality, followed by comparatively less extensive effects for HARV releases. The RARV releases were predicted to have the smallest areas of potential effects. This decreasing progression was the result of highest levels of contamination (i.e., concentration or thickness of oil) that were present for longer periods of time (i.e., durations) for the largest releases, which resulted in greatest exposure and potential for effects. Because the predicted effects are dependent on the duration and exposure to contaminants, emergency response mitigated cases (which contain and collect oil) have comparatively smaller areas of effects, when compared to unmitigated cases.

The largest surface effects were predicted for fur-bearing mammals and dabbling waterfowl. Most of these effects were predicted to occur upstream, closer to the release locations, where the surface oil slicks were thickest and more continuous. The EA-100s and percentages of habitats affected were predominantly influenced by the volume of oil released, with the largest release volumes (FBR) predicted to result in the largest potential for effects. Smaller releases (HARV followed by RARV) generally had the lowest predicted surface effects. Secondarily, surface effects were influenced by river flow conditions at the time of the release. Although higher river flow rates would move oil faster and tend to increase the potential coverage for surface effects, the duration of exposure at any given location was shorter and the greater holding capacity of vegetated shorelines in high river flow, at bank full conditions, was predicted to result in more oil stranding on upstream shorelines. Consequently, surface oil exposures were reduced for those scenarios (especially in the White River), countering some of the influence of faster downstream transport. Presenting the percent of habitat experiencing 100% mortality highlights the importance of scaling predicted areas based upon the changing areas/volumes within the receiving environment, as well as the transport and duration of exposure. Finally, response mitigation had the strongest influence on the potential for surface effects for average river flow conditions, but less so for high flow conditions, particularly in the White River, due to these scenarios having lower surface effects overall (due to the vegetated banks upstream of MCPs retaining more oil), even without mitigation.

The conservative assumptions underlying the models resulted in the largest predictions of acute mortality occurring over as much as one quarter of the modeled portion of the Bad River and two thirds of the White River under average river flow conditions, due to the large release volumes (FBR and HARV), the small size of the rivers, the lower water levels which maximize surface oil (due to less shoreline holding capacity), and the longer duration of exposure. High river flow conditions were predicted to result in approximately 4-20% EA-100 for the Bad River and 5-12% for the White River, predominantly due to the shorter duration of exposure for both rivers, and less oil being present in the White River due to the vegetated banks holding more oil. The largest effects were predicted for fur-bearing mammals and waterfowl, which spend large amounts of time moving through surface waters as they forage, which would expose them to surface slicks. The largest EA-100s were predicted for waterfowl in the FBR, average river flow scenarios, at nearly 4 km^2 of the modeled habitat area in each river. The largest EA-100s for fur-bearing mammals were also predicted in the average

flow, FBR scenarios (~3 km^2). Equivalent areas and percent habitat mortalities were much lower for both wetland wildlife and terrestrial wildlife, which had behaviors that limited their exposure to contaminants. In particular, terrestrial wildlife was predicted to have percent habitat mortalities less than 0.01 km^2 (or 1%). Wetland wildlife effects were consistently less than 0.01 km^2 as well, although those areas represented ranges up to 61% of the habitat areas, which were proportionally much smaller than the total habitat area within each river (Table 4-9, Table 4-10). No surface effects were predicted for releases under low river/ice flow conditions because oil was trapped below the surface of the ice.

The application of emergency response mitigation efforts resulted in reductions in the predicted surface effects on wildlife ranging from approximately 40-90% lower in average flow scenarios and 10-50% lower in high flow scenarios (Table 4-9, Table 4-10). Most of these reductions were predicted to occur in areas downstream of the MCPs, where mitigation activities either prevented surface slicks from transporting entirely or significantly reduced their thickness (e.g., leaving sheens less than 1/1,000[th] the thickness of heavy black oil). As mentioned previously, the effects reductions were smaller for the high flow scenarios because more heavy black oil was predicted to strand on upstream, vegetated banks under bank full conditions, rather than transporting farther downstream, and because the duration of exposure was shorter due to the faster river velocities. All mitigated HARV and RARV scenarios had low predictions of acute mortality, over at most 6% of the model domain, while the FBR scenarios had predicted mortalities covering up to 17% of the model domain.

Table 4-9. River area (km^2) predicted to be affected by acute toxicity for the Bad River FBR, HARV, and RARV release scenarios, expressed as EA-100 (bold) and percentage of wildlife habitat experiencing 100% mortality *(italics)*.

Behavior Group	Bad River - Equivalent Area (km^2) of up to 100% Predicted Mortality													
Surface Effects (km^2)	FBR (9,874 bbl) High Flow	FBR (9,874 bbl) Avg Flow	FBR (9,874 bbl) Low Flow	HARV (1,911 bbl) High Flow	HARV (1,911 bbl) Avg Flow	HARV (1,911 bbl) Low Flow	RARV (334 bbl) Avg Flow	Mit. FBR (9,874 bbl) High Flow	Mit. FBR (9,874 bbl) Avg Flow	Mit. FBR (9,874 bbl) Low Flow	Mit. HARV (1,911 bbl) High Flow	Mit. HARV (1,911 bbl) Avg Flow	Mit. HARV (1,911 bbl) Low Flow	Mit. RARV (334 bbl) Avg Flow
Sensitivity Threshold	10 µm													
Dabbling waterfowl*	**3.0** *21%*	**3.8** *27%*	N/A	**1.0** *7%*	**3.3** *23%*	N/A	**2.2** *16%*	**1.7** *12%*	**2.4** *17%*	N/A	**0.5** *4%*	**0.3** *2%*	N/A	**0.2** *1%*
Wetland wildlife±	**<0.01** *15%*	**<0.01** *<1%*	N/A	**<0.01** *2%*	**<0.01** *<1%*	N/A	**<0.01** *<1%*	**<0.01** *<1%*	**<0.01** *<1%*	N/A	**<0.01** *<1%*	**<0.01** *<1%*	N/A	**<0.01** *<1%*
Terrestrial wildlife¥	**<0.01** *<1%*	**<0.01** *<1%*	N/A	**<0.01** *<1%*	**<0.01** *<1%*	N/A	**<0.01** *<1%*	**<0.01** *<1%*	**<0.01** *<1%*	N/A	**<0.01** *<1%*	**<0.01** *<1%*	N/A	**<0.01** *<1%*
Fur-bearing mammals€	**2.8** *19%*	**3.0** *21%*	N/A	**0.7** *5%*	**2.5** *18*	N/A	**1.7** *12%*	**1.3** *9%*	**1.8** *13%*	N/A	**0.4** *3%*	**0.2** *2%*	N/A	**0.1** *1%*

Percentage of habitat experiencing 100% mortality was calculated by dividing the EA-100 by:

* the habitat in which dabbling waterfowl are modeled as occupying (the entire model domain);

± the habitat in which wetland wildlife are modeled as occupying (all wetlands and mudflats);

¥ the habitat in which terrestrial wildlife are modeled as occupying (all wetlands and shoreline areas); and

€ the habitat in which fur-bearing mammals are modeled as occupying (the entire model domain).

Table 4-10. River area (km²) predicted to be affected by acute toxicity for the White River FBR, HARV, and RARV release scenarios, expressed as EA-100 (bold) and percentage of wildlife habitat experiencing 100% mortality *(italics)*.

Behavior Group	White River - Equivalent Area (km²) of up to 100% Predicted Mortality													
Surface Effects (km²)	FBR (8,517 bbl) High Flow	FBR (8,517 bbl) Avg Flow	FBR (8,517 bbl) Low Flow	HARV (1,911 bbl) High Flow	HARV (1,911 bbl) Avg Flow	HARV (1,911 bbl) Low Flow	RARV (334 bbl) Avg Flow	Mit. FBR (8,517 bbl) High Flow	Mit. FBR (8,517 bbl) Avg Flow	Mit. FBR (8,517 bbl) Low Flow	Mit. HARV (1,911 bbl) High Flow	Mit. HARV (1,911 bbl) Avg Flow	Mit. HARV (1,911 bbl) Low Flow	Mit. RARV (334 bbl) Avg Flow
Sensitivity Threshold	10 µm													
Dabbling waterfowl*	**0.7** *12%*	**3.9** *67%*	N/A	**0.3** *6%*	**3.0** *52%*	N/A	**0.9** *15%*	**0.6** *10%*	**0.5** *9%*	N/A	**0.3** *5%*	**0.2** *4%*	N/A	**0.2** *4%*
Wetland wildlife±	**<0.01** *37%*	**<0.01** *61%*	N/A	**<0.01** *5%*	**<0.01** *59%*	N/A	**<0.01** *8%*	**<0.01** *7%*	**<0.01** *<1%*	N/A	**<0.01** *6%*	**<0.01** *<1%*	N/A	**<0.01** *<1%*
Terrestrial wildlife¥	**<0.01** *<1%*	**<0.01** *<1%*	N/A	**<0.01** *<1%*	**<0.01** *<1%*	N/A	**<0.01** *<1%*	**<0.01** *<1%*	**<0.01** *<1%*	N/A	**<0.01** *<1%*	**<0.01** *<1%*	N/A	**<0.01** *<1%*
Fur-bearing mammals€	**0.5** *9%*	**3.1** *53%*	N/A	**0.3** *4%*	**2.4** *41%*	N/A	**0.7** *12%*	**0.4** *8%*	**0.4** *7%*	N/A	**0.2** *4%*	**0.2** *3%*	N/A	**0.2** *3%*

Percentage of habitat experiencing 100% mortality was calculated by dividing the EA-100 by:

* the habitat in which dabbling waterfowl are modeled as occupying (the entire model domain);

± the habitat in which wetland wildlife are modeled as occupying (all wetlands and mudflats);

¥ the habitat in which terrestrial wildlife are modeled as occupying (all wetlands and shoreline areas); and

€ the habitat in which fur-bearing mammals are modeled as occupying (the entire model domain

4.2.2.2 Shoreline Effects

Potential effects on vegetation were evaluated as the length of shoreline that was predicted to be oiled above a threshold for acute effects (Table 4-11, Table 4-12). Wetlands have large holding capacities for oil, which can result in acute effects to vegetation. The threshold of oiling that was investigated was a thickness greater than 100 μm, which was equivalent to approximately 100 mL of oil per m^2 (10.8 ft^2) of habitat. In scenarios other than low river flow wintertime conditions, with assumed ice cover and completely frozen banks, vegetation effects were predicted within wetland areas that were present and exposed at the river's edge to surface slicks (Table 4-7, Table 4-8). Under high river flow conditions, wetlands covered more than half the length of the White River and nearly 20% of the Bad River, whereas under average flow conditions, the exposed shorelines were predominantly (>90%) sand and mud.

Most shoreline effects were predicted to occur in vegetated areas, closer to the release locations, where the potentials for shoreline exposure were greatest due to surface oil slicks being thickest and more continuous. Shoreline effects were predominantly influenced by river flow conditions and the resulting shore type in contact with the water at the time of the release. Under high river flow bank full conditions, more vegetation was exposed to surface floating oil. Secondarily, shoreline effects were influenced by the volume of oil released, with the largest release volumes (FBR) predicted to result in the largest potential for effects. Smaller releases (HARV followed by RARV) generally had the lowest predicted shoreline effects. Larger river flow rates generally resulted in greater transport and potential for shoreline effects with larger percentages of wetland shorelines (i.e., high river flow conditions) and longer lengths affected. However, in the White River, under average flow conditions, shoreline effects were relatively high (and actually larger than high river flow conditions for the HARV release), due to the exposed wetland areas located upstream of the confluence with the Bad River (Figure 3-2). This allowed for oil to still reach most wetlands in the completely unmitigated scenarios, whereas a smaller, upstream portion of the wetlands was affected during high flow conditions. Finally, response mitigation had a notable influence on the potential for shoreline effects, especially for scenarios where containment and collection efforts removed oil prior to reaching downstream wetlands.

It is important to remember that mortality would only occur if the organisms happened to be present in the areas predicted to be affected by spilled oil at the time of the release. The maximum EA-100 length of vegetated shoreline from any scenario predicted to be affected was 15 km (9.3 mi., or approximately 18% of total vegetated shoreline) for the FBR release in the White River under high river flow conditions (Table 4-7,Table 4-8). However, during average river flow conditions in the White River, model predicted shoreline oiling had the potential to result in mortality over the majority (98-100%) of the vegetated shoreline, because nearly all wetland habitats were in the upper portion of the river, where it was exposed to heavy black oil before slicks thinned to sheens. In the Bad River, the exposed wetlands were located mostly downstream in average river flow conditions (downstream of Highway 2), and surface oil was generally in sheen form before reaching them. No shoreline effects were predicted for low river flow conditions due to the ice layer preventing shoreline adhesion, as banks were assumed to be completely frozen over (i.e., ice).

For response mitigated scenarios under average river flow conditions, there was near complete reduction (~100%) in predicted effects to wetland vegetation (where any initially occurred without mitigation), because a large portion of the surface slicks were contained and collected prior to reaching the predominantly wetland shorelines at downstream Bad River and White River locations as well as within the Bad River Slough (Table 4-11, Table 4-12). As a result, predicted effects for mitigated, average river flow scenarios were below 0.1 km (or <1%), regardless of release volume. Under high river flow conditions, mitigation significantly reduced predicted effects for the FBR release scenarios (23-83% lower than completely unmitigated scenarios), but had

almost no effect on the HARV release scenarios in the White River. For these White River scenarios, the predicted areas of acute mortality covered approximately 3-8% of the model domain, primarily at wetland locations upstream of activated MCPs.

Table 4-11. Shoreline length (km) (bold) and percentage of shoreline habitat experiencing 100% mortality (*italics*) in the Bad River.

Shoreline Type	Bad River -Shoreline Length (km) up to 100% Predicted Mortality													
Shoreline Effects (vegetation) (km)	FBR (9,874 bbl) High Flow	FBR (9,874 bbl) Avg Flow	FBR (9,874 bbl) Low Flow	HARV (1,911 bbl) High Flow	HARV (1,911 bbl) Avg Flow	HARV (1,911 bbl) Low Flow	RARV (334 bbl) Avg Flow	Mit. FBR (9,874 bbl) High Flow	Mit. FBR (9,874 bbl) Avg Flow	Mit. FBR (9,874 bbl) Low Flow	Mit. HARV (1,911 bbl) High Flow	Mit. HARV (1,911 bbl) Avg Flow	Mit. HARV (1,911 bbl) Low Flow	Mit. RARV (334 bbl) Avg Flow
Sensitivity Threshold	100 µm													
Wetlands	**7.8** *17%*	**<0.1** *<1%*	N/A	**3.6** *8%*	**<0.1** *<1%*	N/A	**<0.1** *<1%*	**6.0** *13%*	**<0.1** *<1%*	N/A	**3.6** *8%*	**<0.1** *<1%*	N/A	**<0.1** *<1%*

Table 4-12. Shoreline length (km) (bold) and percentage of shoreline habitat experiencing 100% mortality (*italics*) in the White River.

Shoreline Type	White River - Shoreline Length (km) up to 100% Predicted Mortality													
Shoreline Effects (vegetation) (km)	FBR (8,517 bbl) High Flow	FBR (8,517 bbl) Avg Flow	FBR (8,517 bbl) Low Flow	HARV (1,911 bbl) High Flow	HARV (1,911 bbl) Avg Flow	HARV (1,911 bbl) Low Flow	RARV (334 bbl) Avg Flow	Mit. FBR (8,517 bbl) High Flow	Mit. FBR (8,517 bbl) Avg Flow	Mit. FBR (8,517 bbl) Low Flow	Mit. HARV (1,911 bbl) High Flow	Mit. HARV (1,911 bbl) Avg Flow	Mit. HARV (1,911 bbl) Low Flow	Mit. RARV (334 bbl) Avg Flow
Sensitivity Threshold	100 µm													
Wetlands	**15.0** *18%*	**11.2** *100%*	N/A	**2.3** *3%*	**10.9** *98%*	N/A	**0.5** *4%*	**2.6** *2%*	**<0.1** *<1%*	N/A	**2.3** *3%*	**<0.1** *<1%*	N/A	**<0.1** *<1%*

4.2.2.3 In-Water Effects

Potential effects on in-water species were presented as the EA-100 (in km^2 and acres) based upon two sensitivity levels that were used to bound the range of acute mortality within the water column or in the sediment that may occur following a release. Values were derived based on the calculated river area affected (by habitat grid cell). EA-100s were evaluated for various in-water species, organized by behavior group, for both sensitive and average-sensitivity (Table 4-13; Table 4-14). One should take care when interpreting in-water effects results. They should be read as: "Assuming that all aquatic organisms within the river are sensitive species, the EA-100 would be as high as X km^2 (or acres). However, considering that 50 µg/L is the average sensitivity for the hundreds of species that were considered in this effects modeling, the predicted effects would be closer to Y km^2 (or acres)."

Pelagic (swimming) and demersal (bottom-dwelling) organisms were predicted to have the largest effects, followed by planktonic (drifting) organisms (e.g., early-stage amphibians). As would be expected, sensitive species were predicted to have higher areas of potential effects, when compared to average sensitivity species.

In-water effects were primarily influenced by spill volume and river flow rate. Potential effects to sensitive species were greatest for average river flow conditions, followed by high river flow or low river flow, depending on the oil release volume. This progression was the result of a balance between levels of contamination (i.e., concentrations of hydrocarbons in the water column), downstream transport, and the duration of exposure. Average river flow conditions maximized predicted effects as the downstream transport of oil was predicted to extend along the rivers and river flow rates were slow enough to increase the duration of exposure. For low river flow conditions (i.e., slow velocity), with complete ice coverage, evaporation was prevented, and dissolution was therefore maximized. This resulted in higher dissolved concentrations and longer durations of exposure. However, low river flow conditions had less transport, resulting in lower effects than the average river flow condition scenarios. Under high river flow conditions, because the velocity of the water was increased, the duration of exposure was lower and the volume of water was greater (i.e., dilution), which resulted in reduced mortality. In-water effects were also notably influenced by volume of oil released, with larger release volumes predicted to result in larger potential for effects. Finally, response efforts did reduce the potential for effects slightly in some scenarios, by removing oil and preventing further dissolution. However mitigation had the smallest influence on the potential for in-water effects because the soluble portion would already be dissolved in the water column and would not be removed by response efforts.

Overall, the average river flow scenarios resulted in the largest mortality, with the greatest effects predicted in the FBR scenarios where EA-100s covered approximately 0.5 km^2 (or 120 acres) for sensitive species ranging down to approximately 0.06 km^2 (or 15 acres) for average sensitivity species (

Table 4-13, Table 4-14). Under high river flow conditions, the durations of exposure were reduced and dilution was greatest due to greater volumes of water moving through the river. As seen by comparison of unmitigated and mitigated HARV and FBR scenarios, the application of mitigation activities did not appreciably reduce in-water effects, unlike the surface and shoreline effects. This is because in-water effects are predominantly driven by dissolved hydrocarbons within the water column. This dissolution occurred quickly and near the release point, prior to oil reaching the first CP. Therefore, the DHC moving downstream in the water column were not able to be removed by emergency response equipment that focused on removing surface oil.

Table 4-13. The river area predicted to be affected by acute toxicity for the FBR, HARV, and RARV release scenarios in the Bad River, expressed as Equivalent Area of 100% mortality in km² (bold) or acres (italics).

In-Water Effects (km² or acres) Behavior Group	FBR (9,874 bbl) High Flow 5 µg/L	50 µg/L	FBR (9,874 bbl) Average Flow 5 µg/L	50 µg/L	FBR (9,874 bbl) Low Flow 5 µg/L	50 µg/L	HARV (1,911 bbl) High Flow 5 µg/L	50 µg/L	HARV (1,911 bbl) Average Flow 5 µg/L	50 µg/L	HARV (1,911 bbl) Low Flow 5 µg/L	50 µg/L	RARV (334 bbl) Avg Flow 5 µg/L	50 µg/L	Mit. FBR (9,874 bbl) High Flow 5 µg/L	50 µg/L	Mit. FBR (9,874 bbl) Avg Flow 5 µg/L	50 µg/L	Mit. FBR (9,874 bbl) Low Flow 5 µg/L	50 µg/L	Mit. HARV (1,911 bbl) High Flow 5 µg/L	50 µg/L	Mit. HARV (1,911 bbl) Avg Flow 5 µg/L	50 µg/L	Mit. HARV (1,911 bbl) Low Flow 5 µg/L	50 µg/L	Mit. RARV (334 bbl) Avg Flow 5 µg/L	50 µg/L
Pelagic fish (e.g., trout)	**0.290** *(71.6)*	**0.035** *(8.6)*	**0.485** *(119.8)*	**0.034** *(8.4)*	**0.060** *(14.8)*	**0.039** *(9.7)*	**0.045** *(11.0)*	**0.007** *(1.8)*	**0.281** *(69.4)*	**0.060** *(14.7)*	**0.045** *(11.1)*	**0.025** *(6.1)*	**0.066** *(16.2)*	**0.006** *(1.5)*	**0.290** *(71.6)*	**0.035** *(8.6)*	**0.365** *(90.1)*	**0.034** *(8.4)*	**0.060** *(14.8)*	**0.039** *(9.7)*	**<0.001** *(<0.2)*	**<0.001** *(<0.2)*	**0.281** *(69.4)*	**0.060** *(14.7)*	**0.045** *(11.1)*	**0.025** *(6.1)*	**0.066** *(16.4)*	**0.006** *(1.4)*
Demersal (e.g., crayfish, fish larvae in or at sediments)	**0.318** *(78.5)*	**0.038** *(9.4)*	**0.553** *(136.6)*	**0.042** *(10.3)*	**0.055** *(13.5)*	**0.038** *(9.3)*	**0.044** *(10.7)*	**0.005** *(1.1)*	**0.318** *(78.6)*	**0.070** *(17.3)*	**0.042** *(10.5)*	**0.023** *(5.8)*	**0.073** *(18.1)*	**0.005** *(1.1)*	**0.317** *(78.4)*	**0.038** *(9.4)*	**0.380** *(94.0)*	**0.042** *(10.3)*	**0.055** *(13.5)*	**0.038** *(9.3)*	**<0.001** *(<0.2)*	**<0.001** *(<0.2)*	**0.318** *(78.6)*	**0.070** *(17.3)*	**0.042** *(10.5)*	**0.023** *(5.8)*	**0.072** *(17.7)*	**0.004** *(1.1)*
Planktonic (drifting)	**0.113** *(28.0)*	**0.019** *(4.7)*	**0.116** *(28.6)*	**0.013** *(3.3)*	**0.057** *(14.1)*	**0.034** *(8.4)*	**0.024** *(5.9)*	**0.002** *(0.5)*	**0.107** *(26.4)*	**0.032** *(7.9)*	**0.038** *(9.4)*	**0.017** *(4.2)*	**0.020** *(4.9)*	**0.002** *(0.4)*	**0.113** *(28.0)*	**0.019** *(4.7)*	**0.172** *(42.6)*	**0.013** *(3.3)*	**0.057** *(14.1)*	**0.034** *(8.4)*	**<0.001** *(<0.2)*	**<0.001** *(<0.2)*	**0.107** *(26.4)*	**0.032** *(7.9)*	**0.038** *(9.4)*	**0.017** *(4.2)*	**0.020** *(4.8)*	**0.002** *(0.5)*

Table 4-14. The river area (km²) predicted to be affected by acute toxicity for the FBR, HARV, and RARV release scenarios in the White River, expressed as Equivalent Area of 100% mortality in km² (bold) or acres (italics).

In-Water Effects (km² or acres) Behavior Group	FBR (8,517 bbl) High Flow 5 µg/L	50 µg/L	FBR (8,517 bbl) Average Flow 5 µg/L	50 µg/L	FBR (8,517 bbl) Low Flow 5 µg/L	50 µg/L	HARV (1,911 bbl) High Flow 5 µg/L	50 µg/L	HARV (1,911 bbl) Average Flow 5 µg/L	50 µg/L	HARV (1,911 bbl) Low Flow 5 µg/L	50 µg/L	RARV (334 bbl) Avg Flow 5 µg/L	50 µg/L	Mit. FBR (9,874 bbl) High Flow 5 µg/L	50 µg/L	Mit. FBR (9,874 bbl) Avg Flow 5 µg/L	50 µg/L	Mit. FBR (9,874 bbl) Low Flow 5 µg/L	50 µg/L	Mit. HARV (1,911 bbl) High Flow 5 µg/L	50 µg/L	Mit. HARV (1,911 bbl) Avg Flow 5 µg/L	50 µg/L	Mit. HARV (1,911 bbl) Low Flow 5 µg/L	50 µg/L	Mit. RARV (334 bbl) Avg Flow 5 µg/L	50 µg/L
Pelagic fish (e.g., trout)	**0.158** *(39.1)*	**0.033** *(8.2)*	**0.450** *(111.2)*	**0.059** *(14.5)*	**0.081** *(20.1)*	**0.004** *(1.0)*	**0.036** *(9.0)*	**0.003** *(0.8)*	**0.171** *(42.3)*	**0.018** *(4.5)*	**0.059** *(14.5)*	**0.005** *(1.2)*	**0.044** *(10.8)*	**0.003** *(0.7)*	**0.058** *(14.4)*	**0.033** *(8.2)*	**0.471** *(116.3)*	**0.060** *(14.8)*	**0.081** *(20.1)*	**0.004** *(1.0)*	**0.036** *(9.0)*	**0.003** *(0.8)*	**0.080** *(19.7)*	**0.008** *(2.0)*	**0.059** *(14.5)*	**0.005** *(1.2)*	**0.010** *(2.5)*	**0.003** *(0.7)*
Demersal (e.g., crayfish, fish larvae in or at sediments)	**0.166** *(41.0)*	**0.036** *(8.8)*	**0.462** *(114.2)*	**0.062** *(15.3)*	**0.077** *(19.0)*	**0.004** *(1.0)*	**0.038** *(9.4)*	**0.004** *(0.9)*	**0.173** *(42.7)*	**0.018** *(4.5)*	**0.046** *(11.3)*	**0.003** *(0.8)*	**0.042** *(10.4)*	**0.003** *(0.6)*	**0.166** *(41.0)*	**0.036** *(8.8)*	**0.461** *(114.0)*	**0.063** *(15.4)*	**0.077** *(19.0)*	**0.004** *(1.0)*	**0.038** *(9.4)*	**0.004** *(0.9)*	**0.081** *(19.9)*	**0.006** *(1.4)*	**0.046** *(11.3)*	**0.003** *(0.8)*	**0.008** *(2.1)*	**0.002** *(0.6)*
Planktonic (drifting)	**0.052** *(12.8)*	**0.014** *(3.5)*	**0.102** *(25.1)*	**0.024** *(6.0)*	**0.029** *(7.2)*	**0.001** *(0.3)*	**0.043** *(10.6)*	**0.004** *(0.9)*	**0.071** *(17.4)*	**0.012** *(3.0)*	**0.023** *(5.7)*	**0.002** *(0.4)*	**0.014** *(3.4)*	**0.001** *(0.2)*	**0.052** *(12.8)*	**0.014** *(3.5)*	**0.092** *(22.8)*	**0.018** *(4.4)*	**0.029** *(7.2)*	**0.001** *(0.3)*	**0.043** *(10.6)*	**0.004** *(0.9)*	**0.005** *(1.3)*	**0.005** *(1.1)*	**0.023** *(5.7)*	**0.002** *(0.4)*	**0.005** *(1.2)*	**0.001** *(0.0)*

5   CONCLUSIONS

RPS' SIMAP trajectory, fate, and biological effects models were used to investigate the movement, behavior, and potential effects of a wide range of release scenarios in the Bad River and White River, at their crossings with the Proposed Route of the Line 5 Relocation Project. The scenarios considered included full-bore ruptures (FBR, ~8,500-9,900 bbl), historical accidental release volumes (HARV, ~2,000 bbl), and recent average release volumes (RARV, ~300 bbl). Although they are smaller than the FBR, even the HARV and RARV scenarios targeted conservatively large volume releases. Since 2010, Enbridge has transported approximately 25% of the crude oil produced in North America in its pipelines and recorded 122 total spills, of which 90% were less than 10 bbl, with both the mode and median of these release volumes being less than 1 bbl. Smaller releases, such as 10 bbl, were not modeled and would be expected to have minimal impacts on the environment. Releases were simulated under three different seasonal and corresponding river flow conditions, including wintertime conditions with 100% ice cover. Simulations at the Bad River and White River crossings were allowed to progress unmitigated, providing an illustrative baseline where no emergency response efforts were conducted over the full 4-day model duration (highly unlikely to occur in any real-world release). Each unmitigated scenario was also modeled with response mitigation.

The tiered modeling approach applied herein allowed for quantitative results to be calculated for a variety of metrics related to trajectory, fate, and potential effects. Results were mapped for each release scenario and comparisons were made between them. This Technical Appendix first provides a summary of the trajectory and fate of oil for each of the scenarios and then provides a discussion of the potential biological effects. Discussions are focused on the influences that variable environmental conditions, release volumes, and mitigation efforts have on the results for each simulated release. The findings in this report can be used to identify regions and resources that may be at risk, should there be a large volume release of oil, as well as the estimated magnitude of potential effects. In addition, these results may be used to bound the amount of time that may be available for response mitigation measures to be implemented to protect resources and limit the magnitude and extent of oil contamination.

While it is understood that the identified scenarios are in no way intended to predict a specific future event, the results presented in this document demonstrate a range of potential trajectory and fate, as well as the predicted effects that may result from large volume releases of oil based upon a set of geographic criteria, environmental variability, and biological sensitivities. In the unlikely event of a pipeline rupture or a valve loss resulting in a release of oil in the magnitude modeled here (FBR, HARV, and RARV releases of Bakken crude oil), the potential credible worst case resulting effects are described. The geographic range (i.e., extent) and magnitude of the adverse effects depends on the environmental conditions at the time of the release, the release parameters themselves, and the presence of sensitive receptors. Therefore, the predicted effects identified here are by no means the most expected outcome, as they are highly conservative estimates that tended to err on the side of predicting greater magnitudes and extents of potential effects.

1. Trajectory and Fate - In general, Bakken is a light crude oil with low density and viscosity and a high content of soluble and volatile hydrocarbons. Due to these characteristics, under ice-free conditions, 34-42% of the oil was predicted to evaporate quickly (within ~1 day). Evaporation continued in the simulations up to 40-50% where it was predicted to remain on the surface being transported downstream over an additional three days. In the unmitigated FBR releases under average river flow conditions (for both rivers), which are unlikely and extreme worst-case scenarios, the majority of oil was predicted to form surface slicks that would move downstream, stranding on shorelines and evaporating, with the potential for 35-39% of the release to remain on the surface or enter Lake

Superior at the end of the 4-day simulation. This was not the case for the unmitigated high and low river flow scenarios or any of the mitigated scenarios, where less than 0.1% surface oil was predicted to reach Lake Superior due to stranding on upstream vegetation (high river flow), remaining trapped under the ice surface closer to the release location (low river flow, ice-covered conditions), and the containment and collection of oil by successful emergency response mitigation measures that would be employed. Almost all of the HARV and RARV scenarios were of sufficiently small volume that surface oil was not predicted to reach Lake Superior under any condition, mitigated or even unmitigated. Only the average river flow HARV releases were predicted to have patchy and discontinuous sheens extending north of Highway 2. Of note, surface oil slicks are the primary target of some of the most effective mitigation efforts aimed at containing and collecting released oil (e.g., booms and skimmers). Oil stranding on shoreline would be addressed by Enbridge's SCAT program (Enbridge, 2016). Some limited sediment oiling was predicted in each simulation, but the sedimented oil was patchy and discontinuous, with predicted deposition typically around 0.01 g/m^2 and some localized and patchy areas that reached 0.5 g/m^2 deposition in more quiescent waters.

Seasonal river flow conditions were the dominant factor in downstream transport (e.g., timing) of surface oil in each river, with oil typically being transported fastest and farthest under high river flow conditions, followed by average, and then low river flow conditions. An overbank, flooding scenario was not modeled in this Technical Appendix, but previous analysis of this type of scenario at a different location in the Bad River (the Existing Route Line 5 crossing, Horn et al., 2022) was used to predict that oil could move faster and farther than other seasonal conditions under flood conditions. For the completely unmitigated scenarios, hydrocarbon contamination (whole oil and/or its dissolved constituents) was predicted to reach Lake Superior within approximately 2 days, 3 days, or 4 days following a release for both the White River and Bad River under high, average, and low river flow conditions, respectively. In other words, there would be a 2 to 4 day time lag for response activities to be undertaken to limit oil from reaching the Lake and downstream-most receptors (e.g., the Kakagon-Bad River Slough Complex). Actual response mitigation activation is anticipated to begin at the first CPs within 3.1 to 3.8 hours (see Section 2.1.3 of the Oil Spill Report).

During wintertime low river flow conditions, nearly all (>98%) of the oil in the unmitigated release scenarios was predicted to remain trapped beneath the ice, which prevented evaporation and enhanced dissolution of soluble constituents (which would otherwise preferentially evaporate under ice-free conditions) into the water column. This wintertime scenario used a set of highly conservative assumptions that were intended to bound the upper limit of oil trapped beneath the ice to maximize the potential for in-water effects. Depending on real-world conditions (e.g., partial ice coverage, fissures or leads in the ice, etc.) at the time of release, the amount of oil trapped beneath ice would likely be less than was predicted in these simulations.

Release volume, response mitigation, and the presence of ice were also large factors impacting the predicted oil trajectory, fate, and magnitude of potential effects in the Bad River and White River. Credible worst-case release volumes (i.e., FBR volumes) were generally predicted to result in larger extents with higher concentrations and thicknesses of contamination, which increased the potential for biological exposure and acute mortality. The shortest extents were predicted for the RARV scenarios, where surface and shoreline oiling were predicted to stop before Highway 2 without mitigation and before Copper Falls (Bad River) or before the White River Boreal Forest State Natural Area (White River), with mitigation. For the HARV scenarios in both rivers and the FBR scenarios in the White River, mitigation prevented whole oil (i.e., insoluble fraction) from reaching the wild rice areas, Kakagon-Bad River Slough complex, and Lake Superior. For all wintertime scenarios under 100% ice cover, no

evaporation was simulated, and all of the soluble fraction was predicted to dissolve (with no reduction from volatilization), which resulted in the highest in-water concentrations and potential downstream movement into Lake Superior. In an actual response, substantial additional resources would be deployed at an additional barrier downstream of Highway 2, as well as additional tactics at the CPs (e.g., X-Tex fabric, pom-pom snares, and sorbent booms) that could minimize sheens and help capture submerged oil droplets downstream of turbulent waters.

2. <u>Surface Effects</u> – The most notable surface effects were predicted for fur-bearing mammals and dabbling waterfowl, which spend large amounts of time moving through surface waters as they forage, which would expose them to surface slicks. Most of these effects were predicted to occur in upstream areas, closer to the release locations, where the surface oil slicks were thickest and more continuous. These surface effects assume the presence of fur-bearers and dabbling waterfowl at all points within the river, regardless of whether surveys have identified their presence.

The EA-100s and percentages of assumed habitats affected were predominantly influenced by the volume of oil released, with the largest release volumes (FBR) predicted to result in the largest potential for effects. Smaller releases (HARV followed by RARV), which are of volumes that more closely align with the majority of release data from Enbridge's pipeline system (even though they are still highly unlikely events), generally had the lowest predicted surface effects. No surface effects were predicted for releases under low river/ice flow conditions because oil was trapped below the surface of the ice.

Secondarily, surface effects were influenced by river flow conditions at the time of the release. Although higher river flow rates would move oil faster and tend to increase the potential coverage for surface effects, the duration of exposure at any given location was shorter and the greater holding capacity of vegetated shorelines in high river flow bank full conditions, was predicted to result in more oil stranding on upstream shorelines. Consequently, surface oil exposures further downstream were reduced for those scenarios (especially in the White River), countering some of the influence of faster downstream transport.

Finally, response mitigation had the strongest influence on the potential for surface effects for average river flow conditions, but less so for high flow conditions in the White River, due to these scenarios having lower surface effects overall due to the vegetated banks upstream of MCPs retaining more oil, even without mitigation. The application of emergency response mitigation efforts resulted in reductions in the predicted surface effects on wildlife ranging from approximately 40-90% lower in average flow scenarios and 10-50% lower in high flow scenarios. All mitigated HARV and RARV scenarios had low predictions of acute mortality, over at most 6% of the model domain, while the FBR scenarios had predicted mortalities covering up to 17% of the model domain.

3. <u>Shoreline Effects</u> – In all scenarios other than low river flow wintertime conditions, effects were predominantly predicted within wetland areas. This was due to the prevalence of wetland areas within the model domain and the large oil holding capacity of wetland shorelines themselves, which resulted in acute effects to vegetation. Most effects were predicted to occur in upstream vegetated areas, closer to the release locations, where the potentials for shoreline exposure were greatest due to surface oil slicks being thickest and more continuous.

Shoreline effects were predominantly influenced by river flow conditions and the resulting shore type in contact with the water at the time of the release. Under high river flow bank full conditions, more vegetation was exposed to surface floating oil. Secondarily, shoreline effects were influenced by the

volume of oil released, with the largest release volumes (FBR) predicted to result in the largest potential for effects. Larger river flow rates generally resulted in greater transport and potential for shoreline effects with larger percentages of wetland shorelines (i.e., high river flow conditions) and longer lengths affected. The maximum length of vegetated shoreline from any scenario predicted to be affected was 15 km (9.3 mi., or approximately 18% of total vegetated shoreline) for the FBR release in the White River under high river flow conditions. However, in the White River, under average flow conditions, shoreline effects were relatively high (affecting 98-100% of vegetated shoreline) because nearly all wetland habitats were in the upper portion of the river, where it was exposed to heavy black oil before slicks thinned to sheens. Finally, response mitigation had a notable influence on the potential for shoreline effects, especially for scenarios where containment and collection efforts removed oil prior to reaching downstream wetlands. No shoreline effects were predicted for releases during low river/ice flow conditions because vegetated shorelines were assumed to be covered by a layer of ice.

Response mitigation caused a near complete reduction (~100%) in predicted effects to wetland vegetation (where any initially occurred without mitigation), because a large portion of the surface slicks were contained and collected prior to reaching the predominantly wetland shorelines at downstream Bad River and White River locations as well as within the Bad River Slough. Under average high river flow conditions, predicted effects lengths were below 0.1 km (or <1%), regardless of release volume. Under high river flow conditions, mitigation significantly reduced predicted effects for the FBR release scenarios (23-83% lower than completely unmitigated scenarios), but had almost no effect on the HARV release scenarios in the White River, because acute mortality was predicted primarily at wetland locations upstream of response MCPs (covering approximately 3-8% of the model domain).

4. In-water Effects – Pelagic (swimming) and demersal (bottom-dwelling) organisms were predicted to have the largest effects, followed by planktonic (drifting) organisms (e.g., early-stage amphibians). As would be expected, sensitive species were predicted to have higher areas of potential effects, when compared to average sensitivity species.

In-water effects were primarily influenced by spill volume and river flow rate. Potential effects to sensitive species were greatest for average river flow conditions, followed by high river flow or low river flow, depending on the oil release volume. This progression was the result of a balance between levels of contamination (i.e., concentrations of hydrocarbons in the water column), downstream transport, and the duration of exposure. Greater transport does increase extent, but it reduces duration of exposure. In addition, dilution was greater under high river flow conditions due to greater volumes of water moving through the river. In-water effects were also notably influenced by the volume of oil released, with larger release volumes predicted to result in larger potential for effects.

Because emergency response mitigation efforts focus predominantly on removing whole oil floating on the surface, and dissolution of soluble hydrocarbons largely occurred before the first MCP, in-water effects were not appreciably impacted by response mitigation. The dissolved contaminants within the water column moved downstream, unaffected by response efforts.

5. Mitigation – The response mitigation activities modeled as part of this assessment focused on containing and collecting surface oil, which was predicted to remove between a quarter and nearly all the total volume of released oil, and had a large effect on reducing shoreline oiling and predicted surface effects. At the end of the various mitigated simulations, <0.1% of the oil was predicted to remain on the surface. In other words, mitigation was predicted to remove any oil that had otherwise been able to reach Lake Superior or remained on the surface when no response mitigation was conducted over

the 4-day simulation (i.e., certain scenarios with higher release volumes and greater downstream transport).

Notably, for the mitigated HARV and RARV scenarios, as well as the mitigated FBR scenarios in the White River, mitigation prevented surface slicks from reaching the most downstream portions of the Bad River (north of Highway 2), including the wild rice areas and Bad River Slough. However, for the FBR scenarios in the Bad River, a sufficient oil volume was released that a small amount of surface oil (<1 bbl in total) was predicted to reach the area adjacent to the Bad River Slough and Lake Superior, at levels that were never greater than patchy and discontinuous dull brown or rainbow sheens (<10 µm). In a realistic response, these thin and short-duration sheens (less than a few hours) would be addressed by an additional barrier set up downstream of Highway 2. Although not modeled here, due to the dynamic nature of real spill and environmental conditions, an additional barrier would allow for additional containment and skimming resources to be deployed, as well as additional tactics to minimize sheens and help capture submerged oil droplets downstream of turbulent waters. Even with the equipment modeled here at the planned MCPs, mitigation activities limited oil contact with wetlands and wild rice habitats located in downstream areas, thereby reducing the potential for effects. Downstream surface biological effects were substantially reduced as well. However, mitigation activities did not appreciably reduce dissolved hydrocarbons in the water column, whose transport is not affected by response activities.

6 References

Aamo, O.M., M. Reed, and P. Daling, 1993. A laboratory based weathering model: PC version for coupling to transport models. In Proceedings of the 16th Arctic and Marine Oil Spill Program (AMOP) Technical Seminar, Environmental Protection Service, Emergencies Science Division, Environment Canada, Ottawa, ON, Canada, pp. 617-626.

Alaska Clean Seas (ACS). 2015. Alaska Clean Seas Technical Manual (2 volumes), Revision 12/14, Prudhoe Bay, Alaska, USA, 99734-0022. (Update of 1999 work).

Albers, P.H. and R.C. Szaro, 1978. Effects of No. 2 Fuel Oil on Common Eider Eggs. Marine Pollution Bulletin 9: 138-139.

Albers, P.H., 1980. Transfer of Crude Oil from Contaminated Water to Bird Eggs. Environmental Research 22(2): 307-314.

Allen, A.A. 1978. Case study: Oil Recovery Beneath Ice. Proceedings of the Tenth Offshore Technology Conference. 261-266 pp.

Allen, A.A. 2015. Fate and Behavior of Oil in Ice. Presentation for Shell. Available at: https://s00.static-shell.com/content/dam/shell/static/usa/downloads/alaska/1-fate-behavior-ice.pdf. Accessed: July 2015.

American Society of Civil Engineers, 1969. Design and Construction of Sanitary and Storm Sewers. Manuals and Reports of Engineering Practice, No. 37, New York.

American Society of Civil Engineers Task Committee on Modeling Oil Spills (ASCE), 1996. State-of-the-art Review of Modeling Transport and Fate of Oil Spills, Water Resources Engineering Division, ASCE, Journal of Hydraulic Engineering 122(11): 594-609.

Anderson, E., D. Mendelsohn and E. Howlett, 1995. The OILMAPWin/WOSM Oil Spill Model: Application to Hindcast a River Spill. Proceedings of the Eighteenth Arctic and Marine Oilspill Program (AMOP) Technical Seminar. June 14-16, 1995. Edmonton, Alberta Canada pp. 793.

Anderson, J.W., 1985. Toxicity of dispersed and undispersed Prudhoe Bay crude oil fractions to shrimp, fish, and their larvae. American Petroleum Institute Publication No. 4441, Washington, D.C., USA, August 1985, 52p.

Anderson, J.W., R.G. Riley, S.L. Kiesser, and J. Gurtisen, 1987. Toxicity of dispersed and undispersed Prudhoe Bay crude oil fractions to shrimp and fish. In: Proceedings of the 1987 Oil Spill Conference (Prevention, Behavior, Control, Cleanup), Tenth Biennial, American Petroleum Institute, Washington, D.C., pp.235-240.

Anderson, J.W., S.L. Kiesser, R.M. Bean, R.M., R.G. Riley, and B.L. Thomas, 1981. Toxicity of chemically dispersed oil to shrimp exposed to constant and decreasing concentrations in a flowing system, In: Proceedings of the 1981 Oil Spill Conference, American Petroleum Institute, Washington, D.C., API Publication No. 4334, p. 69-75.

API, 2015. Crude Oil Evaluation Data Sheet (COED), Reference BAKK20140703, Bakken Hi API (Norco RDCC of N0452) generated on 30 November 2015.

Atlas, R. and J. Bragg, 2009. Bioremediation of marine oil spills: when and when not – the Exxon Valdez experience. Microbial Biotechnology 2(2):213-221.

Bad River Tribe, 2020. Maps and GIS Services: Bad River GIS & Map Services Program: Interactive Maps – Wild Rice. Available: https://www.badriver-nsn.gov/natural-resources/maps-gis-services/

Data Hosted:
https://www.arcgis.com/apps/View/index.html?appid=6f44c371217e4ee8b5f1c2c705c7c7c5
Accessed: October 2020

Bad River Watershed Association. 2021. Bad River Watershed Description. Available:
http://www.badriverwatershed.org/index.php/bad-river-watershed. Accessed May 2021

Barnes, P.W., D.M. Schell and E. Reimnitz, (Editors). 2013. The Alaskan Beaufort Sea: Ecosystems and
Environments. Elsevier Publishers - Science.

Blum, D.J. and R.E. Speece, 1990. Determining chemical toxicity to aquatic species, Environmental Science
and Technology. 24: 284-293.

Bonn Agreement, 2009. Bonn Agreement Aerial Operations Handbook, 2009. London, UK. Available:
http://www.bonnagreement.org/site/assets/files/1081/ba-aoh revision 2 april 2012-1.pdf, Accessed: 4
June 2015.

Bonn Agreement, 2011. Bonn Agreement Oil Appearance Code Photo Atlas. Available:
http://www.bonnagreement.org/site/assets/files/1081/photo_atlas_version_20112306-1.pdf.
Accessed: April 2017.

Bradbury, S., R. Carlson, and T. Henry, 1989. Polar narcosis in aquatic organisms. Aquatic Toxicology and
Hazard Assessment 12: 59-73.

Cheng, J. 2022. World of Waterfalls. Copper Falls and Brownstone Falls. Available: https://www.world-of-
waterfalls.com/waterfalls/eastern-us-copper-falls/. Accessed: August 2022.

Clark, R.B., 1984. Impact of Oil Pollution on Seabirds. Environmental Pollution (Series A) 33: 1-22.

Coastal Engineering Research Center (CERC), 1984. Shore Protection Manual, Vol. I. Coastal Engineering
Research Center, Department of the Army, Waterways Experiment Station, U.S. Army Corps of
Engineers, Vicksburg, Mississippi, 1,105p. plus 134p. in appendices.

Cox, J.C., L.A. Schultz, R.P. Johnson and R.A. Shelsby. 1980. The Transport and Behavior of Oil Spilled in
and under Sea Ice. In Environmental Assessment of the Alaskan Continental Shelf. Final Reports of
the Principal Investigators. 1981. Volume 3. Physical Science Studies. Boulder, CO.: National
Oceanic and Atmospheric Administration and Bureau of Land Management. 427.

CSE/ASA/BAT, 1986. Development of a Coastal Oil Spill Smear Model. Phase 1: Analysis of Available and
Proposed Models, Prepared for Minerals Management Service by Coastal Science & Engineering,
Inc. (CSE) with Applied Science Associates, Inc. (ASA) and Battelle New England Research
Laboratory (BAT), 121p.

Daling, P.S. and P.J. Brandvik, 1988. A Study of the Formation and Stability of Water-in-Oil Emulsions. In
Proceedings of the 11th Arctic and Marine Oil Spill Program Technical Seminar. Emergencies
Science Division, Environment Canada, Ottawa, ON, Canada, pp.153-170.

Daling, P.S., D. Mackay, N. Mackay, and P.J. Brandvik, 1990. Droplet size distributions in chemical
dispersion of oil spills: Towards a mathematical model. Oil and Chemical Pollution 7: 173-198.

Daling, P.S. and P.J. Brandvik, 1991. Characterization and prediction of the weathering properties of oils at
sea – A manual for the oils investigated in the DIWO project. IKU SINTEF Group report 91.037,
DIWO report no. 16 02.0786.00/16/91, 29 May 1991, 140p.

Daling, P.S., O.M. Aamo, A. Lewis, and T. Strom-Kritiansen, 1997. SINTEF/IKU Oil-Weathering Model:
Predicting Oil's Properties at Sea. In: Proceedings of the 1997 Oil Spill Conference, Publication No.
4651, American Petroleum Institute, Washington, D.C., pp. 297-307.

Dangerous Goods Transport Consulting (DGTC), 2014. A Survey of Bakken Crude Oil Characteristics Assembled for the U.S. Department of Transportation. Submitted by American Fuel & Petrochemical Manufacturers. Prepared by Dangerous Goods Transport Consulting, Inc. May 14, 2014

Deltares, D., 2022. D-Flow FM user manual. Deltares Delft, The Netherlands, 330 p.Delvigne, G.A.L. and C.E. Sweeney, 1988. Natural Dispersion of Oil. Oil and Chemical Pollution 4: 281-310.

Delvigne, G.A.L., 1993. Natural dispersion of oil by different sources of turbulence. Proc. Oil Spill Conf.-1993. Sponsored by U.S. Coast Guard, EPA and API, Tampa, FL, March, pp. 415-419.

Dickins, D.F., J. Bradford and L. Steinbronn. 2008. Detection of Oil on and Under Ice: Phase III Evaluation of Airborne Radar System Capabilities in Selected Arctic Spill Scenarios. Report submitted to US Department of Interior, Minerals Management Service. July 2008. 68 pp.

Di Toro, D.M. and J.A. McGrath, 2000. Technical basis for narcotic chemicals and polycyclic aromatic hydrocarbon criteria. II. Mixtures and sediments. Environmental Toxicology and Chemistry 19(8): 1971-1982.

Di Toro, D.M., J.A. McGrath, and D.J. Hansen, 2000. Technical basis for narcotic chemicals and polycyclic aromatic hydrocarbon criteria. I. Water and tissue. Environmental Toxicology and Chemistry 19(8): 1951-1970.

Drozdowski, D., S. Nudds, C.G. Hannah, H. Niu, I. Peterson, and W. Perrie, 2011. Review of oil spill trajectory modelling in the presence of ice. Canadian Technical Report of Hydrographic and Ocean Sciences 274 Fisheries and Oceans Canada. Bedford Institute of Oceanography, Dartmouth, NS, Canada

Engelhardt, F.R., 1983. Petroleum Effects on Marine Mammals. Aquatic Toxicology 4: 199-217.

Enbridge. 2016. Guide: Shoreline Cleanup Assessment Technique (SCAT) Guidance. Version 1.0, 06/30/2016. Effective date 6/30/2016. 99 p.

Enbridge. 2018. Enbridge Inland Spill Response Tactics Guide. Prepared by Enbridge, Elastec, QualiTech, LAMOR, and Riverspill Response Canada, Ltd.

Enbridge, 2020. MP-4 – Plan and Profile, 30-iinch Pipeline Crossing of the White River by Horizontal Direction Drilling. Sheet number 1. Project Enbridge/1948. 1 p.

Enbridge, 2022a. Response documentation received by RPS (Matt Horn) from Enbridge (Dan Quick, Kurtis Fleet) via email. May 17, May 31, June 9.

Enbridge, 2022b. SURCP0877 Control Point site sheet. Received from Dan Quick, Enbridge, on May 17, 2022

Enbridge, 2022c. Email re: Enbridge response tactics. Received from Dan Quick, Enbridge, on September 13, 2022

Environment Canada Oil Property Database, 2017. Sweet Blend (http://www.etcentre.org/spills) as described in Jokuty et al. (1999). Now available at https://www.etc-cte.ec.gc.ca/databases/OilProperties/oil_prop_e.html. Accessed: May 2021

Fay, J.A., 1971. Physical processes in the spread of oil on a water surface. In: Proceedings, Conference on Prevention and Control of Oil Spills, sponsored by API, EPA, and US Coast Guard, American Petroleum Institute, Washington, D.C., June 15 17, 1971, pp. 463-467.

Fingas, M., 1996. The Evaporation of Crude Oil and Petroleum Products. Ph.D. Dissertation, McGill University, Montreal, Canada, 181p.

Fingas, M., 1997. The Evaporation of Oil Spills: Prediction of Equations Using Distillation Data. In Proceedings of the 20th Arctic and Marine Oil Spill Program (AMOP) Technical Seminar, Emergencies Science Division, Environment Canada, Ottawa, ON, Canada, pp. 1-20.

Fingas, M., B. Fieldhuse, and J.V. Mullin, 1997. Studies of Water-in-Oil Emulsions: Stability Studies. In: Proceedings of 20th Arctic and Marine Oil Spill Program (AMOP) Technical Seminar, Emergencies Science Division, Environment Canada, Ottawa, ON, Canada, pp. 21-42.

Fingas, M.F., 1998. Studies on the Evaporation of Crude Oil and Petroleum Products: II. Boundary Layer Regulation. Journal of Hazardous Materials, Vol. 57, pp.41-58.

Fingas, M.F., 1999. The Evaporation of Oil Spills: Development and Implementation of New Prediction Methodology. In: Proceedings of the 1999 International Oil Spill Conference, American Petroleum Institute, Washington, D.C., pp. 281-287.

Fischer, H.B., 1973. Longitudinal Dispersion and Turbulent Mixing in Open Channel Flow. Annual Review of Fluid Mechanics: pp 59-78.

French, D.P. and F.W. French III, 1989. The biological effects component of the Natural Resource Damage Assessment Model system. Oil and Chemical Pollution 5:125 163.

French, D.P., 1991. Estimation of exposure and resulting mortality of aquatic biota following spills of toxic substances using a numerical model, Aquatic Toxicology and Risk Assessment: Fourteenth Volume, ASTM STP 1124, (M.A. Mayes and M.G. Barron, Eds.) American Society for Testing and Materials, Philadelphia, pp. 35-47.

French, D.P., M. Reed, K. Jayko, S. Feng, H. Rines, S. Pavignano, T. Isaji, S. Puckett, A. Keller, F.W. French III, D. Gifford, J. McCue, G. Brown, E. MacDonald, J. Quirk, S. Natzke, R. Bishop, M. Welsh, M. Phillips, and B.S. Ingram, 1996. Final Report, The CERCLA Type A Natural Resource Damage Assessment Model for Coastal and Marine Environments (NRDAM/CME), Technical Documentation, Vol. I - V., Office of Environmental Policy and Compliance, U.S. Department of the Interior, Washington, DC, Contract No. 14-0001-91-C-11.

French, D.P. and H. Rines, 1997. Validation and use of spill impact modeling for impact assessment. In: Proceedings, 1997 International Oil Spill Conference, Fort Lauderdale, Florida, American Petroleum Institute Publication No. 4651, Washington, DC, pp-829-834.

French, D.P., H. Rines, and P. Masciangioli, 1997. Validation of an Orimulsion spill fates model using observations from field test spills. In: Proceedings, Twentieth Arctic and Marine Oil Spill Program Technical Seminar, Vancouver, Canada, June 10-13, 1997.

French, D., H. Schuttenberg, and T. Isaji, 1999. Probabilities of Oil Exceeding Thresholds of Concern: Examples from an Evaluation for Florida Power and Light. In: Proceedings of the 22nd Arctic and Marine Oil Spill Program (AMOP) Technical Seminar, June 2-4, 1999, Calgary, Alberta, Environment Canada, pp.243-270.

French-McCay, D.P., 2001. Development and Application of an Oil Toxicity and Exposure Model, OilToxEx. Final Report to Damage Assessment Center, Silver Spring, MD, January 2001, 50p plus appendices.

French-McCay, D.P. and J.R. Payne, 2001. Model of Oil Fate and Water concentrations with and without application of dispersants. In: Proceedings of the 24th Arctic and Marine Oil Spill Program (AMOP) Technical Seminar, Emergencies Science Division, Environment Canada, Ottawa, ON, Canada, pp. 601-653.

French-McCay, D.P., 2002. Development and Application of an Oil Toxicity and Exposure Model, OilToxEx. Environmental Toxicology and Chemistry 21(10): 2080-2094.

French-McCay, D.P., 2003. Development and Application of Damage Assessment Modeling: Example Assessment for the North Cape Oil Spill. Marine Pollution Bulletin, Volume 47, Issues 9-12, September-December 2003, pp. 341-359.

French-McCay, D.P., 2004. Oil release impact modelling: Development and validation. Environmental Toxicology and Chemistry 23(10): 2441-2456.

French-McCay, D.P. and J.J. Rowe, 2004. Evaluation of Bird Impacts in Historical Oil Release Cases Using the SIMAP Oil Release Model. Proceedings of the Twenty-seventh Arctic and Marine Oil Spill Program (AMOP) Technical Seminar. Emergencies Science Division, Environment Canada, Ottawa, ON, Canada. pp. 421-452.

French-McCay, D.P., 2009. State-of-the-Art and Research Needs for Oil Release Impact Assessment Modelling. In: Proceedings of the 32nd AMOP Technical Seminar on Environmental Contamination and Response, Emergencies Science Division, Environment Canada, Ottawa, ON, Canada, pp. 601-653.

French-McCay, D., K. Jayko, Z. Li, M. Horn, T. Isaji, and M. Spaulding, 2017. Simulation Modeling of Ocean Circulation and Oil Spills in the Gulf of Mexico - Annex A to Appendix II Oil Transport and Fate Model Technical Manual: Oil Fate Model Algorithms. Prepared by RPS ASA for the US Department of the Interior, Bureau of Ocean Energy Management, Gulf of Mexico OCS Region, New Orleans, LA. BOEM OCS Study.

Geraci, J.R. and D.J. St. Aubin, 1988. Synthesis of Effects of Oil on Marine Mammals, Report to U.S. Department of the Interior, Minerals Management Service, Atlantic OCS Region, OCS Study, MMS 88 0049, Battelle Memorial Institute, Ventura, CA, 292 p.

Gerritsen, H. Gerritsen, de Goede, E.D., Platzek, F.W., van Kester, J.a.Th.M., Genseberger, M., Uittenbogaard, R.E. 2008. Validation Document Delft3D-FLOW; a software system for 3D flow Simulations. Technical Report. X0356, M3470. September.

Great Lakes Drive, 2022. Red Granite Falls. Available: http://greatlakesdrive.com/GLD/property/red-granite-falls/#:~:text=Red%20Granite%20Falls%20is%20located,Copper%20Falls%20and%20Brownstone%20Falls. Accessed: August 2022.

Great Lakes Waterfalls and Beyond, 2009. Waterfalls Page – Copper Falls. Available: http://www.gowaterfalling.com/waterfalls/copper.shtml. Accessed: August 2022.

Great Lakes Waterfalls and Beyond, 2013. Waterfalls Page – Granite Falls. Available: http://www.gowaterfalling.com/waterfalls/redgranite.shtml. Accessed: August 2022.

Gundlach, E.R., 1987. Oil Holding Capacities and Removal Coefficients for Different Shoreline Types to Computer Simulate Spills in Coastal Waters. In: Proceedings of the 1987 Oil Spill Conference, pp. 451-457.

Hines, A.L. and R.N. Maddox, 1985. Mass Transfer Fundamentals and Application. Prentice-Hall, Inc., Englewood Cliffs, New Jersey, 542p.

Hodson, P.V., D.G. Dixon, and K.L.E. Kaiser, 1988. Estimating the Acute Toxicity of Waterborne Chemicals in Trout from Measurements of Median Lethal Dose and the Octanol-Water Partition Coefficient. Journal of Environmental Toxicology and Chemistry 7:443-454.

Hoffman, D.J., 1978. Embryotoxic Effects of Crude Oil in Mallard Ducks and Chicks. Toxicology and Applied Pharmacology 46: 183-190.

Horn, M., Robinson, H., McStay, L., Frediani, M., 2022. Rebuttal Report – Enbridge Line 5. Redesignated version. April 8. 339 p.

Huang, W. and M. Spaulding, 1995. 3D Model of Estuarine Circulation and Water Quality Induced by Surface Discharges. Journal of Hydraulic Engineering 121: 300-311.

Incardona, J.P., M.G. Carls, L. Holland, T.L. Linbo, D.H. Baldwin, M.S. Myers, K.A. Peck, M. Tagal, S.D. Rice, and N.L. Scholz, 2015. Very low embryonic crude oil exposures cause lasting cardiac defects in salmon and herring. Scientific Reports 5.

Jenssen, B. M. and M. Ekker, 1991a. Dose Dependent Effects of Plumage-Oiling on Thermoregulation of Common Eiders Somateria mollissima Residing in Water. Polar Research 10: 579-84.

Jenssen, B. M. and M. Ekker, 1991b. Effects of Plumage Contamination with Crude Oil Dispersant Mixtures on Thermoregulation in Common Eiders and Mallards. Archives of Environmental Contamination and Toxicology 20: 398-403.

Jenssen, B.M., 1994. Review article: effects of oil pollution, chemically treated oil, and cleaning on thermal balance of birds. Environmental Pollution. 86(2):207-215.

Jones, R.K., 1997. A Simplified Pseudo-Component of Oil Evaporation Model. In Proceedings of the 20th Arctic and Marine Oil Spill Program (AMOP) Technical Seminar, Environment Canada, pp. 43-61.

King, K.A. and C.A. Lefever, 1979. Effects of Oil Transferred from Incubating Gulls to Their Eggs. Marine Pollution Bulletin 10: 319-321.

Kirstein, B.E., J.R. Clayton, C. Clary, J.R. Payne, D. McNabb, Jr., G. Fauna and R. Redding, 1985. Integration of Suspended Particulate Matter and Oil Transportation Study. Year One Interim Report. Minerals Management Service, OCS Study MMS87-0083, Anchorage, Alaska, 216p.

Kolluru, V., M.L. Spaulding, and E. Anderson, 1994. A three dimensional subsurface oil dispersion model using a particle based approach. In Proceedings of 17th Arctic and Marine Oil Spill Program (AMOP) Technical Seminar, Vancouver, British Columbia, June 8-10, 1994, Emergencies Science Division, Environment Canada, Ottawa, ON, Canada, pp. 867-893.

Kooijman, S.A.L.M., 1981. Parametric analysis of mortality rates in bioassays. Water Res. 15:107-119.

Kullenberg, G. (ed.), 1982. Pollutant transfer and transport in the sea. Volume II. CRC Press, Boca Raton, Florida. 66 p.

Lehr, W.J., D. Wesley, D. Simecek-Beatty, R. Jones, G. Kachook, and J. Lankford, 2000. Algorithm and interface modifications of the NOAA oil spill behavior model. In Proceedings of the 23rd Arctic and Marine Oil Spill Program (AMOP) Technical Seminar, Vancouver, BC, Environmental Protection Service, Environment Canada, pp. 525-539.

Lewis, E.L. 1976. Pacific Marine Science Report 76-12. Institute of Ocean Sciences. Victoria, BC.

Li, Z. and D. French-McCay, 2017. Simulation Modeling of Ocean Circulation and Oil Spills in the Gulf of Mexico - Annex C to Appendix II Oil Transport and Fates Model Technical Manual: Review of Biodegradation Rates of Crude Oil and Hydrocarbons in Seawater. Prepared by RPS ASA for the US Department of the Interior, Bureau of Ocean Energy Management, Gulf of Mexico OCS Region, New Orleans, LA. BOEM OCS Study. Included in "French-McCay et al. 2017."

Lunel, T., 1993a. Dispersion: Oil droplet size measurements at sea. In: Proceedings of the 16th Arctic Marine Oilspill Program (AMOP) Technical Seminar, Environment Canada, Calgary, Alberta, June 7-9, 1993, pp. 1023-1056.

Lunel, T., 1993b. Dispersion: Oil droplet size measurements at sea. In: Proceedings of the 1993 Oil Spill Conference, pp. 794-795.

Lyman, C.J., W.F. Reehl, and D.H. Rosenblatt, 1982. Handbook of Chemical Property Estimation Methods. McGraw-Hill Book Co., New York, 960p.

Mackay, D. and R.M. Matsugu, 1973. Evaporation rates of liquid hydrocarbon spills on land and water. Canadian Journal of Chemical Engineering 51: 434-439.

Mackay, D. and P.J. Leinonen, 1977. Mathematical model of the behavior of oil spills on water with natural and chemical dispersion. Prepared for Fisheries and Environment Canada. Economic and Technical Review Report EPS-3-EC-77-19, 39p.

Mackay, D., S. Paterson, and K. Trudel, 1980. A mathematical model of oil spill behavior. Department of Chemical and Applied Chemistry, University of Toronto, Canada, 39p.

Mackay, D, W.Y. Shiu, K. Hossain, W. Stiver, D. McCurdy, and S. Peterson, 1982. Development and calibration of an oil spill behavior model. Report No. CG-D-27-83, U.S. Coast Guard, Research and Development Center, Groton, Connecticut, 83p.

Mackay, D. and W. Zagorski, 1982. Studies of Water-In-Oil Emulsions. Environment Canada Manuscript Report EE-34, Ottawa, Ontario, Canada, 93p.

Mackay, D., H. Puig and L.S. McCarty, 1992. An equation describing the time course and variability in uptake and toxicity of narcotic chemicals to fish. Environ. Toxicol. Chemistry 11: 941-951.

Malins, D.C. and H.O. Hodgins, 1981. Petroleum and marine fishes: a review of uptake, disposition, and effects. Environmental Science & Technology 15(11):1272-1280.

McAuliffe, C.D., 1987. Organism exposure to volatile/soluble hydrocarbons from crude oil spills – a field and laboratory comparison. In Proceedings of the 1987 Oil Spill Conference, API, p. 275-288.

McAuliffe, C.D., 1989. The Weathering of Volatile Hydrocarbons from Crude Oil Slicks on Water. In: Proceedings of the 1989 Oil Spill Conference, San Antonio, Texas, American Petroleum Institute, Washington, D.C., pp. 357-364.

McCarty, L.S., 1986. The Relationship Between Aquatic Toxicity QSARs and Bioconcentration for Some Organic Chemicals. Journal of Environmental Toxicology Chemistry 5:1071-1080.

McCarty, L.S., D. Mackay, A.D. Smith, G.W. Ozburn, and D.G. Dixon, 1992a. Residue-based Interpretation of Toxicity and Bioconcentration QSARs from Aquatic Bioassays: Neutral Narcotic Organics. Journal of Environmental Toxicology and Chemistry 11:917-930.

McCarty, L.S., G.W. Ozburn, A.D. Smith, and D.G. Dixon, 1992b. Toxicokinetic modeling of mixtures of organic chemicals. Environmental Toxicology and Chemistry 11: 1037-1047.

McCarty, L.S., and D. Mackay, 1993. Enhancing Ecotoxicological Modeling and Assessment. Journal of Environmental Science and Technology 27(9):1719-1728.

Mendelsohn, D., E. Howlett, and J.C. Swanson, 1995. WQMAP in a Windows Environment. In: Proceedings of the 4th International Conference on Estuarine and Coastal Modeling, October 26-28, 1995, San Diego, CA.

Mendelsohn, D., S. Peene, W. Saunders, and M. Goodrich, 2003. Three-Dimensional Modeling Of Anthropogenic Impacts To Dissolved Oxygen In A Stratified Estuarine Environment: Savannah River Estuary. In: Proceedings, TMDL 2003, Chicago, Ill, Nov 16-19, 2003. Water Environment Federation.

Milton, S., P. Lutz, and G. Shigenaka, 2003. Oil Toxicity and Impacts on Sea Turtles. In: Shigenaka, G. (ed.), Oil and Sea Turtles: Biology, Planning, and Response. National Oceanic and Atmospheric Administration, 116 p.

Muin, M. and M.L. Spaulding, 1997. Three-dimensional boundary fitted circulation model. Journal of Hydraulic Engineering, Vol. 123, No. 1, January 1997, p. 2-12.

Muin, M., 1993. A three dimensional boundary fitted circulation model in spherical coordinates. Ph.D. Thesis, Department of Ocean Engineering, University of Rhode Island, Kingston, RI.

National Oceanic and Atmospheric Administration (NOAA), 2015. National Centers for Environmental Information – Comparative Climatic Data through 2015. Available: http://www1.ncdc.noaa.gov/pub/data/ccd-data/CCD-2015.pdf. Accessed: November 2017.

National Oceanic and Atmospheric Administration (NOAA), 2016a. Open water oil identification job aid for aerial observation. U.S. Department of Commerce, Office of Response and Restoration [http://response.restoration.noaa.gov/oil-and-chemical-spills/oil-spills/resources/open-water-oil-identification-job-aid.html].

National Research Council (NRC), 1985. Oil in the Sea: Inputs, Fates and Effects. National Academy Press, Washington, D.C. 601p.

National Research Council (NRC), 2003. Oil in the Sea III: Inputs, Fates and Effects. National Academy Press, Washington, D.C. 280p.

Neff, J.M. and J.W. Anderson, 1981. Response of Marine Animals to Petroleum and Specific Petroleum Hydrocarbons. Applied Science Publishers Ltd., London and Halsted Press Division, John Wiley & Sons, NY. 177p.

Neff, J.M., J.W. Anderson, B.A. Cox, R.B. Laughlin, Jr., S.S. Rossi, and H.E. Tatem, 1976. Effects of petroleum on survival respiration, and growth of marine animals. In: Sources, Effects and Sinks of Hydrocarbons in the Aquatic Environment. American Institute of Biological Sciences, Washington, D.C. 515-539p.

Nirmalakhandan, N. and R.E. Speece, 1988. Structure-activity relationships, quantitative techniques for predicting the behavior of chemicals in the ecosystem. Environmental Science and Technology 22:606-615.

Okubo, A., 1971. Oceanic diffusion diagrams. Deep-Sea Research 8:789-802.

Okubo, A. and R.V. Ozmidov, 1970. Empirical dependence of the coefficient of horizontal turbulent diffusion in the ocean on the scale of the phenomenon in question. Atmospheric and Ocean Physics 6(5):534-536.

Payne, J.R. and G.D. McNabb Jr., 1984. Weathering of Petroleum in the Marine Environment. Marine Technology Society Journal 18(3):24-42.

Payne, J.R., B.E. Kirstein, G.D. McNabb, Jr., J.L. Lambach, R. Redding R.E. Jordan, W. Hom, C. deOliveria, G.S. Smith, D.M. Baxter, and R. Gaegel, 1984. Multivariate analysis of petroleum weathering in the marine environment – sub Arctic. Environmental Assessment of the Alaskan Continental Shelf, OCEAP, Final Report of Principal Investigators. US Dept. of Commerce, National Oceanic and Atmospheric Administration; US Dept. of the Interior, Minerals Management Service, Alaska OCS Region. Vol. 1 technical results, 686p. and Vol. 2 appendix, 209p., Jan. 1984.

Payne, J.R., B.E. Kirstein, J.R. Clayton, Jr., C. Clary, R. Redding, G.D. McNabb, Jr., and G. Farmer, 1987. Integration of suspended particulate matter and oil transportation study. Final Report. Minerals Management Service, Environmental Studies Branch, Anchorage, AK. Contract No. 14-12-0001-30146, 216 p.

Peakall, D.B., P.G. Wells and D. Mackay, 1985. A hazard assessment of chemically dispersed oil spills and seabirds a novel approach. In: Proc. 8th Tech. Sem. Annual Arctic Marine Oil Spill Program, 18-20 June 1985. Environmental Protection Service Environmental Canada. Edmonton, Alta., pp. 78-90.

Pipeline and Hazardous Materials Safety Administration (PHMSA), 2017. PHMSA Pipeline Incident Statistics. Available: http://www.phmsa.dot.gov/pipeline/library/data-stats/pipelineincidenttrends. Accessed: September 2017.

Reed, M. and E. Gundlach, 1989. Hindcast of the Amoco Cadiz event with a coastal zone oil spill model. Oil and Chemical Pollution 5: 451-476.

Rice, S.D., J.W. Short, and J.F. Karinen, 1977. Comparative oil toxicity and comparative animal sensitivity, p. 78-94. In: D.A. Wolfe (ed.). Fate and Effects of Petroleum Hydrocarbons in Marine Ecosystems and Organisms. Pergamon Press, NY.

Seo, I.W. and K.O. Baek, 2004. Estimation of the Longitudinal Dispersion Coefficient Using the Velocity Profile in Natural Streams. Journal of Hydraulic Engineering. March 2004.

Socolofsky, S.A. and G.H. Jirka, 2005. Environmental Fluid Mechanics Draft Textbook.

Sørstrøm, S.E., P.J. Brandvik, I. Buist, P. Daling, D. Dickins, L-G. Faksness, S. Potter, J. Fritt-Rasmussen and I. Singsaas, 2010. Joint Industry Program on Oil Contingency for Arctic and Ice-Covered Waters. Summary Report. Report No. 32. SINTEF A14181, ISBN-no. 978-82-14-04759-2.

Spaulding, M.L., 1984. A vertically averaged circulation model using boundary fitted coordinates. Journal of Physical Oceanography, May, pp. 973-982.

Spaulding, M.L., 1988. A State-of-the-Art Review of Oil Spill Trajectory and Fate Modeling. Oil and Chemical Pollution 4(1):39-55.

Spies, R.B., S.D. Rice, D.A. Wolfe, and B.A. Wright, 1996. The Effects of the Exxon Valdez Oil Spill on the Alaskan Coastal Environment. In: Proceedings of the Exxon Valdez Oil Spill Symposium 18, American Fisheries Society, Bethesda, MD, pp. 1-16.

Sprague, J.B., 1969. Measurement of pollutant toxicity to fish. I. Bioassay methods for acute toxicity. Water Research 3: 793-821.

Stiver, W. and D. Mackay, 1984. Evaporation rate of oil spills of hydrocarbons and petroleum mixtures. Environmental Science and Technology 18: 834-840.

Swanson, C., D. Mendelsohn, D. Crowley, and Y. Kim, 2012. Monitoring and modeling the thermal plume from the Indian Point Energy Center in the Hudson River. In: Proceedings of the Electric Power Research Institute Third Thermal Ecology and Regulation Workshop, Maple Grove, MN, 11-12 October 2011.

Swanson, J. C., 1986. A three dimensional numerical model system of coastal circulation and water quality. Ph.D. Thesis, Dept. of Ocean Engineering, University of Rhode Island, Kingston, RI.

Swanson, J.C., M. Spaulding, J-P Mathisen and O.O. Jenssen, 1989. A Three Dimensional Boundary fitted Coordinate Hydrodynamic Model, Part I: Development and Testing. Dt. Hydrog, Z. 42, 1989, p. 169-186.

Swartz, R.C., D.W. Schults, R.J. Ozretich, J.O. Lamberson, F.A. Cole, T.H. DeWitt, M.S. Redmond, and S.P. Ferraro, 1995. ΣPAH: A Model to Predict the Toxicity of Polynuclear Aromatic Hydrocarbon Mixtures in Field-Collected Sediments. Journal of Environmental Toxicology and Chemistry 14(11): 1977-1987.

Tatem, H.E., B.A. Cox, and J.W. Anderson, 1978. The toxicity of oils and petroleum hydrocarbons to estuarine crustaceans. Estuarine and Coastal Marine Science 6:365-373.

Territory Supply, 2022. 11 Waterfalls in Wisconsin Not to be Missed. Copper Falls. Available: https://www.territorysupply.com/wisconsin-waterfalls. Accessed: August 2022.

Thorpe, S.A., 1984. On the Determination of K in the Near Surface Ocean from Acoustic Measurements of Bubbles. Journal of Physical Oceanography 14: 855-863.

U.S. Environmental Protection Agency (U.S. EPA), 2000. AQUIRE ECOTOX database. Internet database for aquatic toxicity data. http://www.epa.gov/ecotox/.

U.S. Environmental Protection Agency (U.S. EPA), 2003. Procedures for the Derivation of Equilibrium Partitioning Sediment benchmarks (ESBs) for the Protection of Benthic Organisms (PDF). PAH Mixtures. EPA-600-R-02-013. Office of Research and Development. Washington, DC.

U.S. Environmental Protection Agency (U.S. EPA), 2008. Procedures for the Derivation of Equilibrium Partitioning Sediment benchmarks (ESBs) for the Protection of Benthic Organisms (PDF). Compendium of Tier 2 Values for Nonionic Organics. U.S. Environmental Protection Agency, Office of Research and Development: Washington DC. EPA/600/R-02/016. PB2008-107282. March 2008.

U.S. Fish and Wildlife Service, 2020. National Wetlands Inventory – Wetlands Data by State. Available: https://www.fws.gov/wetlands/Data/State-Downloads.html Accessed: October, 2020

U.S. Geological Survey (USGS), 2020a. Surface water data for USA: USGS Surface-Water Monthly Statistics for USGS 04027000 BAD RIVER NEAR ODANAH, WI Available: https://waterdata.usgs.gov/usa/nwis/uv?04027000. and for USGS 04026450 BAD RIVER NEAR MELLEN, WI Available: https://waterdata.usgs.gov/usa/nwis/uv?04026450 Accessed: June 2020.

U.S. Geological Survey (USGS), 2020b. The National Map – National Hydrography Dataset. Available: http://nhd.usgs.gov/.

U.S. Geological Survey (USGS), 2022. Surface water data for USA: USGS Surface-Water Monthly Statistics for USGS 04027500 WHITE RIVER NEAR ASHLAND, WI Available: https://waterdata.usgs.gov/usa/nwis/uv?04027500. Accessed: June 2022.

Vargo, S., P. Lutz, D. Odell, E. Van Vleep, and G. Bossart, 1986. Final Report: Study of Effects of Oil on Marine Turtles. Technical Report OCS study MMS 86-0070. Vol. 2, 181 p.

Varhaar, H.J.M, C.J. VanLeeuwen, and J.L.M. Hermens, 1992. Classifying Environmental Pollutants, 1: Structure-activity Relationships for Prediction of Aquatic Toxicity. Chemosphere 25:471-491.

Varoujean, D.H., D.M. Baltz, B. Allen, D. Power, D.A. Schroeder, and K.M. Kempner, 1983. Seabird Oil Spill Behavior Study, Vol 1: Executive Summary, Volume 2: Technical Report, Volume 3: Appendices. Final Report to U.S. Dept. of the Interior, Minerals Management Service, Reston, VA, by Nero and Associates, Inc., Portland, OR, MMS QN TE 83 007, NTIS #PB84 17930, 365 p.

WDNR. 1966. Wisconsin Department of Natural Resources 608-266-2621 White River Flowage – Ashland County, Wisconsin DNR Lake Map Date – Sep 1966 - Historical Lake Map - Not for Navigation. Available: https://dnr.wi.gov/lakes/maps/DNR/2894200a.pdf Accessed: August 2022.

Wisconsin Department of Natural Resources, 2020. Wild Rice Map Service. Available: https://dnrmaps.wi.gov/arcgis/rest/services/WT_SWDV/WT_Wetlands_Plants_and_Habitat_WTM_Ext_v2/MapServer/6 Accessed: October, 2020

Wisconsin Department of Natural Resources (WI DNR), 2023. Wild rice waters - polyline and polygon layers. Available: https://dnrmaps.wi.gov/arcgis/rest/services. Accessed January 2023.

Wolfe, J.L. and R.J. Esher, 1981. Effects of Crude Oil on Swimming Behavior and Survival in the Rice Rat. Environmental Research 26: 486-489.

Youssef, M. and M.L. Spaulding, 1993. Drift current under the action of wind waves, Proceedings of the 16th Arctic and Marine Oil Spill Program Technical Seminar, Calgary, Alberta, Canada, pp. 587-615.

Zahed, M.A., H.A. Aziz, M.H. Isa, L. Mohajeri, S. Mohajeri, and S.R.M. Kutty, 2011. Kinetic modeling and half-life study on bioremediation of crude oil dispersed by Corexit 9500. Journal of Hazardous Materials 185(2-3):1027-1031.